UNDERSTANDING THE ROLE OF LYSINE-SPECIFIC DEMETHYLASE 1 IN EMBRYONIC GENE REGULATION

Thesis submitted for the degree of

Doctor of Philosophy

at the University of Leicester

by

Charles Thomas Foster MSc (Leicester)

Department of Biochemistry

University of Leicester

August 2011

Abstract

Understanding the Role of Lysine-Specific Demethylase 1 in Embryonic Gene Regulation

Charles T Foster

Histone proteins provide a means of packaging DNA over 10,000-fold in order to allow the accommodation of genetic material as chromatin in the nucleus of the cell. However, the chemical manipulation of histones underpins an array of additional biological functions of chromatin. The unstructured N-terminal tails of histones are covalently modified in a variety of fashions, with many of these modifications implicated in the regulation of gene expression. Lysine specific demethylase 1 (LSD1), which demethylates mono- and di-methylated histone H3 lysine 4 (H3K4) as part of a complex including CoREST and histone deacetylases (HDACs), is essential for embryonic development in the mouse beyond embryonic day (E)6.5. The aim was to determine the role of LSD1 during this early period of embryogenesis through generation and analysis of conditional knockout mouse embryonic stem (ES) cells, which are the *in vitro* counterpart of the epiblast. Prior analysis of post-implantation loss-of-function genetrap embryos revealed that LSD1 expression, and therefore function, is restricted to the epiblast. Conditional deletion of LSD1 in mouse ES cells revealed a reduction in CoREST protein and associated HDAC activity, resulting in a global increase in histone H3K9 and H3K56 acetylation, but only minor increases in global H3K4 methylation. Despite this biochemical perturbation, LSD1 deleted ES cells proliferate normally and retain stem cell characteristics. However, differentiation of these ES cells is associated with significant cell death. Loss of LSD1 causes the aberrant expression of 588 genes, including transcription factors with roles in anterior/posterior patterning and tissue specification. *Brachyury*, a key-regulator of mesodermal differentiation, is a direct target gene of LSD1 and is over-expressed in E6.5 *Lsd1* genetrap embryos. Thus, LSD1 regulates the expression and appropriate timing of a key developmental regulator, as part of the LSD1/CoREST/HDAC complex, during early embryonic development. Notably, rescue experiments show that the catalytic activity of LSD1 is not required for gene repression and it is proposed that the regulatory role of LSD1/CoREST/HDAC complex is governed by the ability to target HDACs to genomic regions or to prevent promoter access of gene-activating complexes with H3K4 tri-methylation catalytic activity.

Acknowledgements

Naturally there are many people I wish to thank for their support and guidance during the course of my PhD. Firstly I would like to thank my supervisor, Dr Shaun Cowley, who has provided me with this opportunity to contribute to scientific knowledge. I must convey particular gratitude to Shaun for allowing me independence in exploring certain avenues of investigation as well as encouraging me to independently attend international conferences. Shaun has provided some fantastic insight and has always been available for discussion, being true to his word when insisting that he likes to keep the office door open. Oliver Dovey has been a pillar of support and inspiration over the last 4 years. We embarked on our PhD studies around the same time, as the lab was just establishing itself following Shaun's arrival in Leicester. Oliver's thorough and professional attitude, combined with a realistic view of day to day life, has kept me motivated throughout. He is beginning this writing up process as I finish and I wish him all the best. Overall, being a part of this small research team of three ('The HDAC Army') has been a very rewarding experience.

My mum, dad and sister have been unceasingly supportive; so I thank them for everything they have done. I thank Vidya Ramesh for her love and comfort over last few years, especially during the writing-up months. Alistair Ray has been a common fixture in all of my residences in Leicester and provided the comedic antidote to the occasional struggles in scientific research. Cheers Ali! I must also thank numerous other friends I have made during the course of my studies; in the workplace, on the cricket pitch and on the squash courts. I am also very grateful for the academic input of Professors' Ian Eperon and John Schwabe, who have seen me through the PhD process as members of my thesis committee. Jivan Rees provided helped with proof-reading, for which I am grateful. Finally I must acknowledge the guitar-work of Alexi Laiho, which has provided the backing soundtrack each day of writing this thesis.

Contents

Chapter 1 Introduction 12
1.1 Chromatin 12
1.2 Histone modifications 15
1.3 Lysine methylation 19
1.3.1 H3K4 methylation 21
1.3.2 H3K27 methylation 22
1.3.3 H3K9 methylation 25
1.3.4 H3K36 methylation 27
1.3.5 H4K20 methylation 28
1.4 Lysine demethylases (KDMs) 29
1.4.1 Identification of KDMs 29
1.4.2 Lysine-specific demethylase 1 (LSD1/KDM1A) 34
1.4.2.1 Discovery 34
1.4.2.2 LSD1 knockout studies 38
1.4.2.3 LSD1/CoREST function in transcriptional regulation 39
1.4.2.4 LSD1 function in other complexes 41
1.4.2.5 Non-histone targets of LSD1 42
1.5 Histone acetylation 44
1.5.1 Effects of acetylation 44
1.5.2 Histone Deacetylases 46
1.6 Class I HDAC repressor complexes 50
1.6.1 Sin3 complex 50
1.6.2 NuRD complexes 52
1.6.3 CoREST complex 54
1.7 Crosstalk of histone modifications 57
1.8 Mouse embryonic stem cells 60
1.8.1 Origins and applications 60
1.8.2 Maintenance of mouse ES cell pluripotency 62
1.8.3 Core pluripotency factor network: Oct4, Nanog and Sox2 64
1.8.4 An extended pluripotency regulatory network 66
1.8.5 Molecular mechanisms in pre-gastrulation embryonic development 68

1.8.6 *In vitro* differentiation of ES cells 70
1.8.7 Mesoderm development 74
1.9 Chromatin state of pluripotent and differentiated ES cells 77
1.9.1 ES cell chromatin state 77
1.9.2 Bivalent domains 78
1.9.3 Histone modification change upon ES cell differentiation 81
Chapter 2 Materials and Methods 86
2.1 Chemicals and reagents 86
2.2 Generation of LSD1 knock out mouse 86
2.3 Growth and maintenance of mouse ES cells 87
2.3.1 Culture of ES cells 87
2.3.2 Passage of ES cells by trypsinisation 87
2.3.3 Long term storage of ES cells 88
2.3.3.1 Freezing in cryovials 88
2.3.3.2 Freezing in 96-well plates 88
2.3.4 Revival of cells from frozen aliquots 89
2.3.5 Extraction of DNA from ES cells 89
2.3.5.1 Extraction in from cells in 96-well plates 89
2.3.5.2 Extraction from cell pellets 90
2.3.6 Extraction of RNA from ES cells and Embryoid bodies (EBs) 90
2.3.7 Media and reagents used for ES cells and EB manipulations 91
2.4 Polymerase Chain Reaction (PCR) 94
2.5 Transfection of ES cells 95
2.5.1 Transfection of ES cells by electroporation 95
2.5.2 Transfection of ES cells by lipofection 95
2.6 Generation of conditional LSD1 knock-out ES cell lines 96
2.6.1 pCAGGs-Flpe vector transfection 96
2.6.2 ES cell colony screening 96
2.6.2.1 Targeted ES cell colony growth and colony picking 96
2.6.2.2 'HygΔTK' cassette-removed ES cell growth and colony picking 97
2.6.3 Deletion of exon 3 ($\Delta 3$) from the targeted allele 97
2.6.4 Genotyping of WT, Lox and Δ3 alleles by PCR 98
2.6.5 Southern blotting to identify allelic genotypes 98

2.6.5.1 Southern Blotting 98
2.6.5.2 Strategy for identification of the *Lsd1* targeted clones 99
2.6.5.3 Strategy for identification of '*HygΔTK*' cassette-removed clones 99
2.6.5.4 Strategy for identification of deletion of exon 3 100
2.6.5.5 Agarose gel electrophoresis for Southern blotting 100
2.6.5.6 DNA Transfer onto the nylon membrane 101
2.6.5.7 DNA Probe labelling 101
2.6.5.8 Hybridisation, washing and developing of the membrane 102
2.6.6 Analysis of LSD1 protein deletion 102
2.6.7 Growth curve analysis of ES cells 102
2.7 DNA methylation analysis by Southern Blot 104
2.7.1 Restriction digestion and gel electrophoresis 104
2.8 Generation of *Lsd1*$^{Lox/\Delta 3}$ Mouse Embryonic Fibroblasts (MEFs) 105
2.9 ES cell *in vitro* differentiation analysis 106
2.9.1 Alkaline Phosphatase and Colony Formation Assays 106
2.9.2 Differentiation of ES cells as Embryoid Bodies 107
2.9.3 Differentiation with Retinoic Acid 107
2.9.4 Differentiation in N2B27 media 108
2.10 Flow Cytometry 109
2.10.1 Cell cycle analysis by propidium iodide (PI) staining 109
2.10.2 GFP analysis 109
2.11 Protein and enzymatic analysis 110
2.11.1 Immunoblotting 110
2.11.2 Immunoprecipitation 110
2.11.3 In-House Histone Deacetylase assay 111
2.11.4 Histone extraction and modification analysis 112
2.11.5 Protein stability assay 113
2.11.6 Histone demethylase assay 113
2.12 Reverse Transcription, Microarray Hybridisation and Quantitative Real-Time PCR 114
2.12.1 Reverse transcription 114
2.12.2 Illumina Microarray 114
2.12.2.1 Array hybridisation 114

2.12.2.2 Illumina microarray quality control 116
2.12.2.3 Analysis of microarray hybridisation 116
2.12.3 Quantitative Realtime PCR (qRT-PCR) for gene expression analyses..... 117
2.13 Chromatin Immunoprecipitation..... 118
2.13.1 Crosslinking of cells for chromatin immunoprecipitation 118
2.13.1.1 Double crosslinking 118
2.13.1.2 Single crosslinking 119
2.13.1.3 Cell extract preparation 119
2.13.2 Sonication of cells using the Diagenode Bioruptor 200 119
2.13.3 Immunoprecipitation..... 120
2.13.4 Washing and processing of immunoprecipitated material 121
2.13.4.1 Washing and crosslink reversal..... 121
2.13.4.2 Digestion of protein and RNA and DNA purification 121
2.13.5 Buffers used in ChIP..... 122
2.13.6 PCR validation of histone antibodies for ChIP..... 122
2.13.7 Validation of ChIP primers..... 123
2.13.8 Quantitative RT-PCR for ChIP 124
2.14 Molecular Biology and Engineering of DNA constructs 126
2.14.1 Bacterial cultures..... 126
2.14.2 Storage and revival of bacterial strains 126
2.14.3 Culturing bacterial cells for miniprep and maxiprep..... 127
2.14.4 Plasmid purification from bacteria..... 127
2.14.5 Generation of EGFP-LSD1 fusions by PROTEX cloning service 127
2.14.6 Amplification of large regions by PCR 128
2.14.7 In-Fusion^{TM} advanced PCR cloning 129
2.14.8 Transformation of In-Fusion^{TM} cloned plasmid into bacterial cells..... 130
2.14.9 PCR screening of transformed bacteria..... 131
Chapter 3 Generation of Conditional LSD1 Knockout Mouse Embryonic Stem Cells and Examination of Growth and *In Vitro* Differentiation Potential..... 132
3.1 Introduction 132
3.2 Results 138
3.2.1 Generation of conditional LSD1 knockout ES cell lines 138
3.2.1.1 Removal of the HygΔTK selection cassette from Lsd1$^{Lox\text{-}Hyg\Delta TK/\Delta 3}$ ES cells141

3.2.1.2 Deletion of exon 3 from Lsd1$^{Lox/\Delta 3}$ ES cells 144
3.2.1.3 Deletion of LSD1 protein 147
3.2.2 Generation of LSD1-null MEFs 150
3.2.3 Analysis of undifferentiated LSD1 knockout ES cells 153
3.2.4 *In vitro* differentiation analysis of LSD1 knockout ES cells 159
3.3 Conclusions 169
Chapter 4 Understanding the role of LSD1 in embryonic gene regulation 170
4.1 Introduction 170
4.2 Results 173
4.2.1 Loss of LSD1 causes a reduction in the level of CoREST 173
4.2.2 Loss of LSD1 results in increased global histone acetylation 180
4.2.3 LSD1 regulates the embryonic transcriptome 183
4.2.4 Chromatin state changes in up-regulated genes 193
4.2.5 *Brachyury* is a direct target of LSD1 197
4.2.6 *Brachyury* is up-regulated in E6.5 *Lsd1*$^{\beta\text{-}geo/\beta\text{-}geo}$ embryos 205
4.3 Conclusions 207
Chapter 5 Investigating the requirement for the catalytic activity of LSD1 208
5.1 Introduction 208
5.2 Results 210
5.2.1 Generation of LSD1 expression constructs 210
5.2.2 Expression of pCAGGS EGFP-LSD1 constructs in ES cells 216
5.2.3 Analysis of recombinant LSD1 protein interactions 218
5.2.4 Analysis of the ability for re-expressed wild-type LSD1 to rescue CoREST levels and gene expression 220
5.2.5 LSD1 demethylase activity is not required for gene repression 223
5.3 Conclusions 229
Chapter 6 Discussion 230
6.1 An essential role for LSD1 in early embryonic development 230
6.2 LSD1 regulates the transcriptome during embryonic development 236
6.3 LSD1 knockout ES cells have reduced CoREST levels and increased histone acetylation 243
6.4 Catalytic activity of LSD1 is dispensable for gene regulation 247
6.5 Concluding Remarks 252

Appendices.....254
Table A1 List of antibodies used in the study.....254
Table A2 List of primers used quantitative RT-PCR.....255
Table A3 List of genes that are de-regulated >1.4-fold in LSD1 knockout ES cells.....258
Bibliography.....266

List of Abbreviations

ADP	adenosine diphosphate
ATP	adenosine triphosphate
bME	betamercaptoethanol
bp	base pair
BSA	bovine serum albumin
cDNA	complementary DNA
ChIP	chromatin immunoprecipitation
CoREST	co-repressor of REST
Ct	cycle threshold
°C	degrees centigrade
dpc	days post conception
dCTP	2'-deoxycytosine 5'-triphosphate
DMSO	dimethylsulphoxide
DNA	deoxyribose nucleic acid
DNMT	DNA methyltransferase
dNTPs	2'-deoxynucleotide 5'-triphosphate
EB	embryoid body
EDTA	ethylenediaminetetraacetic acid
ES cell	(mouse) embryonic stem cell
EtBr	ethidium bromide
FCS	foetal calf serum

G418	geneticin
HAT	histone acetyltransferase
HCP	high CpG content promoter
HDAC	histone deacetylase
hr	hours
ICM	inner cell mass
IP	immunoprecipitation
kb	kilobase
KDa	kilodalton
KDM	lysine demethylase
KMT	lysine methyltransferase
KO	knockout
LCP	low CpG content promoter
LSD1	Lysine-specific demethylase 1
M	molar
MEF	mouse embryonic fibroblast
mM	millimolar
μM	micromolar
mRNA	messenger RNA
ng	nanogram
NMD	nonsense mediated decay
NPC	neural progenitor cells
NRSF	neuronal restrictive silencing factor
O/N	overnight
PBS	phosphate-buffered saline
PcG	polycomb group
PCR	polymerase chain reaction
pmol	picomol
Pol II	DNA-dependent RNA polymerase II

PRC	polycomb repressor complex
PRE	polycomb response element
PTM	posttranslational modification
qRT-PCR	quantitative real-time PCR
REST	RE1 silencing transcription factor
RNA	ribose nucleic acid
rRNA	ribosomal RNA
SAHA	suberoylanilade hydroxamic acid
S.E.M	standard error of the mean
ssRNA	single stranded RNA
TE	Tris-EDTA
TRE	Trithorax response element
TrxG	Trithorax Group
TSA	Trichostatin A
TSS	transcriptional start site
V	volt
v/v	volume per volume
w/v	weight per volume
WT	wild-type

1 Introduction

1.1 Chromatin

The function of a cell is defined by its ability to utilise the genetic material within the nucleus. The genome is the entirety of the DNA sequence and genes within the genome must be expressed to produce proteins that are crucial for cellular processes. The regulation of gene expression is highly complex and overall it may be controlled by many factors, including extracellular stimuli, intracellular signalling, protein access to DNA and transcriptional mechanisms. Gene expression occurs in a chromatin environment and therefore the packaging of the genome into chromatin is now known to be a critical feature of gene regulation mechanisms.

Histones are one of the oldest families of proteins known, first being described by Albrecht Kossel in 1884 (Kossel 1884). Kossel showed that a substance called nuclein (which was discovered by the Swiss biochemist Johann Meischer several years earlier and thought to be a phosphorous-rich protein) was composed of a non-protein and protein fraction. Ultimately histones were characterised as basic proteins that combine with nucleic acids to form chromatin. The formation of chromatin is not only a way to package DNA to form the chromosomes, but it is also fundamental to the regulation of gene expression (reviewed in Zhang and Reinberg 2001). Cellular state is therefore closely related to 'chromatin state' and this regulation is accomplished by many interrelated mechanisms including covalent modifications of histone tails, DNA

methylation at CpG residues, incorporation of histone variants and chromatin remodelling events (reviewed in Surani *et al*., 2007, Kouzarides 2007).

The fundamental subunit of chromatin, the nucleosome, is composed of approximately 146bp of DNA wrapped 1.75 turns around an octameric complex of four globular core histones H2A, H2B, H3 and H4 (Kornberg 1974). Original nucleosome studies identified a $(H3)_2(H4)_2$ tetramer with two (H2A) (H2B) hetero-dimers binding either side (Kornberg 1974). This repeat unit was discovered through micrococcal nuclease digestion of unwrapped 'linker' DNA and electron microscopy (Hewish & Burgoyne 1973, Noll 1974, Finch *et al*., 1975, Oudet *et al*., 1975). Roughly 50bp of DNA acts as a linker sequence between the core histone octamers to organise nucleosomes into the polynuclesome 11nm-fibre; or the 'beads on a string' architecture (Oudet *et al*. 1975, Turner 2005). Linker DNA is accessible to 'non-core' histones and other proteins, which facilitate further packaging into 30nm-fibres with six nucleosomes per turn in a spiral or solenoid arrangement (reviewed in Kornberg & Lorch 1999, Hayes & Hansen 2001). This architecture ultimately lays the foundation for the formation of chromosomes, resulting in an overall 10,000-fold packaging of DNA. This packaging is repressive towards processes requiring access of proteins to the DNA, therefore the unfolding of the 30nm-fibre to the 11nm-fibre and the further remodelling of polynucleosomes is required to generate templates for transcription (reviewed in Zhang & Reinberg 2001). As a result, signals that mediate transcriptional responses must integrate mechanisms to overcome nucleosomal repression before they can influence the core transcriptional machinery (Wolffe 1998). Seminal studies

revealed protein complexes capable of altering chromatin structure either by utilising the energy derived from ATP hydrolysis to mobilise the nucleosome or by covalently modifying the histone polypeptides (Pazin & Kadonaga 1997, Hassig *et al*. 1998, Kadosh & Struhl 1998, Kuo *et al.* 1998, Kingston & Narlikar 1999, Sterner & Berger 2000, Viganli *et al*. 2000, reviewed in Wu & Grunstein 2000, Kuzmichev & Reinberg 2001). These studies collectively demonstrated that gene expression was regulated by affecting the dynamics of chromatin structure and modulating DNA accessibility. A variety in the extent of chromatin packaging is therefore observed in interphase cell nuclei, which is representative of the different functional requirements for regions of the genome.

1.2 Histone modifications

In the mid-1960s, before the fundamental subunit of chromatin was discovered, histone proteins were shown to be subject to multiple post-translational modifications (PTMs) (Allfrey *et al*. 1964). Today, the most important branch of chromatin biology relates to a striking feature of histones, namely the large number and type of modified residues found on their N-terminal tails. It is now known that there are at least eight distinct types of modifications found on histones, including acetylation, methylation, phosphorylation, ubiquitination, sumoylation, ADP ribosylation, deimination and proline isomerisation; with all of these modifications regulating transcription in some way (reviewed in Kouzarides 2007). A vast array of enzymes that catalyse the addition and removal of these modifications have hence been characterised as regulators of transcription (reviewed in Grunstein 1997, Cheung *et al.,* 2000, Kouzarides 2007, Zhang & Reinberg 2001, Turner 2002). The result of these studies provided a new layer of understanding of gene regulation, especially concerning the role of chromatin as a regulatory element rather than a passive structural scaffold (Schreiber & Bernstein 2002). Modified histones behave as regulatory molecules by providing docking sites for proteins that can initiate molecular processes involving DNA. Histone modifying enzymes interplay with transcription factors at the pinnacle of signal transduction pathways, to control the recruitment or exclusion of additional factors to alter chromatin structure and facilitate the DNA-associated function of transcription factors (Bannister *et al.* 2001, Lachner *et al*. 2001, Carmen *et al.* 2002, Nishioka *et al.* 2002, Zeng & Zhou 2002).

The unstructured N-terminal tails of histone H3 and H4 tails, which are external to the core structure of the nucleosome (Luger *et al.* 1997), are the most extensively modified region of the core histone octamer (Zhang & Reinberg 2001, Lachner *et al.* 2003) (Figure 1.1). Residues on the tails of H2A and H2B tails as well as some residues contained within the structured protein regions can be manipulated too. The identification of a multitude of histone modifications, led to the proposal that they constitute a 'histone code' that predicts the transcriptional state of a gene (Strahl & Allis 2000). This stated that "multiple histone modifications, acting in a combinatorial or sequential fashion on one or multiple histone tails, specify unique downstream functions". Recently though, layers of complexity have been added to the understandings of signalling through chromatin, which has revealed an intriguing language of histone crosstalk, as opposed to a strict code (Lee *et al.* 2010). The functional complexity is increased due to this interplay between various modifications.

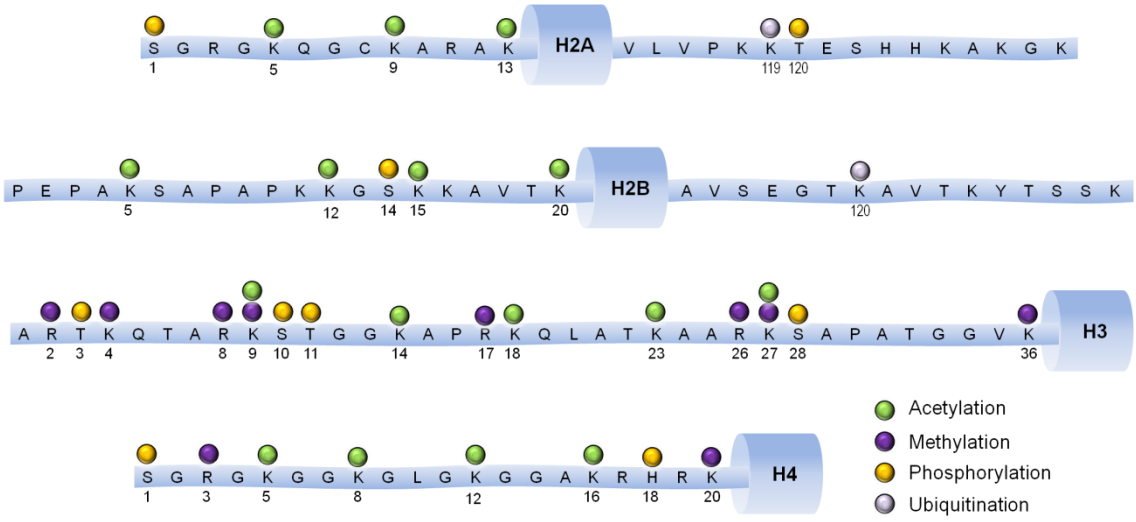

Figure 1.1. Post translational modifications of core histone tail. Specific amino acids within the unstructured N-terminal tails of histone H2A, H2B, H3 and H4 are subject to various types of post-translational modification. Acetylation, methylation, phosphorylaion and ubiquitination are the most extensively studied modifications. The globular core of these histones may also be modified, which is not illustrated in this figure.

Covalent modifications to histones have been closely linked to transcriptional regulation and are required for many biological processes, including the differentiation of pluripotent stem cells into specific tissue lineages (Dodge *et al.* 2004, Margueron *et al.* 2005, Lin & Dent 2006, Torres-Padilla *et al.* 2007), which is the process of primary interest of this thesis. Histone modifications have been implicated in a variety of cellular process in addition to transcriptional regulation, including splicing (Spies *et al.* 2009, Luco *et al.* 2010), DNA replication (Goren *et al.* 2008, Lande-Diner *et al.* 2009), DNA repair (Ikura *et al.* 2000, Stucki & Jackson 2004), recombination during meiosis (Borde *et al.* 2009, Buard *et al.* 2009) and somatic recombination in lymphocytes (Giambra *et al.* 2008). The inability to maintain specific histone modifications has also been identified as a common hallmark of human cancer (Fraga *et al.* 2005). Modifications primarily regulate the recruitment of proteins to genomic sites by providing docking sites for proteins (Figure 1.2). These proteins will often be transcriptional co-activators or co-repressors, which themselves can further recruit factors involved in transcriptional regulation. Thus, histone modifications and the protein complexes they recruit modulate the accessibility of the genetic information and therefore the biological role played by the DNA sequence (reviewed in Zhang & Reinberg 2001, Kouzarides 2007). Notably, there is a correlation between transcriptionally 'active' chromatin marks and CpG islands (CGIs), as well as between repressive marks and highly conserved non-coding regions of the genome (Bernstein *et al.* 2006a, Barski *et al.* 2007, Tanay *et al.* 2007). Mutual exclusivity of different modifications also emphasises their functional importance, where active histone marks can inhibit the deposition of repressive marks and vice versa (Rea *et al.* 2000, Nishioka *et al.* 2002). Lysine methylation and acetylation will be primarily discussed as

the focus of my research is the role of proteins involved in removing these modifications.

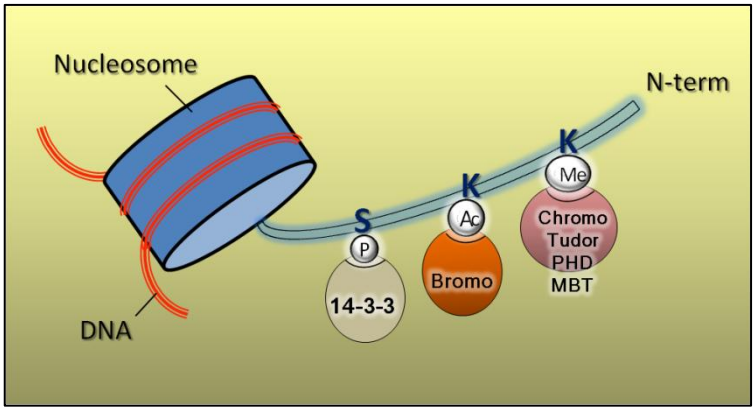

Figure 1.2 Recruitment of protein domains to histone tails. The domains used by various proteins for recognition of phosphorylated serines, acetylated lysines, or methylated lysines present on the unstructured N-terminal tails of core histone proteins.

1.3 Lysine methylation

Histones can be methylated on lysine and arginine residues of histone tails (Shilatifard 2006, Kouzarides 2007). Lysines can be methylated on lysines 4, 9, 27, 36 and 79 of histone H3 and lysine 20 of histone H4. Many studies have highlighted the importance of histone methylation on specific lysines with respect to gene regulation. The consequence of lysine methylation on gene expression can be either positive or negative, depending on the context of the particular lysine residue and the number of methyl moieties added (Jenuwein & Allis 2001, Kouzarides 2007). Importantly, methylation does not change the charge of the amino acid, and the effects of methylation state are manifested through recognition of the methyl moieties by other factors. Thus, four states of lysine residues, unmodified (me0), mono-methylated (me1), di-methylated (me2) and tri-methylated (me3), are interpreted by subsequent binding of chromatin-associated proteins with a cognate chromodomain, PHD finger or TUDOR domain to dictate downstream signalling from chromatin (Ruthenburg *et al.* 2007, Taverna *et al.* 2007) (Figure 1.2). For example, the PHD domain of the DNA methyltransferase, DNMT3L recognises histone H3 tails that are unmethylated at K4 and induces de novo DNA methylation by recruitment of DNMT3A (Ooi *et al.* 2007). In this instance, H3K4me0 is a signalling molecule to dictate DNA methylation. Methylation on a particular residue can stimulate or prevent methylation on other residues (Nishikawa *et al.* 1998), with distinct site-specific histone methylation patterns defining euchromatic and heterochromatic chromosomal domains (Noma *et al*. 2001). Studies have also revealed extensive crosstalk with histone acetylation, phosphorylation and ubiquitination (Noma *et* al. 2001, Nishioka *et al.* 2002).

Lysine methylation *in vivo* is controlled by the opposing activities of lysine methyltransferases (KMTs) and lysine demethylases (KDMs). The machinery and sites of histone methylation are, for the most part, conserved from yeast to human. Of all the enzymes that modify histones, KMTs are the most specific. Early biochemical studies on the H3K4- and H3K9-specific KMTs, SET7 and Su39h1, respectively, indicated that the SET domain in the SET domain-containing proteins is essential for methyltransferase activity (Rea *et al.* 2000, Wang *et al.* 2001). The SET domain is found in many proteins demonstrated to mediate lysine methylation (Zhang & Reinberg 2001, Jenuwein & Allis 2001, Lachner & Jenuwein 2002). Now, three families of enzymes are known to methylate lysine residues on histones H3 and H4: the PRMT1 family, the SET domain-containing protein family, and the non-SET domain-containing proteins DOT1 and DOT1L (reviewed in Martin & Zhang 2005).

In vertebrates, the MLL family of proteins (MLL1-5), homologous to the yeast Set1 family and *Drosophila trithorax*, are present in protein complexes that catalyse H3K4 methylation (Milne *et al.* 2002, Hughes *et al.* 2004). These complexes are similar to Set1-containing COMPASS (COMplex of Protein ASsociated with Set1) (Miller *et al.* 2001). KMTs specific to H4K9me3 in mammals are Suv39h1, Suv39h2, G9a, GLP, ESET and RIZ1 (Rea *et al.* 2000, Tachibana *et al.* 2001, Shilatifard 2006). These enzymes catalyse this repression-associated methylation of H3K9 and some interact with other factors involved in transcriptional repression and silencing such as DNA methyltransferases and heterochromatin-associated protein 1 (HP1) isoforms (Dong *et al.* 2008, Tachibana *et al.* 2008, Epsztejn-Litman *et al.* 2008). The SET domain-

containing EZH2 protein catalyses H3K27 di- and tri-methylation (O'Carroll *et al.* 2001), NSD1 and SMYD2 (homologous to yeast Set2) methylate H3K36 (Brown *et al.* 2006) and DOT1 methylates H3K79 (van Leeuwen *et* al. 2002). PR-Set7 (also known as Set8), Suv4-20h1 and Suv4-20h2 catalyse histone H4K20 mono-, di- and tri-methylation respectively (Schotta *et al.* 2004, Xiao *et al.* 2005). Crosstalk between methyltransferases and demethylases also occurs to synchronise the deposition of active marks with the removal of repressive histone modifications (Issaeva *et al.* 2007). One of the MLL enzymes, MLL2, can co-ordinate its activity with a H3K27-specific demethylase, UTX to reduce the antagonist effects of H3K27 methylation on H3K4 methylation during cell differentiation.

1.3.1 H3K4 methylation

Trimethylation of K4 on histone H3 (H3K4me3) is associated with transcriptionally active regions (Noma *et al*. 2001, Litt *et al.* 2001, Santos-Rosa *et al.* 2002, Schneider *et al.* 2004). H3K4me3 localises primarily to the 5' end of active genes, correlating with localisation of the initiated form of RNA polymerase II (phosphorylated at serine 5 of its C-terminal domain) (Barski *et al.* 2007). The deposition of H3K4me3 precedes the establishment of initiated RNA polymerase II machinery though, in yeast, Set1 interacts with RNA polymerase II and elongation machinery to mediate the transition between intitiation and elongastion and to maintain H3K4 hypermethylation, in order to provide a molecular memory of recent transcriptional activity (Ng *et al.* 2003). The H3K4me2 modification is also considered as an active mark, correlating positively with gene expression and found to peak just downstream

of the TSS (Barski *et al.* 2007). Di- and tri-methylation are thought to co-exist at promoters of active genes, though in some cell types a subset of H3K4me2+/H3K4me3- genes have been identified (Orford *et al.* 2008). However, ChIP-on-chip and ChIP-seq datasets from Orford *et al.* and Meissner *et al.* indicate that, in mouse embryonic stem (ES) cells, the vast majority of promoters positive for H3K4me3 are also positive for H3K4me2. Mono-methylation of H3K4 is associated with enhancer elements of genes and is linked to both transcriptional activation and repression (Barski *et al.* 2007, Heintzman *et al.* 2007, Heintzman *et al.* 2009). Several factors involved in active transcription have been reported to interact with di- and tri-methylated H3K4, including the ATP-dependent chromatin remodelers CHD1 and NURF, which bind through their chromodomains (Sims & Reinberg 2006, Wysocka *et al.* 2006), as well as the H3K9me3/K36me3 demethylase, JMJD2A, which binds through its tandem TUDOR domains, and removes the repressive H3K9 methylation mark (Huang *et al.* 2006, Kim *et al*. 2006). Crosstalk with histone deacetylation can be co-ordinated by H3K4me2/me3, as the Sin3A/HDAC-associated protein ING2 can interact with high affinity to H3K4me3 through its PHD finger (Shi *et al.* 2006). The association of HDACs with actively transcribed genes is a phenomenon described by Keji Zhao lab and will be discussed further in 1.5 (Wang *et al*. 2009b, Dovey *et al*. 2010a).

1.3.2 H3K27 methylation

H3K27 methylation is a chromatin mark associated with gene repression and silencing (Turner 2002, Lachner & Jenuwein 2002, Boyer *et al.* 2006, Lee *et al.* 2006, Roh *et al.* 2006, Barski *et al.* 2007, Kouzarides 2007). H3K27me2/me3 has similar distributions at

silent gene promoters, though H3K27me1 signals have actually been seen higher at active promoters than silent promoters (Barski *et al.* 2007). This modification was originally implicated in silencing of *HOX* gene expression, X chromosome inactivation and genomic imprinting (Schuettengruber *et al.* 2007). Research on *HOX* genes ultimately revealed that the H3K4me3 and H3K27me3 states impose an inherited state of gene regulation that is independent of the genetic information encoded by the DNA itself. This is achieved through the recruitment of the Trithorax Group (TrxG) and Polycomb Group (PcG) complexes, which can maintain an active or repressive expression state of a gene after the initial transcriptional regulators disappear (originally identified in *D. Melanogaster*; review in Schuettengruber *et al.* 2007). The presence of these modifications is therefore a form of epigenetic cellular memory.

Distinct classes of TrxG and PcG complexes contain KMTs and KDMs specific to H3K4 and H3K27. Work in *Drosophila* led to the identification of DNA regulatory elements, known as TrxG and PcG response elements (TREs and PREs), which recruit these TrxG and PcG factors, respectively, to chromatin. The deposition of histone marks then mediates recruitment of other TrxG and PcG complexes to their chromatin targets, which serve as effectors of the transcriptional state (Figure 1.3). In vertebrates, one class of TrxG complexes includes the SET domain-containing factor MLL, which can methylate H3K4 (Milne *et al.* 2002). A second class of TrxG factors includes components of ATP-dependent chromatin remodelling complexes like SWI/SNF and NURF, though the chromatin recruitment mechanisms are largely unknown (Hughes *et al.* 2004, Wysocka *et al*. 2006). PcG complexes have been extensively investigated in

recent years. Two PcG complexes exist: PRC2 and PRC1; the former being a 'writer' of H3K27 methylation, through the EZH2 KMT, and the latter being a 'reader' of this modification, through specific recognition of H3K27me3 by chromodomain-containing proteins within the complex (Fischle *et al.* 2003). The deletion of the EZH2, SUZ12 or EED component of PRC2 causes embryonic lethality at E7.5 due to defects in gastrulation (O' Carroll *et al.* 2001, Pasini *et al*. 2004, Cao & Zhang 2004, Montgomery *et al*. 2005, Boyer *et al.* 2006). Most notably, the deletion of these components results in inappropriate expression of PcG target genes and unscheduled differentiation (Pasini *et al*. 2004, Boyer *et al*. 2006, Lee *et al*. 2006, Azuara et al. 2006, Agger et al. 2007, Shen *et al*. 2008b); this confirms that H3K27 methylation is essential to repress developmental regulators in ES cells and maintain the pluriopotent state (Boyer *et al*. 2006) (1.9). The central components of PRC1 are Cbx, Rnf2 (Ring1) and Bmi1 proteins (Schuettengruber *et al*. 2007). PRC1 is thought to be subservient to PRC2, manifested through chromodomain recognition of H3K27me3. This is supported by the knockdown of EZH2 resulting in significant mis-localisation of the PRC1 complex component Bmi1 (Hernandez-Munoz *et al*. 2005). The chromodomain-containing protein, Cbx, binds the H3K27me3 modification catalysed by EZH2 (Bernstein *et al*. 2006b). Rnf2 has a RING motif that ubiquitinates H2A119 to prevent the binding of the transcription elongation complex, FACT, thus manifesting a state of transcriptional repression (Stock *et al*. 2007, Zhou *et al*. 2008). Balance of H3K4me3 and H3K27me3 is further regulated by lysine demethylation (1.4). The histone H3K27-specific demethylases (UTX and JMJD3), which remove H3K27me3, interact with the H3K4-specific methyltransferase (MLL2) of TrxG complex at the *Hoxb1* promoter upon

retinoic acid-induced differentiation to synchronise changes in chromatin state (Agger *et al*. 2007, Lan *et al*. 2007, Lee *et al*. 2007b, De Santa *et al*. 2007).

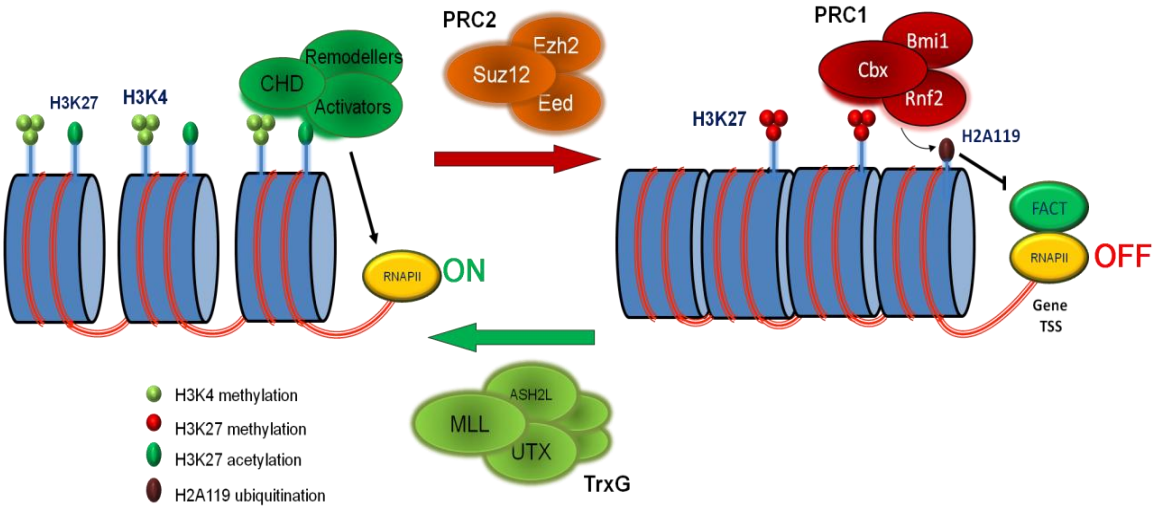

Figure 1.3 Antagonistic roles of TrxG and PcG complexes. Two protein complexes modulate the levels of H3K4 and H4K27 trimethylation at gene promoters. MLL and EZH2 methylate H3K4 and H3K27, respectively via SET domains. The methylation state of these sites will determine the expressional fate of genes due to recruitment of further proteins. The chromodomain of CHD1 recognises H3K4me3 for transcriptional activator and chromatin remodeller recruitment. The chromodomain of Cbx recognises H3K27me3 and brings the ubiquitin ligase Rnf2/Ring1 to modify H2AK119. The ubiquitination of this residue physically blocks the binding of the transcriptional elongation protein, FACT.

1.3.3 H3K9 methylation

Trimethylation of K9 of histone H3 (H3K9me3) is generally associated with the formation of constitutive or facultative heterochromatin (Rea *et al*. 2000, Nakayam *et al*. 2001, Nakayam *et al*. 2001, Peters *et al*. 2002), involving the recruitment of HP1 to the promoter of repressed genes and subsequent association of co-repressors such as the Retinoblastoma (Rb) proteins (Lachner *et al*. 2001) and KAP1. The binding of the

HP1α and HP1β protein has a key role in heterochromatinisation (Bannister *et al*. 2001, Lachner *et al*. 2001). This processes also involves the docking of *de novo* methyltransferases, DNMT3a/3b, via HP1 for effective silencing of genomic regions (Feldman *et al.* 2006). This is also important in euchromatic gene repression, for example E-cadherin and E- and A-type cyclin genes (Shi *et al*. 2003, Nielsen *et al*. 2001). Suv39h KMTs, that apply the H3K9me3 modification, contain a chromodomain that bind this modification and therefore these proteins have the potential to cause the physical spread of the H3K9me3 modification across chromatin regions through a self-propagating effect of recognition and catalysis (Lachner *et al*. 2001). The H3K9me3 modification is rarely found in ES cell/early embryonic chromatin, but becomes abundant as cells differentiate, functioning to restrict patterns of gene expression and reduce the rate of cell division in differentiating embryos (for review see (Bhaumik *et al*. 2007). Notably, an accumulation H3K9 methylation and subsequent de novo DNA methylation at the *Oct4* locus is essential for repression of this pluripotency gene in differentiating ES cells and embryonic development (Feldman *et al*. 2006, Epsztejn-Litman *et al.* 2008). In this situation, an increase in H3K9 methylation is accompanied by loss of H3K4 methylation. This dogma—that H3K9 methylation and HP1 recruitment is always repressive—has been challenged though, with the identification of HP1γ association with H3K9me3 at the promoter and body of actively transcribed genes (Vakoc *et al.* 2005).

1.3.4 H3K36 methylation

H3K36 methylation is catalysed by SET2, NSD1 and SMYD2, which are SET/MYND domain-containing KMTs and homologous of yeast Set2. This modification is implicated in repression and activation of transcription as well as linking transcription with splicing (Carrozza *et al.* 2005, Brown *et al.* 2006, Kolasinska-Zwierz *et al.* 2009, Luco *et al.* 2010). The H3K36me3 modification is tightly associated with the serine 2-phosphorylated elongating form of RNA polymerase II and is highly enriched within transcribed regions of active genes (Bannister *et al.* 2005, Barski *et al.* 2007). Due to the association of H3K36 methylation with actively transcribed genes, H3K36me3 signals are elevated sharply after TSSs in active genes following the peak of H3K4me3 around the promoter (Barski *et al.* 2007). This modification is primarily implicated in recruiting other factors that regulate chromatin structure and is effectively a repression-inducing modification due to its coupling to histone deacetylation. H3K36me2/me3 modifications play a key role in suppressing intragenic transcription initiation through recruitment of Rpd3S complex (a Sin3A-HDAC complex homologue) via Eaf3 (an MRG15 homologue) in order to deacetylate histones H3 and H4 and re-compact chromatin in the wake of the elongating polymerase (Carrozza *et al.* 2005, Joshi & Struhl 2005, Keogh *et al.* 2005, Brown *et al.* 2006, Li *et al.* 2009). In contrast, H3K36 methylation in yeast can prevent binding of the Sir2 deacetylase and the associated formation of heterochromatin, in order to prevent global repression in regions to be actively transcribed (Brown *et al*. 2006). H3K36me3 has also been implicated in regulation of pre-mRNA splicing by recruiting PTB via MRG15 (Luco *et al*. 2010).

1.3.5 H4K20 methylation

The tri-methylation of H4K20 by Suv4-20h2 allows the formation of heterochromatin at constitutively silenced centromeric DNA, repeat DNA regions and the inactive X chromosome. The sequential induction of H3K9 and H4K20 trimethylation is thought to index repressive chromatin domains, with the H4K20 modifications having an almost identical distribution to H3K9 modifications, respectively (Schotta *et al*. 2004, Barski *et al.* 2007). H4K20me3 and H4K20me2/1, however, have distinct distribution in the genome. Tri-methylation is enriched at pericentric heterochromatin, whereas the mono-methyl mark is dispersed in euchromatin, therefore possibly involved in gene regulation (Schotta *et al*. 2004, Kohlmaier *et al*. 2004, Talasz *et al*. 2005, Vakoc *et al*. 2006, Barski *et al.* 2007).

1.4 Lysine demethylases (KDMs)

1.4.1 Identification of KDMs

Following the discovery of KMT involvement in regulation of chromatin in 2000, the methylation modification was still considered a permanent mark and the existence of demethylases was contentious (Rea *et al*. 2000, Bannister *et al*. 2002, Kouzarides 2007). The dogma that methylation was an irreversible process was supported by early studies looking at the turnover of methyl groups in bulk histones, where the half-life of histones and methyl-lysine residues within them were the same (Byvoet *et al.* 1972, Duerre & Lee 1974). The permanent nature of this mark fitted with an understanding of the role of methylation in cellular epigenetic inheritance of transcriptionally silenced states. However, there is evidence from the 1970s that active turnover of methyl groups does take place at low but detectable levels (Borun *et al*. 1972). A hunt for a demethylase was in fact instigated over fourty-five years ago, where in 1964, Paik and co-workers published the purification of an enzyme from rat kidney capable of demethylating free mono- and di-N-methyllysine (Kim *et al.* 1964). The same group described enzymatic demethyaltion towards histones a few years later and then partially purified this enzymatic activity (Paik & Kim 1973, Paik & Kim 1974). They ultimately failed to relate this activity to a specific protein due to limitations of protein characterisation techniques in the 1970s. This early work was considered with emerging evidence from the Kouzarides lab in 2001, showing that histone methylation plays a role in dynamic regulation of gene expression, to fuel an strong arguement that enzymes that actively reverse methylation must exist (Bannister *et al*. 2002, Santos-Rosa *et al*. 2002). Numerous chemical mechanisms for

active demethylation were proposed and even monoamine oxidases had been suggested to be candidate histone demethylases (Bannister *et al.* 2002).

Eventually, the first lysine demethylase was discovered by Yang Shi and colleagues, which was named Lysine-specific demethylase 1 (LSD1/KDM1A/AOF2/BHC110) (Shi *et al*. 2004). This paved the way for characterisation of many other histone demethylases over the next few years. KDMs are now known to appear in two varieties, the amine oxidases (LSD1 and LSD2) and the far more numerous JmjC-domain (JMJD) containing hydroxylase enzymes (Cloos *et al*. 2006, Klose *et al*. 2006, Tsukada *et al*. 2006, Whetstine *et al*. 2006, Yamane *et al*. 2006; for review see Cloos *et al*. 2008). The JmjC domain is conserved from yeast to humans and belongs to the superfamily of Fe^{2+}-dependent dioxygenases. These enzymes are divided into subgroups based on their similarities within the JmjC domain. So far, seven subgroups of lysine demethylase have been shown to have activity towards histone H3 and H4 substrates (Table 1.1).

Family	Human Genes	Substrate
AOF/KDM1	LSD1 LSD2	H3K4me2/1; H3K9me2/1
JHDM1/KDM2	JHDM**1A** JHDM**1B**	H3K36me2; H3K4me3
JHDM2/KDM3	JMJD**1A** JMJD**1B** JMJD**1C**	H3K9me2
JMJD2/KDM4	JMJD**2A** JMJD**2B** JMJD**2C** JMJD**2D**	H3K9me3/2; H3K36me3/2
JARID/KDM5	JARID**1A** JARID**1B** JARID**1C** JARID**1D**	H3K4me3/2
JMJD3/KDM6	UTX UTY JMJD**3**	H3K27me3/2

Table 1.1 Lysine demethylases families, their members and substrate specificity

LSD1 has been shown to demethylate H3K4 and H3K9 (Shi *et al*. 2004, Metzger *et al*. 2005, Shi & Whetstine 2007), but can only demethylate mono- and di-methylated forms of the substrate due to the requirement of a protonatable methyl ammonium group (Forneris *et al*. 2008). Recently, LSD2 (KDM1B) was discovered and demonstrated to also demethylate H3K4me2/me1 (Karytinos *et al*. 2009). It was soon after identified as being important in establishing maternal genomic imprints (Ciccone *et al*. 2009). Yi Zhang and co-workers isolated the first JmjC domain protein, JHDM1A (KDM2A), upon purification of a H3K36 demethylase activity from cells using formaldehyde release as the readout (Tsukada *et al.* 2006). Since then, numerous JmjC enzymes have been identified that have unique histone substrates specificity,

with the ability to demethylate distinct moieties of H3K4, H3K9, H3K27 and H3K36. The JmjC-driven demethylase reaction mechanism is different to the amine oxidase, with original identification through speculation that hydroxylation of a methylated lysine residue by a JmjC protein could undergo spontaneous conversion to unmethylated lysine (Trewick *et al*. 2005). This mechanism is compatible with demethylation of mono-, di- and tri-methylated lysines; in most cases favouring a tri-methylated substrate (Couture *et al*. 2007, Ng *et al*. 2007). The reaction mechanisms of these two classes of enzyme are outlined in Figure 1.4.

As with KMTs, several KDMs appear to have an important function in ES cell self-renewal and differentiation (1.9). Demethylases specific to H3K9 (JMJD1c/JMJD2a) are activated by *Oct4* expression, in order to prevent the repression of *Nanog* and *Tcl1* in ES cells (Loh *et al*. 2007) (section 1.8). Upon ES cell differentiation, the repression of *Oct4* corresponds with loss of expression of *JMJD1a/JMJD2c*, facilitating rapid reprogramming of *Nanog* and *Tcl1* to a silent state (Loh *et al*. 2007). As mentioned, the H3K27 demethylases, UTX and JMJD3 have been shown to remove the H3K27me3 modification at *HOX* gene promoters in order to permit their activation upon differentiation (Agger *et al*. 2007, Lee *et al*. 2007b).

A Amine Oxidase reaction

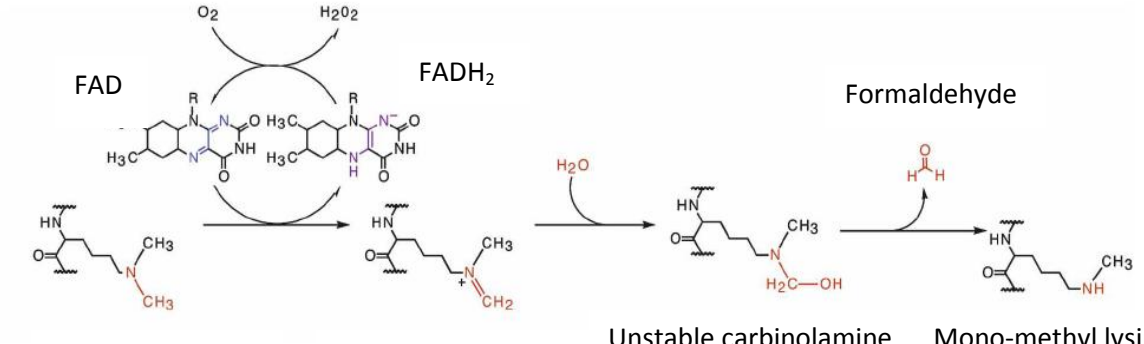

B JmjC hydroxylation reaction

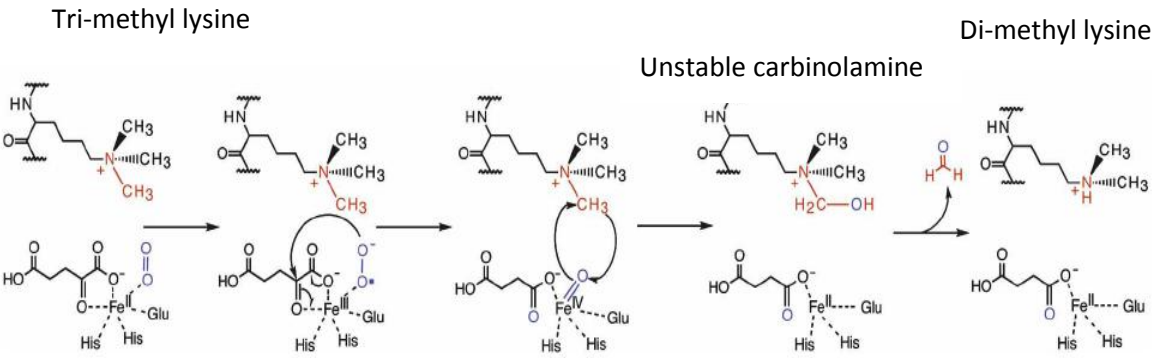

Figure 1.4 Two reaction mechanisms of lysine demethylation. (A) The amino group α-carbon bond is oxidised to produce an imine intermediate, which will spontaneously hydrolyse to form formaldehyde and a corresponding amine reside by a non-enzymatic. Substrate oxidation leads to the two electron reduction of the FAD cofactor, which is re-oxidised by molecular oxygen to form hydrogen peroxide (Binda *et al*. 2002). Protonation of the nitrogen is essential in this reaction and hence the enzyme can only demethylate mono- and di-methylated lysines. (B) Conversion of a methyl group to a hydroxyl-methyl by JmjC domain-containing enzymes occurs using of 2-oxoglutarate and Fe^{2+} as cofactors, in the presence of oxygen. Formaldehyde is then released, resulting in demethylation of the lysine.

1.4.2 Lysine-specific demethylase 1 (LSD1/KDM1A)

1.4.2.1 Discovery

Investigation of the repression of broad neurogenic transcriptional programmes, mediated by the RE1 silencing transcription factor (REST; also known as NRSF) (Schoenherr & Anderson 1995, Chong *et al*. 1995), led to the discovery of the co-repressor of REST (CoREST; also known as Rcor1), a SANT domain-containing protein that interacts with specific histone deacetylases (HDACS) (Andres *et al*. 1999, Ballas *et al*. 2001, Lunyak *et al*. 2002) (1.6.3). CoREST was subsequently found to be a component of a larger purified complex, which included carboxy-terminal binding protein (CtBP), HDACs and an uncharacterised 110kDa FAD-binding protein (BHC110), which was speculated to contribute a novel enzymatic activity (Tong *et al.* 1998, You *et al*. 2001, Humphrey *et al*. 2001, Hakimi *et al*. 2002, Shi *et al*. 2003). An enzymatic function and direct role in transcriptional repression of this novel protein was however eventually identified by Yang Shi in 2004, after recognition that the chemistry used by FAD-dependent polyamine oxidases could be used to catalyse lysine demethylation within histones (Shi *et al*. 2004). It has been found to specifically demethylate mono- and dimethylated H3K4, but not trimethylated H3K4 *in vitro* (Shi *et al*. 2004, Lee *et al*. 2005, Forneris *et al*. 2007, Rudolph *et al*. 2007). However, reports of alternative substrate, H3K9me2/me1, have been been forthcoming (Metzger *et al*. 2005, Wissmann *et al.* 2007, Garcia-Bassets *et al*. 2007, Wang *et al*. 2007). Overlall, it has been demonstrated that the nature of associating proteins dictates the H3K4 or H3K9 substrate preference of LSD1.

The dispute in substrate specificity has largely been resolved through structural studies (Forneris *et al*. 2006, Yang *et al*. 2007). Structural data has shown there are strict steric constraints that support specificity of LSD1 towards the H3K4 residue (Yang *et al*. 2007). Structural determination of LSD1 bound to histone H3 peptides initially proved difficult due to a weak binding affinity (mM range *K*m) (Forneris *et al*. 2005b). A mechanism-based approach using peptide inhibitors provided solutions and ultimately a stable LSD1-H3 peptide complex was produced, in which the substrate analogue was covalently linked to the FAD cofactor. This led to a crystal structure which indicated that only residues 1-7 of histone H3 fit into the active-site cavity of LSD1 (Yang *et al*. 2007). The extreme N-terminus of H3 is anchored into the catalytic pocket with no more than three residues permitted on the N-terminal side of the methyl-lysine, which itself is situated above the isoalloxazine ring of FAD for catalysis. Consistent with H3K4me2 (an active mark of transcription) as a substrate, LSD1 is found in cells as part of a core complex with the corepressor CoREST and HDAC 1 and 2 (You *et al*. 2001, Humphrey *et al.* 2001, Hakimi *et al.* 2002). Structural data has shown that other modifications to the tail of histone H3 must be removed before K4 demethylation can efficiently occur (Forneris *et al*. 2006). Association with HDAC1/2 creates a 'double-blade razor' that first eliminates acetyl groups from lysine residues and then removes methyl groups from H3K4 (Forneris *et al*. 2006). The biochemistry of this complex will be further discussed in 1.6.3.

The interaction with CoREST prevents LSD1 degradation and is essential for the recognition and demethylation of nucleosomal substrates (Lee *et al*. 2005, Shi *et al*.

2005). Hence, LSD1 alone can only demethylate H3K4me1/me2 in peptides or bulk histones, but in order to efficiently demethylate nucleosomes it must be in a complex with CoREST. Binding to CoREST is mediated through an extended helical region termed the 'TOWER' domain (Chen *et al*. 2006, Yang *et al*. 2006, Forneris *et al*. 2007) (Figure 1.5A and B). The enzymatic activity of LSD1 is contained within the large amine oxidase-like (AOL) domain (Chen *et al*. 2006) (Figure 1.5A and B). The TOWER domain is an antiparallel coiled-coil, with two extended α-helices that pack together in a left-handed superhelix with a repeating pattern of seven residues (Chen *et al*. 2006). Not only does this domain possess the interaction interface between LSD1 and CoREST, but it is also indispensible for the demethylase activity of LSD1 towards bulk histone substrates (Chen *et al*. 2006). LSD1 also contains an N-terminal 'SWIRM' (Swi3p, Rsc8p and Moira) domain, which is a conserved motif that is thought to be important for protein stability and implicated in histone tail recognition (Qian *et al*. 2005, Da *et al*. 2006). The N-terminus of the protein is an unstructured region dispensable for LSD1 demethylase activity *in vitro* (Forneris *et al*. 2005b). The related amine oxidase LSD2 notably lacks the TOWER domain essential to bind CoREST (Figure 1.5C); hence there is no redundancy between these proteins (Ciccone *et al*. 2009, Karytinos *et al*. 2009).

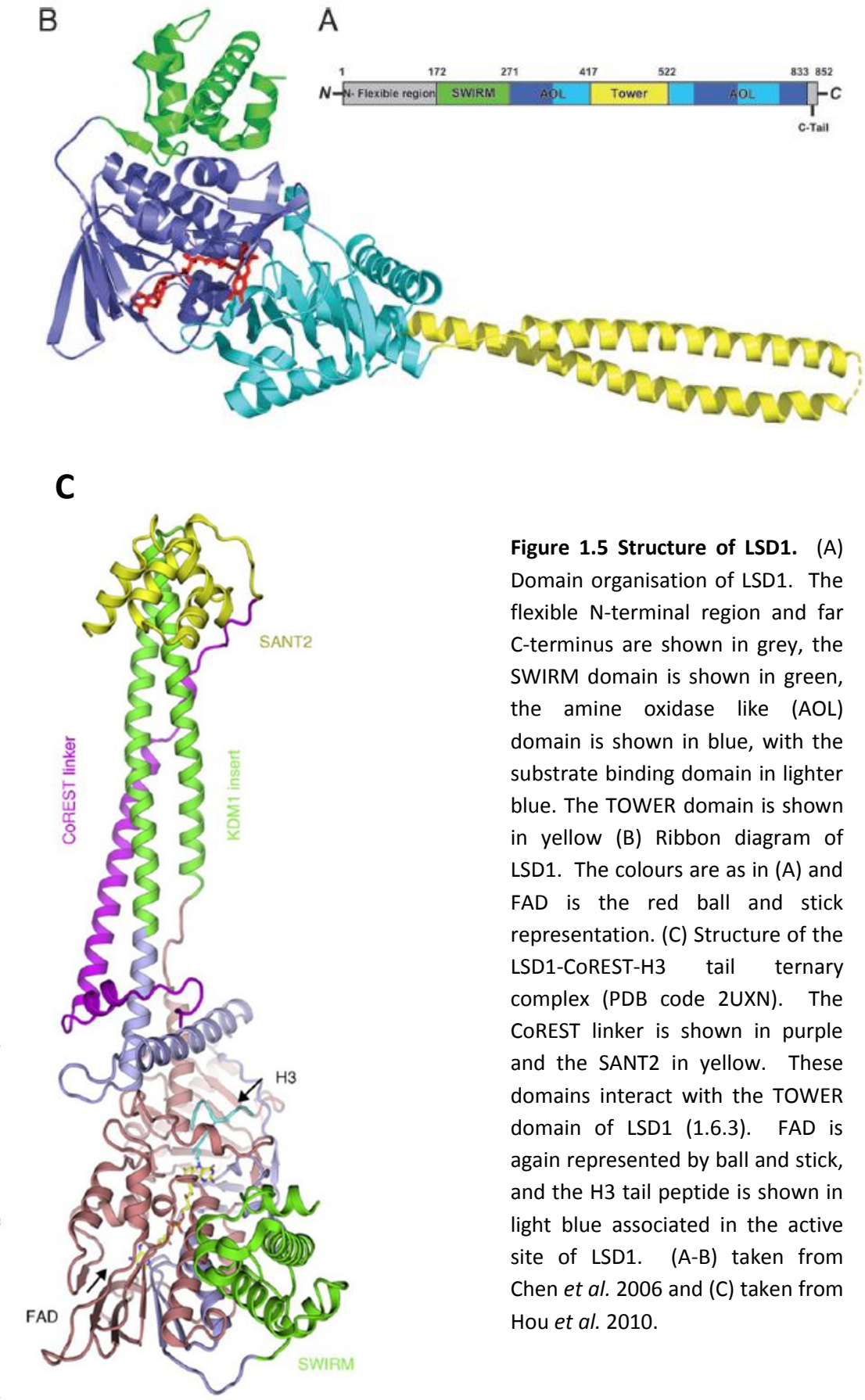

Figure 1.5 Structure of LSD1. (A) Domain organisation of LSD1. The flexible N-terminal region and far C-terminus are shown in grey, the SWIRM domain is shown in green, the amine oxidase like (AOL) domain is shown in blue, with the substrate binding domain in lighter blue. The TOWER domain is shown in yellow (B) Ribbon diagram of LSD1. The colours are as in (A) and FAD is the red ball and stick representation. (C) Structure of the LSD1-CoREST-H3 tail ternary complex (PDB code 2UXN). The CoREST linker is shown in purple and the SANT2 in yellow. These domains interact with the TOWER domain of LSD1 (1.6.3). FAD is again represented by ball and stick, and the H3 tail peptide is shown in light blue associated in the active site of LSD1. (A-B) taken from Chen *et al.* 2006 and (C) taken from Hou *et al.* 2010.

1.4.2.2 LSD1 knockout studies

The first LSD1 knockout mouse study showed that germline deletion of LSD1 leads to the developmental block at around embryonic day (E)7.5. In order to circumvent this early embryonic lethality, a conditional, pituitary-specific LSD1 deletion was generated to investigate the role of LSD1 during organogenesis. Pituitary development and the appropriate expression of pituitary-specific hormones were found to be dependent on LSD1 in the mouse and conclusions of this study work stated that LSD1 is required for late cell lineage determination and differentiation during pituitary organogenesis (Wang *et al*. 2007). This data could not explain death at E7.5 as complete loss of LSD1 was only achieved in the pituitary beyond E9.0-9.5 and the majority of analyses were performed in pituitaries at E17.5 (Wang *et al*. 2007). A second publication of an LSD1 knockout mouse also reported an arrest in embryonic development at E6.5 (Wang *et al*. 2009). Analysis of knockout ES cells derived from gene targeting identified a dramatically reduced global DNA methylation. This phenotype was attributed to decreased levels of the maintenance DNA methyltransferase DNMT1 as a result of LSD1 loss (Wang *et al*. 2009). Demethylation of DNMT1 by LSD1 is crucial for protein stability and hence correct regulation of genomic methylation. The loss of genomic methylation would likely lead to aberrant activation of silenced genes and repetitive DNA elements as well as genomic instability (Wang *et al*. 2009). However, embryonic lethality observed in the *Lsd1* knockout mice is unlikely to be solely caused by loss of DNMT1, since *Dnmt1* mutant embryos survive to mid-gestation, whereas *Lsd1* mutants die at the onset of gastrulation (Li *et al*. 1992, Wang *et al*. 2007). Very recently, after publication of results from our lab, another mouse knockout of *Lsd1* showed embryonic lethality at the onset of gastrulation, however, DNMT1 protein levels and

global DNA methylation remained unchanged in the *Lsd1* mutant ES cells derived from the inner cell mass of the embryo (Macfarlan *et al*. 2011). In order to ensure that DNMT1 levels had not been restored by a compensatory mutation during ES cell isolation, the generation of a conditional deletion by ES cell gene targeted was also performed. These cells also showed stable levels of DNMT1 through multiple passages (by immunofluorescence-assessment of individual cells); thus, these discrepancies between two reports are unresolved. Therefore, in this most recent publication, LSD1 was dissociated from DNMT1 and alternatively was characterised in repression of retrotransposable elements (REs) by controlling histone modifications. The removal of LSD1 resulted in activation of endogenous retroviral LTRs as well as genes that contain an LTR in their promoter resulting in developmental arrest at gastrulation (Macfarlan *et al*. 2011).

1.4.2.3 LSD1/CoREST function in transcriptional repression

The LSD1 hetero-dimeric partner, CoREST, is a co-repressor for the REST, which represses neuronal genes in non-neuronal cells (Ballas *et al*. 2001). Inhibition of LSD1 function causes increased expression of CoREST targets such as acetycholine receptor (AchR), synapsin and sodium channels (SCNA1A, SCNA2A, SCNA3A) in non-neuronal cells (Shi *et al*. 2004, Lee *et al*. 2005, Shi *et al*. 2005); therefore identifying them as LSD1 target genes. Inhibiting the activity of HDACs, by Trichostatin A (TSA) treatment, results in de-repression of SCNA2 and SCNA3A, suggesting that hyperacetylation of histone tails constitute an inferior substrate for LSD1 activity (Shi *et al*. 2005) (1.6.3). Subsequent studies have shown that these SCNA genes are up-regulated in both CoREST and LSD1 stable knockdown cells (Hu *et al.* 2009, Ouyang *et al.* 2009). The

regulation of haematopoietic differentiation by Growth factor independent (Gfi) transcription factors is also mediated by association with the CoREST complex (Saleque *et al*. 2007). The LSD1/CoREST/HDAC complex also regulates transcriptional activities of the TAL1 transcription factor during haematopoiesis (Hu *et al*. 2009). Here, LSD1 plays an important role in the repression of the TAL1-target genes in undifferentiated murine erythroleukemia (MEL) cells by demethylation of H3K4. Erythroid differentiation is accompanied by a reduction in TAL1-associated LSD1 and HDAC1 activities (Hu *et al*. 2009). LSD1 is implicated in maintaining neural stem cell proliferation through interaction with the orphan nuclear receptor, TLX, as well as co-operation with HDAC5, in order to repress p21 and PTEN expression (Sun *et al*. 2010). It has recently been recognised that posttranslational modification of CoREST by the small ubiquitin-related modifier SUMO regulates LSD1/CoREST/HDAC function in transcriptional repression (Ouyang *et al*. 2009). Promoter occupancy, gene repression and associated histone modification of SCNA1A and SCNA3A, but not SCNA2A, depends on binding of SUMO-2 to CoREST via a SUMO interaction motif (SIM) present between amino acids 255 to 275 of CoREST (Ouyang *et al*. 2009). The binding of SUMO-2 does not influence the ability of CoREST to bind LSD1, though overall there is a gene-specific requirement for SUMOylation of COREST protein within the CoREST complex. In addition to canonical functions of LSD1 in the CoREST complex, it was recently shown to be recruited to the NuRD complex via interaction with MTA1-3 in MCF-7 breast cancer cells (Wang Y *et al*. 2009).

1.4.2.4 LSD1 function in gene activation

The association of LSD1 with the androgen receptor (AR) has been reported, which switches its substrate specificity to H3K9me1/me2, thus, implicating a role in gene activation (Metzger *et al*. 2005, Wissmann *et al*. 2007). LSD1 has also been shown to co-operate with the H3K9me3 demethylase, JMJD2C, to activate these AR-responsive gene targets (Wissmann *et al*. 2007). The inhibition of LSD1 results in an increase in H3K9 methylation of AR targets and a concomitant decrease in their expression. This effect is also seen in C2C12 mouse myoblast cells at the *myogenin* and *MCK* promoters, to reveal an activating role for LSD1 in skeletal muscle development (Choi *et al*. 2010). Here, LSD1 interaction with myogenic transcription factors (Mef2c and MyoD) has been reported to induce skeletal muscle differentiation (Choi *et al*. 2010). Furthermore, the link of LSD1 to Estrogen Receptor (ER) signalling supports a role for LSD1 in gene activation, where RNAi-mediated inhibition of LSD1 led to a decrease in expression of ERα targets co-occupied by LSD1, but not those not occupied by LSD1 alone (Garcia-Bassets *et al*. 2007). Studies performed on LSD1 orthologs in *D.melanogaster* and *S.pombe* have corroborated the notion that LSD1 can act as a H3K4 or as a H3K9 demethylase, though in each case it is implicated in establishing euchromatin/heterochromatin boundaries (Nicolas *et al*. 2006, Lan *et al*. 2007, Rudolph *et al*. 2007). The composition of LSD1 containing complexes therefore has the ability to alter both target gene recruitment and substrate specificity. In addition to this, neighbouring histone marks surrounding the substrate are important in determining specificity (Forneris *et al*. 2006, Forneris *et al*. 2005b). The presence of HDAC1/2 in the CoREST and NuRD complexes suggest a co-ordinate modification of histone tails, which is supported by evidence that hypoacetylated histone tails are the

preferred substrate for LSD1 (Lee *et al*. 2005, Forneris *et al*. 2006, Forneris *et al*. 2005b, Shi *et al*. 2005). This parallels with the feature of H3K4 methylation often being associated with increased acetylation of H3 by p300 and other histone acetyltransferases (HATs). Both features support the notion that H3K4 and H3K9 methylation inhibit each other (Wang *et al*. 2001). Each of these roles mentioned above involves direct recruitment to target genes and the manipulation of histone substrates. Much of the literature reveals that LSD1 is recruited by transcription factors, such as REST, Gfi1/1b and TAL1, as part of the CoREST complex to repress differentiation-specific genes in undifferentiated cell types (Ballas *et al*. 2001, Hu *et al*. 2009, Saleque *et al*. 2007).

1.4.2.5 Non-histone targets of LSD1

LSD1 demethylates other proteins in addition to histone H3. DNMT1 was recently identified as a substrate for LSD1, though non-histone substrates were recognised before this. The pro-apoptotic tumour suppressor, p53, is known to be regulated by numerous posttranslational modifications, possessing multiple sites for lysine methylation (Chuikov *et al.* 2004, Huang *et al*. 2007). LSD1 has been implicated in the DNA damage response by demethylating p53, which restrains the interaction of p53 with its cofactor p53BP1, thereby repressing p53-mediated transcriptional activation and inhibiting the role of p53 in promoting apoptosis (Huang *et al*. 2007). LSD1 depletion might be expected to cause accumulation of p53 methylated on K370 and thereby aberrantly stimulating pro-apoptotic transcriptional events (especially if histone modifications are affected in concert; see 1.7). LSD1 also functions to regulate

p53-independent cell death upon DNA damage by controlling E2F1 stability through demethylation of K185. LSD1 demethylation prevents ubiquitin-mediated E2F1 degradation, allowing it to activate the expression of pro-apoptotic target genes, including p73 (Kontaki & Talianidis 2010). Taken together, this suggests that LSD1 demethylation causes commitment to p73- and not p53-mediated apoptosis. Whereas, Set9 methylation would result in stimulation of p53 function and limited activation of p73 through E2F1.

1.5 Histone acetylation

1.5.1 Effects of acetylation

Acetylation was first identified on histones in 1964 as a potential regulator of RNA synthesis (Allfrey *et al*. 1964). A direct link between core histone acetylation and active genes was identified through studies in chicken erythroid cells (Hebbes *et al*. 1985). Lysine acetylation, on many residues of the four core histones, is a highly dynamic process and differs to methylation in its effect, as it is almost invariably associated with active transcription (Roth *et al.* 2001, Zhang & Reinberg 2001, Kouzarides 2007, Mellor *et al.* 2008). Histone acetyltransferases (HATs) catalyse the addition of the acetyl group to the ε-amino group of lysine amino acids (Brownell & Allis 1996). HATs can be divided into three main groups: GNAT, MYST and CBP/p300, where each functioning enzyme often modifies more than one lysine (Sterner & Berger 2000). Deacetylation, catalysed by histone deacetylases (HDACs), is the reversal of acetylation and generally correlates with transcriptional repression. HDACs are found in numerous co-repressor complexes in the cell (described in greater detail in 1.6). Many cellular processes are regulated by histone acetylation, including the assembly of newly synthesised histones into nucleosomes, the spreading of heterochromatic regions and gene transcription (Shahbazian & Grunstein 2007). Lysine acetylation regulates local histone-DNA interaction as well as higher order structure of chromatin, where histone acetylation creates more open chromatin architecture.

The effects of acetylation on chromatin are manifested through three processes. Firstly, lysine acetylation perturbs the electrostatic charge attraction between the negatively charged DNA backbone and the long, positively charged, basic histone tails (Clark & Kimura 1990, Sun *et al.* 2005). This ultimately loosens the association of DNA with the nucleosome. Secondly, the compaction of the 30nm fibre is prevented by the presence of acetyl-lysines. A histone octamer with twelve acetylated residues (46% maximal site occupancy) is completely inhibited from forming a higher-order folded chromatin structure, and subsequently leads to an enhancement of transcription (Tse *et al*. 1998). Specifically, H3K14Ac has been shown to inhibit formation of a compacted fibre and to inhibit the ability of the ATP-utilising remodelling enzyme ACF to mobilise the nucleosome, thereby preventing formation of higher order chromatin (Shogren-Knaak *et al*. 2006, Robinson *et al*. 2008). Acetylation also prevents core histone octamer association with linker histone H1, which stabilises the structure of the polynucleosome, further hindering intra- and inter-nucleosomal interaction (Shogren-Knaak *et al*. 2006, Ridsdale *et al*. 1990). Thirdly, acetyl-lysines are recognised by specific proteins with bromodomains (Dhalluin *et al*. 1999), and these protein modules are often found in core transcription factors and transcriptional activators with further acetylating ability (for review see Taverna *et al*. 2007). For example, H3K9Ac and H3K14Ac are required for transcription initiation by recruiting the transcription factor TFIID (Agalioti *et al*. 2002).

1.5.2 Histone Deacetylases

HDACs remove the acetyl moiety from acetyl-lysine residues in histone protein substrates. The first HDAC (HDAC1) was purified from cow-protein extracts in 1996 using an inhibitor as an affinity tag (Taunton *et al*. 1996). HDAC1 was discovered to be an orthologue of yeast Rpd3, which had already been established as a global gene regulator (Vidal & Gaber 1991). Eleven members of this orthologous family of proteins have since been identified in mammalian genomes, all containing a conserved deacetylase domain (Yang & Seto 2008) (Figure 1.6). These enzymes are zinc-dependent and classified based on their homology to yeast Rpd3/Hda1 deacetylases; now designated as the 'classical' family since the discovery of another family of proteins known as the Sirtuins, which are not zinc-dependent but have a requirement for NAD+ (Taunton *et* al. 1996, De Ruijter *et al*. 2003). The classical HDAC family is grouped into classes I, II and IV, with class II being further divided into two subclasses (IIa and IIb). These HDACs differ in structure, function, sub-cellular localisation and expression patterns in mammals. Class I HDACs (HDACs 1, 2, 3 and 8) are highly conserved enzymes present in the nucleus of all cells, which display high enzymatic activity towards histone substrates (Van der Wyngaert *et al.* 2000, Bjerling *et al.* 2002, De Ruijter *et al*. 2003). HDAC1 and 2 are nearly identical and are generally found together in co-repressor complexes such as the Sin3, NuRD, CoREST and PRC2 complexes (Yang & Seto 2008) (1.6). Due to their ability to form multi-protein complexes, they have been implicated in a variety of cellular process, including: the regulation of cell cycle progression (Brehm *et al*. 1998, Luo *et al.* 1998, Magnaghi-Jaulin *et al*. 1998), differentiation (Liu *et al*. 2009, Montgomery *et al*. 2009), cellular ageing (Pegoraro *et al*. 2009) and cancer (Ropero *et al*. 2006).

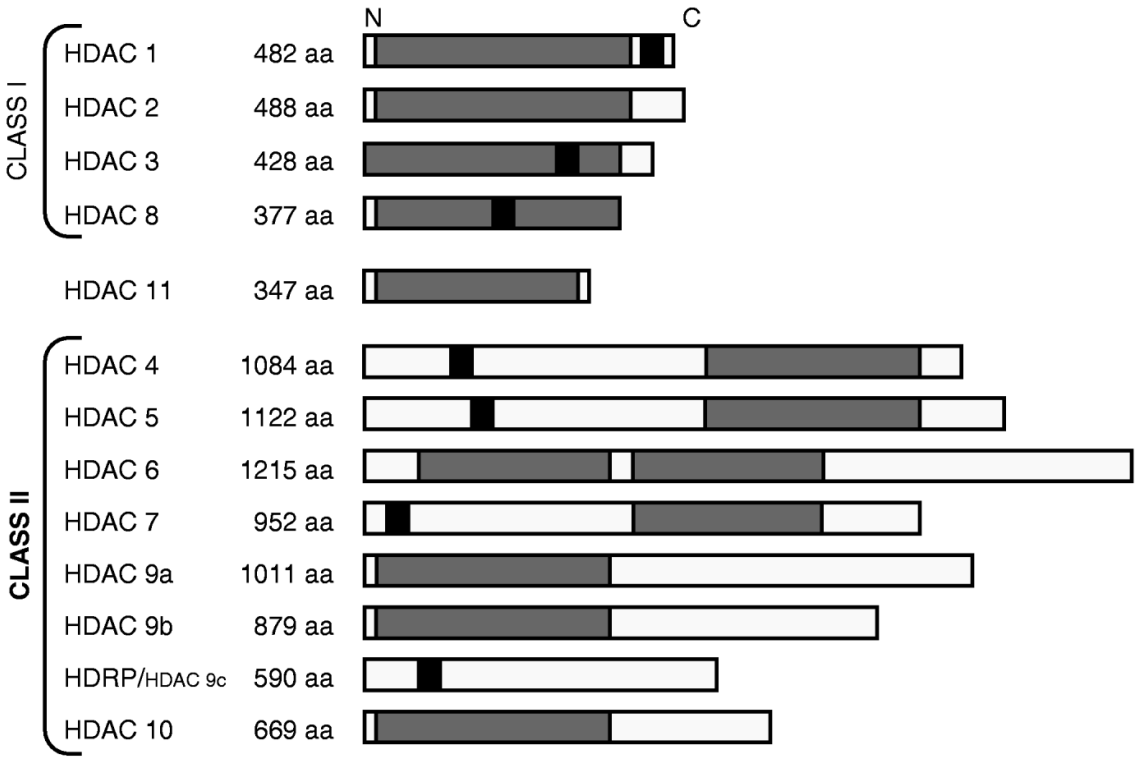

Figure 1.6 Schematic of the classical HDAC family members. Class I HDACs share significant sequence similarity with relatively simple structures, consisting of the conserved deacetylase domain (grey box) with short N- and C-terminal extensions. These HDACs are ubiquitously expressed nuclear proteins. Class IIa HDACs include HDAC4, 5, 7. They have large N-terminal extensions with conserved binding sites for the MEF2 transcription factor and the 14-3-3 chaperone protein. These proteins can be shuttled between the nucleus and the cytoplasm. HDAC6 and 10 form the class IIb family, with HDAC6 being the main cytoplasmic deacetylase in mammalian cells with cytoskeletal protein targets. HDAC11 is the sole class IV HDAC; classified due to the presence of a deacetylase domain that shows homology to class I and II domains. Black boxes indicate the nuclear localisation sequence. Figure adapted from De Ruijter *et al.* 2003.

The obvious extension of the correlation between gene activity and acetylation is that HDACs must therefore function in gene repression. This dogma is supported by the following knowledge: reduced acetylation promotes the formation of more condensed chromatin; class I HDACs are found as the catalytic components of multi-protein repressor complexes; and that HDAC1 tethered directly to DNA in the vicinity of gene

promoters using heterologous DNA binding domains, results in transcriptional repression (Ridsdale *et al*. 1990, Nagy *et al*. 1997, Shogren-Knaak *et al*. 2006, Yang & Seto 2008). However, data on the correlation of HDAC binding and gene expression insinuates that HDACs can negatively and positively regulate transcription (Kadosh & Struhl 1997, Xie *et al*. 1999, Kurdistani *et al*. 2002, Wang *et* al. 2002, Robert *et al*. 2004). This latter observation suggests that a major function of HDACs is to remove the acetyl group added by HATs at active gene promoters, thereby resetting the chromatin modifications following transcriptional activation (Wang *et* al. 2002, Dovey *et al*. 2010a). The strongest evidence for a positive role in transcription comes from two separate studies by the Grunstein and Zhao laboratories in yeast and human cells, respectively (Kurdistani *et al*. 2002, Wang *et al*. 2009b). Genome-wide mapping of HATs and HDACs in human T cells demonstrated that HDAC1 is predominantly localised at active gene loci, co-localising with many HATs, including p300/CBP, p/CAF, GCN5 and MOF (Wang *et al*. 2009b). Strikingly, the block of HDAC activity with HDAC inhibitors and the knockdown of mSin3A and HDAC1 and 2 causes a dramatic reduction in *Nanog* expression in undifferentiated ES cells (coupled with loss of active histone marks), indicating that the mSin3A-HDAC complex positively regulates *Nanog* expression (Baltus *et al*. 2009). One potential explanation is that transcriptional activation involves a 'cyclical' utilisation of HATs and then HDACs to initiate and then reset chromatin state between rounds of RNA polymerase II recruitment (Wang *et al*. 2009b). HDACs therefore have a role in promoter clearance that necessitates re-initialisation of RNA polymerase II transcription (Dovey *et al*. 2010b)

HDACs are of significant research interest due to the great therapeutic potential of HDAC inhibitors (HDACi). Many small molecule HDAC inhibitors exist, with most being 'pan-HDAC', that is, they block the activity of all isoforms (except class IIa), but some being isoform-specific (Haberland *et al*. 2009). Ongoing human clinical trials are investigating the use of HDAC inhibitors as treatment for a wide variety of disorders, including cancer. Notably, suberoylanilade hydroxamic acid (SAHA; marketed as Vorinostat) has been approved for treatment of cutaneous manifestations of advanced, refractory T-cell lymphoma (Duvic *et al*. 2007). Inhibition of HDAC activity can induce cell cycle arrest, differentiation or apoptosis of cancer cells *in vitro* and *in vivo*. However, normal cells are relatively resistant to HDACi-induced cell death. Indeed, a number of inhibitors are currently being tested in the clinic as potential chemotherapeutic agents (for review see Marks & Xu 2009). Considering that histone acetylation and deacetylation is involved in so many aspects of development and tissue homeostasis, it is striking that systemic HDAC inhibition with compounds that broadly inhibit most or all HDACs is well tolerated *in vivo,* with differing phenotypes to HDAC gene deletions. An explanation for these discrepancies is that HDACs participate in multi-protein transcriptional complexes. Genetic deletion of an HDAC perturbs the complex in which it would normally be associated, whereas inhibitors are believed to block enzymatic activity without necessarily disrupting the entire complex (Haberland *et al*. 2009). The importance of this aspect of HDAC biochemistry is elaborated upon in the next two sections.

1.6 Class I HDAC repressor complexes

With the exception of HDAC8, all class I members have been observed to exist in large multi-subunit protein complexes**,** leading to co-operation with other chromatin modifiers and proteins with chromatin binding domains (Ng *et al*. 2000). Among the class I HDACs, HDAC1 and 2 are the most similar (83% sequence identity) and in mammalian cells, they interact together (Taplick *et al*. 2001) to form the catalytic core of a number of these complexes, including Sin3A, NuRD, CoREST and NODE (Figure 1.7). The CoREST complex is a key focus in this thesis. The N-CoR/SMRT complex contains HDAC3, but will not be discussed in detail.

1.6.1 Sin3 complex

Sin3 repressor complexes were first identified in yeast. *S.cerevisiae* contains two Sin3 complexes; one deacetylates histones at promoter regions (Rpd3L), and the other targets transcribed regions to suppress intragenic transcription (Rpd3S). This latter complex contains the Eaf3 subunit that recognises H3K36me3 via its chromodomain (1.3.4) (Rundlett *et al*. 1996, Kasten *et al*. 1997, Carrozza *et al.* 2005, Keogh *et al*. 2005). Mammals have two Sin3 homologues, mSin3A and mSin3B, which show high sequence similarity and are both essential in mouse development (Cowley *et al*. 2005, Dannenberg *et al.* 2005, David *et al*. 2008). mSin3A is one of the best characterised class I HDAC-containing complexes (Figure 1.7).

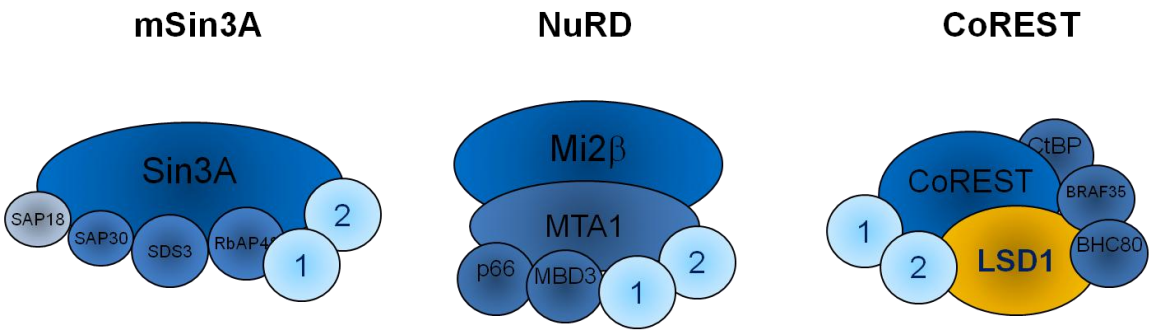

Complex	Component	Protein domain
Sin3	HDAC1, HDAC2	Class I deacetylase
	RbAp46, RbAp48	WD40 repeat
	Sin3A	PAH motifs, ELM2
	Sds3	Coiled coil
	RBP1	
	SAP30	
	SAP18	Ubiquitin fold
	ING1/2	PHD finger
NuRD	HDAC1, HDAC2	Class I deacetylase
	RbAp46, RbAp48	WD40 repeat
	Mi-2α/β	Helicase
	MTA1-3	SANT domain
	MBD2, MBD3	Methyl CpG binding
	p66α/β	
CoREST	HDAC1, HDAC2	Class I deacetylase
	CoREST	SANT domain, ELM2
	LSD1	SWIRM, AOL, Tower
	BHC30	PHD finger
	BRAF35	
	CtBP	Dehydrogenase

Figure 1.7 Repressor complexes containing HDAC1 and HDAC2. The simple schematic shows how HDAC1 and 2 are common to these unique complexes with differing functions. Core components are displayed and different isoforms of each component may also be incorporated. The detailed list of components and structural motifs present is adapted from Yang & Seto 2008. The importance of some of these motifs is discussed in the main text.

The interaction of Sin3A and HDAC1 and 2 *in vivo* was originally identified in the Eisenman lab, where this discovery also elucidated a mechanism of Mad-Max transcriptional repression through Sin3A association (Laherty *et al*. 1997). The mSds3 component is critical for maintenance of Sin3-associated HDAC activity (Alland *et al*. 2002) and the retinoblastoma associated proteins, RbAp46 and -48 are thought to stabilise the interaction with the nucleosome (Lai *et al*. 2001). The mSin3A complex itself lacks any DNA-binding activity; therefore, it must be targeted to genomic regions by interacting with DNA-binding factors, such as p53, E2F and Ikaros (for a review see Silverstein & Ekwall 2005). mSin3A has an essential role in early embryonic development and T cell development (Cowley *et al*. 2005, Dannenberg *et al.* 2005). mSin3A knockout MEFs exhibit de-regulation of genes involved in cell cycle control, DNA replication, DNA repair, apoptosis, chromatin modification and mitochondria function as well as mis-localisation of HP1α (Cowley *et al*. 2005, Dannenberg *et al*. 2005). mSin3B has a critical role in later stage of development in the mouse, with depletion causing defective differentiation of multiple lineages due to de-repression of E2F target genes (David *et al*. 2008).

1.6.2 NuRD complexes

The nucleosome remodelling and deacetylase (NuRD) complex was first characterised as a complex containing the ATP-dependent chromatin remodelling protein Mi-2 and MTA (metastasis associated) proteins (Tong *et al*. 1998, Zhang *et al*. 1998). This co-repressor complex has been shown to be recruited to DNA by transcription factors such as Ikaros and hunchback (Kim *et al*. 1999). The catalytic core of NuRD is HDAC1,

HDAC2, RbAp46 and RbAp48. Distinct NuRD complexes are formed depending on the isoforms of the components, including: MTA1-3, Mi-2α/β, p66 proteins and MBD (methyl CpG-binding domain) 2 and 3. The MTA isoforms contain SANT domains and are crucial for the integrity and deacetylase activity of NuRD (Denslow & Wade 2007). The complex is involved with DNA methylation events through the MBD2 component and complex association with MeCP1 and MeCP2. However, MBD2 and MBD3 are exclusively associated within NuRD to form distinct complexes and the discovery that MBD3 is unable to bind methyl-CpGs resulted in a reassessment of the overall importance of NuRD in targeting methylated cytosines (Hendrich & Bird 1998, Saito & Ishikawa 2002, Le Guezennec *et al.* 2006). MBD3 is necessary for MTA and HDAC association within NuRD and is essential for mouse development, whereas MBD2 is not (Hendrich *et al.* 2001); therefore, the importance of MBD3 is conveyed through its role in protein-protein interactions (Saito & Ishikawa 2002) . It has since been shown that ES cells lacking MBD3 are unable to differentiate due to inability to repress the *Oct4* gene (Keji *et al.* 2006).

A variant of the NuRD complex, lacking MBD3, was recently found associated with Oct4 and Nanog proteins, which mediates repression of Oct4/Nanog target genes to control ES cell pluripotency (Liang *et al*. 2008) (1.8 and 1.9). This unique complex was named NODE (Nanog- and Oct4-associated DEacetylase). MTA1 is the preferred isoform found within NODE and HDAC activity is comparable to that of the NuRD complex. Upon knockdown of NODE components, ES cells spontaneously differentiate into endodermal cell types due to de-repression of development-specific Oct4/Nanog

target genes. Therefore the function of NODE, which is to repress developmental genes in undifferentiated cells, contrasts with the function of the NuRD complex, which is to mediate *Oct4* repression upon ES cell differentiation (Kaji *et al.* 2006, Liang *et al*. 2008).

1.6.3 CoREST complex

The CoREST complex was initially identified as a complex containing HDAC1 and 2 that was composed of polypeptides distinct from the previously characterised HDAC1/2-containing complexes, Sin3 and NuRD (You *et al.* 2001). CoREST was initially cloned as a co-repressor to REST/NRSF, which represses neuronal specific genes (Andres *et al.* 1999, Ballas *et al*. 2001). However, when CoREST and HDAC1/2 were first co-purified, REST was not detected bound to CoREST (You *et al*. 2001, Hakimi *et al*. 2002). A 110kDa protein with homology to polyamine oxidases was, however, identified, which was later characterised as LSD1 (You *et al.* 2001, Shi *et al.* 2004). Other complex members include the co-repressor, CtBP (C-terminal binding protein) (Shi *et al.* 2003, Shi *et al*. 2005), an HMG domain containing protein, BRAF35 (Hakimi *et al*. 2002, Lee *et al*. 2005) and BHC80, which contains a PHD finger that specifically recognises unmodified H3K4 (Lan *et al*. 2007). This binding is a contrast to other PHD fingers, such as the bromodomain PHD finger transcription factor (BPTF) in the nucleosome remodelling NURF complex and ING2 in the Sin3a complex, which bind methylated H3K4 (Shi *et al*. 2006, Li *et al*. 2006). Thus, PHD finger-containing proteins are important effecter molecules that are recruited to various methyl lysine moieties. CoREST contains two SANT (Swi3, Ada3, NCoR, TFIIB) domains that resemble the DNA-

binding domains of Myb-related proteins that are also present in MTA proteins and the transcription factors from which SANT is named (Aasland *et al.* 1996). Structural and biochemical studies have shown that a SANT domain (SANT1) and a linker region of CoREST interact with the LSD1 TOWER domain (Chen *et al*. 2006, Lee *et al*. 2006a). A C-terminal SANT domain (SANT2) within CoREST facilitates the association with chromatin by interacting directly with DNA (Shi *et al*. 2005, Yang *et al*. 2006). An ELM2 domain, located N-terminally of the SANT1 domain, is essential for interaction with HDACs and confers nucleosomal deacetylation within the CoREST complex (Lee *et al.* 2006a). This ELM2 domain was previously shown to associate with HDAC1 in other transcription factors (Solari *et al.* 1999, Ding *et al.* 2003).

The main functional interconnection between deacetylation and demethylation activities was elucidated through two biochemical studies in 2006. One of these studies showed that inhibition of deacetylase activity with HDACi decreased nucleosomal demethylation, with similar magnitudes of inhibition of deacetylation and demethylation observed as the concentration of TSA was increased (Lee *et al.* 2006a). This effect was independent of changes in subunit composition in the CoREST complex. These results implied that deacetylation precedes demethylation and corroborated earlier suggestions that acetylated histone tails are an inferior substrate for the activity of LSD1 in the complex (Shi *et al*. 2005). Subsequent experiments in the Mattevi lab characterised the substrate specificity and recognition by LSD1, with biochemical assays on histone peptides showing that essentially all covalent modifications on the 21 N-terminal amino acids of histone H3 cause a significant

reduction in LSD1 enzymatic activity (Forneris *et al*. 2006). This confirmed that lysines (notably K9) must be deacetylated by HDACs with the CoREST complex in order to remove biophysical restraints on the demethylation of H3K4 by LSD1. Thus, a model of CoREST complex function was proposed: it operates as a "double-blade razor" that first eliminates the acetyl groups from acetylated lysine residues and then removes the methyl group from lysine 4 (Forneris *et al*. 2006).

The complex is targeted to specific gene loci by DNA-binding transcription factors, such as REST, TAL1 and Gfi proteins (1.4.2.3) that associate with CoREST and LSD1. CtBP was identified as a 48kDa cellular phospho-protein that binds to the C-terminal region of the human adenovirus E1A proteins (Boyd *et al*. 1993, Schaeper *et al.* 1995). CtBP also directly interacts with many DNA-binding transcription factors and the identification of its role as a transcriptional co-repressor was initially through its co-purification with HDAC1 and 2 (reviewed in Chinnadurai 2002). CtBP can also co-ordinate histone modification to act as a co-repressor through more than one mechanism, which is elaborated on in the next section.

1.7 Crosstalk of histone modifications

As both methylation and acetylation play important roles in regulating gene expression, it is no surprise these modifications are often tightly co-ordinated. This crosstalk is exemplified by the presence of a LSD1 demethylase and deacetylases in the LSD1/CoREST/HDAC protein complex. Removal of H3K4 methylation and H3K9/K14 acetylation has repressive functions. Evidence strongly indicates that changes in acetylation states precede changes in methylation: LSD1 is more active towards hypomethylated H3 (Lee *et al*. 2005, Shi *et al.* 2005, Forneris *et al*. 2006); and the KMT, MLL, has increased methyltransferase activity towards H3 peptides acetylated at K9 and K14 (Milne *et al*. 2002). Furthermore, treatment with HDACi increases H3K4 methylation *in vivo* and decreases demethylation *in vitro* (Lee *et al.* 2006a). The presence of a PHD finger in an LSD1 complex partner, BHC80, which binds unmethylated H3K4, is an interesting feature that is suggested to be a targeting system for LSD1 to the propagate H3K4 demethylation (Lan *et al.* 2007). CtBP also manifests crosstalk between histone substrates, where HDACs, LSD1 and H3K9 KMTs are linked through a CtBP supercomplex. Two CtBP subcomplexes have been identified: one containing LSD1/CoREST/HDAC/BHC80; the other containing REST/G9a/EuMT (Shi *et al*. 2003). Therefore, propagation of a repressive state in euchromatic regions can occur through a stepwise model that synchronises H3K9 deacetylation, H3K4 demethyaltion and H3K9 methylation (see Lan *et al.* 2008) (Figure 1.8). HDAC1/2-mediated deacetylation of H3K9 is followed by CoREST recruitment to hypoacetylated histone tails, which targets LSD1 to the H3K4me2/me1 substrate. This is preceded by BHC80 binding to unmethylated H3K4 and potential stabilisation of

additional CtBP supercomplex members in the vicinity of the unmodified H3K9 substrate.

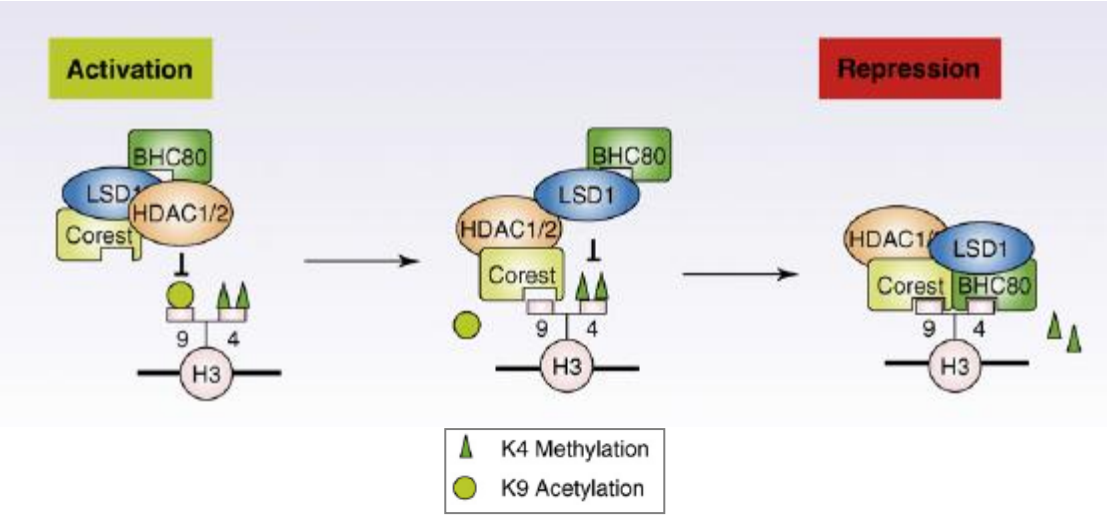

Figure 1.8 Mechanism of CoREST complex-mediated targeting of LSD1 to H3K4 and contribution to euchromatic gene repression. This stepwise model shows that HDAC1/2 deacetylates H3K9, which provides a hypoacetylated substrate for CoREST-LSD1 targeting. LSD1 subsequently demethylates H3K4me2/me1 creating a moiety for BHC80 PHD finger recognition. This binding maintains repression to prevent re-methylation of H3K4 as well as crosstalk with H3K9 methylation through KMT activity in the CtBP complex. Figure adapted from Lan *et al*. 2008.

In an analogous fashion, the mSin3A complex will deacetylate histones in a methylation-dependent manner (Pena *et al.* 2006, Shi *et al*. 2006). The ING2 component has a PHD finger domain that recognises H3K4me2/me3, in order to tether the repressive mSin3A complex to highly active, proliferation-specific genes. This represents a mechanism of feedback to actively shut-off highly transcribed genes. The Eaf3/MRG15 chromodomain within the mSin3A-HDAC-Mrg15 complex is recruited to

H3K36me3 to deacetylate histones within the gene body. This occurs to compact chromatin behind the elongating RNA polymerase complex in order to suppress intragenic transcription initiation (Brown *et al.* 2006). This process has been well characterised in *S.cerevisiae*, where deletion of Set2 or one of the Rpd3S components results in spurious transcription from intragenic start sites (Carrozza *et al.* 2005).

1.8 Mouse embryonic stem cells

1.8.1 Origins and applications

Mouse embryonic stem (ES) cells are derived from the inner cell mass (ICM) of the E3.5 pre-implantation embryo, known as the blastocyst (Figure 1.9). Cells of the ICM will give rise to the embryo proper. ES cells possess two distinctive properties that make them unique to any other cell type: they are 'pluripotent' as they can differentiate into all cell types of the adult organism; and they can divide indefinitely without losing the capacity to self-renew. ES cells were first derived from mouse embryos in 1981 (Evans & Kaufman 1981, Martin 1981). When maintained in cell culture, undifferentiated ES cells are thought to generally reflect cells of the epiblast (E4.5–5.5 stage of development) (Doetschman *et al.* 1985, Brook & Gardner 1997).

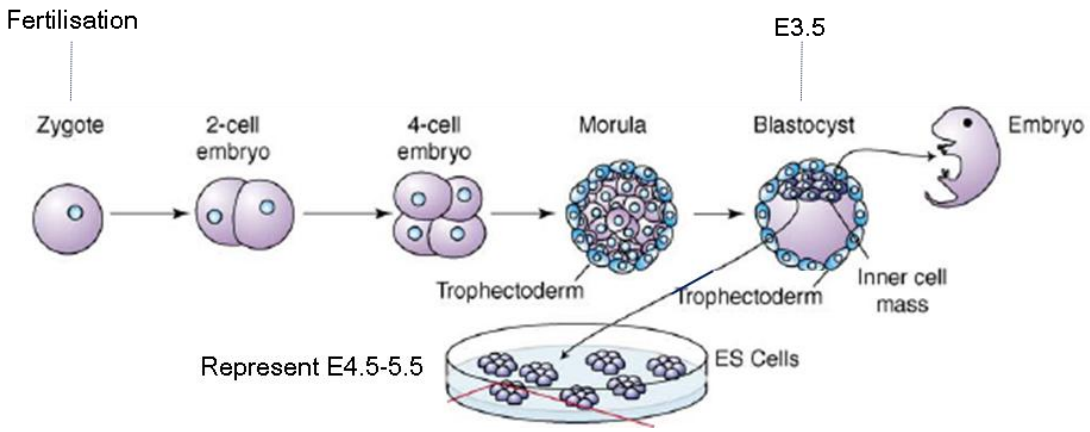

Figure 1.9 Mouse ES cells are derived from the ICM of the E3.5 blastocyst and can be maintained in cell culture. During mouse gestation, the pre-implantation stage involves progression from the zygote to the blastocyst. The ICM has formed in the blastocyst at E3.5 and contains pluripotent cells that will form the embryonic tissue. These cells can be extracted and maintained in an undifferentiated state either on a feeder layer of mouse embryonic fibroblasts (MEFs) or on gelatin-coated dishes in serum-containing media supplemented with LIF (Smith *et al.* 1988, Williams *et al.* 1988. Figure adapted from Boyer *et al.* 2006.

Mouse ES cells came to the fore within scientific research due to their ability to create knockout mice (Bradley *et al*. 1984). The marriage of ES cell biology with homologous recombination techniques, which were pioneered independently by Mario Capecchi and Oliver Smithies, created a new technology known as gene targeting; this could ultimately be utilised to knockout gene function the mouse (Folger *et al.* 1982, Smithies *et al.* 1985, Thomas & Capecchi 1987). Gene targeting requires the creation of a specific vector with DNA sequences homologous to the region in which it is to be integrated. Ultimately, the method can be used to delete a whole gene, remove exons, add a gene and introduce point mutations. These methods of altering the genome of ES cells in culture created the ability to generate mice with targeted mutations. To target genes in mice, the manipulated ES cells are injected into diploid blastocysts followed by implantation into a pseudo pregnant surrogate mouse. These ES cells will follow the course of development that the endogenous pluripotent cells of the ICM will undertake, with the surrogate mother giving birth to chimeric mice; representing the two distinct genetic backgrounds present in the blastocyst (see http://www.eucomm.org/docs/protocols/mouse_protocol_1_Sanger.pdf). The transmission of the targeted ES cells can be monitored by coat colour, as ES cell lines used in culture are of a different genetic background (agouti coat colour) to the common C57BL/6, inbred strain of laboratory mouse (dark brown/black coat colour). Chimeras will therefore have mixed coat colour, indicative of their genetic mix. The targeted ES cells can eventually contribute to the germline and therefore the entirety of animals' tissue following sufficient breeding of chimeras (Robertson *et al*. 1986).

Another important feature of ES cells is that they epitomise cells found in an early stage embryo and they have the ability to differentiate into the three primary embryonic germ layers (Keller 1995). Their differentiation may be viewed as a counterpart to embryogenesis, making them a potent tool for embryology research and an ideal *in vitro* counterpart in which to study loss of gene function in the early embryo (Doetschman *et al*. 1985, Brook & Gardner 1997). They are also suitable as they have a normal karyotype (diploid) and large numbers of homogenous cells can be generated from a single cell due to their capacity to indefinitely self-renew. Understanding the nature of ES cell biology has also allowed investigators to gauge the success of reprogramming somatic cells into pluripotent stem cells (known as induced pluripotent stem cells, or iPS cells) (Takahashi & Yamanaka 2006, Yu *et al*. 2007, Takahashi *et al*. 2007, Wernig *et al*. 2007, Okita, Ichisaka & Yamanaka 2007, Meissner *et al.* 2007, Maherali *et al.* 2007, Lowry *et al*. 2008, Okita *et al*. 2008, Park *et al.* 2008, Stadtfeld *et al.* 2008). The generation of patient specific iPS cells could potentially be used for cell replacement therapies. Finally, ES cells are a useful tool for studying chromatin biology and epigenetics during early embryonic development. ES cell differentiation is governed by remodelling of the epigenome and chromatin structure, therefore the ES cell system is ideal for investigating the specific roles of histone-modifying enzymes.

1.8.2 Maintenance of mouse ES cell pluripotency

Mouse ES cells can be maintained in cell culture by supplementing the culture media with a cytokine called leukaemia inhibitory factor (LIF) (Smith *et al.* 1987 and 1988). LIF is a member of the interleukin 6-family of cytokines that binds to the gp130

receptor, resulting in activation of the STAT3 signalling pathway (Ernst *et al.* 1996, Niwa *et al.* 1998). The presence of serum or bone morphogenic protein (BMP4) suppresses differentiation signals through Smad activation and subsequent induction of Inhibitor-of-differentiation (Id) proteins (Ying *et al.* 2003). The MAPK pathway is proposed to induce differentiation rather than self-renewal in ES cells. FGF4 is produced by undifferentiated ES cells and autocrine activation of the FGF receptor stimulates downstream MAPK signalling (Ma *et al.* 1992, Rathjen *et al.* 1999). The importance of MAPK signalling in lineage commitment is highlighted by observations that FGF4 ablation in ES cells restricts the ability to differentiate (Kunath *et al*. 2007). The activation of differentiation-specific factors is, however, overridden by STAT3 and BMP4 signalling. The requirement for extrinsic LIF and BMP4 stimuli is now known to be dispensable for maintenance of the stem cell state and the minimal requirements for self-renewal has been attributed mainly to the elimination of differentiation-inducing signals emanating from the FGF receptor and MAPK signalling, which requires neither LIF nor serum/BMP4 (Ying *et al*. 2008). These experiments showed that the culture of ES cells with three selective small-molecule inhibitors (3i: SU5402, to inhibit the FGF receptor; PD184352, to inhibit MEK; and CHIR99021, to inhibit GSK3 kinase) can maintain the pluripotent state, and that action of these chemical antagonists occurs upstream of differentiation-counteracting functions of LIF and BMP4.

1.8.3 Core pluripotency factor network: Oct4, Nanog and Sox2

The molecular networks that govern this stem cell state have been much scrutinised within the three decades since mouse ES cells were first described. The expression of a few key transcription factors are known to maintain pluripotency and self-renewal in mouse ES cells (for reviews see Smith 2001, Boyer *et al.* 2006). Oct4 (Pou5f1) is a POU-family transcription factor that was the first identified master regulator of pluripotency, which prevents differentiation into the trophectoderm lineage and thereby 'locks' the pluripotent capacity (Niwa *et al.* 2000). Nanog is a homeodomain transcription factor identified as essential for maintenance of pluripotency in mouse epiblast and ES cells (Mitsui *et al*. 2003). Sox2 is a high mobility group (HMG)-containing transcription factor that functions in a combinatorial fashion with Oct4 to maintain pluripotency and self-renewal through control of *FGF4* expression (Ambrosetti *et al.* 1997, Avilion *et al*. 2003, Chew *et al*. 2005).

The original mapping of Oct4, Nanog and Sox2 genome binding sites in human and mouse ES cells indicated that many of their gene targets overlap and that they formed the basis for circuitry consisting of auto-regulatory and feed-forward loops (Boyer *et al*. 2005b, Loh *et al*. 2006) (Figure 1.10). In mouse ES cells, a core set of 345 genes are targeted by both Oct4 and Nanog, with 30 DNA-binding transcriptional regulators encoded among these genes, *Oct4*, *Nanog* and *Sox2* included (Loh *et al*. 2006) (Figure 1.10). Some of these common targets, such as *STAT3* and Wnt-responsive genes, are activated in order to drive self-renewal (Chambers & Smith 2004, Sato *et al*. 2004, Anton *et al.* 2007, Pardo *et al*. 2010). The other major function of core pluripotency

factors is to co-ordinate the repression of differentiation programs (Niwa *et al.* 2000, Mitsui *et al*. 2003, Chambers *et al*. 2003). This is achieved by directly mediating gene repression as well as by activating genes encoding transcription factors that can regulate transcription repression, such as *Esrrb, Rif1* and *REST* and activating genes encoding components of chromatin remodelling and histone-modifying complexes, such as *ESET* and *Jarid2,* which will mediate gene repression (Loh *et al*. 2006). Notably, knockdown of *Esrrb, Rif1* and *REST* causes differentiation of ES cells (Loh *et al*. 2006). Differentiation is also suppressed by activation of Tgf-β signalling by Nanog (Chambers & Smith 2004, Boyer *et al*. 2005a). The core factors also directly repress genes encoding transcription factors that will drive differentiation, notably homeodomain, T-box, SRY-box and zinc finger transcription factors (Kim *et al.* 2008).

Most relevantly, the direct positive and negative regulation of gene targets by the core factors occurs through the interaction with chromatin remodelling/histone-modifying proteins. Sox2 interacts with mSin3A-HDAC complex to positively regulate *Nanog* expression (Baltus *et al*. 2009). Oct4 and Nanog are associated with PcG (1.3.2) and NuRD (1.6.2) repressor complex components, linking them to K27-specific KMTs and HDAC1/2, respectively, thereby mediating the repression of developmental regulators in ES cells through H3K27 methylation and histone deacetylation (Boyer *et al*. 2006, Wang *et al.* 2006, Liang *et al*. 2008, Pardo *et al*. 2010). LSD1/CoREST/HDAC were recently recognised as low affinity binding partners of Oct4, suggesting that this complex has a role in Oct4-directed transcriptional repression (Pardo *et al*. 2010). Down-regulation of core pluripotency factors will lead to the removal of repressive

complexes from development-specific genes and enable exit from the pluripotent state. Deletion of these histone-modifying factors that interact with Oct4, Nanog and Sox2 often results in increased expression of developmental genes and spontaneous ES cell differentiation (Liang *et al*. 2008), similar to effects seen upon removal of Oct4, Sox2 and Nanog (Nichols *et al*. 1998, Mitsui *et al*. 2003, Avilion *et al*. 2003, Chambers *et al*. 2003).

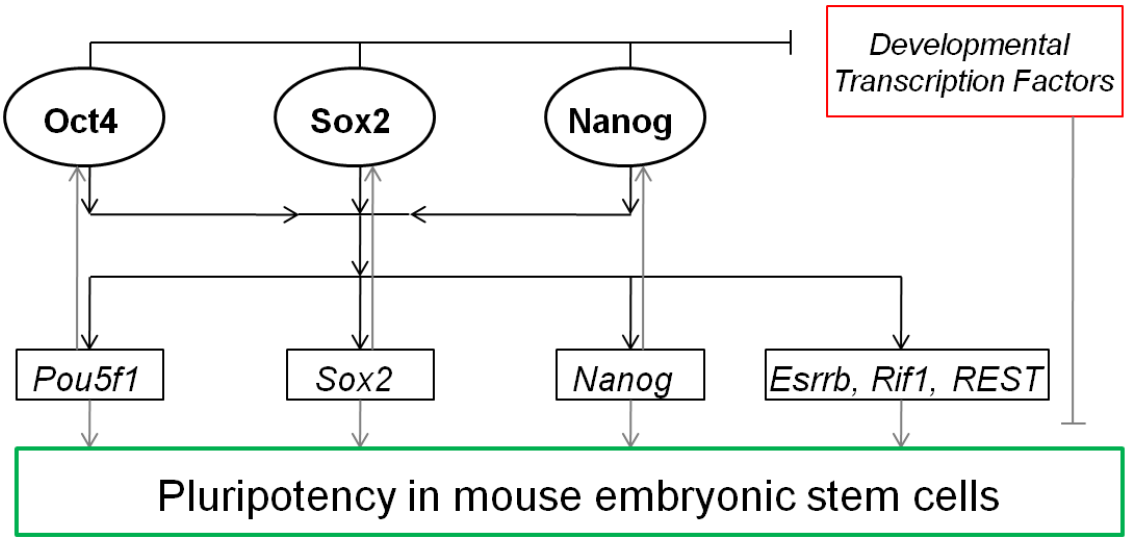

Figure 1.10 Oct4, Sox2 and Nanog regulatory network controlling pluripotency in mouse ES cells. The core pluripotency factors are represented by ovals, and the genes (printed in italics) are represented by rectangles. A black arrow indicates a transcription factor binding to a gene and positively regulating that gene with arrows denoting the synthesis of gene products from their respective genes. The core factors can repress tissue-specific transcription factor genes and activate transcription factors involved in repression of differentiation (*Esrrb, Rif1* and *REST).*

1.8.4 An extended pluripotency regulatory network

Pluripotency factors act in a highly combinatorial fashion to hold differentiation-promoting genes in check, while also driving the expression of genes encoding

proteins required for self renewal. Subsequently, ES cell differentiation is a complex process that requires the simultaneous activation of lineage-specific genes and repression of self-renewal genes. Recently, a network of nine transcription factors that controls ES cell state have been described (Kim *et al.* 2008). This revealed further intricacy of control of the pluripotent state and extended the network beyond control by Oct4, Nanog and Sox2. Nine factors (Oct4, Sox2, Nanog, Dax1, Nac1, Klf4, Zfp281, Rex1 and Myc) occupy one third of mouse ES cell gene promoters in varying combinations (Kim *et al*. 2008). Whereas 345 genes were initially found to be co-occupied by Oct4, Sox2 and Nanog in ES cells (Loh *et al*. 2006), more than 800 promoters were found to be occupied by at least four out of nine factors examined in the study from the Orkin lab (Kim *et al*. 2008). Distinct effects on gene expression and associated histone modification was ascribed to the specific combination. Single or dual occupancy is the most prevalent situation (5093 out of 6632 promoters) and Myc occupies more promoters than any other factor (18% of all promoters). Myc and Rex1 were segregated from the other factors as they mainly occupy active genes implicated in protein metabolism. The other factors are, however, found mainly at genes involved in developmental processes, with genes bound by six factors implicated most frequently in developmental processes. An expanded network recognised transcriptional interconnectivity of the nine factors as well as other important targets of these factors, which are involved in the regulation of developmental decisions, signalling pathways and chromatin remodelling. Important multi-factor target genes include *Tcll, Il6st (*gp130), and *Bmp4.* TcII promotes ES cell self-renewal through participation in the PI3K/Akt cell survival pathway; gp130 is a receptor important in

LIF/STAT3 signalling; BMP4 is a critical signalling molecule for inhibition of ES cell differentiation.

1.8.5 Molecular mechanisms in pre-gastrulation embryonic development

Oct4 is essential for the establishment of the ICM in the early embryo (Rosner *et al*. 1990). Restriction of Oct4 expression and expression of the caudal-type homeodomain transcription factor, Cdx2, is required for trophectoderm development, which becomes the extra-embryonic tissue. This balance of these two factors affects the first overt lineage differentiation in the embryo (Niwa *et al*. 2005). Indeed, loss of Oct4 in ES cells will cause inappropriate differentiation into trophectoderm (Niwa *et al*. 2005, Strumpf *et al*. 2005). Over-expression of Oct4, on the other hand, induces commitment to extra-embryonic endoderm and mesoderm lineages (Niwa *et al.* 2000). Overall, a strict regulation of Oct4 levels is required in the pre-implantation embryo. During early gestation, LIF is secreted from the oviduct and the extra-embryonic primitive endoderm layer forms in the blastocyst (Shen & Leder 1992). A balance between Nanog and Gata4/Gata6 expression determines commitment to the primitive endoderm lineage (Fujikura *et al*. 2002, Mitsui *et al*. 2003, Capo-chichi *et al*. 2005). ES cells lacking Nanog will spontaneously differentiate into primitive endoderm (an effect also seen with forced over-expression of Gata4 or Gata6) (Mitsui *et al*. 2003, Chambers *et al*. 2003, Fujikura *et al*. 2002) and the over-expression of Nanog can promote mouse ES cell self-renewal in the absence of LIF (Mitsui *et al*. 2003). Sox2 plays an important role in early embryonic development through interaction with Oct4

at promoters, though expression of this factor is not restricted to pluripotent cells (Avilion *et al*. 2003).

Pre-gastrulation events involve rapid proliferation, intense differentiation and specific migration of cells, which is governed by expression of specific genes. The emergence of the three primary germ layers occurs at gastrulation. These are the definitive ectoderm, mesoderm and definitive endoderm. Germ layers eventually give rise to all an animal's tissues and organs through the process of organogenesis. The derivatives of these germ layers are presented in Table 1.3. The formation of primitive ectoderm and differentiation into the primary germ layers requires the withdrawal of LIF (Shen & Leder 1992, Murray & Edgar 2001). Repression of *Rex1* and the up-regulation of *FGF5* are associated with development of the primitive ectoderm (Haub & Goldfarb 1991, Rogers *et al.* 1991, Hebert *et al.* 1991), which will eventually form the epiblast following mass apoptosis and cavitation (Coucouvanis & Martin 1995). Primitive ectoderm cells at this point are still pluripotent, but cannot contribute to chimera formation following injection into blastocysts (Rossant & Ofer 1977, Beddington 1983). The epiblast responds to extrinsic signals to give rise to the primary germ layers as well as primordial germ cells (Gardner & Rossant 1979, Ginsburg *et al.* 1990). The primary germ layers in the embryo are formed during the onset of gastrulation around E6.5-7.0 (Tam & Behringer 1997). The primitive streak arises upon gastrulation with complete Oct4 repression being evident at this point. Differentiation into mesoderm and definitive endoderm occurs by epiblast cell movement through the posterior and anterior streak respectively, where epithelial-to-mesenchymal transition (EMT) of cells

occurs. Cells in the most anterior region of the epiblast do not move through the primitive streak and will form ectoderm (Tam & Behringer 1997, Kinder *et al*. 1999). All these processes are thought to involve interplay of the expression of Tgfβ family genes including BMP4 and Nodal, and the Wnt and FGF families. It is important to note that Oct4 continues to be expressed in the primordial germ cells and maturing oocytes of the female (Holland & Hogan 1988, Rosner *et al*. 1990).

ECTODERM	MESODERM	ENDODERM
• Epidermis of the skin and derivatives (hair, nails, sweat glands, sensory receptors) • Nasal, oral epithelium • Nervous system • Cornea and lens of eye • Adrenal medulla • Posterior pituitary • Tooth enamel	• Notochord • Skeletal system • Muscular system • Muscle layer of stomach and intestine • Excretory system • Circulatory and lymphatic systems • Urogenital system (except germ cells) • Dermis of skin • Lining of body cavity • Adrenal cortex	• Digestive tube (except for mouth, pharynx, end of rectum) • Lining of urinary bladder and urethra • Thymus • Thyroid gland • Anterior pituitary gland • Accessory digestive organs (pancreas, liver, gallbladder) • Auditory structures • Epithelial lining of respiratory system

Table 1.3. A list of the tissues in mammals that originate from each primary germ layer of the early embryo.

1.8.6 *In vitro* differentiation of ES cells

The assays of *in vitro* differentiation aim to recapitulate early embryogenesis, where an intricate series of morphological and molecular changes occur. The ability to differentiate ES cells to generate various lineages under appropriate conditions in

culture provides a valuable tool to study early precursor populations that are difficult to access *in vivo* (Doetschman *et al*. 1985, Risau *et al*. 1988, Wiles & Keller 1991, Millerhance *et al*. 1993, Rohwedel *et al*. 1994, Bain *et al*. 1995). The mechanisms of emergence of the three embryonic germ layers may be analysed in cell culture by generation of embryoid bodies (EBs) from ES cells (Doetschman *et al*. 1985, Keller 1995, Coucouvanis & Martin 1995). *In vivo* analysis of gene function is complicated if the gene deletion results in early embryonic lethality, therefore the study of gene function during these stages may be done in culture.

Three approaches can be used to initiate the formation of the three primary germ layers *in vitro.* Aggregation of ES cells as 'hanging drops' in the absence of LIF to form embryoid bodies is the most common method. This involves initial formation of primitive endoderm as the outer layer of EBs and subsequent differentiation as three-dimensional structures (Shen & Leder 1992). The second method involves culturing ES cells on stromal cells, such as the OP9 cell line, where differentiation takes place in contact with these cells (Nakano *et al.* 1994). Thirdly, ES cells can be differentiated in a monolayer on extracellular matrix proteins (Nishikawa *et al.* 1998). In addition to this method of *in vitro* differentiation, other techniques can be used including simple removal of LIF and serum (BMP4) to induce spontaneous differentiation, as well as the addition of factors such as retinoic acid, Wnt proteins, PPARγ and insulin to stimulate differentiation towards specific lineages. LIF withdrawal relieves cells of inhibitory effects of STAT3 on mesoderm differentiation and BMP4 withdrawal reduces inhibitory effects of Id proteins on neuroectoderm differentiation.

ES cell aggregation in the EB simulates early embryonic pre-gastrulation events. The withdrawal of LIF stimulus is not required here and is supported by the observation that primitive endoderm can form by ES cell aggregation in the presence of LIF (Shen & Leder 1992, Murray & Edgar 2001, Hamazaki *et al*. 2004). EB differentiation in the absence of LIF allows recapitulation of development from the primitive ectoderm in the epiblast. Cells with characteristics of primitive ectoderm (FGF5-positive; Rex1-negative) have in fact been identified in culture by growth in conditioned media from hepatocellular carcinoma cell lines. These cells, named early primitive ectoderm-like (EPL) cells, can be differentiated into EBs and have been seen to form mesoderm and derivative cell populations more efficiently and rapidly than ES cells (Rathjen *et al*. 1999, Lake *et al*. 2000). The point of gastrulation in the embryo is thought to be represented at about day 3 in EB differentiation, even though the development of a structure comparable to the primitive streak does not occur (Figure 1.11). At this point, in both systems, *Brachyury (T)* expression can be observed (section 1.8.7). The regulation of germ layer induction is now understood to be influenced by the mixture of growth factors and inhibitors present in serum, as well as additional factors that can be supplemented in the culture media. Adding BMP4 can induce posterior mesoderm derivatives; a gradient of activin/Nodal signalling from low to high is implicated in mesoderm and definitive endoderm induction, respectively; and FGF will drive neuroectoderm formation, with Wnt, BMP4 and activin inhibiting early stages of this pathway (for more details see Keller 2005).

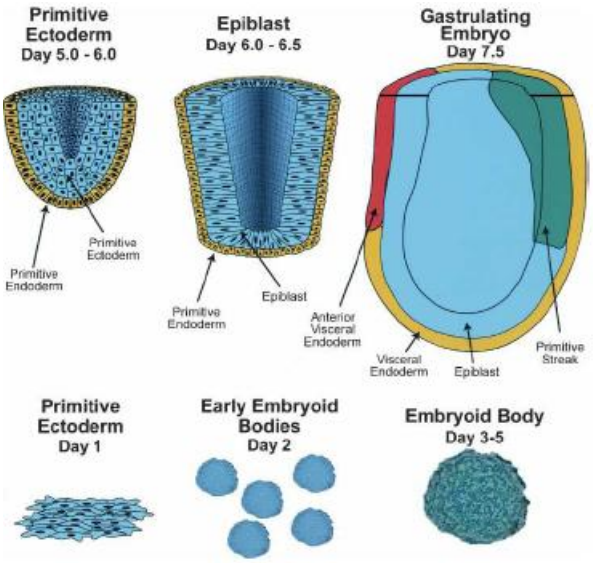

Figure 1.11 Comparison of the stages of early embryonic development and EB differentiation of ES cells. Primitive ectoderm forms from ES cells when LIF exposure is removed (or when cultured as EPL cells) and represents accumulation of this cell type in the embryo and formation of the epiblast at E6.0. Gastrulation occurs around E6.5, which indicated by *Brachyury* expression in the primitive streak. *Brachyury* is upregulated in EBs at day 3 of culture. Figure from Keller 2005.

The examination of lineage differentiation in EBs can be performed using certain well-established markers. Visceral and parietal endoderm arises from the primitive endoderm and markers include *Gata4*, *Gata6*, *hepatocyte nuclear factor (HNF)* family genes, *alpha-fetoprotein (AFP)* and *transthyretin* (*TTR*). *Wnt3* and *Brachyury* are common markers of mesoderm (Fehling *et al*. 2003, Liu *et al.* 1999) and *FGF5* is a strong primitive ectoderm marker (Haub & Goldfarb 1991, Hebert *et al.* 1991). Presence of distinct lineages in EBs can be analysed by harvesting RNA and measuring transcript abundance of these genes. Additional markers are well established, many of which have been used in this study to test the presence of primary lineages and more restricted lineages, such as cardiomyocyte, muscular, haematopoietic and neuronal lineages (Figure 1.12).

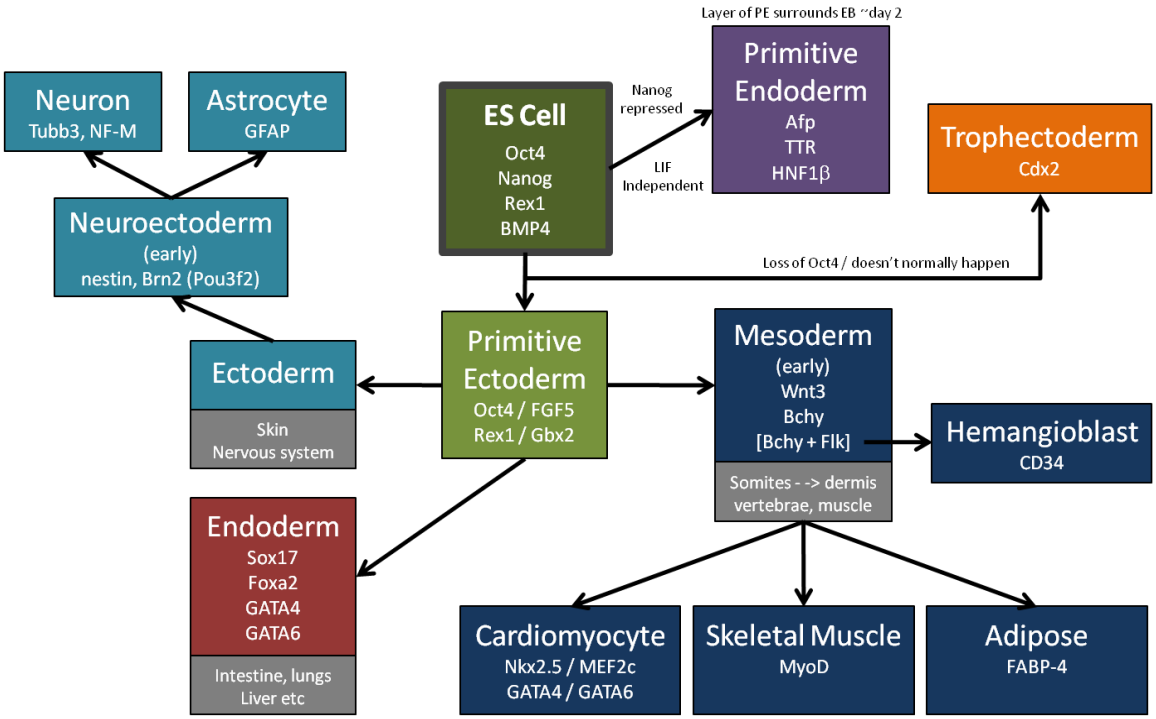

Figure 1.12 Markers of lineage differentiation in embryoid bodies. ES cells express Oct4, Nanog and Rex1. The primitive endoderm and trophectoderm constitute the extra-embryonic tissues of the late blastocyst and trophectoderm can differentiate into a variety of extra-embryonic cell types, including placenta. Primitive endodermal cells constitute the surrounding layer of EBs as Nanog is repressed. AFP, TTR and HNF1b are up-regulated in these cells. Oct4 and FGF5 expression with Rex1 and Gbx2 repression is exhibited in the primitive ectoderm (which constitutes the pluripotent population of cells derived from the ICM). Definitive endoderm, mesoderm and ectoderm arise from these cells as gastrulation occurs at E6.5-7.0 in the embryo. Sox17, Foxa2, Gata4 and Gata6 expression signifies definitive endoderm in EBs. Early mesoderm markers include Wnt3 and Brachyury (T). Specific mesodermal lineages and markers are indicated. The neuroectoderm develops from ectoderm, where Nestin and Pou3f2 are expressed. Further neural markers include β-III tubulin (Tubb3), NF-M and GFAP.

1.8.7 Mesoderm development

Mesoderm induction occurs through formation of the primitive streak. It differentiates to give rise to a number of tissues and structures including bone, cartilage, muscle, adipose tissue, connective tissue (including that of the dermis), blood, vascular, reproductive, excretory and urinogenital systems and some glands

(Table 1.3). The development of the haematopoietic system, derived from mesoderm, is the most thoroughly analysed developmental program. Mesodermally-derived cell populations representing the hematopoietic, vascular, cardiac and skeletal muscle, the osteogenic, the chrondrogenic and adipogenic lineages have been generated from ES cells differentiated in culture. The hematopoietic, vascular and cardiac lineages have been among the easiest to generate from ES cells and have been studied in considerable detail. The first mesodermal cells contribute predominantly to the haematopoietic and vascular cells of the yolk sack. In fact, hematopoietic progenitors are found in the developing yolk sac as early as E7.0, approximately 12 hours following the beginning of gastrulation (Keller 2005).

The embryo and EB systems display an extremely similar sequence of events with regards to this development, as defined by the onset of expression of specific genes. The *Brachyury (T)* gene encodes a transcription factor that is essential for mesoderm development and correct development of the primitive streak and notochord morphogenesis in the embryo (Wilkinson *et al.* 1990, Kispert & Herrmann 1994). *Brachyury* mutant mice have defective tail development (Herrmann *et al*. 1990, Wilkinson *et al.* 1990). *Brachyury* transcript and protein are present in the primitive streak from the onset of gastrulation (E6.5) and this expression persists in the streak throughout the period of axis formation and elongation (Kispert & Herrmann 1994). *Brachyury* is down-regulated as cells undergo patterning and specification into derivative tissues including skeletal muscle, cardiac muscle, blood and endothelium. *Brachyury* has often been used to track mesoderm induction during ES cell

differentiation. Expression is barely detectable in undifferentiated ES cells until induced at day 5 of differentiation, and is silenced by day 10 (Keller *et al*. 1993).

1.9 Chromatin state of ES cells and changes upon differentiation

1.9.1 ES cell chromatin state

ES cell chromatin displays characteristics of transcriptionally permissive euchromatin, such as the abundance of acetylated histones and increased accessibility to nucleases (Boyer *et al.* 2006*)*. Analysis of global chromatin dynamics, by measuring the exchange rate of chromatin-associated proteins using fluorescent recovery after photobleaching (FRAP), has revealed a far more dynamic association of structural chromatin proteins (core and variant histones, linker histones and HP1α) within the chromatin of pluripotent cells compared to that of differentiated cell types (Phair *et al.* 2004, Meshorer *et al.* 2006). These increased rates reflect loose binding of proteins to chromatin, rendering it more accessible to transcription factors and histone modifiers. This study also showed that replacement of histone H1 with a version that binds more tightly to chromatin inhibited ES cell differentiation, indicating that this feature of ES cell chromatin enables rapid reorganisation of chromatin structure during differentiation (Meshorer et al. 2006). Core pluripotency factors induce the expression of chromatin remodelers (*SMARKD1*), H3K4 KMTs (*MLL*) and HATs (MYST) to maintain a 'transcriptionally-permissive' chromatin state (Boyer *et al.* 2005). Expressed genes in ES cells (including pluripotency factors and active genes bound by these factors) expectedly have hyperacetylated histones and are enriched for H3K4me3 with minimal H3K9me3 modification and less promoter CpG DNA methylation than somatic cells (Mikkelsen *et al.* 2007, Kim *et al.* 2008, Fouse *et al.* 2008) (Figure 1.13). The identification that lineage-specific genes, which are silent in undifferentiated ES cells, might be in a semi-permissive transcriptional state was an

initial suggestion this 'open' chromatin state is not just conveyed by expressed genes, but it is also a feature of inactive genes (Chambeyron *et al*. 2005, Szutorisz *et al*. 2005).

1.9.2 Bivalent domains

Two reports soon revealed the existence of a dual chromatin mark or 'bivalent' domain, consisting of the repressive H3K27me3 modification and the active H3K4me3 modification, at a large set of developmentally important genes that are not expressed in ES cells but activated upon differentiation (Azuara *et al.* 2006, Bernstein *et al.* 2006). At these gene promoters, the active mark is physically present at the same or adjoining nucleosomes as repressive chromatin marks. This domain is unique to ES cells in order to maintain lineage-specific genes in a quiescent or 'poised' state. It ensures that no gene is truly off, as ES cells must have the capacity to rapidly induce the expression of appropriate genes to become any cell type. The chromatin state at these genes is transcriptionally-permissive, though the genes are not expressed. The plastic chromatin state reflects that approximately a quarter of all CpG island-containing promoters in ES cells are poised for activation, through the nature of the bivalent modification (Mikkelsen *et al*. 2007, Pan *et al*. 2007, Ku *et al*. 2008). In addition to these histone marks, initiated RNA polymerase II, phosphorylated at serine 5 of its C-terminal domain, is found associated with these bivalent promoters; this is important in conferring the poised nature of genes (Stock *et al.* 2007). The presence of H3K27me3 is important in establishing this state, as this poised RNA polymerase configuration is enforced by PRC1-mediated ubiquitination of histone H2AK119 (section 1.3.2). As ES cells differentiate, rapid induction of 'poised' genes essential for cell-type specialisation is enabled by resolution into a H3K4me3 univalent chromatin

state and thus removal of PcG-imposed restraints on transcriptional elongation (Figure 1.13) (Bernstein *et al*. 2006a, Mikkelsen *et al*. 2007, Stock *et al*. 2007). On the other hand, tissue-specific genes associated with alternative developmental pathways will be resolved into a H3K27me3 univalent state and therefore silenced upon differentiation (Azurara *et al.* 2006, Bernstein *et al.* 2006) (Figure 1.13).

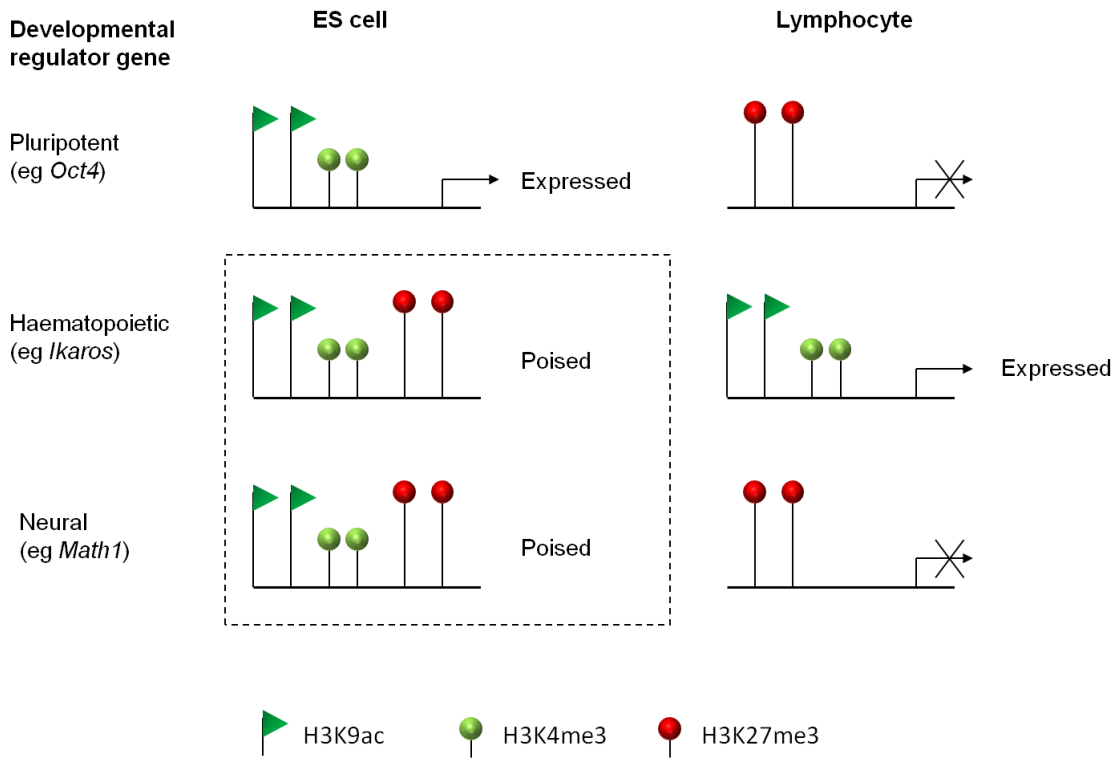

Figure 1.13 The bivalent chromatin domain in ES cells. In ES cells, the promoters of a range of repressed developmental genes contain conflicting modifications that are either associated with active chromatin states (H3K4me2/me3) or inactive chromatin states (H3K27me3). These genes are poised for expression in response to the appropriate developmental cue. ES cell differentiation corresponds with resolution of the bivalent state to a univalent methylation state, leading to either activation of required tissue-specific genes or silencing of loci associated with alternative developmental pathways.

The PcG and TrxG proteins have predominantly been implicated in 'cellular memory' in order to maintain repressed or active transcriptional states of developmentally

important genes through many rounds of cell division (Ringrose & Paro 2004). However, over the last five years it has become clear that chromatin state is equally as important as core pluripotency factor expression in regulating the ES cell transcriptional profile, where the inability to maintain H3K27me3 results in large alterations in the ES cell transcriptional profile (Boyer *et al*. 2006, Lee *et al*. 2006, Bracken *et al.* 2006, Surani *et al.* 2007). This indicates that the transcriptional switches required upon ES cell differentiation are governed by histone-modifying enzymes. Deletions of PRC2 components results in de-repression of developmental transcription factor genes, including *HOX* genes, and often lead to spontaneous differentiation of ES cells, early embryonic lethality and failure to derive ES cells from the ICM (Cao & Zhang 2004, Azuara et al. 2006, Boyer et al. 2006, Lee et al. 2006, Agger et al. 2007). Moreover, removal of the PRC1 component, RING1B, which restrains RNA polymerase II in a poised state, results in de-repression of bivalent genes, emphasising the essential requirement for downstream implementers of the H3K27me3 modification (Stock *et al*. 2007). Overall, around 500 transcription factors with roles in a variety of developmental processes have bivalent genes and are bound by PcG complexes (Bernstein *et al*. 2006a, Boyer *et al.* 2006, Fouse *et al.* 2008, Ku *et al*. 2008). Localisation of PcG complexes to these genes is regulated by pluripotency factors, Oct4, Nanog and Sox2 (Loh *et al.* 2006, Boyer *et al.* 2005a) (section 1.8.3). A recent study in human ES showed that LSD1 is important in regulating H3K4 methylation levels at bivalent genes, which is mediated by Oct4 and Nanog association (Adamo *et al.* 2011).

1.9.3 Chromatin changes upon ES cell differentiation

ES cell differentiation requires a co-ordinated change in gene expression programmes in order to restrict the new cell type to a particular lineage and diminish the capacity to self-renew. This restriction in developmental potential is associated with reorganisation of the transcriptional profile and a marked decrease in genome plasticity. As chromatin state closely reflects transcriptional state in ES cells, proteins involved in the chromatin regulation serve an important function in differentiation. The feature that lineage-specific genes are cued for activation upon differentiation by chromatin modification also emphasises the importance of histone-modifying enzymes. Change in chromatin state necessitates the activation of some genes and repression of others; hence, components of histone modification complexes are often essential for development with knockout mice displaying embryonic lethality (Hendrich *et al.* 2001, O'Carroll *et al.* 2001, Lagger *et al.* 2002, Dodge *et al*. 2004, Pasini *et al*. 2004, Cowley *et al*. 2005, Kaji *et al*. 2006, Wang *et al*. 2007, Foster *et al.* 2010)

The pluripotency genes *Oct4* and *Nanog* are associated with low levels of H3K27me3 in ES cells, consistent with their high expression (Boyer *et al*. 2006). Although these genes become silenced upon ES cell differentiation, H3K27me3 levels at these genes appear not to change significantly (Hattori *et al.* 2004, Boyer *et al*. 2006, Feldman *et al.* 2006). The accumulation of methylation at H3K9 and histone deacetylation underpins the repression of *Oct4*, where ChIP analysis of the *Oct4* promoter region in ES cells and P19 embryonic carcinoma cells shows a dramatic increase of H3K9 methylation and a concomitant decrease of H3K4 methylation and H3K9 acetylation during the first 48

hours of differentiation (Lee *et al.* 2004a, Feldman et al. 2006). The orphan nuclear receptor GCNF is known to mediate *Oct4, Nanog* and *Sox2* repression through direct promoter binding, and depletion of GCNF prevents the repression *Oct4* upon differentiation (Fuhrmann *et al.* 2001, Gu *et al.* 2005). Ultimately, the critical mechanism in *Oct4* repression was identified in the Bergmann laboratory; which is the targeting of the H3K9 KMT (G9a) to the *Oct4* locus to initiate the facultative heterochromatinisation via the binding of HP1α and for subsequent de novo methylation at the promoter by the enzymes Dnmt3a/3b (Feldman *et al.* 2006). However, subsequent work from the same lab demonstrated that a point mutation in the G9a SET domain prevents heterochromatinisation, but still allows *de novo* methylation and silencing of *Oct4* (Epsztejn-Litman *et al.* 2008). This is because G9a itself is capable of bringing about *de novo* methylation through recruitment of Dnmt3a and Dnmt3b by its ankyrin domain (Epsztejn-Litman *et al.* 2008). The accumulation of H3K9me3 is crucial for the repression of *Nanog*, where down-regulation of *Nanog* expression is facilitated through decrease in expression of H3K9-specific KDMs, JMJD1a and JMJD2c, which are activated by Oct4 binding (Loh *et al.* 2007).

Ablation of the HDAC-containing NuRD complex also restricts the ability to repress *Oct4,* where *Mbd3*$^{-/-}$ ES cells fail to differentiate upon removal of LIF (Kaji *et al.* 2006). This requirement for HDAC-containing repressor complexes for stem cell factor repression is also emphasised by the report of prevention of differentiation in ES cells treated with the an HDAC inhibitor (TSA) and the re-activation of the *Oct4* gene in trophoblast stem cells cultured with TSA (Hattori *et al.* 2004, Lee *et al.* 2004a).

Conversely, the mSin3A/HDAC complex positive regulates *Nanog* expression to maintain *Nanog* expression in ES cells, where the knockdown of mSin3A, but not HDAC1 and 2 alone, reduces *Nanog* expression (Baltus *et al.* 2009). This shows that the co-repressor is essential for regulating the dynamics of histone acetylation at the *Nanog* locus. Recent data from our lab has shown that HDAC1 is required to restrict developmental gene expression. The deletion of HDAC1 in ES cells, which results in reduced deacetylase activity associated with the Sin3A, NuRD and CoREST complexes, causes precocious differentiation into mesodermal and ectodermal lineages in EBs (Dovey *et al.* 2010b). These data underpin the need for further understanding of the role of LSD1/CoREST/HDAC complex in ES cell gene expression, especially as deletion of LSD1 in the mouse results in embryonic lethality at a similar time to *Oct4, Nanog* and *Sox2* (Nichols *et al.* 1998, Avilion *et al.* 2003, Mitsui *et al*. 2003). In fact, LSD1 and CoREST are known to directly bind *Oct4* in P19 embryonic carcinoma cells (derived from the primitive ectoderm cells of the epiblast) and inhibition of LSD1 demethylase activity with a non-selective monoamine oxidase inhibitor shows de-repression of *Oct4,* accompanied by an increase in H3K4me2 (Lee *et al.* 2006). This data implies a potential role for LSD1 in facilitating the repression of *Oct4* upon ES cell differentiation. This justifies an investigation of HDAC-containing complex function in embryonic gene regulation.

Changes in development-specific gene expression are equally important as changes in pluripotency factor expression in defining new transcriptional networks upon ES cell differentiation. Expressional fates of these genes are also mediated through changes

in chromatin state and often operate through the bivalent chromatin domain at gene promoters. The rapid switch of transcriptional states in response to developmental cues relies on manipulation of H3K4 and H3K27 methylation at the appropriate genes. *HOX* genes are well characterised bivalent genes and TrxG and PcG proteins are well-known regulators of these genes (Ringrose & Paro 2004, Schuettengruber *et al*. 2007). A decrease in the H3K27me3 mark during ES cell differentiation is mediated through down-regulation of pluripotency factors, whose expression is required to recruit PcG complexes (containing H3K27 KMT activity) to a significant subset of promoters (Lee *et al.* 2006). As LSD1 has been identified as a binding protein of Oct4 in ES cells, it would follow that Oct4 expression can direct LSD1-mediated gene repression to a subset of developmental gene promoters in pluripotent cells (Pardo *et al.* 2010). Down-regulation of Oct4 would facilitate the removal of LSD1/CoREST/HDAC from these promoters upon differentiation, corresponding with an increase in H3K4 methylation and gene expression. Thus, the genomic targeting of H3K27- and H3K4-specific repressor complexes by core pluripotency factors may operate in concert to repress developmental genes in pluripotent cells. In fact, the recently discovered H3K27me3 KDM (UTX) is found to associate with MLL2/3 complexes, revealing a mechanism for transcriptional activation of developmental genes involving cycles of H3K4 methylation by MLL2/3 linked to the demethylation of H3K27me2/me3 (Agger *et al*. 2007, De Santa *et al.* 2007, Lee *et al.* 2007b). Overall, ES cell and embryonic loss of function analyses of the H3K27-specific KMT, such as EZH2, may be comparable to loss of function analyses of LSD1; an early indicator being that EZH2, SUZ12, EED and LSD1 knockout mice die during the post-implantation period of embryogenesis, displaying severe developmental defects (Faust *et al*. 1995, O'Carroll *et al*. 2001, Pasini *et al.* 2004, Wang

et al. 2007). This knowledge underpins investigation of LSD1 function within ES cells, which are equivalent to the embryonic epiblast, in order to understand the cause of developmental arrest in the absence of LSD1. The expectation would be to identify overlap in genes that are de-repressed in the absence of PRC2 components and LSD1.

2 Materials and Methods

2.1 Chemicals and reagents

All commonly used stocks, solutions and buffers were prepared as outlined in Current Protocols in Molecular Biology, Ausubel *et al.* 1994-1998 (Wiley). Unless otherwise stated, all chemicals were supplied by Sigma Aldrich or Fisher Scientific, analytical grade or higher.

2.2 Generation of LSD1 knock out mouse

The LSD1 knock out mouse was generated by Dr Shaun Cowley in the Bradley lab. An E14 murine embryonic stem (ES) cell line containing a genetrap construct in the *Lsd1* gene locus (clone X102) was obtained from the Sanger Institute Gene Trap Resource (www.sanger.ac.uk/resources/mouse/sigtr/).

2.3 Growth and maintenance of mouse ES cells

The constituents of all reagents used in tissue culture are listed in 2.3.9.

2.3.1 Culture of ES cells

The majority of cellular analysis in this thesis was performed on the E14 mouse ES cell line (hereby referred to as ES cells), kindly supplied by David Adams. ES cells were grown on tissue culture grade plates from NUNC. Plates were coated in 0.1% Gelatin solution in PBS for ES cell adherence. ES cells were maintained in an undifferentiated state by culture in standard ES cell medium (M15+LIF) and were grown in a 5% CO_2 incubator at 37°C. ES cells were monitored daily and media was changed when the phenol red indicator in the media turned orange (indicating pH change due to build up of respiration waste products).

2.3.2 Passage of ES cells by trypsinisation

Culture media was aspirated and cells were washed twice with room temperature PBS. For cells in a 10cm plate, 3ml trypsin solution was added and the cells were incubated at 37°C for 5min. 3ml of ES cell medium was added to neutralise the trypsin and the suspension was passed through a pipette several times to disaggregate the cells. The cells were centrifuged for 5min at 1200rpm, the supernatant aspirated, and the pellet was re-suspended in an appropriate volume of ES cell medium for splitting into new gelatinised plates. Newly plated cells were shaken from side-to-side in the plate to ensure an even dispersal of cells in the dish.

For splitting of 96 well plates, 50µl of trypsin was used and 150µl of ES cell medium added for inactivation after the 5min incubation at 37°C. 150µl fresh media was added to the wells of the new gelatinised 96-well plates. Cells were disaggregated by pipette and a 1:4 split of the 200µl volume into the new plates was usually employed.

2.3.3 Long term storage of ES cells

2.3.3.1 Freezing in cryovials

ES cells were frozen back when approximately 70% confluent in tissue culture plates. Roughly $5x10^6$ cells were stored in each freezing vial in order to be revived into 10cm plates as a 1:3 ratio split. In this instance, cells cultured on 6cm plates were frozen as individual aliquots for 10cm plate revival (due to a 1:3 surface area ratio between 6cm and 10cm plates). Cells were trypsinised as described in 2.3.2 and resuspended in 0.5ml ES cell medium and 0.5ml 2X freezing media per freezing aliquot. 1ml aliquots were transferred to 1.5ml cryovials. Controlled freezing of cells at 1°C/min was required, therefore vials were inserted into freezing pots filled with iso-propanol and placed at -80°C. After 24-48hr, cryovials were transferred to liquid nitrogen storage racks.

2.3.3.2 Freezing in 96-well plates

As with larger plates, ES cells were frozen back when approximately 70-80% confluent. 50µl trypsin was added to the wells as in 2.3.2 and 50µl 2X freezing media was used to inactivate the trypsin following incubation. Cells were pipetted up and down, and

then the plate and lid were secured with tape and blue roll before freezing at 1°C/min within a Tupperware in the -80°C freezer.

2.3.4 Revival of cells from frozen aliquots

Cryovials were removed from liquid nitrogen as required and thawed rapidly in a 37°C water bath (the caps of the vials were loosened upon removal otherwise the vials were likely to explode). The 1ml of thawed cells was transferred to 5ml of pre-warmed ES cell medium in a 15ml falcon and centrifuged at 1200rpm for 5min to remove the DMSO-containing freezing media. The cell pellet was re-suspended in ES cell medium and plated on gelatine-coated plates as described in 2.3.1.

2.3.5 Extraction of DNA from ES cells

2.3.5.1 Extraction in from cells in 96-well plates

Cells were grown beyond confluency for genomic DNA harvesting in 96 well plates. DNA was prepared by incubating cells in the wells at 55°C overnight in a humidity chamber with 50µl lysis buffer followed by precipitation with 50µl isopropanol and two washes with 70% ethanol. Precipitation of DNA in the bottom of the well was achieved by vigorous shaking of the plate and careful decanting of the liquid onto paper towel.

2.3.5.2 Extraction from cell pellets

The cell pellet from a 6-well plate was incubated in 200μl cell lysis buffer by rotation in the 55°C oven overnight. Addition of 200μl isopropanol and spooling of DNA was possible to precipitate DNA, which could be transferred by a pipette tip to new tubes for washing with 70% ethanol. DNA was air-dried and re-dissolved in 100μl TE. 20-fold dilution was further required for PCR with 1μl of DNA.

2.3.6 Extraction of RNA from ES cells and Embryoid bodies (EBs)

All chemicals and equipment used in RNA extraction were RNA grade and kept free of RNAses by treatment with RNAseZap spray (Ambion). ES cells were harvested in 6-well plates and EBs were collected in 1.5ml Eppendorf tubes for harvesting. Multiple samples within a single experiment were routinely collected by harvesting in TRIzol reagent and stored at -80°C until RNA extraction. For ES cells, 1ml of TRIzol was used per $1x10^7$ cells. TRIzol was left on the plate for 5min before transfer to a 1.5ml Eppendorf. The amount of TRIzol used for EBs was more arbitrary as exact cell numbers were unknown; though 1ml TRIzol was often used per 15cm dish of EBs. Day 12-15 cultured EBs required further disruption with a handheld homogeniser. Three 10sec high speed pulses with 20sec pauses between was often sufficient to break up the EBs.

Following thawing of -80°C-stored samples, 10min incubation at 37°C was allowed before addition of chloroform (1/5 volume of the TRIzol reagent used). Samples were

inverted 10 times and left to stand at RT for 5min. The samples were then transferred to Phase Lock Gel Heavy Tubes (5 Prime, Hamburg, GmbH) and centrifuged for 15min at 13000rpm at 4°C. The top aqueous phase was carefully decanted into a 1.5ml Eppendorf. An isopropanol volume equal to half that of the starting TRIzol volume was added and tubes were inverted several times. Samples were left at 4°C for 30min then centrifuged for 15min at 13000rpm at 4°C. The supernatant was removed, the RNA pellet washed once in 70% EtOH, and centrifuged again for 10min at 7500rpm at 4°C. The supernatant was removed and the pellet left to air-dry for 10min. DEPC H_2O was used to re-dissolve the RNA, the volume of which depended on the quantity of RNA. This volume was adjusted to normalise RNA concentrations following Nanodrop™ quantification of nucleic acid. 37°C incubation and agitation ensured complete dissolving of the RNA. Samples were snap-frozen for -80°C storage before use. Phenol-choroform cleanup of the RNA was often employed.

2.3.7 Media and reagents used for ES cells and EB manipulations

M15+LIF ES cell media

Knockout DMEM + L-Glucose –Pyruvate (GIBCO)	500ml
Fetal Calf Serum (Hyclone)	90ml
100X Glutamine/Penicillin/Streptomycin	6ml
100mM β-mercaptoethanol	600μl
Leukaemia Inhibitory Factor (Synthesised In House)	50μl

EB media

Knockout DMEM + L-Glucose –Pyruvate (GIBCO)	500ml
Fetal Calf Serum	90ml
100X Glutamine/Penicillin/Streptomycin	6ml

MEF media (M10)

DMEM + L-Glucose –Pyruvate (GIBCO)	445ml
Fetal Calf Serum	50ml
Glutamine/Penicillin/Streptomycin 100X (GIBCO)	5ml

2.5% trypsin solution

PBS (GIBCO)	500ml
0.5M EDTA	500µl
Trypsin solution (Invitrogen)	20ml
Chicken serum (Invitrogen)	5ml

Trypsin was stored in 40ml aliquots at -20°C

2X Freezing Media

Knockout DMEM (GIBCO)	60%
Fetal Calf Serum (Hyclone)	20%
DMSO (Invitrogen)	20%

0.1% Gelatin

PBS (GIBCO)	500ml
2% Bovine gelatin solution	25ml

Retinoic acid differentiation media

M15+LIF	600ml
100mM ATRA	60μl (10μM working concentration)

N2B27 differentiation media

Knockout DMEM/F12 (GIBCO)

N2 supplement (Invitrogen)

B27 supplement (Invitrogen)

Cell lysis buffer

50mM Tris-HCl

100mM NaCl

10mM EDTA

1% SDS

0.2mg/ml Proteinase K

2.4 Polymerase Chain Reaction (PCR)

PCR was performed routinely to amplify DNA fragments for a variety of purposes including genotyping ES cells and mice, cloning, generation of DNA probes, screening transformed bacteria, gene expression analysis and fragment enrichment in chromatin immunoprecipitation (ChIP) experiments. Thermo Taq (Thermo Scientific) was often used for genomic PCR and bacterial screens; High Fidelity Platinum *Taq* (Invitrogen) or KOD polymerase (Novagen) was often used in cloning; Universal probe library (Roche) reagents were used for quantitative real-time PCR in gene expression analysis. A standard genomic PCR program is shown below:

95°C	2min	
95°C	30sec	⎫
Annealing temp	30sec	⎬ 35 cycles
72°C	30sec	⎭
72°C	5min	
12°C	∞	

A typical 25µl PCR reaction mix consisted of:

10X Buffer	2.5µl
$MgCl_2$	1.5µl
dNTPs	0.15µl
5'primer	0.25µl
3'primer	0.25µl
Taq	0.1µl
ddH_20	21µl

2.5 Transfection of ES cells

2.5.1 Transfection of ES cells by electroporation

$1x10^7$ cells were electroporated in 800μl of ES cell media with 10μl and 30μl of linearised targeting vector (from 50μl elution following gel purification) within a 0.4ml cuvette (Biorad). Electroporation was performed at 0.23V and 500μF with a routinely recorded time constant of 8.0.

2.5.2 Transfection of ES cells by lipofection

Transfection with Lipofectamine 2000 (Invitrogen) was performed in 6-well plates. $1x10^6$ cells were plated the night before transfection. Media was changed the next morning and transfection reagents were set up. 6-10μl of Lipofectamine was added to 250μl of knockout DMEM in an Eppendorf and left for 5min. Meanwhile, 2-2.5μg DNA was added to 250μl DMEM in a separate Eppendorf. The two volumes were combined together and mixed by tapping. Lipofection complexes were left to form over 20min before the mixture was pipetted drop-wise into the culture media. For transfection in 6cm plates, all the reagents were scale-up 2-fold.

2.6 Generation of conditional LSD1 knock-out ES cell lines

Specific details of the *Lsd1* gene targeting strategy are described in Chapter 3. Targeting vector electroporation methodology is described in 2.5.1.

2.6.1 pCAGGS-Flpe vector transfection

Removal of the selection cassette by *FRT* site recombination required expression of the FLP recombinase in the cells. A fresh maxiprep of the pCAGGS-FLPe plasmid (Buchholz *et al.* 1998) was made as described in section 2.13.6. The plasmid was verified by *Hind*III restriction enzyme digestion to produce 6426bp and 1302bp bands. Transfection of the plasmid was performed on ES cells in a 6-well plate using Lipofectamine 2000 as described in section 2.5.2. 48hr after transfection the cells were trypsinised and seeded at two different quantities of 20000 and 5000 cells in 10cm plates in the presence of 1-(2-deoxy-2-fluoro-1-D-arabinofuranosyl)-5-iodouracil (FIAU).

2.6.2 ES cell colony screening

2.6.2.1 Targeted ES cell colony growth and colony picking

Following electroporation with the targeting vector, 5000 and 20000 ES cells were plated in M15+LIF. The following day, selection drug was added to the culture media and colonies were grown over 10-12 days until picking and screening for correct allele targeting. For *Lsd1* gene targeting, hygromycin was added to the media to a concentration of 100μg/ml. When colonies were of sufficient size, 96 were picked in

7ml PBS under the phase contrast microscope and transferred into 50µl trypsin in wells of a 96-well round-bottomed plate. Cells were allowed to trypsinise until 50µl of M15+LIF was added to each well and the total volume of each well was transferred to 96-well for culture. Selected ES cells were grown for 3 days until passage into three 96-well plates. Two plates were allowed to grow to high confluence for DNA preparation, with one plate frozen down in the -80°C freezer at 80% confluence. These frozen cells would be recovered appropriately once targeted clones had been identified by Southern blotting.

2.6.2.2 'HygΔTK' cassette-removed ES cell growth and colony picking

Negative selection of clones containing the cassette was achieved by growing colonies in the presence FIAU over 10-12 days. This drug selected for cells that did not express thymidine kinase from the *HygΔTK* gene. Surviving colonies were picked as before and cultured until passage for DNA preparation followed by Southern blotting and freezing back. Six positive clones were selected for propagation into the $Lsd1^{Lox/\Delta 3}$ cell lines.

2.6.3 Deletion of exon 3 (*Δ3*) from the targeted allele

Six targeted clones were revived into wells of 24-well plates and cultured for generation of stocks of $Lsd1^{Lox/\Delta 3}$ cell lines. Once sufficient stocks had been generated for freezing and analysis, specific cell numbers were plated in wells of 6-well plate for an assessment of the time period for deletion of the *LoxP* site-flanked (floxed) region. Induction of *LoxP* site recombination required the addition of 0.1µM 4-OHT to the

culture media for 48hr. Genomic DNA was harvested from ES cells at specific time points after the addition of 4-OHT. Time points and cell numbers plate were as follows: 0hr, $2x10^6$; 6hr, $2x10^6$; 12hr, $2x10^6$; 24hr, $1x10^6$; 48hr, $0.5x10^6$; 72hr, $0.25x10^6$; 96hr, $0.25x10^6$. Cells were plated the night before the morning that the media was supplemented with 4-OHT. *Lsd1*$^{Lox/\Delta 3}$ cells were harvested before 4-OHT addition as time-point 0d. DNA was harvested as described (2.3.5) for Southern Blotting.

2.6.4 Genotyping of WT, Lox and Δ3 alleles by PCR

Genomic PCR was performed as described (2.4) on DNA extracted from ES cells (2.3.5). Two PCR reactions using 2 combinations of 3 primers could identify *WT, Lox* and *Δ3* alleles. The band sizes produced from PCR are as follows:

- Primer 1 and 2: *Lox* 390bp , *WT* 280bp
- Primer 1 and 3: *Δ3* 465bp , *Lox* 1427bp

2.6.5 Southern blotting to identify allelic genotypes

2.6.5.1 Southern Blotting

Southern blotting is a method routinely used in molecular biology for detection of a specific DNA sequence in DNA samples. Southern Blotting was developed by Edwin Southern in 1975 (Southern 1975). The method involves the restriction digestion of DNA, followed by the transfer of electrophoresis-separated DNA to a membrane and subsequent fragment detection by radiolabelled probe hybridisation. The result identifies the DNA sequence that is complementary to the probe. With prior knowledge of restriction enzyme cut sites, the size of the band detected reveals the

context of the complementary sequence, therefore allowing genotyping of DNA sequences. The method is also semi-quantitative, indicating relative amounts of DNA species that the complementary sequence is present in.

2.6.5.2 Strategy for identification of the Lsd1 targeted clones

A strategy using a 5' external probe and an *Eco*RV restriction enzyme digest was used to distinguish *Lsd1*$^{+/Lox}$ cells from *Lsd1*$^{+/+}$ and *Lsd*$^{Lox/\Delta 3}$ cells from Lsd1$^{+/\Delta 3}$ in each allele targeting step. Following DNA preparation, DNA was allowed to dry in a 30°C incubator prior to *Eco*RV restriction enzyme (1.5µl) digestion in the wells at 37°C overnight. This digestion was performed in 50µl.

2.6.5.3 Strategy for identification of 'HygΔTK' cassette-removed clones

Lsd1$^{Lox/\Delta 3}$ *-HygΔTK* needed to be distinguished from *Lsd1*$^{Lox/\Delta 3}$ cells and some possible contaminating WT cells in mixed cell population colonies. A strategy involving an internal 3' probe and a *Hind*III restriction digest was developed. Probe hybridisation would result in bands of the following sizes corresponding to each allelic genotype: WT, 1.9kb; *Lox,* 2.6kb; *Lox-HygΔTK,* 5kb; *Δ3,* 1.9kb. The lack of 5kb band and presence of a 2.6kb band would indicate '*HygTK*-out' *Lsd1*$^{Lox/\Delta 3}$ cells.

The 380bp probe was synthesised by PCR from the targeting vector in 50µl reactions (2.4). Primers used were: LSD1_3_Int1 and LSD1_3_Int2. The probe was gel extracted and purified using Qiagen Gel Extraction Kit according to manufacturer's instructions

and quantified by Nanodrop™. Genomic DNA was harvested in 96-well plates (2.3.5.1). *Hind*III digestion of genomic DNA in 96-well plates and allele characterisation using an internal probe was performed.

2.6.5.4 Strategy for identification of deletion of exon 3

DNA was prepared by incubating cells at 55°C with lysis buffer (10mM Tris pH 7.5, 10mM EDTA, 10mM NaCl, 0.5% SDS, 200μg/ml Proteinase K) followed by precipitation with isopropanol and two washes with 70% ethanol. For Southern blotting 5μg of genomic DNA was digested overnight with *Stu*I restriction enzyme before hybridisation using a $dCTP^{32}$ labelled 3' internal probe (for details on probe location see Chapter 3, Figure 3.3).

2.6.5.5 Agarose gel electrophoresis for Southern blotting

Following digestion of DNA in 50μl volumes, 10μl of 6X DNA loading buffer (60mM Tris pH7.5, Glycerol, Bromophenol blue) was added and the entire volume loaded onto an 0.8% agarose gel for resolution of digested genomic DNA. The DNA was resolved at 20V overnight. Resolution of larger fragments required the DNA to be electrophoresed a significant distance. This distance was decided on when appropriately required. The following day the gel was viewed on the UV transilluminator to ensure complete digestion of DNA and location of the DNA ladder. The gel was washed once in distilled water to remove the ethidium bromide (EtBr) and then twice in alkaline transfer buffer (1M NaCl, 0.4M NaOH). The apparatus for

capillary transfer onto Hybond XL membrane in alkaline transfer buffer was subsequently assembled.

2.6.5.6 DNA Transfer onto the nylon membrane

Hybond XL membrane was equilibriated in alkaline transfer buffer before capillary transfer apparatus was set up. The transfer was usually performed overnight. The following day the position of the wells was marked onto the membrane in pencil and the membrane was neutralised with two 15min washes in neutralisation buffer (1M NaCl, 0.5M Tris-HCl pH 6.8). The membrane was then dried in the 37°C incubator before hybridisation. A pre-hybridisation step was required by incubation of the membrane for 1hr at 65°C in hybridisation buffer (Amersham). Membrane pre-hyb and hybridisation was carried out in a roller bottle in the hybridisation oven.

2.6.5.7 DNA Probe labelling

The double stranded probe required radiolabelling by the incorporation of $dCTP^{32}$. Firstly, 25ng of the probe was diluted in 45µl of TE (10mM Tris pH7.5, 1mM EDTA). The double stranded probe had to first be denatured by boiling at 95°C for 6min. It was then quenched on ice for 5min before transfer to the radiation area and addition of 1.85Bq (5µl) of $dCTP^{32}$ and random primer, dNTPs and Klenow mix (Amersham Bioscience). The labelling reaction was allowed to occur for 1hr before purification of the labelled probe through a sepharose column (Amersham). The purified probe was then monitored for radiolabel incorporation; at least 30% incorporation was deemed

acceptable to proceed with. Finally the probe was boiled at 95°C prior to addition to the hybridisation buffer in the roller bottle.

2.6.5.8 Hybridisation, washing and developing of the membrane

Hybridisation occurred overnight at 65°C by rotation of the roller bottle in the hybridisation oven. The following day the buffer was poured away down the designated sink and the radioactivity of the membrane was monitored. The membrane was washed twice in 2X SSC/0.2% SDS buffer at RT and then twice in 0.2X SSC/0.1%SDS buffer at 65°C. The membrane was exposed to X-ray film in a cassette placed at -80°C overnight, then developed.

2.6.6 Analysis of LSD1 protein deletion

Three independent *Lsd1*$^{Lox/\Delta 3}$ cell lines from the six clones recovered were initially analysed for LSD1 protein deletion and cell growth characteristics. Immunoblot figures in results chapters show data from a single cell line, which is representative of the three independent clones. ES cell protein was harvested as described in 2.11**.** Antibodies used in Western blotting are indicated in Table A1.

2.6.7 Growth curve analysis of ES cells

Once the protein deletion had been assessed, 5 day frozen cells were recovered for 3 days then plated to analyse the growth rate of *Lsd1*$^{\Delta 3/\Delta 3}$ cells compared to controls. To assess the proliferative potential of ES cell lines 2.5 x 10^4 cells were seeded in triplicate

in 6-well plates 8 days after induction of LSD1 protein deletion and counted each day over 5 days using a haemocytometer. Two days into the growth rate analysis, cells were harvested for propidium iodide (PI) staining to assess the cell cycle profile by FACS, as described in 2.10.

2.7 DNA methylation analysis by Southern Blot

2.7.1 Restriction digestion and gel electrophoresis

Genomic DNA was harvested from *Lsd1*$^{Lox/\Delta 3}$ and *Lsd1*$^{\Delta 3/\Delta 3}$ cells at the appropriate time points. 20µg DNA was digested with *Hpa*II and 20µg with *Msp*1, using 30µl of the correct NEB buffer, 6µl enzyme, and sufficient dH_2O to make a total reaction volume of 300µl. Samples were incubated at 37°C for 3 hours, before another 3µl enzyme was added and they were left at 37°C overnight. *Hpa*II and *Msp*I are isoschizomers (cutting site: C↓CG↑G), but *Hpa*II is methylation-sensitive and will only cut when the recognition sequence is not methylated. *Msp*I will cut regardless of the presence of methylation at the recognition sequence. Thus, because the enzymes cut at regular intervals (roughly every 250bp), the difference in restriction digestion between the two enzymes is proportional to the amount of CpG methylation in the DNA sample.

After digestion, the samples were precipitated, air-dried, resuspended in 40µl TE. The DNA concentration was quantified and 5µg of each sample was loaded and run overnight at 20V on a 1% agarose gel. When the samples had migrated 16-18cm from the wells, the gel was photographed to check for even loading. The gel was then washed twice for 10min on the shaker in depurination solution (0.2M HCl, 1M NaCl). This reduced the molecular weight of any very large fragments so that they could be transferred more easily onto the membrane. The gel was then washed twice for 10min in alkaline transfer buffer before capillary transfer and hybridisation (2.6.5.6-2.6.5.8). The IAP DNA probe used in the hybridisation was kindly provided by Dr Christine Armstrong.

2.8 Generation of *Lsd1*$^{Lox/\Delta 3}$ Mouse Embryonic Fibroblasts (MEFs)

Lsd1$^{Lox/\Delta 3}$; *ROSA26*$^{CreER\text{-}PURO}$ ES cells were tested for Mycoplasma by the Geneta Service at the University of Leicester before preparation for blastcocyst injection. Chimaeric animals were born and their embryos were harvested at E14.5 for MEFs by standard protocols. MEFs were cultured in M10 media with puromycin to select for MEFs containing *puro*^{R} gene at the *ROSA26* locus. Genomic PCR was performed to identify successful selection of *Lsd1*$^{Lox/\Delta 3}$ MEFs using primers 1 and 2 and primers 1 and 3 as described in 2.4 and 2.6.5. *LoxP* recombination and protein deletion timecourse experiments were carried out as with ES cells (2.6.5 and 2.6.7). Genomic PCR was performed to assess deletion of exon 3 using primers 1 and 2.

2.9 ES cell *in vitro* differentiation analysis

All three original cell lines were assessed for *in vitro* differentiation potential. In order to ensure no residual LIF remained in the culture media when transferring cells to LIF-free culture conditions, ES cells were trypsinised and washed twice in PBS before plating at low density or as hanging drops in fresh MI5 without LIF. In all of the differentiation studies except differentiation in N2B27 media (Ying & Smith 2003), the media contain 15% FCS. Alkaline phosphatase staining was accessed under the microscope and methylene blue staining was assessed by eye. EB number at 5 days could be counted under the microscope at low magnification. EB diameters were measured using the scale bar in the Leica® microscope software.

2.9.1 Alkaline Phosphatase and Colony Formation Assays

For alkaline phosphatase assays, cells were plated at 7 x 10^2 cells per well in 6-well plates in the presence of LIF. After overnight culture, cells were cultured in the presence or absence of LIF for 6 days. They were fixed with 4% formaldehyde for 2min, washed twice in PBS + 0.1% Tween ($T_{0.1}$), and stained with 1ml of a commercial Alkaline Phosphatase Assay Reagent (Millipore) for stem cell colony identification. This reagent required prior combination of Fast Red Violet, Napthol and water in a ratio of 2:1:1. Cells were incubated at RT in the dark for 15min followed by a final wash in PBS- $T_{0.1}$. Undifferentiated and mixed colonies that had strong and intermediate purple staining, respectively, were counted. Differentiated colonies that were often totally unstained were difficult to identify; hence colonies were counterstained with

methylene blue and counted to calculate the total number of colonies and identify the number of differentiated colonies.

2.9.2 Differentiation of ES cells as Embryoid Bodies

Embryoid bodies (EBs) were created by suspending 600 cells in 15μl hanging drops on 15cm tissue culture dishes for 48 hours. Cell aggregates were washed down and carefully collected in PBS then transferred to low-adherence 15cm petri dishes. Plates were maintained in the CO_2 incubator on a shaking platform to allow the development of EBs. RNA was harvested from EBs at specific time points by homogenisation in TRIzol and chloroform phase separation in phase lock gel tubes as described in 2.3.6. Cellular RNA was precipitated using isopropanol and glycogen carrier. RNA was extracted under strict RNase-free conditions and the quantity and quality of RNA recovered was analysed on the Nanodrop™ spectrophotometer. Further quality control was performed by agarose gel electrophoresis; RNA was routinely of a very good quality. RNA samples were all normalised to 0.5μg/μl concentrations for cDNA synthesis (2.12.1). Methods for qRT-PCR using the Roche Universal Probe Library system of the Roche Light Cyclers are explained in detail in 2.12.3.

2.9.3 Differentiation with Retinoic Acid

For retinoic acid (RA) differentiation, ES cells were seeded in 6cm plates with M15+LIF the day before commencement of the experiment. Differential cell numbers were plated as follows: day 0, $1x10^6$; day 1, $0.75x10^6$; day 2, $0.5x10^6$; day 3 $0.3x10^6$. The

following day, day 0 cells were harvested and 100mM RA was diluted to 10μM in fresh MI5 for addition to the other plates. Cells were harvested for cell cycle analysis as described in 2.10.1.

2.9.4 Differentiation in N2B27 media

The same numbers of ES cells were plated in 6cm plates as for RA differentiation. On day 0, fresh N2B27+LIF was replaced with N2B27 without LIF. Cells were harvested for cell cycle analysis as described in 2.10.1.

2.10 Flow Cytometry

2.10.1 Cell cycle analysis by propidium iodide (PI) staining

For FACS analysis of RA and N2B27 differentiation, the media was not changed before harvesting of cells. The culture media was collected in addition to trypsinised cells in order to harvest dead cells floating in the media. All cells were centrifuged and fixed by drop-wise addition of -20°C-stored 70% ethanol under vortex. Cells were washed twice in PBS at RT and propidium iodide was diluted from a 2.5mg/ml stock in PBS to a working concentration of 50μg/ml. 1mg/ml RNaseA was also diluted in the PI solution for use at 10μg/ml. 500μl staining solution was added to each fixed ES cell sample and incubated at 37°C for 30-60min. FACS analysis was performed on the BD FACSCanto®. Individual ES cells were identified based on FSC and SSC characteristics and PI staining measured on the PE-A (FL-2) laser channel to reveal DNA content of cells.

2.10.2 GFP analysis

ES cells were harvested by trypsinisation (2.3.2) and washed twice in PBS at RT. Live cells were immediately analysed on the BD FACSCanto® where viable ES cells were gated based on FSC and SSC, followed by measurement of GFP expression in individual cells by the FITC-A channel.

2.11 Protein and enzymatic analysis

2.11.1 Immunoblotting

Nuclear extracts were routinely prepared from ES cells for Western blotting. 3 x 10^7 ES cells were washed twice in PBS at RT before scraping in ice cold PBS. Cells were washed twice more in cold PBS then resuspended in 1ml hypotonic buffer (10mM KCl, 20mM Hepes pH7.9, 1mM EDTA, protease inhibitor cocktail (Sigma #P8340) and 1mM DTT) and incubated on ice for 20min. Extracts were then vortexed for 10sec with 50μl 10% NP-40 and nuclei spun down at 1500rpm for 5min at 4°C. Supernatant was removed and nuclei were resuspended in 200μl of hypertonic lysis buffer (400mM NaCl, 20mM Hepes pH7.9, 10mM EDTA, 25% glycerol, 1mM DTT and protease inhibitor cocktail) for direct immunoblotting. Nuclear debris was spun down at 13000rpm for 10min at 4°C. Protein concentrations were quantified using Bradford reagent in a spectrophotometer. Immunoblots were performed on 20μg of nuclear extract resolved by 4-12% gradient SDS-PAGE. A list of antibodies used for immunoblotting is presented in Table A1.

2.11.2 Immunoprecipitation

For immunoprecipitation, ES cells were cultured in 10cm plates until 80% confluent, washed twice in PBS at RT, scraped in 5ml cold PBS, pelleted at 1200rpm, washed again in cold PBS and then 500μl 'IP buffer' was used to extract whole cell protein (250mM NaCl, 10mM Hepes pH7.9, 1mM EDTA, 0.5% NP-40 and protease inhibitors). Protein was extract with rotation at 4C for 1hr. Extracts were then cleared of cell debris by centrifugation at 13000rpm for 15min. Protein concentration was then

quantified using Bradford reagent on a spectrophotometer. 100μg of extract was incubated overnight at 4˚C with 1μg antibody. 50μl of Protein-G sepharose beads (GE Life Sciences) were washed twice in cold PBS then blocked with 1% BSA in PBS at 4°C overnight. The following day the beads and immune complexes were combined for 4hr at 4˚C. After 3 washes in IP buffer, beads were split into two aliquots. One aliquot was used to assess the enzymatic activity of the immunoprecipitates using a commercially available deacetylase assay (Active Motif, Rixensart, Belgium); 20μl taken from 80μl bead suspension in HDAC assay buffer was used for each reaction in 25μl reactions using 5μM assay substrate. Colorimetric reactions were performed in 96-well plates and analysed on a plate reader in the Toxicology Unit. The remaining aliquot was resolved by SDS-PAGE and probed with antibodies raised against known components of the immunoprecipitated complexes. A list of antibodies used for immunoblotting of immunoprecipitates is presented in Appendix Table A1.

2.11.3 In-House Histone Deacetylase assay

Following three washes of immunoprecipitations, the beads were resuspended in 10mM Tris, 1mM EDTA, 50mM NaCl and split in two. One half of the beads was then resuspended in 130μl deacetylase buffer (20mM Tris pH8, 0.25mM EDTA, 250mM NaCl) and this suspension was aliquoted into three 40μl quantities in wells of 96-well plate reader plate. Once all of the samples were applied to the 96-well plate, 30mM BOC acetyl-lysine substrate was dilute to 500μM (1:60) in deacetylase buffer. 10μl of the substrate was simultaneously added, using a multichannel pipette, to the wells; making a final substrate concentration of 100μM. The plate was incubated in the dark

at 37°C for 90min. Quenching of the deacetylase activity and trypsin cleavage of the substrate was then performed by adding 50μl of 2μM Trichostatin A (TSA; 200μM stock) in 10μg/μl trypsin solution (made up in 50mM Tris pH7.5, 100mM NaCl). The samples were left to develop at room temperature for 15min before measuring the fluorescence with an excitation wavelength of 360nm and an emission wavelength of 470nm on a plate reader.

2.11.4 Histone extraction and modification analysis

Acid extraction of histones was performed to assess global histone modification levels on denatured acid soluble histones. Cells were harvested by scraping in 5ml of ice cold PBS from 10cm plates and nuclei were harvested as described (2.11.1). Acid extraction was performed according to the method described by Shechter et al. 2007 and all steps were carried out at 4°C. Nuclei were resuspended in 400μl of 0.2M H_2SO_4 and incubated by rotation overnight. The following day the samples were centrifuged at 13000rpm for 10min, supernatant removed and 132μl TCA added drop-wise to the pellets. This suspension was incubated on ice for 30min and the chromatin centrifuged at 13000rpm for 10min. Chromatin was washed twice with ice-cold acetone and resuspended in ddH_2O. This extract could be flash-frozen and -80°C stored. 5μg of extract was loaded in each lane and membranes probed using a panel of antibodies raised against a number of histone modifications (Table A1). Membranes were scanned using the Odyssey Infrared Imaging System and quantification of proteins achieved using the appropriate IRDye conjugated secondary antibodies (LiCOR Biosciences, Cambridge, UK). Histone modification bands were

normalised to the total histone H3 loading and analysis was done using three biological replicates grown from single cell cloned colonies.

2.11.5 Protein stability assay

$2x10^6$ cells were plated in 6cm plates overnight. The following day, MG132 was added to the culture media at a concentration of 30μM. Control plates with no inhibitor were also used. Cells were harvested after 4hr for Western blotting as described (2.11.1)

2.11.6 Histone demethylase assay

Measurement of the demethylase activity of ES cell extracts was performed in 50μl reaction volumes with 5μl of extract (10μg) using a fluorescent histone demethylase assay kit (Active Motif). 4X assay buffer was diluted to 1X and 12.5μl was used in each reaction. A recombinant histone H3K4me2 substrate used in the assay mimics a native histone substrate. This peptide was reconstituted in 500μl 1X assay buffer and 5μl was used in each reaction. Reactions were made up to 50μl with ddH_2O with the substrate added last. Reactions were incubated at 37°C for 1hr. 50ml fluorescent detection reagent was then added and incubated for 30-60min. The Detection Reagent reacted with each formaldeyde molecule to generate a fluorescent signal equivalent to the overall production of formaldehyde. The fluorescent signal was measured using a fluorescent microplate reader with an excitation wavelength of 410 nm and an emission wavelength of 480 nm.

2.12 Reverse Transcription, Microarray Hybridisation and Quantitative Real-Time PCR.

2.12.1 Reverse transcription

Total RNA was isolated from ES cells and embryos using a standard TRIzol (Invitrogen) protocol and Phase Lock Gel Heavy Tubes as described (2.3.6). Total RNA was reverse transcribed using Q-Script one step Supermix (Quanta Biosciences, Gaithersburg, MD, USA). All RNA samples were quantified and assessed for purity using the Nanodrop™ spectrophotometer then normalised to a concentration of 0.5μg/μl. 2μg was also run on an agarose gel to assess the integrity of the RNA prep. 2μg total RNA was used in a 40μl Q-Script cDNA synthesis reaction. This reaction consisted of 5X reaction buffer, the appropriate volume of RNA and DEPC H_2O. cDNA synthesis was carried out in the thermocycler with the following conditions:

25°C	5 minutes
42°C	30 minutes
85°C	5 minutes
4°C	Hold

2.12.2 Illumina Microarray

2.12.2.1Array hybridisation

RNA preparation was performed according to manufacturer's instructions using the Illumina TotalPrep® RNA amplification kit which ultimately generated hundreds to thousands of biotinylated, antisense RNA copies of each mRNA in a sample for hybridisation with the Illumina Bead Array. The kit is based on the RNA amplification protocol developed in the laboratory of James Eberwine (Vangelder *et al.* 1990) . The

procedure consists of reverse transcription with an oligo(dT) primer bearing a T7 promoter using a reverse transcriptase enzyme engineered to produce higher yields of first strand cDNA than wild type enzymes. This enzyme catalyzes the synthesis of virtually full-length cDNA, which is the best way to ensure production of reproducible microarray samples. The cDNA then undergoes second strand synthesis and clean-up to become a template for in vitro transcription (IVT) with T7 RNA Polymerase. Biotin UTP is included to generate labelled cRNA from the IVT.

Microarray gene expression profiling in *Lsd1*$^{Lox/\Delta 3}$ cells and *Lsd1*$^{\Delta 3/\Delta 3}$ cells 10 days after induction of LSD1 deletion was performed using the Illumina MouseWG-6 v2 Expression BeadChip platform. The hybridisation was performed in triplicate using three biological clones A6, B12 and C10. The MouseWG-6 v2.0 BeadChip platform covers 45,200 different mouse transcripts. The probe content is derived from the NCBI RefSeq database, supplemented with probes from Mouse Exonic Evidence Based Oligonucleotide (MEEBO) set a well as examplar protein-coding sequence described in the RIKEN FANTOM2 database. Six samples in total were prepared and these were hybridised simultaneously to each of the six identical bead arrays present on the BeadChip. The probe design consists of nanoscopic beads tiled on the array, which are attached with a short address sequence with a 50bp gene-specific probe linked. Labelled nucleic acid prepared from the total RNA were hybridised to the probes on the Chip at 65°C. The amount of hybridised cRNAs is detected using the biotin label and corresponds to original transcript abundance. The Sentrix Barcodes of the Chips used were 4769263016A—F.

2.12.2.2 Illumina microarray quality control

Illumina quality control was performed by Cambridge Genomics Services. The hybridisation controls showed an increasing intensity from low to high of at least 3 fold at each step; therefore the hybridization performed well. The stringency of the hybridisation was also shown to be good through comparing mismatch probes to perfect match probes. The biotin labelled showed a good level of intensity and the background to noise ratio was very acceptable. Regarding the efficacy of the samples, small variations in degradation and signals of the samples was reported, confirming that the assay was a success.

2.12.2.3 Analysis of microarray hybridisation

Raw expression data was managed in Illumina BeadStudio and statistical and analyses were performed by Dr Jinli Luo (MRC Toxicology Unit) using ArrayTrack bioinformatics software, developed by USFDA (http://www.fda.gov/ScienceResearch/Bioinformatics

Tools/Arraytrack/default.htm). Data was normalised using a median scaling normalisation method and then the triplicate $Lsd1^{Lox/\Delta 3}$ versus $Lsd1^{\Delta 3/\Delta 3}$ datasets were compared using a Welch T-test. Significant differentially expressed genes were selected using $p<0.05$ and 1.4-fold change cut-offs. A gene ontology analysis of PANTHER terms for biological processes was performed using DAVID bioinformatics software (Huang *et al.* 2009).

2.12.3 Quantitative Realtime PCR (qRT-PCR) for gene expression analyses

For the relative quantification of gene expression, primers were designed using the Roche-applied-science assay design centre online. GAPDH was used as an endogenous control gene in the single-well multiplex PCR with which to normalise target gene Ct values to. All primer sequences are displayed in the appendix along with the specific hydrolysis probe from a set of 110, which was used in the reaction (Appendix Table A2). Probes consisted of Lock Nucleic Acid technology, which upon binding of the reaction amplicon, released a HEX or FAM fluorophore. This also provided an additional level of specificity to the gene of interest in the qRT-PCR. 2µl of diluted cDNA was used in all subsequent multiplex qRT-PCR reactions using the Light Cycler Probes Master Mix (Roche) as per the manufacturer's instructions. All reactions were performed in wells of 96-well PCR plates on the Roche Light Cycler 480 under the following conditions: initial denaturation for 10min at 94°C followed by 40 cycles of 10sec at 94°C, 20sec at 55°C and 5sec at 72°C. Advanced relative quantification analysis using the Roche LightCycler software generated a relative expression value based on the comparative Ct calculations ([delta][delta]C_t = [delta]$C_{t,sample}$ - [delta]$C_{t,reference}$).

2.13 Chromatin Immunoprecipitation

For ChIP assays, many features of experimentation had to be optimised. These included cell number used per IP, method and time period of crosslinking, chromatin extraction, chromatin sonication procedure and purification of DNA. Additionally PCR primers had to be tested before use on the immunoprecipitated DNA. Varying cell numbers (ranging from $0.5x10^6$ to $1.5x10^6$) were originally tested for length of time required to shear chromatin to enrich for 300-500bp fragments. Ultimately $1x10^6$ cells were used and sonication times for single crosslinking (10min formaldehyde) and double crosslinking (10min EGS + 10min formaldehyde) were evaluated. 15min sonication using the Diagenode Bioruptor on setting 'HIGH' (2.13.2) was seen to be optimum for single crosslinking and 20 minutes was needed for double crosslinking (Chapter 4; Figure 4.15).

2.13.1 Crosslinking of cells for chromatin immunoprecipitation

2.13.1.1 Double crosslinking

For LSD1 and CoREST ChIP, double crosslinking was performed as described by (Zeng et al. 2006). Approximately $1x10^7$ ES cells were used for each IP (half of 80% confluent 10cm plate) and cells were crosslinked as a monolayer in a 10cm plate. For double crosslinking a 20mM EGS stock (Thermo #21565) was prepared in DMSO on the day of use (0.0913g in 10ml). The culture media was aspirated and 6.5ml PBS added to the 10cm plate. 0.5ml EGS (20mM→1.5mM) was added to the PBS and incubated at RT for 10min. 1/16 volume fresh 16% formaldehyde (1% final) was then added directly to the plate and incubated with intermittent swirling at RT for 10min. 1/10

volume 1.25M glycine was added to quench crosslinking (0.125M final concentration). The plate was aspirated and washed twice in PBS at RT. Cells were then scraped in 5ml cold PBS and spun down at 1200rpm before either snap-freezing on liquid nitrogen and -80°C storage or proceeding immediately to chromatin extraction.

2.13.1.2 Single crosslinking

Single crosslinking with formaldehyde only was performed for histone modification immunoprecipitation. Single crosslinking required 1/16 dilution of 16% formaldehyde directly in culture media and incubation with swirling for 10min. Quenching, washing and scraping were performed as described (2.13.1.1).

2.13.1.3 Cell extract preparation

Protease inhibitor cocktail (Sigma) was added to all lysis buffers immediately before use (333X dilution). Cell pellets for individual IPs were resuspended in 500µl of *LB1*. Cells were lysed by rotation at 4°C for 10min and nuclei were spun down at 1,350xg for 5min at 4°C. Nuclear pellets were resuspended in 500µl of *LB2* and rotated gently at RT for 10min. Insoluble chromatin was isolated by spinning at 1,350xg for 5min at 4°C. This was resuspended in 300µl *LB3*, which was the sonication buffer.

2.13.2 Sonication of cells using the Diagenode Bioruptor 200

300µl volumes of chromatin extracts were transferred to pre-chilled 1.5ml polycarbonate tubes prior to sonication. The Diagenode Bioruptor 200 water bath was

pre-chilled with ice up to an hour before use. This ice was allowed to melt to ice slush, and topped up with cold water just prior to sonication. Six tubes could be sonicated simultaneously; therefore three *Lsd1*$^{Lox/\Delta 3}$ samples and three *Lsd1*$^{\Delta 3/\Delta 3}$ samples were sonicated in the same run. The Bioruptor setting was on HIGH for all sonications. 20min with 30sec on-off intermittency was required for ideal chromatin shearing in double crosslinked samples, with 15min adequate for single crosslinked samples. This procedure was optimised by testing different times and cell numbers for each crosslinking method. Following sonication, 30µl 10% triton was added to sonicated lysate and briefly vortexed. Samples were then centrifuged at 20,000xg for 10min at 4°C to pellet unsheared debris. *Lsd1*$^{Lox/\Delta 3}$ and *Lsd1*$^{\Delta 3/\Delta 3}$ samples were combined and 50µl of sonicated material was removed for input DNA (stored at -20°C). Equal volumes were then removed for individual IPs.

2.13.3 Immunoprecipitation

20µl protein G-conjugated Dynabeads were used for each IP. Beads were washed twice with 1ml block solution (0.5% BSA in PBS) and collected each time using the Dynal magnetic stand. Supernatant was aspirated once the beads had been collected to the side of the tube. The beads were resuspended in 250µl block solution and 2µg of appropriate antibody was added (Appendix Table A1). For histone modification ChIP, 2µl of unmodified histone H3 peptide (Abcam) was also added to the bead suspension. Antibody was linked to protein G by overnight incubation on the rotating wheel at 4°C. The following day, blocked beads were collected and resuspended in 100µl of block buffer, before being combined with sonicated chromatin.

Immunoprecipitation of chromatin was allowed to occur over overnight at 4°C on the rotating wheel.

2.13.4 Washing and processing of immunoprecipitated material

2.13.4.1 Washing and crosslink reversal

The following day all apparatus was taken into the cold room for washing of the IPs. Each sample was washed with 1ml RIPA buffer 3 times, each time rotating the tubes, collecting the beads and aspirating. A final wash with 1ml TE + 50mM NaCl was performed before centrifuging the samples at 960xg for 3min at 4°C. TE/NaCl buffer was carefully removed and 210µl of elution buffer was added. Chromatin was eluted from the antibody by 15min incubation at 65°C; with brief vortexing to resuspend the beads every 2min. Centrifugation at 16,000xg for 1min at RT pelleted the beads in order to remove 200µl of the supernatant to a new labelled tube. The input sample reserved after sonication were thawed and 150µl (3 volumes) of elution buffer added. Crosslinking was reversed by adding 8µl 5M NaCl (200mM final) and incubating O/N at 65°C.

2.13.4.2 Digestion of protein and RNA and DNA purification

200µl of TE was added to each tube the following day to dilute the SDS in the elution buffer. RNAseA was added to each sample to a final concentration of 0.2mg/ml and incubated for 2hr at 37°C. Proteinase K was then added to each sample to a final concentration of 0.2mg/ml and incubated for 2hr at 55°C. DNA was column purified

through Qiagen PCR purification columns and eluted in 50µl TE. The input samples were diluted 10-fold.

2.13.5 Buffers used in ChIP

Block solution

PBS, 0.5% (w/v) IgG-free BSA (Sigma)

LB1

50mM Hepes-KOH pH7.5, 140mM NaCl, 1mM EDTA, 10% Glycerol, 0.5% NP-40, 0.25% Triton X-100

LB2

10mM Tris-HCl pH8, 200mM NaCl, 1mM EDTA, 0.5mM EGTA

LB3

10mM Tris-HCl pH8, 100mM NaCl, 1mM EDTA, 0.5mM EGTA, 0.1% Na-deoxycholate, 0.5% N-lauroylsarcosine

RIPA buffer

50mM Hepes-KOH pH7.5, 500mM LiCl, 1mM EDTA, 1% NP-40, 0.7% Sodium Deoxycholate

TE + NaCl buffer

10mM Tris-HCl pH8.0, 1mM EDTA, 50mM NaCl

Elution Buffer

50mM Tris-HCl pH8.0, 10mM EDTA, 1% SDS

2.13.6 Testing of histone antibodies for ChIP

In order to test the quality of histone modification antibodies in immunoprecipitation, ChIP was performed using H3K4me2 (Sigma D5692) and H3K4me3 (Millipore 07-473)

antibodies and PCR was performed using primers to genomic regions with known levels of H3K4 methylation (Table 2.1). Purified DNA was quantified by Nanodrop™ in order to use equal input and IP DNA amounts in qRT-PCR. 40 cycle amplification was performed using the Corbett 6000 machine with Rotor-Gene 6000 series software analysis. Histone modification IP "cycle threshold" (C_t) values were subtracted from the input C_t values and this figure was converted into the fold enrichment by $2^{(\text{input Ct} - \text{IP Ct})}$.

Name	Genomic locus	Forward	Reverse	Reference
K4me3$^-$#1	Chr17:14505850 -145506450	AAGCTGAGTGAGCCTGTGCT	AAGGGTATTTGCTGCCACTG	Mikkelsen *et al.* 2006
K4me3$^-$#2	Chr19:6212200 -6212800	TACCCTGTGGATTAGGCACC	ATGGGTATCTGGCACTGAGC	Mikkelsen *et al.* 2006
K4me3$^+$#1	Chr9:110150000 -110150600	CTGAGAGCAGCACAATGGTC	ACTCGAGTCAGCCAATCAGG	Mikkelsen *et al.* 2006
K4me3$^+$#2	Oct4 promoter	GGCTCTCCAGAGGATGGCTGAG	TCGGATGCCCCATCGCA	Stock *et al.* 2008

Table 2.1 Details of primers used for validation of histone modification antibodies

2.13.7 Validation of ChIP primers

Having examined the quality of antibodies to be used in ChIP, primers for the DNA fragment enrichment of candidate genes also had to be tested. Primers used to identify regions at the *Brachyury* locus were tested at two concentrations (700nM and 350nM) on input DNA (undiluted and 1:10 dilution). The dilution of input DNA was required to imitate the speculated potential yields of immunoprecipitated DNA. The observation of a single peak upon melt curve analysis was indicative of amplification of a single PCR product and the height peaks was indicative of the amount of product

produced. Six primer pairs were tests between -600bp and +400bp of the TSS, with two pairs identified as being appropriate for PCR analysis (Table 2.2). A number of primer pairs between -3000bp and -4500bp were also assessed, with one chosen to be used in PCR analysis of a region remote to the *Brachyury* TSS (Table 2.2).

2.13.8 Quantitative RT-PCR for ChIP

PCR was performed in triplicate with 1μl DNA using Dynamo SYBR Green (Finnzymes) in the Corbett 6000 machine. Reactions were assembled in 20μl volumes (10μl SYBR Green mix, 1μl 14μM/7μM primer mix, 8ml PCR grade H_2O, 1μl DNA). Primers were initially tested using input DNA (undiluted and 1/10 diluted) to assess the number and amount of products amplified (melt curve/gel electrophoresis) using 700nM and 350nM working concentrations.

PCR amplification cycle was as follows:

95°C	2min	
95°C	20sec	40 cycles
58°C*	20sec	
72°C	25sec	
4°C	∞	

(*4°C touchdown to 58°C @ 1°C/min first 4 cycles of annealing)

Region	Forward	Reverse	Conc.
Brachyury -4500	gcttgctcagtggttaaggc	gaggtggagttacaggcagc	350nM
Brachyury -600	agggtcgctatctgttcgtct	actgccactaactcccacctc	350nM
Brachyury +400	gagcatcttttcttcccaacc	gaaagttcccgagaaaccaag	700nM
Hoxd8 -4000	tcctccccatatccttctcc	agtccccctctttcatcagg	700nM
Hoxd8 -400	catttacccttgacgcactg	tctcagcgacactcatgtcc	350nM
RASGRP3 -3700	tgctgtgaagggattgtcac	gaggaaggggaggatgtagc	700nM
RASGRP3 -150	ggttccgttttcttgctgac	gccacttgattagcatgcag	350nM
RASGRP3 +400	tgtggtcttcttagccacactg	ccatcagctcctatccactg	700nM

Table 2.2 Details of primers used in ChIP qRT-PCR

2.14 Molecular Biology and Engineering of DNA constructs

2.14.1 Bacterial cultures

Lucigen *E.cloni*® 10G chemically competent cells were used for transformation and propagation of plasmids. 2YT media was routinely used to grow bacterial cultures.

2YT:

Bacto-tryptone	16g
Bacto-yeast	10g
NaCl	5g
H_2O	1000ml

Where appropriate:

Ampicillin	100 μg/ml
Kanamycin	100μg/ml

2.14.2 Storage and revival of bacterial strains

Transformed bacterial strains were prepared as glycerol stocks for long-term storage at -80°C. 500μl of bacteria grown overnight in 2TY media with the appropriate antibiotic was added to 500μl sterile 50% glycerol in a screw-top 1.5ml cryovial. This was vortexed briefly to ensure mixing, then stored at -80°C. Revival of bacterial strains was achieved by picking a small quantity of the glycerol stock with a pipette tip and inoculating an agar plate or 5ml 2YT starter culture for overnight incubation at 37°C.

2.14.3 Culturing bacterial cells for miniprep and maxiprep

Bacterial colonies were picked from agar plates with a sterile pipette tip and used to inoculate 5ml of 2YT media containing an appropriate antibiotic. These were incubated overnight in a 37°C shaker before either eing used to harvest plasmids by miniprep or to inoculate a larger culture volume for plasmid maxipreps. 100µl from the starter culture was diluted in 100ml of 2YT with antibiotic for overnight incubation for maxiprep.

2.14.4 Plasmid purification from bacteria

All extraction methods are adapted from the original alkaline lysis plasmid purification method described in (Birnboim *et al.* 1979) , followed by binding of plasmid DNA to an anion-exchange resin under appropriate salt and pH conditions and subsequent elution in elution buffer or TE. Minipreps were prepared using Qiagen Plasmid Miniprep kits as per manufacturer's instructions. Endotoxin-free maxipreps were prepared using NucleoBond® EF kits (Macherey-Nagel GmbH) according to manufacturer's instructions. Eluted maxiprep plasmid DNA was further purified by isopropanol precipitation, ethanol wash and re-dissolving in endotoxin-free H_2O (2.3.5).

2.14.5 Generation of EGFP-LSD1 fusions by PROTEX cloning service

Full length LSD1 and all mutants required fusion to EGFP by cloning into pLEIC21. PCR primers were designed with arms of homology to amplify various forms of LSD1 from an IMAGe cDNA clone for insertion into pLEIC21 (family D homology vector with

Kanamycin resistance gene). Mutagenesis to make the demethylase dead LSD1 was also performed by the PROTEX service, thought mutagenesis to create the TOWER domain mutation was performed by 2-step PCR in house once the $LSD1^{FL}$ was cloned into pLEIC21. Plasmids were purified from bacterial clones as described (2.14.4) and DNA sequencing of the EGFP-LSD1 fusion inserts was performed by the PNACL service using pLEIC21-Seq-F and pLEIC21-Seq-R primers to ensure of no mutations. Glycerol stocks were subsequently made as described (2.14.2).

2.14.6 Amplification of large regions by PCR

The pCAGGS vector backbone was linearised by PCR amplification using KOD Hot Start Polymerase (Novagen). The EGFP-LSD1 fusions were also amplified with arms of homology to the pCAGGS vectors in order to insert the fusion into this vector using the In-Fusion™ Advantage PCR cloning kit (Clontech) for CAG promoter-driven expression in ES cells. 50µl PCR reaction contained: 5µl 10X KOD buffer, 2µl 25mM MgSO4, 5µl dNTPs (2mM each), 2.5µl DMSO, 1.5µl 5'primer (125ng), 1.5µl 3' primer (125ng), 1µl KOD Hot Start DNA polymerase (1U/µl), 1ml DNA template (20ng) and 31.5µl PCR grade H_2O. A typical PCR cycle for amplification of large templates with KOD is shown below:

95°C	2min	
95°C	20sec	30 cycles
Annealing temp	10sec	
70°C	25sec/kb	
70°C	10min	
12°C	∞	

5µl of vector PCR product was analysed by agarose gel electrophoresis and the remainder was purified with QIAGEN PCR purification columns and quantified by Nanodrop™.

Primer	Sequence 5' to 3'	Annealing Temp °C	Notes
LSD1_1_D_5	GTATTTTCAGGGCGCCATGTTGTCTGGGAAGAA	58	Cloning of LSD1 into pLEIC21
LSD1_166_D_5	GTATTTTCAGGGCGCCGAAAGTGAGCCGGAAGA	58	
LSD1_277_D_5	GTATTTTCAGGGCGCCAAAAAGACAGGAAAGGTGATT	58	
LSD1_853_D_3	GTCGACTGCAGAATTTCACATACTTGGGGACT	58	
LSD1_KA_5	GATTTGGCAACCTTAACAAGGTGGTGTTATGCTT	58	Mutagenesis oligos used with LSD1_1_D_5 and LSD1_853_D_3
LSD1_KA_3	AAGCATAACACCACCTTGTTAAGGTTGCCAAATC	58	
LSD1_TOWER_5	GAAAGAGCTTGATAATAAGATGGAGAATTTGAAGG	58	Mutagenesis oligos used with EGFP_CAGtail_5 and LSD1_CAGtail_3
LSD1_TOWER_3	CCTTCAAATTCTCCATCTTATTATCAAGCTCTTTC	58	
EGFP_CAG tail_5	AAGAATTACCCGCCGCCACCATGGTGAGCAAGGG	58	1-853 **3360bp** 166-853 **2859bp** 277-853 **2580bp**
LSD1_CAG tail_3	GCTATCGATCCATGCATGTCACATACTTGGGGACT	58	
pCAG_5	GCATGGATCGATAGCCTCGAC	56	pCAG vector backbone **5134bp**
pCAG_3	CGGCGGGTAATTCTTTGCCAA	56	

Table 2.3 Primers used in generation of LSD1 rescue constructs

2.14.7 In-Fusion™ advanced PCR cloning

5µl of EGFP-LSD1 PCR product was also analysed by gel electrophoresis and then 5µl of unpurified PCR product was treated with 2µl of Cloning Enhancer. This mix was incubated at 37°C for 15min, then at 80°C for 15min in the thermocycler. Cloning Enhancer treated PCR product was either stored at -20°C or used immediately in the In-Fusion Cloning procedure. The pCAGGs vector backbone was 5.1kb therefore 150ng of vector was used in the reaction.

The In-Fusion reaction was set up in 10µl as follows:

5X In-Fusion Reaction Buffer	2µl
In-Fusion Enzyme	1µl
Vector	2µl (70ng/µl)
PCR insert	2µl
ddH2O	3µl
Total volume	10µl

Positive and negative control reactions were also set up utilising a 2kb control insert (40ng/µl) and a linearised pUC19 control vector (50ng/µl) supplied with the Clontech reagents. The reactions were incubated for 15min at 37°C, followed by 15min at 50°C, then placed on ice. The reaction volume was then made up to 50µl with TE buffer and mixed well.

2.14.8 Transformation of In-Fusion™ cloned plasmid into bacterial cells

Nutrients agar plates were prepared by microwave heating Agar + Ampicillin sachets () in 200ml of ddH_2O to dissolve. Agar was then poured into 10cm bacterial petri dishes under the Bunsen flame and allowed to set. *E. cloni*® chemically competent cells (Lucigen) were removed from the -80°C freezer and allowed to thaw completely on wet ice for 10min. One Eppendorf per transformation was pre-chilled on ice and 40µl of cells were added to each. 2.5µl of the diluted In Fusion reactions and 1ml of a pUC plasmid as a transformation positive control were added to the cells on stirred briefly with the pipette tip. Cells were incubated for 30min on ice. Following this, they were

heat-shocked for 45sec at 42°C then returned to ice for 2min. 960µl of RT Recovery Medium (Lucigen) was added and the cells in medium transferred to 10ml miniculture tubes to shake at 200rpm for 1hr at 37°C. Transformed cells were spread on agar plates and incubated overnight at 37°C. 100µl were plated with the remainder centrifuged and re-suspended in another 100µl of Recovery Medium and also plated.

2.14.9 PCR screening of transformed bacteria

Colony PCR was performed using primers spanning between the vector backbone and the insert to identify bacterial colonies successfully transformed with plasmids.

3 Generation of Conditional LSD1 Knockout Mouse Embryonic Stem Cells and Examination of Growth and *In Vitro* Differentiation Potential

3.1 Introduction

LSD1 knockout mice were originally generated by Shaun Cowley in the laboratory of Allan Bradley. The initial embryos analyses were also performed by Shaun Cowley (Figure 3.1). The rationale for creating a mouse embryonic stem (ES) cell line where LSD1 can be conditionally inactivated was underpinned by the failure for LSD1 knockout embryos to develop beyond embryonic day (E)6.5. This block in development suggested that is would not be possible to derive viable ES cells from the inner cells mass. Notably, conditional knockout mice are create to circumvent embryonic lethality. Working with cells in culture is more feasible than early stage embryo analyses and because ES cells represent cells in the embryonic epiblast and differentiation of ES cells into embryoid bodies (EBs) is comparable to events in early embryogenesis, this *in vitro* approach was pursued. Two LSD1 knockout mice have been previously published: the first knockout was generated in the Rosenfeld lab, using gene targeting in mouse ES cells, however the embryonic phenotype was not studied, and rather a pituitary-specific gene deletion was generated for investigation (Wang *et al.* 2007). The second knockout was published from the lab of Taipeng Chen in early 2009 along with conditional LSD1 knockout ES cells (Wang *et al*. 2009). In this study, ES cells were used to investigate causes of early embryonic lethality; however *in vitro* differentiation assays and transcriptional analyses were not pursued in this study. Reduced Dnmt1 protein levels and subsequent genomic DNA hypomethylation

accounted for the essential requirement for LSD1 during embryogenesis (Wang et al. 2009). However, disparities between the time of embryonic lethality in LSD1 knockout and Dnmt1 knockout mice raised questions about additional functions of LSD1 in the early embryo, specifically as a transcription regulator (Li *et al.* 1992, Wang *et al*. 2009). The ability to induce the deletion of LSD1 in ES cells would allow a more accurate evaluation of resulting transcriptional changes and would provide a way to remove LSD1 at stages of various differentiation assays to understand the role of LSD1 during specific lineage commitment programs.

The LSD1 knockout mouse was created using a genetrap insertion into the 3rd exon of the *Lsd1* gene (Figure 3.1A). This genetrap truncates the open reading frame within the SWIRM domain (Figure 3.1B), prior to the amine oxidase-like (AOL) domain, which is essential for the catalytic activity of LSD1, as described in the Chapter 1 (Shi *et al*. 2004, Forneris *et al*. 2005b)**.** Intercrosses between *Lsd1*$^{+/\beta\text{-}geo}$ mice produced only wild-type and heterozygous animals, with no *Lsd1*$^{\beta\text{-}geo/\beta\text{-}geo}$ pups, indicating an embryonic lethal phenotype and consistent with previous reports of LSD1 knockout mice (Fig 3.1C) (Wang *et al.* 2007, Wang *et al.* 2009). The latest point at which *Lsd1*$^{\beta\text{-}geo/\beta\text{-}geo}$ embryos were observed was at E6.5 (Figure 3.1C). At E6.5, *Lsd1*$^{\beta\text{-}geo/\beta\text{-}geo}$ embryos were much reduced in size compared to *Lsd1*$^{+/\beta\text{-}geo}$ controls, which suggested a developmental block around this stage (Figure 3.1G). Published histological analysis of sagittal sections has demonstrated that these embryos blocked in development are resorbed by E7.5 (Wang *et al.* 2009). The introduction of the *β-galactosidase* open reading frame into the endogenous *Lsd1* locus allowed an approximation of LSD1

protein expression patterns in cells and embryos using X-gal staining. The expression of LSD1 at E8.5 and E10.5 was essentially ubiquitous (Figure 3.1D and E). Interestingly, X-gal staining of the early post-implantation embryo revealed that LSD1 expression was restricted to the embryonic portion of the embryo, with little or no expression in the extra-embryonic tissue (Figure 3.1F and G). Based on the expression pattern of LSD1 and the developmental block at or before E6.5, it seems that the essential embryonic role of LSD1 is restricted to the developing epiblast. LSD1 is expressed in the inner cell mass (ICM) at the blastocyst stage (Figure 3.1I and J); supporting a role in epiblast cell development. This is also consistent with the genetrap selection in ES cells, as they are derived from the ICM (Chapter 1). It is possible however that lack of LSD1 expression may perturb the development of the extra-embryonic trophectoderm, as this region is clearly underdeveloped at E6.5.

At the E3.5-6.5 stage of development, the epiblast consists of primitive ectoderm cells that are rapidly proliferating before the onset of intense differentiation at gastrulation (Snow 1977). The restriction of expression to this region, the reduced size of E6.5 *Lsd1*$^{\beta\text{-}geo/\beta\text{-}geo}$ embryos and reports from Wang *et al.* that LSD1 knockout ES cells have reduced proliferation in culture, suggested that cells lacking LSD1 may have reduced proliferative potential (Wang *et al.* 2009). Proliferative capacity of inner cell mass (ICM) cells was therefore tested by performing blastocyst outgrowth assays. This involved isolating *WT*, *Lsd1*$^{+/\beta\text{-}geo}$ and *Lsd1*$^{\beta\text{-}geo/\beta\text{-}geo}$ blastocysts, plating them on gelatin-coated plates and culturing them under standard ES cell conditions for 6 days. Similar expansion of the ICM cells was observed (Figure 3.1K, L and M), thus implying that loss

of LSD1 does not cause significant reduction in proliferation. Embryonic lethality was therefore likely not resultant of a general defect in cell cycle progression. Importantly, this assay indicated that ES cells could be derived from the ICM and cultured as cells that retain pluripotent capacity. However, very few X-gal negative trophoblast cells appear as giant cells surrounding the ICM outgrowth (Figure 3.1M), confirming a defect in extra-embryonic tissue development in *Lsd1*$^{\beta\text{-}geo/\beta\text{-}geo}$ embryos (Figure 3.1G). As a consequence of these results, further investigation into the developmental role of LSD1 in the embryonic epiblast was proposed.

ES cells are the *in vitro* counterpart of epiblast cells and their differentiation mimics many of the processes and changes in gene expression associated with embryonic development (Doetschman *et al.* 1985). The conditional deletion of LSD1 allows temporal control of removal of a functioning gene in ES cells and conditional knockout mouse embryonic fibroblasts (MEFs) were also generated using the established *Lsd1*$^{Lox/\Delta 3}$ ES cell lines. ES cell culture and differentiation provides a platform to investigate the role of a gene in cellular proliferation, differentiation and death and gene expression. EB differentiation is a well established system of differentiation that was primarily utilised in this investigation. Interestingly, Wang *et al.* reported that LSD1 knockout ES cells failed to form EBs and instead underwent massive cell death upon differentiation. Our analyses, before these observations were published, indicated that EBs could form, providing reasons to follow this route of investigation. The ability to form EBs confirms the potential to construct primitive endoderm through molecular mechanisms discussed in Chapter 1.7. The successful formation of

EBs would also lead to questions of the role of LSD1 in processes of primitive ectoderm development or possibly at the onset of gastrulation. To answer these questions, gene expression throughout differentiation was analysed to understand which cell types could develop in the absence of LSD1. Gene expression data could potentially reveal involvement of LSD1 within transcriptional networks in the early embryo.

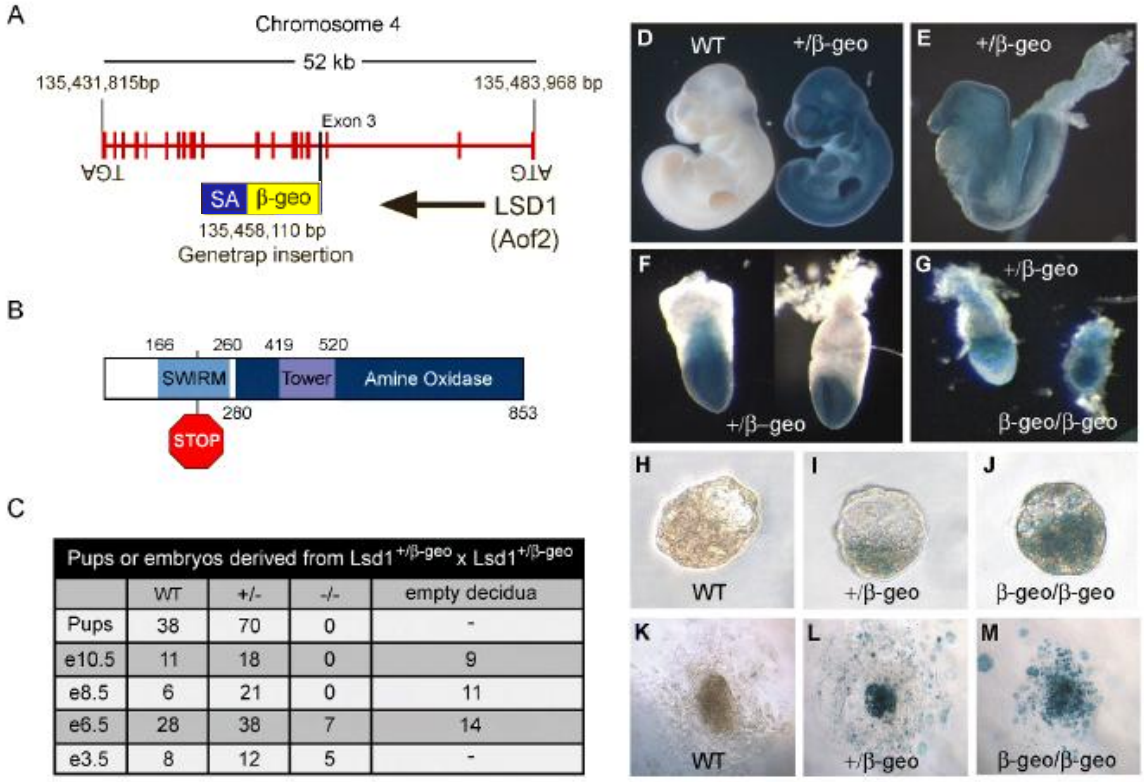

Pups or embryos derived from Lsd1$^{+/\beta\text{-geo}}$ x Lsd1$^{+/\beta\text{-geo}}$				
	WT	+/-	-/-	empty decidua
Pups	38	70	0	-
e10.5	11	18	0	9
e8.5	6	21	0	11
e6.5	28	38	7	14
e3.5	8	12	5	-

Figure 3.1 A genetrap insertion inactivates *Lsd1* and reveals embryo-specific expression. (A) A mouse ES cell line containing a genetrap vector in the *Lsd1* gene locus (clone X102) was used to generate *Lsd1*$^{+/\beta\text{-geo}}$ mice. The genetrap vector, which consists of a splice acceptor site linked to a β-geo selectable marker, was found to be inserted into the 3rd intron of the *Lsd1* gene on chromosome 4. (B) Schematic representation of the LSD1. The position of the genetrap insertion (STOP), downstream of exon 3, truncates the LSD1 open reading frame within the SWIRM domain. This is prior to the amine oxidase-like (AOL) domain, which is essential for the catalytic activity of LSD1 (C) Table shows that *LSD1* KO embryos are not viable beyond E6.5 with empty deciduas being prevalent from e6.5 to e10.5. At E6.5. *Lsd1*$^{\beta\text{-geo}/\beta\text{-geo}}$ pups are born at numbers below Mendelian ratios. (D), Wild-type and *Lsd1*$^{+/\beta\text{-geo}}$ embryos isolated at E10.5 (Theiler Stage (TS) 17) were stained with X-gal to detect *β-galactodase* reporter gene activity approximating to *Lsd1* expression patterns. Similar X-gal staining experiments were performed using embryos isolated at, (E), E8.5 (TS 12), (F), E8.0 dpc (TS 11), (G), E6.5 (TS 8) and (H-J), E3.5 (TS 5). The genotype of individual embryos is indicated (K-M) X-gal staining of blastocyst out-growth cultures shows *WT*, *Lsd1*$^{+/\beta\text{-geo}}$ and *Lsd1*$^{\beta\text{-geo}/\beta\text{-geo}}$ that were isolated at E3.5 and cultured on gelatinized plates for 6 days. On day 6 blastocyst outgrowth cultures were stained with X-gal to determine *β-galactosidase* expression and then genotyped.

3.2 Results

3.2.1 Generation of conditional LSD1 knockout ES cell lines

An E14 embryonic stem (ES) cell line expressing a Cre/Estrogen Receptor fusion protein from the *ROSA26* locus was used to generate *Lsd1*$^{Lox/\Delta 3}$; *ROSA26*$^{CreER\text{-}Puro}$ cells. E14 ES cells and the *ROSA26-CreER* targeting vector were kindly provided by David Adams. Sequential gene targeting using an *Lsd1cKO-HygTK* targeting vector, which conferred Hygromycin resistance, was performed (Figure 3.2). This targeting vector was created by Dr Shaun Cowley in the lab of Alan Bradley. *CreER-puro*^{R} expressing ES cells were used for targeting of the endogenous *LSD1* locus with the vector, which was linearised by *Ahd*1 restriction enzyme digestion for genomic integration by homologous recombination. The 5' arm of homology was 4.4kb and the 3' arm of homology was 4.6kb. Following electroporation, all cells were added to 10cm plates with fresh M15+LIF. The following day the media was supplemented with hygromycin, to select for integration of the vector containing the *HygTK* gene, and puromycin, to maintain selection for *CreER-puro*^{R} cells. The first allele was targeted to create *Lsd1*$^{+/Lox}$ cells, in which exon 3 was flanked by *LoxP* sites. This allele was deleted by addition of 4-hydroxytamoxifen (4-OHT) to the cells to activate the Cre, generating *Lsd1*$^{+/\Delta 3}$ cells (lacking exon 3) before targeting of the second allele with the *Lsd1cKO-HygTK* vector to create *Lsd1*$^{Lox/\Delta 3}$ cells. This generated ES cells where one allele has exon 3 flanked by two *LoxP* sites and the second allele has exon 3 deleted (Figure 3.2). Correct gene targeting (verified by Southern blotting as described in Chapter 2.5.6.4) resulted in a modified locus in which exon 3 of the endogenous LSD1 gene was flanked by 34bp *LoxP* sites. Deletion of exon 3 from the second allele was achieved using the

same Cre-Lox method as when deleting exon 3 from the first allele. The knockout was designed so that removal of exon 3 would disrupt the open reading frame of LSD1, and hense a premature stop codon is introduced into exon 4. Transcription from the LSD1 promoter can occur, though synthesis of full length protein is impeded. This truncated protein was expected to be degraded though, due to proteolytic mechanisms that function to remove incorrectly synthesised or folded protein. Regardless of these mechanisms, any protein synthesised would be non-functional due to lack of the enzymatic amine oxidase like (AOL) domain and most significantly, the catalytically essential lysine 661 residue, encoded by exon 15 (Lee *et al.* 2005).

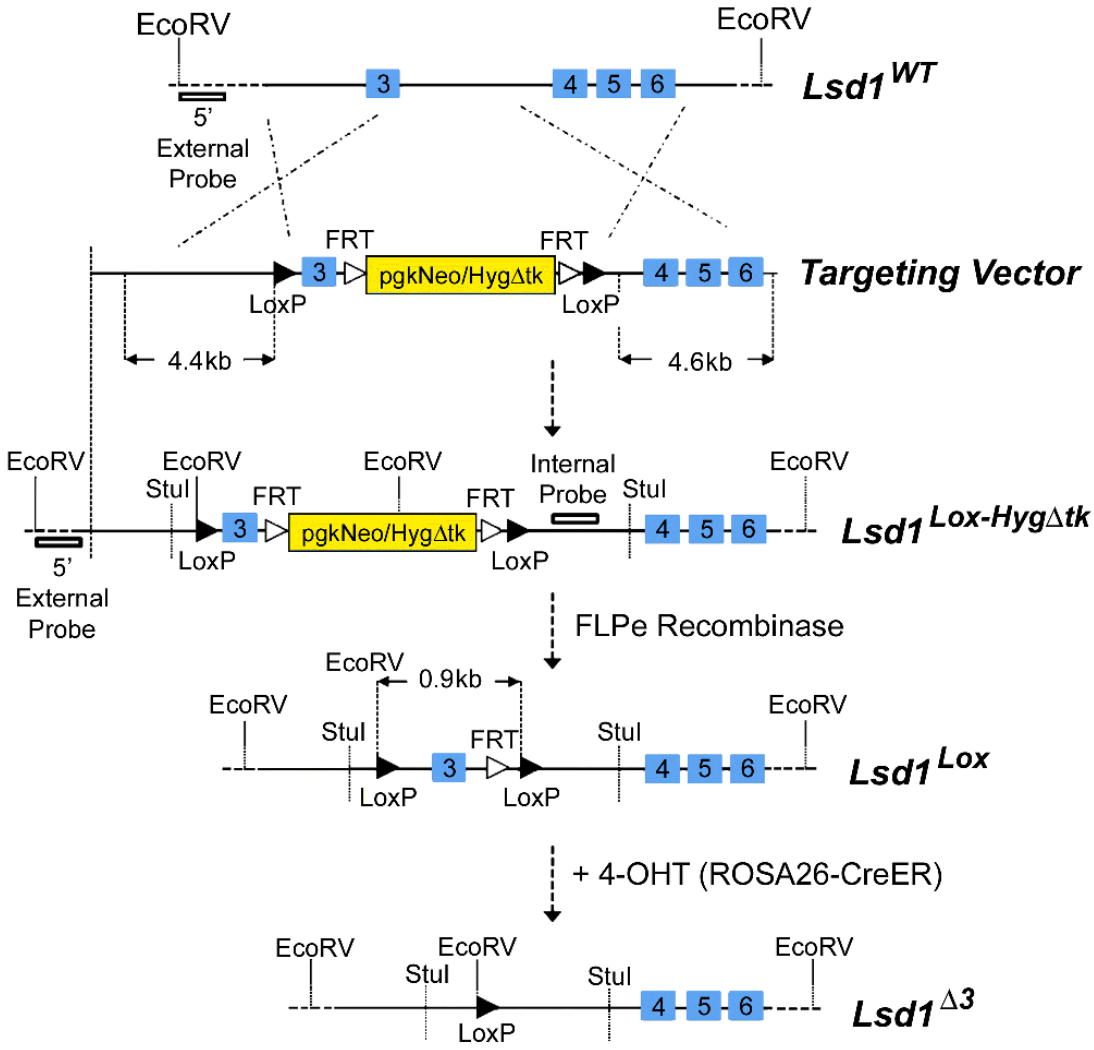

Figure 3.2 Generation of the conditional LSD1 knockout ES cell line (A) E14 mouse ES cells expressing a Cre/ER fusion protein from the *ROSA26* locus were used to produce a 4-OHT inducible conditional knockout system. Exon 3 of the *Lsd1* gene was flanked by LoxP sites (floxed) using an '*Lsd1cKO-HygΔTK'* gene targeting vector. The size of the arms of homology and postion of the *LoxP* and *FRT* sites is indicated. Correct gene targeting was assessed by Southern blotting using a 5' external probe following an *Eco*RV restriction digest of genomic DNA. Targeted $Lsd1^{+/Lox\text{-}Hyg\Delta TK,}$ cells were treated with 4-OHT for 24 hours to induce *LoxP* site recombination and generate $Lsd1^{+/\Delta 3}$ cells. Successfully recombined cells were identified by Southern blotting using an internal probe and *Stu*I digest. The second *WT* allele of the $Lsd1^{+/\Delta 3}$ cells was targeted with the same targeting vector to produce $Lsd1^{Lox\text{-}Hyg\Delta TK/\Delta 3}$ cells. Transient transfection of the $Lsd1^{Lox\text{-}Hyg\Delta TK/\Delta 3}$ cells with the FLPe recombinase was used to remove the selection cassette and produce $Lsd1^{Lox/\Delta 3}$ cells used in the study.

3.2.1.1 Removal of the HygΔTK selection cassette from Lsd1$^{Lox\text{-}Hyg\Delta TK/\Delta 3}$ ES cells

Before the targeted ES cells could be used for deletion of the floxed region, a clone of *Lsd1*$^{Lox\text{-}Hyg\Delta TK/\Delta 3}$ ES cells was transfected with the FLPe recombinase to remove the *FRT* site-flanked selection cassette from the *Lox-HygΔTK* allele (Figure 3.3A). *FRT* site recombination is known to be less efficient than *LoxP* site recombination and therefore following transfection, single cell plating and colony growth, 96 colonies were picked and screened. Generation of pure *Lsd1*$^{Lox/\Delta 3}$ ES cell clones depended on the efficiency of plasmid transfection, the level of FLPe expression in individual cells, the efficiency of recombination, efficacy of drug selection and preventing contamination between ES cell colonies during colony picking. Colonies were grown under the selection of 1-(2-deoxy-2-fluoro-1-D-arabinofuranosyl)-5-iodouracil (FIAU) and puromycin, which would kill cells expressing thymidine kinase (TK) and cells no longer expressing *puro*^{R} from the *ROSA26* locus, respectively. As expected, many cells were killed as they retained the *HygΔTK* cassette, which indicated that either transfection efficiency was much less than 100% and/or FRT site recombination was inefficient.

Following screening of surviving colonies by Southern blotting using an internal probe (Figure 3.3A), 100% of targeted cells lacked the *HygΔTK* cassette. This was no surprise, as FIAU selection had killed thymidine kinase-expressing cells (Figure 3.3B lane 1, 6,7 and 9). However, the Southern blotting result identified the *WT* allele in addition to *Lox* and *Δ3* alleles, which had an identical size to the *Δ3* allele (1.9kb) (Figure 3.3B lanes 2, 3, 4, 5 and 8). This contamination occurred as some *Lsd1*$^{+/\Delta 3}$ cells, which had

not been effectively targeted with the *Lsd1cKO-HygTK* vector in the second round of targeting and had survived hygromycin selection, remained in the population of ES cells. Six *Lsd1*$^{Lox/\Delta 3}$ clones were analysed by genomic PCR to ensure no confirm these cells possessed the targeted *Lsd1*^{Lox} allele (Figure 3.3C). These six *Lsd1*$^{Lox/\Delta 3}$ clones were chosen for further experimentation and established in cell culture from which to induce recombination in the floxed allele (to generate *Lsd1*$^{\Delta 3/\Delta 3}$ cells); these clones were A6, B12, C10, E5, F4 and G9.

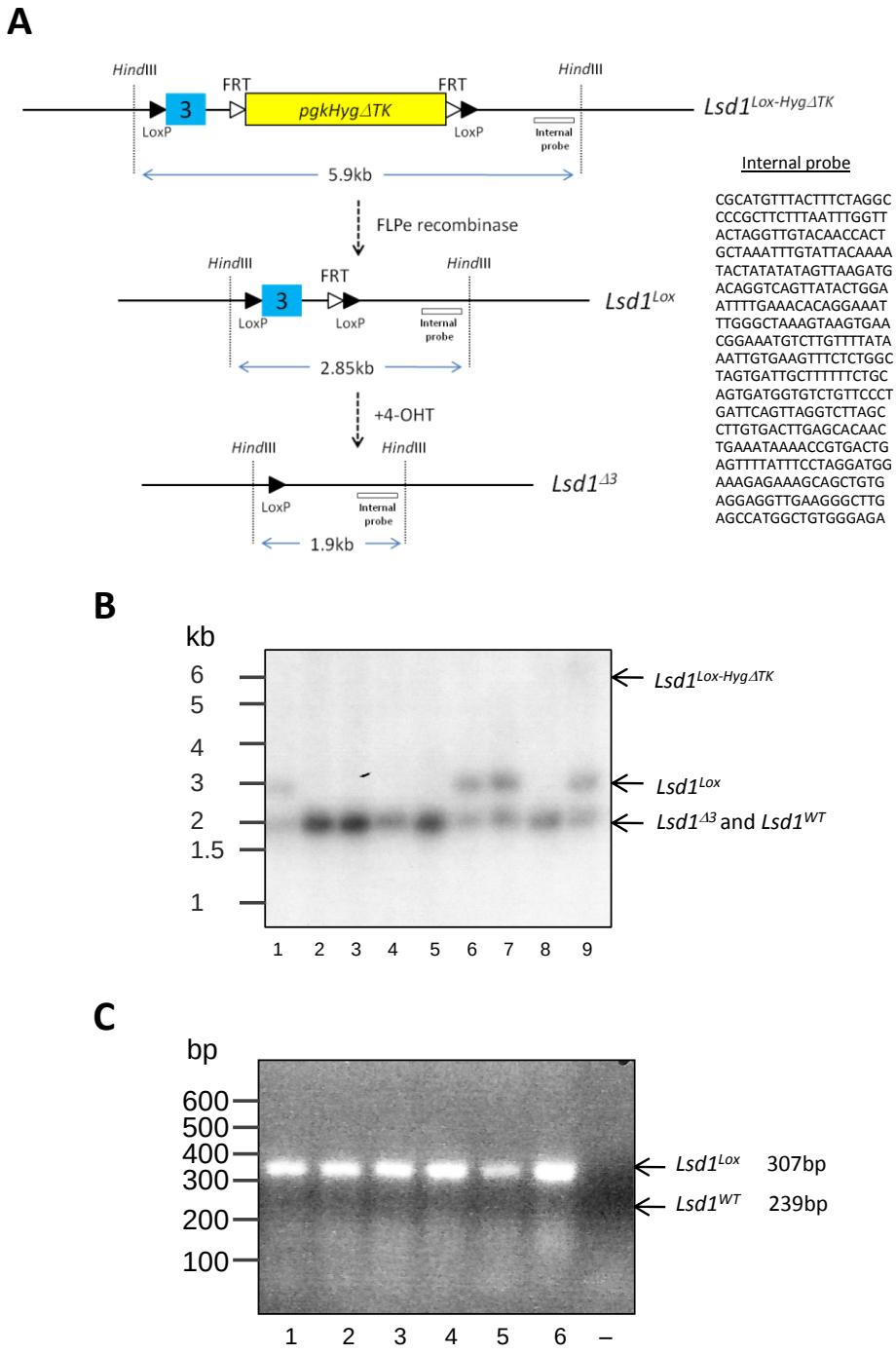

Figure 3.3 Identification of *Lsd1*$^{Lox/\Delta3}$ ES cell clones by Southern blotting. (A) Identification of *Lsd1*$^{Lox/\Delta3}$ clones with successfully removed *Hyg⊿TK* selection cassette was achieved by Southern blotting using digestion with *Hind*III and hybridisation with an 367bp internal probe (B) A representation of the screen of 96 clones shows that the original cell used for transfection of FLPe were a mix of *Lsd1*$^{+/\Delta3}$ and *Lsd1*$^{Lox\text{-}Hyg\Delta TK/\Delta3}$ cells and that deletion of the selection cassette from *Lsd1*$^{Lox\text{-}Hyg\Delta TK}$ allele was very efficient (4 out of 4 clones; lanes 1, 6, 7 and 9). (C) PCR was performed on six *Lsd1*$^{Lox/\Delta3}$ clones used in the study to confirm the genotype.

3.2.1.2 Deletion of exon 3 from Lsd1$^{Lox/\Delta 3}$ ES cells

Cre-Lox recombination is a special type of site-specific recombination developed by Brian Sauer, commonly used to spatially and temporally control the deletion of a gene in animals and cells (Sauer 1987, Sauer & Henderson 1988). Cre (Causes recombination) is a 343 amino acid protein with a C-terminus similar in structure to the domain in the Integrase family of enzymes isolated from lamba (λ) phage. The *LoxP* (locus of X over P1) site is a 34bp DNA sequence from the Bacteriophage P1. An 8bp sequence exists between two 13bp palindromic sequences. The result of recombination depends on the orientation of the *LoxP* sites. Inverted *LoxP* sites will cause an inversion of a DNA sequence, while direct repeats of *LoxP* sites cause a deletion event. The latter mechanism is employed in these experiments. The CreER^{T} system was pioneered by Pierre Chambon in the 1990s (Metzger *et al.* 1995, Feil *et al.* 1996). Cre fused to the Estrogen Receptor (ER) renders it inactive in the cytoplasm of these ES cells (Figure 3.4A). It is sequestered by the Hsp70 chaperone protein until the activation of this nuclear receptor by ligand binding allows release from Hsp70 and translocation into the nucleus. The ER ligand-binding domain contains a mutation (glutamic acid 521→arginine) however, which renders it unresponsive to the endogenous *17β*-estrodial (estrogen) ligand. It can only be activated by 4-hydroxy tamoxifen (4-OHT), an analogue of estrogen. Translocation of Cre into the nucleus will permit access to the *LoxP* sites within the genomic sequence (Figure 3.4A). Addition of 0.1μM 4-OHT to the culture media for 48hr caused translocation of the Cre/ER fusion protein (Figure 3.4A) and subsequent Cre-mediated recombination of the *LoxP* sites within 6 hours of addition of 4-OHT (Figure 3.4B). Genomic DNA was harvested for Southern blotting as described in Chapter 2. The generation of *Lsd1$^{\Delta 3/\Delta 3}$*cells could

also be recognised by PCR (Figure 3.4C) though this method would not allow quantification of the amount of a DNA species. However, PCR was used to confirm future generation of *Lsd1*$^{\Delta 3/\Delta 3}$ cells, as it was a more convenient procedure.

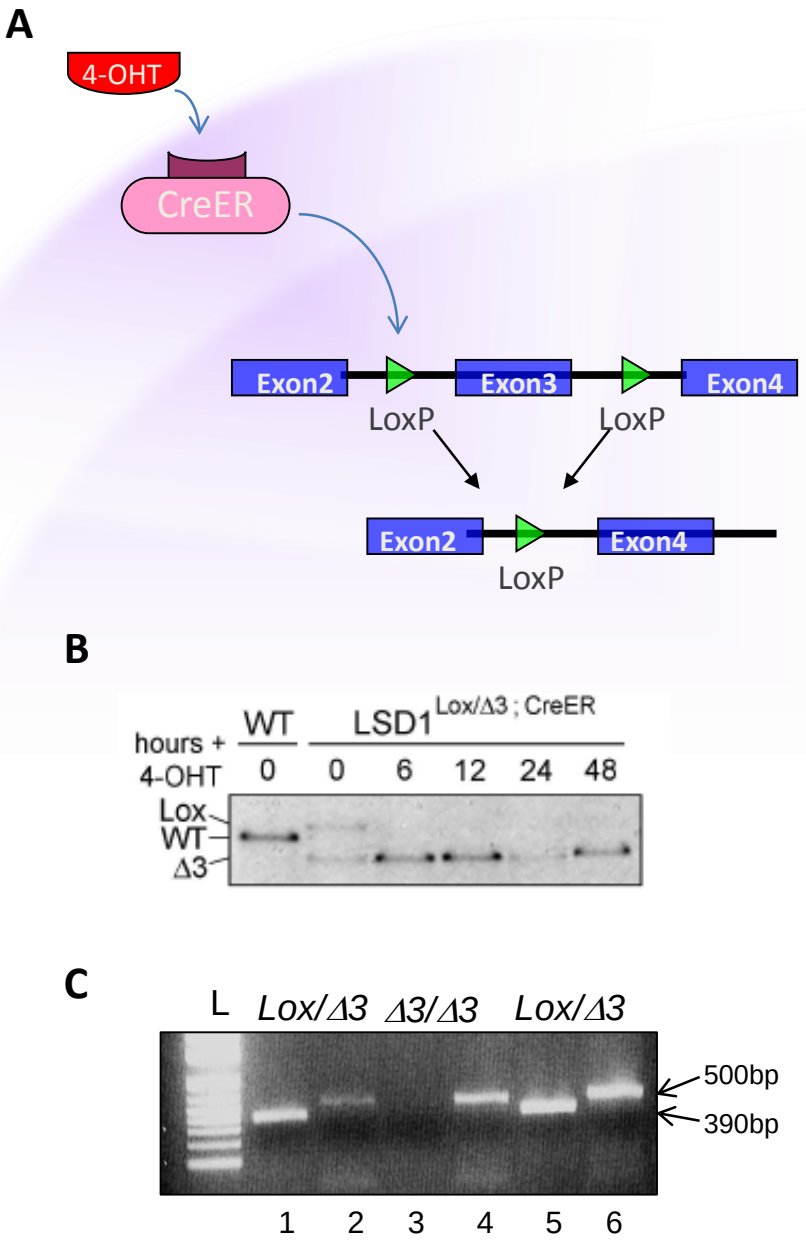

Figure 3.4 Full recombination of LoxP sites occurs within 6 hours of addition of 4-OHT. (A) A schematic to show ligand-activation of CreER, which results in translocation of Cre to the nucleus for catalysis of *LoxP* site recombination. Tandem *LoxP* site recombination causes removal of the floxed genomic DNA sequence, which contains exon 3 of LSD1. (B) *LoxP* site recombination was identified by Southern blotting. Hybridisation of an internal probe revealed shortening of DNA sequence following recombination to create the *Δ3* allele from the *Lox* allele. Complete conversion of *Lox* into *Δ3* is observed at 6 hours. (C) PCR to identify *LoxP* site recombination. Lane 1-4 shows PCR to genotype $Lsd1^{Lox/\Delta3}$ and $Lsd1^{\Delta3/\Delta3}$ cells. The *Lox* PCR generates a band of 390bp and the *Δ3* PCR generates a band of 500bp. The absence of 390bp band in *Lox* PCR indicates recombination. Lane 5 and 6 shows PCR on $Lsd1^{Lox/\Delta3}$ control cells to ensure both PCR reactions from master-mixes were successful in the genotyping.

3.2.1.3 Deletion of LSD1 protein

Following confirmation that the genetic alteration of the *Lox* allele occurred by 6 hours, the half-life of LSD1 protein following exon deletion was analysed by harvesting cellular protein from *Lsd1*$^{Lox/\Delta 3}$ cells + 4-OHT over a 10 day timecourse. This timescale used was based on previous experience with conditional deletion of HDAC1, 2 and 8 in the laboratory (Dovey *et al.* 2010a). LSD1 forms a stable protein complex with HDACs (You *et al.* 2001, Shi *et al.* 2004); therefore a similar time period for complete depletion of LSD1 was expected. Protein depletion relied on the inability to synthesise full length protein from the mRNA as well as protein complex turnover to remove the functioning cellular protein.

Progressive loss of LSD1 protein was observed over 4 days (Figure 3.5A). When creating a knockout through single exon deletion, there is always the chance that exon skipping mechanisms may allow production of a shortened, functional protein by alternative splicing back into frame using a downstream exon. The frame of exon 5 starts with the same phase as the end of exon 2 (phase 1), therefore just one exon could be skipped to splice exon 2 to exon 5 and resume the correct reading frame. As well as this, the use of an alternative start codon, in the correct frame, downstream of exon 3 could be utilised to produce a functional protein with an AOL domain. To ensure that a shortened, possibly functional protein did not arise following exon 3 deletion, an antibody specific to an epitope at the C-terminus of LSD1 was used in addition to an N-terminal antibody. This would recognise the possible accumulation of a smaller protein throughout the timecourse of deletion. The C-terminal antibody was

used to assess the deletion over the timecourse and LSD1 protein appears to be completely removed at 4 days post induction with no smaller protein observed (Figure 3.5A). The reduction in the level of LSD1 transcript (Figure 3.5B) is validation that a successful nonsense mutation was created. This depletion of transcript is indicative of nonsense mediated decay (NMD) as the 5' and 3' primers used in the qRT-PCR anneal in exon 4 and 5 respectively, downstream of the exon deletion and the premature stop codon, which is 14 codons into exon 4. The presence of a premature stop codon in exon 4 before the final exon would be detected by mRNA surveillance mechanisms to trigger the degradation of aberrant mRNA species and prevent the expression of truncated proteins (Hentze & Kulozik 1999). However, the occurrence of exon 4 skipping would remove the 5' primer binding site and may account for this result. This was ruled out due to the lack of any smaller protein products in western blots and microarray-identified reduction of LSD1 transcripts in *Lsd1*$^{\Delta 3/\Delta 3}$ cells (Chapter 4). *Lsd1*$^{Lox/\Delta 3}$ ES cells were used as control cells for much of the functional analysis. These cells are heterozygous for *Lsd1* and were considered an appropriate control genotype to compare *Lsd1*$^{\Delta 3/\Delta 3}$ cells to; as they showed identical levels of LSD1 protein expression to *WT* cells (Figure 3.5C). Given the kinetics of exon 3 deletion and protein half-life, in subsequent experiments *Lsd1*$^{Lox/\Delta 3}$ cells were compared to *Lsd1* $^{\Delta 3/\Delta 3}$ cells at 7-15 days after 4-OHT treatment.

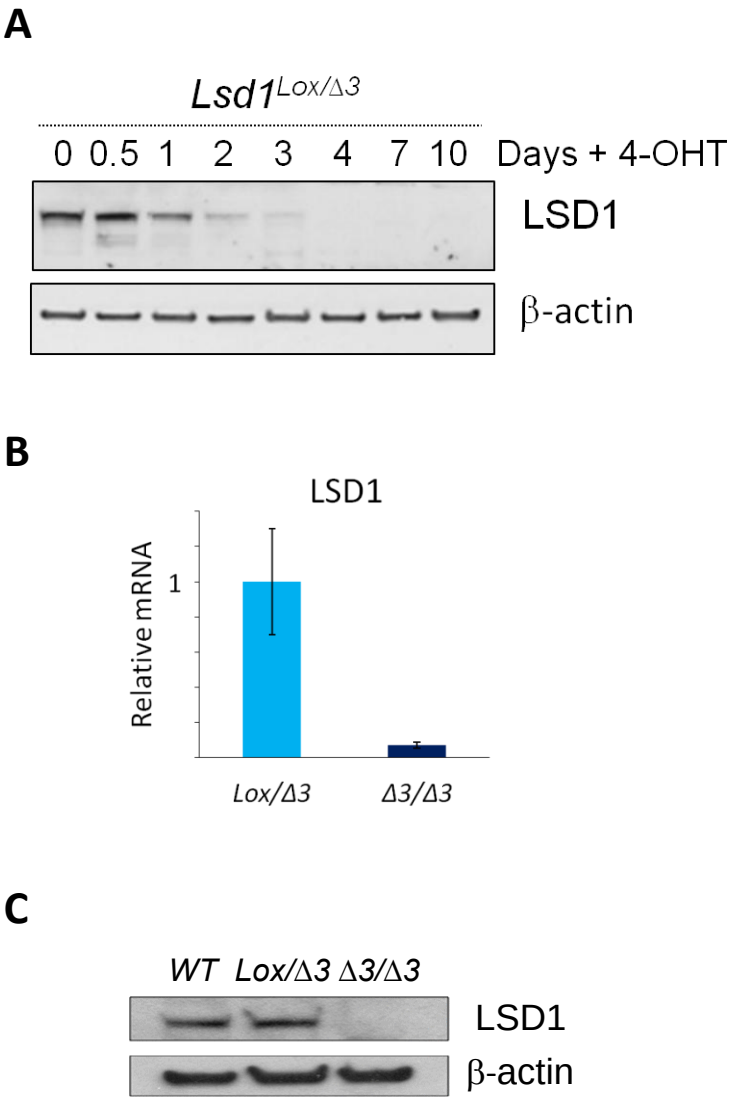

Figure 3.5 Induction of the conditional deletion results in loss of LSD1 protein after 4 days. (A) Western blot shows ligand-inducible deletion of LSD1 protein in nuclear extracts of *Lsd1*$^{Lox/\Delta 3}$ ES cells. Cells were cultured for up to 10 days to assess the timescale of protein depletion (0-2 days in the presence of 4-OHT). The signal at 110kDa is lost over time with no evidence of the appearance of a slightly smaller protein that would result from alternative splicing from exon 2 to exon 5. β-actin was used to normalise for protein loading. (B) Quantitative RT-PCT reveals a decrease in LSD1 mRNA levels due to nonsense mediated decay following exon 3 deletion**.** (C) Western blot shows that LSD1 protein levels are equivalent in *WT* and *Lsd1*$^{Lox/\Delta 3}$ ES cells. *Lsd1*$^{Lox/\Delta 3}$ cells are used as a control through the study of LSD1 function.

3.2.2 Generation of LSD1-null MEFs

The question of whether ES cells that had undergone numerous rounds of targeting and selection are still functionally pluripotent can be resolved by observing their ability to contribute to the germ line of a mouse following blastocyst injection. In addition to this, teratoma formation assays can be implemented to test if all three primary lineages could develop from the pluripotent state. Mouse embryonic fibroblasts (MEFs) can be harvested from chimeric embryos that develop from injected blastocysts. *Lsd1*$^{Lox/\Delta 3}$; *ROSA26*$^{CreER\text{-}Puro}$ ES cells were injected into blastocysts by the Geneta Gene Targeting and Transgenic Service at the University of Leicester. MEFs were harvested from E14.5 chimaeras and cells were cultured in the presence of puromycin to select for *Lsd1*$^{Lox/\Delta 3}$ cells over 4 days. Genomic PCR identified the presence of a small amount of contaminating *WT* cells (Figure 3.6A), we therefore continued to supplement the culture media with puromycin. Deletion of exon 3 within the *Lsd1*^{Lox} allele by 0.1μM 4-OHT treatment was analysed over a 5 day timecourse. PCR was used to assess the temporal nature of *LoxP* site recombination, which showed that full recombination occurred by 3 days (Figure 3.6B). This method is not quantitative; however the lack of any detectable amplified band at 3 days post 4-OHT treatment suggested complete recombination of *LoxP* sites. The kinetics of LSD1 protein depletion in MEFs was similar to that observed in the *Lsd1*$^{\Delta 3/\Delta 3}$ ES cells, where LSD1 protein was lost by 4 days (Figure 3.6C). *Lsd1*$^{\Delta 3/\Delta 3}$ MEFs were frozen back at day 5 after induction of deletion. These cells were not used further in functional analyses due to time limitations; though they would provide a useful tool for study, as the

aspects of chromatin and histone modifications are different in MEFs to mouse ES cells. Notably, these results validated that MEFs could be generated from ES cells used in this investigation.

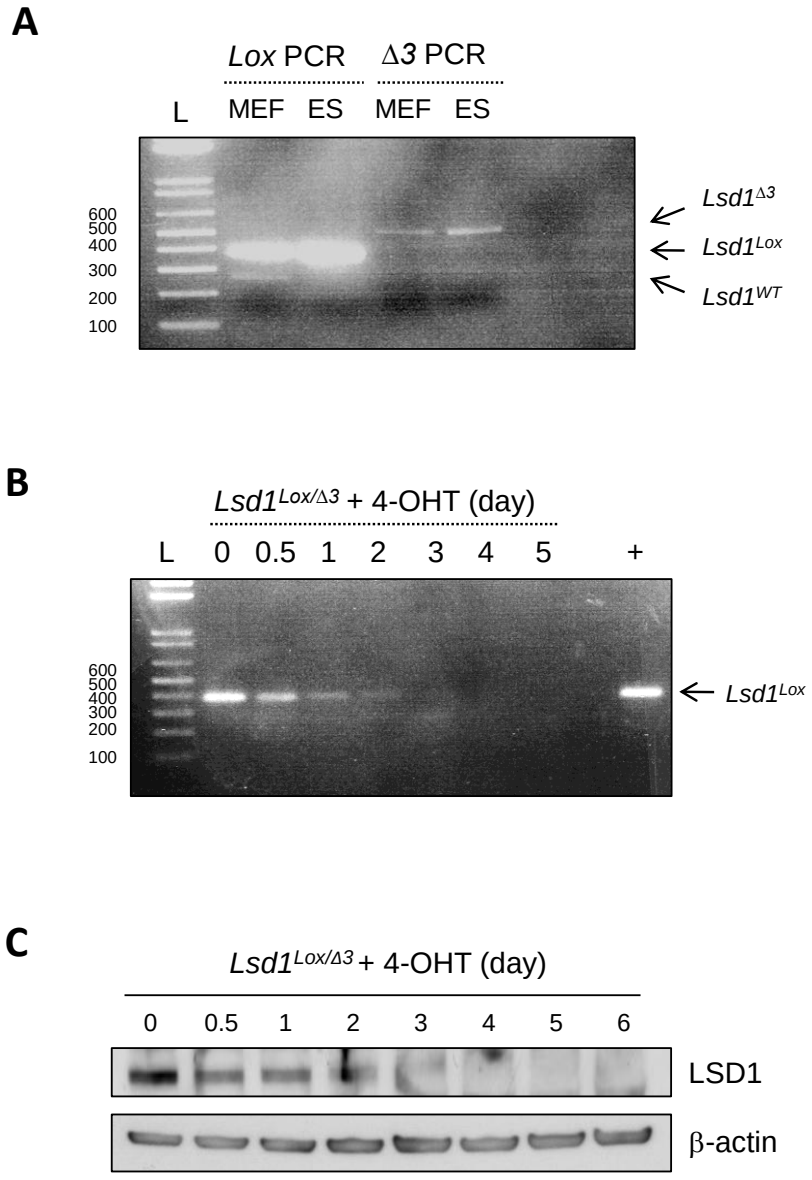

Figure 3.6 Generation of LSD1-null MEFs. (A) PCR reactions identified successful establishment of *Lsd1*$^{Lox/\Delta3}$ MEFs through puromycin selection. Two PCR reactions were performed separately to identify *Lox* and *Δ3* alleles. The result shows that there was residual quantity of *WT* cells. *Lsd1*$^{Lox/\Delta3}$ ES cells were used as a positive control. (B) PCR was performed to assess the temporal nature of *LoxP* site recombination within the *Lox* allele following +4-OHT treatment. *Lsd1*$^{Lox/\Delta3}$ ES cells were used as a positive control. (C) Western blot shows ligand-inducible deletion of LSD1 protein in nuclear extracts from *Lsd1*$^{Lox/\Delta3}$ MEFs. Cells were cultured for up to 6 days to assess the timescale of protein depletion (0-2 days in the presence of 4-OHT). β-actin was used to normalise for protein loading.

3.2.3 Analysis of undifferentiated LSD1 knockout ES cells

Analysis of the growth rate (Figure 3.7A) and cell cycle profile (Figure 3.7B) of *Lsd1*$^{\Delta 3/\Delta 3}$ cells revealed that the deletion of LSD1 had little effect on the proliferative potential of undifferentiated ES cells, consistent with the embryo outgrowth phenotype (Figure 3.1K-M). Over a 5 day period the rate of ES cell growth were very similar, which was supported by similar numbers of cells identified in each stage of the cell cycle. Very similar percentages of cells were undergoing cell death (6% v 7% cells with sub-G1 DNA content); 3% more *Lsd1*$^{\Delta 3/\Delta 3}$ cells were in the G1 stage of the cell cycle; 28% and 30% of control and knockout cells, respectively, were within the period of DNA replication (S-phase); and 6% less *Lsd1*$^{\Delta 3/\Delta 3}$ cells were in mitosis (G2/M) (Figure 3.7B). Discrepancies in the cell cycle percentages overall had little effect on rate of growth (Figure 3.7A). The generation of LSD1 knockout MEFs (Figure 3.6) was performed with the intention of investigating these results further.

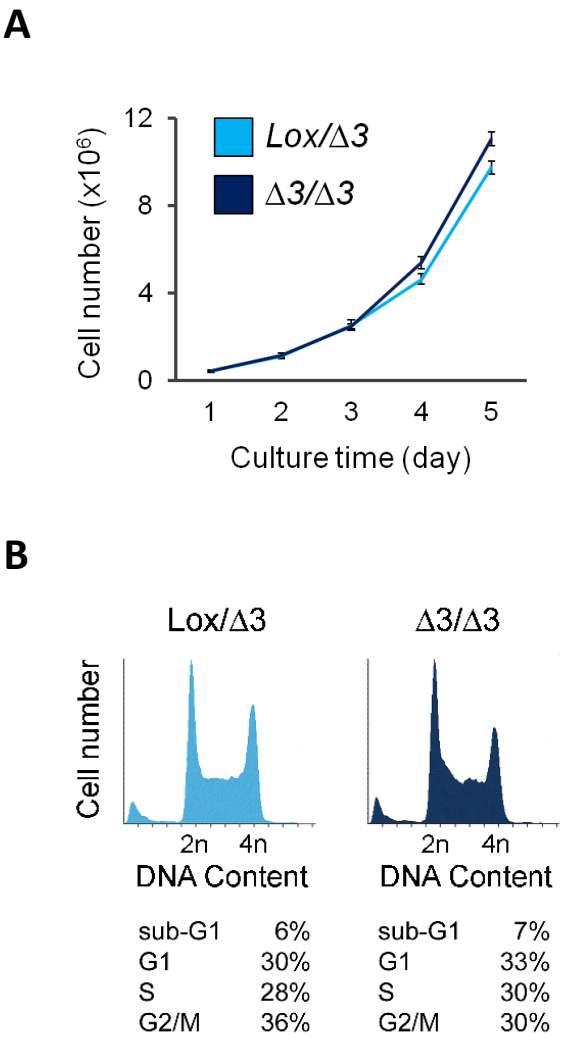

Figure 3.7 Deletion of LSD1 has no effect on the growth rate and cell cycle profile. (A) The growth rate of the indicated cells was assessed by counting cells over a 5 day period from initial plating of 2.5 x 10^4 cells in 6cm plates. *Lsd1*$^{\Delta 3/\Delta 3}$ cells were plated at day 10 after induction of the deletion. (B) Propidium iodide (PI) staining and FACS analysis reveals similar cell cycle profiles of *Lsd1*$^{Lox/\Delta 3}$ and *Lsd1*$^{\Delta 3/\Delta 3}$ ES cells. The percentage of cells with a sub-G1, G1 (2n), S-phase or G2/M) (4n) content is indicated.

Dnmt1 levels were assessed by Western blot due to the previous suggestion that LSD1 regulates Dnmt1 levels in ES cells (Wang *et al.* 2009). Dnmt1 is a key enzyme that maintains DNA methylation patterns following DNA replication due to specificity to hemi-methylated CpG dinucleotides (Li *et al.* 1992, Bird 2002, Goll & Bestor 2005). Reduced Dnmt1 is translated into defects in maintenance of global DNA methylation (Wang *et al.* 2009). Loss of global DNA methylation may result in the expression of genomic regions that are usually silenced (reviewed in Bird 2000). It was important to know the state of global DNA methylation following LSD1 deletion in order to rule out effects of DNA hypo-methylation on transcriptional changes. The continued culture of ES cells lacking LSD1 for up to 25 days results in a progressive decrease in Dnmt1 levels (Figure 3.8A and B). The onset of this progressive reduction in Dnmt1 correlates with the point of complete LSD1 protein deletion (compare Figure 3.5A with 3.8B). However, a substantial reduction in protein levels is not observed in *Lsd1*$^{\Delta 3/\Delta 3}$ ES cells until beyond 10 days after induction of LSD1 deletion (Figure 3.8B). This result supports the published role of LSD1 in regulating the stability of Dnmt1 by demethylation of K1096 in mouse ES cells (Wang *et al.* 2009). Importantly, global DNA methylation levels in *Lsd1*$^{\Delta 3/\Delta 3}$ cells were comparable to control cells at 10 days after induction of LSD1 deletion, as measured by incomplete digestion of endogenous retroviral elements (IAP) using a methylation-sensitive restriction enzyme, *Hpa*II (Figure 3.9A). This repetitive DNA sequence is heavily methylated at CpG dinucleotides within the ES cell-represented developmental stage (Mayshoopes, *et* al. 1983). The presence of methylation can be identified by digestion of genomic DNA with an enzyme that only cuts at the unmethylated form of the CC$^{\downarrow}$GG restriction site (*Hpa*II), and comparing it to digestion with an isoschizomer that cuts regardless of

methylation state (*Msp*I) (Mcclelland *et al.* 1981). At day 10, this site is clearly still methylated, based on the inability for *Hpa*II to recognise and cut this site (Figure 3.9A, lane 3). Complete digestion of this site by *Msp*I results in a hybridisation of the IAP probe to approximately 0.5kb fragments (Figure 3.9A, lanes 2 and 4; Mcclelland *et al.* 1981). The continued culture of these ES cells lacking LSD1 (up to 25 days post 4-OHT addition) results in decreased global DNA methylation (Figure 3.9B, lane 7, arrow), consistent with the results of Taipeng Chen and colleagues (Wang *et al.* 2009). This is identified by the appearance of smaller fragments of DNA in the *Hpa*II digested DNA (Figure 3.9B, arrow), indicative of loss of cytosine methylation on the second C of the $CC^{\downarrow}GG$ site. This data provided assurance that analysis of ES cell differentiation from day 7 onwards following LSD1 deletion could reveal insights into the role of LSD1 in ES cell differentiation through direct gene regulation.

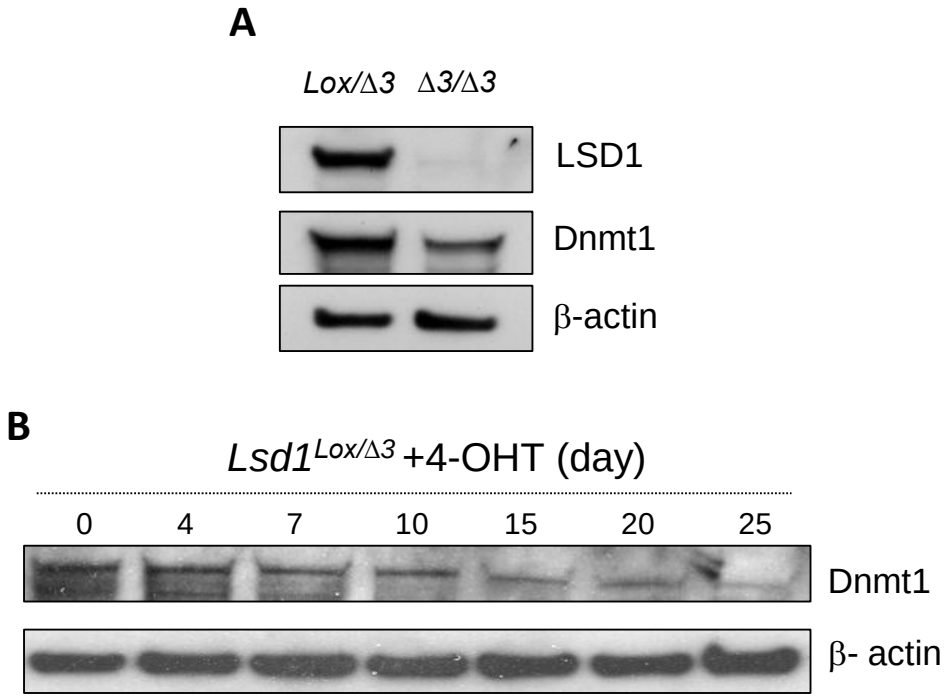

Figure 3.8 Loss of LSD1 causes a reduction in Dnmt1 protein levels. (A) A Western blot shows that after 25 days (7-8 passages) following induction of LSD1 deletion, protein levels of Dnmt1 are decreased, as previously reported (Wang *et al*. 2009) . (B) Western blotting over the 25 day period indicates that there is a progressive reduction in Dnmt1, clearly in response to LSD1 deletion. β-actin was used to normalise for protein loading.

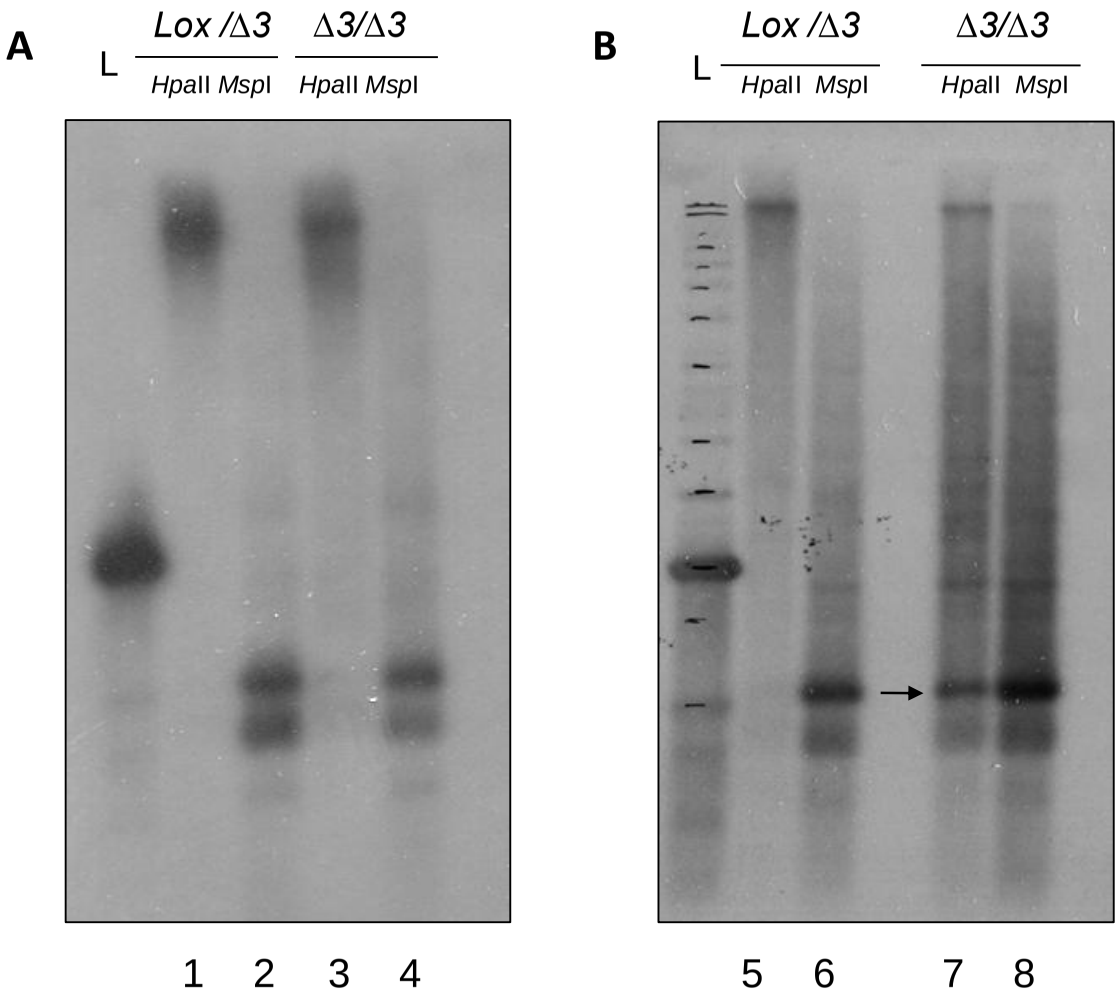

Figure 3.9 Deletion of LSD1 results in loss of genomic methylation after multiple passages. Southern blotting was used to assess the level of genomic methylation at the intracisternal A-particle (IAP) LTR retrotransposon elements at, (A) 10 days, and (B) 25 days after the induction of LSD1 deletion. Genomic DNA was digested with either *Hpa*II (methylation sensitive) or *Msp*I (methylation resistant) restriction enzymes and then hybridised with an IAP DNA probe.

3.2.4 *In vitro* differentiation analysis of LSD1 knockout ES cells

As the LSD1 knockout embryos die just before the onset of gastrulation and the proliferative capacity of undifferentiated ES cells is unperturbed by loss of LSD1, *Lsd1*$^{Lox/\Delta 3}$ and *Lsd1*$^{\Delta 3/\Delta 3}$ cells were compared for their ability to differentiate. The first differentiation assay involved plating ES cells at clonal density (700 cells/6-well) and culturing them for a further 5 days in the presence, or absence of LIF. Subsequent staining of cells with alkaline phosphatase (AP), a marker of pluripotency, tested the ability of cells to retain pluripotency in the presence of LIF and the potential to differentiate without it. *Lsd1*$^{\Delta 3/\Delta 3}$ cells could retain pluripotency in the presence of LIF as well as spontaneously differentiate over the course of 5 days in the absence of LIF (Figure 3.10A). *Lsd1*$^{\Delta 3/\Delta 3}$ cells also showed a similar percentage of differentiated colonies to *Lsd1*$^{Lox/\Delta 3}$ controls in the presence of LIF, though the proportion of differentiated cells was less in the absence of LIF (Figure 3.10B). Interestingly, the overall number of *Lsd1*$^{\Delta 3/\Delta 3}$ colonies observed, by methylene blue staining, in the absence of LIF was reduced by approximately 60% (Figure 3.10C). This result, along with a lower proportion of differentiated colonies surviving 5 days in the absence of LIF, suggests that *Lsd1*$^{\Delta 3/\Delta 3}$ cells can differentiate, but differentiation is associated with increased cell death. Another observation was that LSD1-deficient ES cells, when plated at low density, generated more colonies in the presence of LIF (Figure 3.10C); supporting a slightly increased growth rate of *Lsd1*$^{\Delta 3/\Delta 3}$ cells (Figure 3.7A). The observation that *Lsd1*$^{\Delta 3/\Delta 3}$ cells can also survive upon differentiation, meant that some developmental lineages can propagate in the absence of LSD1. Further differentiation experiments were required to understand which lineages could develop and if the phenotype was reproducible in other assays of *in vitro* differentiation.

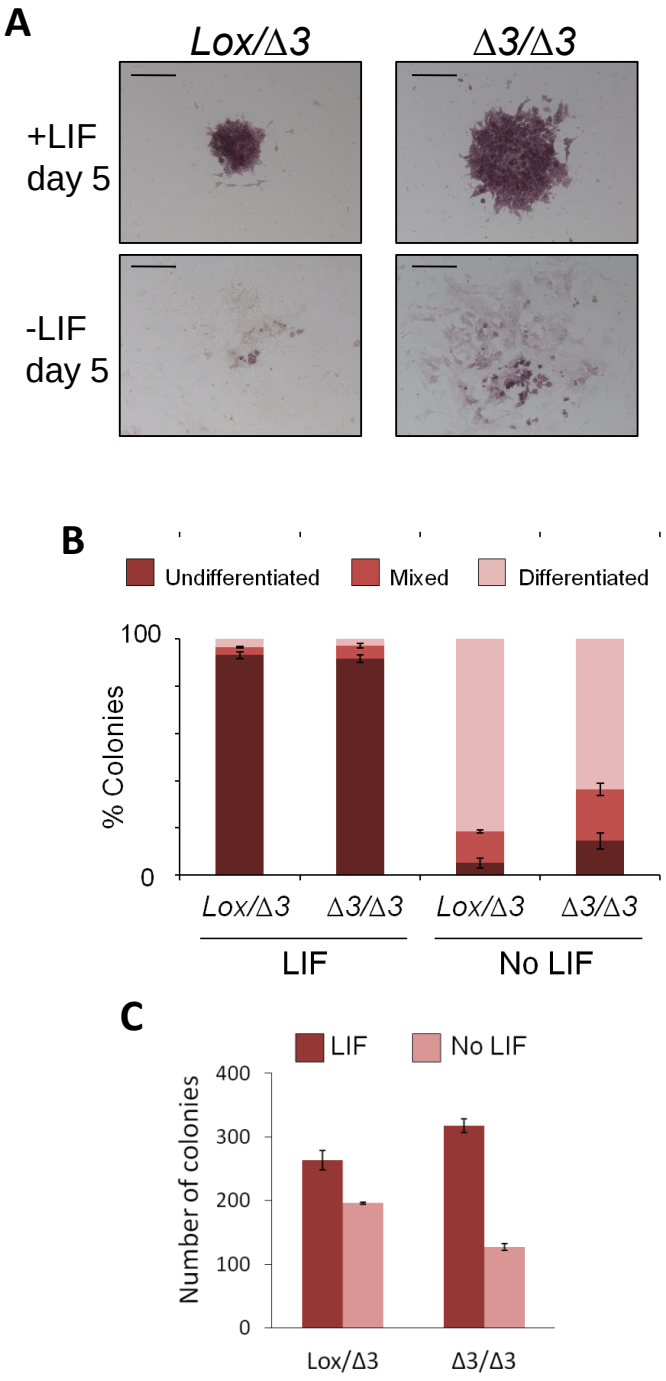

Figure 3.10 ES cells lacking LSD1 are allowed to differentiate upon LIF withdrawal, however with reduced survival of colonies. (A-B) Differentiation potential; ES cells of the indicated genotype were plated at low density in the presence or absence of LIF and cultured for 5 days before being stained for the presence of alkaline phosphatase (a marker of pluripotency) and imaged under the microscope to record a representative image and to be scored as undifferentiated (intense purple), mixed (weak purple), or differentiated (no staining). Scale bar = 200μMeter. (C) Colonies were subsequently stained with methylene blue and total numbers were counted to calculate colony numbers and percentages for the bar graph in (B). Mean values were plotted (n=3) +/- S.E.M .

The generation of embryoid bodies (EBs) by hanging drop culture in the absence of LIF demonstrated that *Lsd1*$^{\Delta 3/\Delta 3}$ cells had the ability to aggregate to form embryoid bodies (Figure 3.11A). However, fewer *Lsd1*$^{\Delta 3/\Delta 3}$ cells formed aggregates effectively by day 1, as shown in the representative image (Figure 3.11A, top panel). By day 5, 50-60% less *Lsd1*$^{\Delta 3/\Delta 3}$ EBs compared to controls was observed (Figure 3.11B); a similar figure to the reduction in *Lsd1*$^{\Delta 3/\Delta 3}$ cell survival after 5 days in the absence of LIF (Figure 3.10C). In addition, the surviving EBs were reduced in size by roughly a third at day 5 (Figure 3.11C). These data suggest that ES cell aggregation can occur to form the outer layer of primitive endoderm, though further differentiation may be perturbed, either resulting in death of the EB or reduced capacity to differentiate and grow.

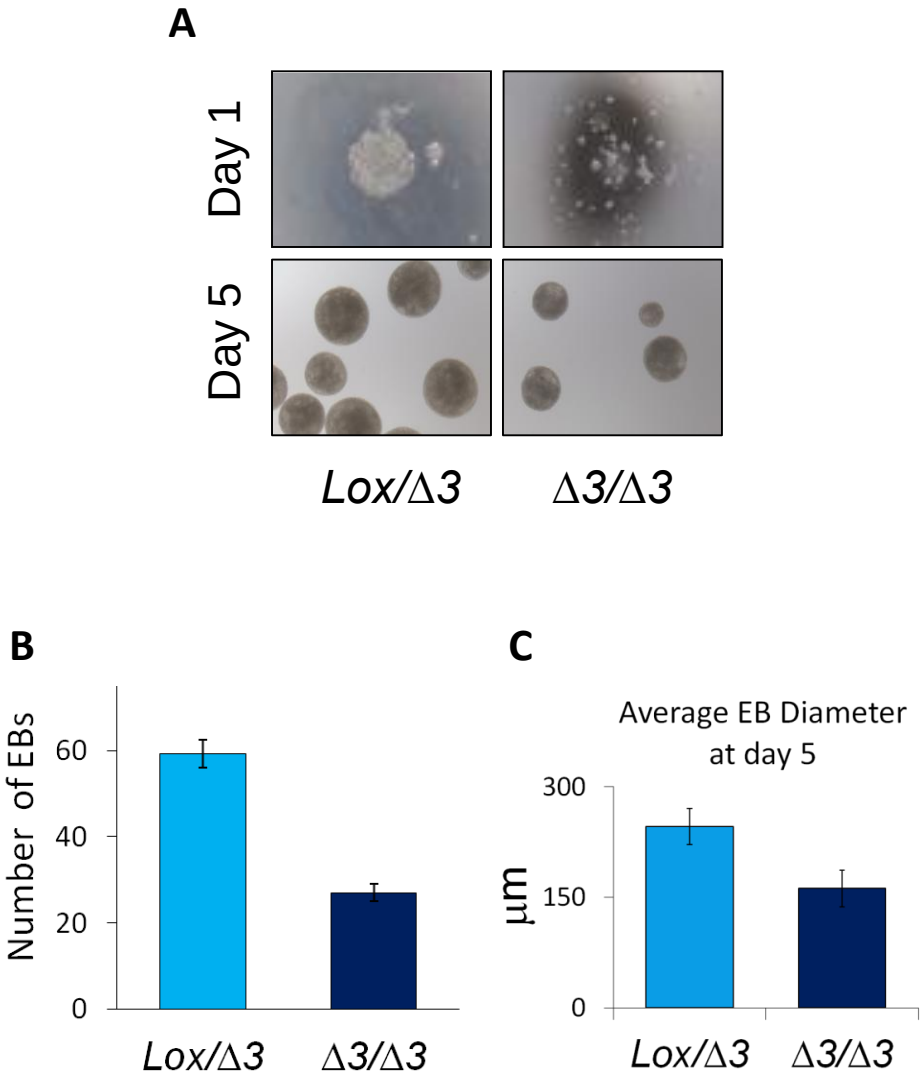

Figure 3.11 ES cells depleted in LSD1 have defects in differentiation as embryoid bodies. (A) Images representative of EBs at 1 and 5 days of culture shows that some EBs *Lsd1*$^{\Delta 3/\Delta 3}$ EBs fail to aggregate as expected as well as reduced size at day 5. Bar graphs show (B) the number of EBs and (C) the average size of EBs of the indicated genotype obtained after 5 days of culture.

To confirm whether increased cell death is associated with differentiation in the absence of LSD1, *Lsd1*$^{Lox/\Delta 3}$ and *Lsd1*$^{\Delta 3/\Delta 3}$ cells were cultured in the presence of retinoic acid (RA) to stimulate differentiation and measure the accumulation of cells with sub-G1 DNA content. Prior to RA treatment, both sets of cells display small populations of dead cells (Figure 3.12A, day 0). In contrast, after 3 days of RA treatment, 58% of *Lsd1*$^{\Delta 3/\Delta 3}$ cells showed a sub-G1 DNA content, over 2-fold more than controls (Figure 3.12A, day 3). As RA addition is a powerful driver of differentiation, a more subtle differentiation assay was subsequently employed by removing LIF in neuronal differentiation serum-free media (N2B27). Even before the withdrawal of LIF, 4-fold more *Lsd1*$^{\Delta 3/\Delta 3}$ cells possessed sub-G1 DNA content, most likely accounted for by the lack of differentiation-inhibiting serum in media (Figure 3.12B day 0), as serum/BMP4-inhibits differentiation through induction of Id proteins (Ying *et al.* 2003). Loss of BMP4 signalling may therefore account for increased cell death. Notably though, an almost 4-fold larger percentage of dead cells was observed upon the withdrawal of LIF in this media (Figure 3.12B, day 3). Overall, these data suggest that ES cells lacking LSD1 are far more susceptible to cell death in differentiation-inducing conditions, and that much of this death occurs within 3 days of exit from the pluripotent state, which is consistent with a 50-60% reduction in the number of EBs over a similar time period.

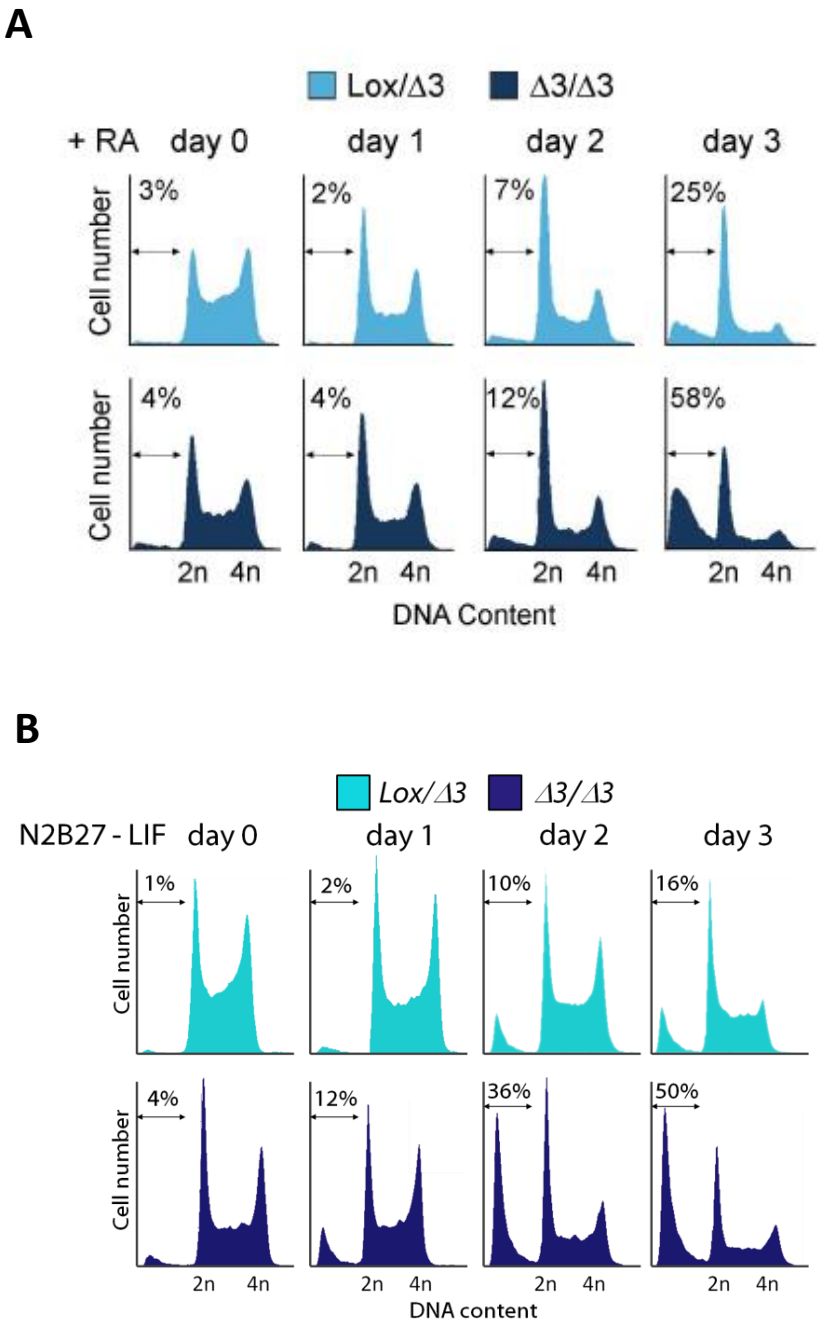

Figure 3.12 Differentiation of ES cells lacking LSD1 is associated with apoptotic cell death. (A) The percentage of dead cells was determined by propidium iodide staining and FACS analysis after treatment of cells with 1mM retinoic acid over 3 days . (B) The same analysis was done after culture in N2B27 media with removal of LIF over 3 days. In each case the percentage of cells with a sub-G1 DNA content is indicated.

Gene expression analysis of EBs was performed in order to reveal molecular mechanisms that might underpin the observed cell death. Firstly, as expected following observations of AP down-regulation in the absence of LIF, EBs lacking LSD1 retained the ability to switch off the pluripotent factor genes *Oct4*, *Nanog* and *Rex1* (Figure 3.13A). This signifies that LSD1 is not involved in repression of these genes upon exit from the pluripotent state. The formation of primitive ectoderm (indicative of the embryonic epiblast cells before E6.5) was unaffected, since activation of *FGF5* was observed at day 2 (Figure 3.13B, left panel). At day 5, endoderm lineages appeared to develop to a similar extent in EBs derived from $Lsd1^{Lox/\Delta 3}$ and $Lsd1^{\Delta 3/\Delta 3}$ cells, as indicated by *GATA6* activation (Figure 3.13B, right panel). This agrees with the ES cell aggregation and down-regulation of *Nanog* expression at day 5 to form primitive endoderm (Chambers *et al*. 2003, Mitsui *et al.* 2003, Hamazaki *et al*. 2004). However, defects in mesoderm development were apparent. The level of *Brachyury* mRNA was notably higher in both undifferentiated ES cells and day 2 EBs lacking LSD1 (Figure 3.13B, middle panel), indicating an altered pattern of gene expression that could potentially perturb differentiation. Classically, induction of *Brachyury* is not observed upon differentiation in the presence of serum until day 3 (Fehling *et al.* 2003, Keller 2005). The significant reduction of *Brachyury* expression in LSD1-deleted cells between day 2 and 5 suggests that cell types over-expressing this gene may have died. This idea was supported by the observation of 12%→58% sub-G1 cells between day 2 and 3 of RA-induced differentiation (Figure 3.12A). It is also noteworthy that day 2 of EB differentiation corresponds to E6.5 of the developing embryo (Keller 2005; see Chapter 1.8.6), suggesting that *Brachyury* over-expression, large differentiation-associated cell death and a block in embryonic development may be linked. The

survival however of some *Lsd1*$^{\Delta 3/\Delta 3}$ EBs suggested that some early stage EBs withstood the de-regulation of mesodermal gene expression due to a redundancy in gene expression control.

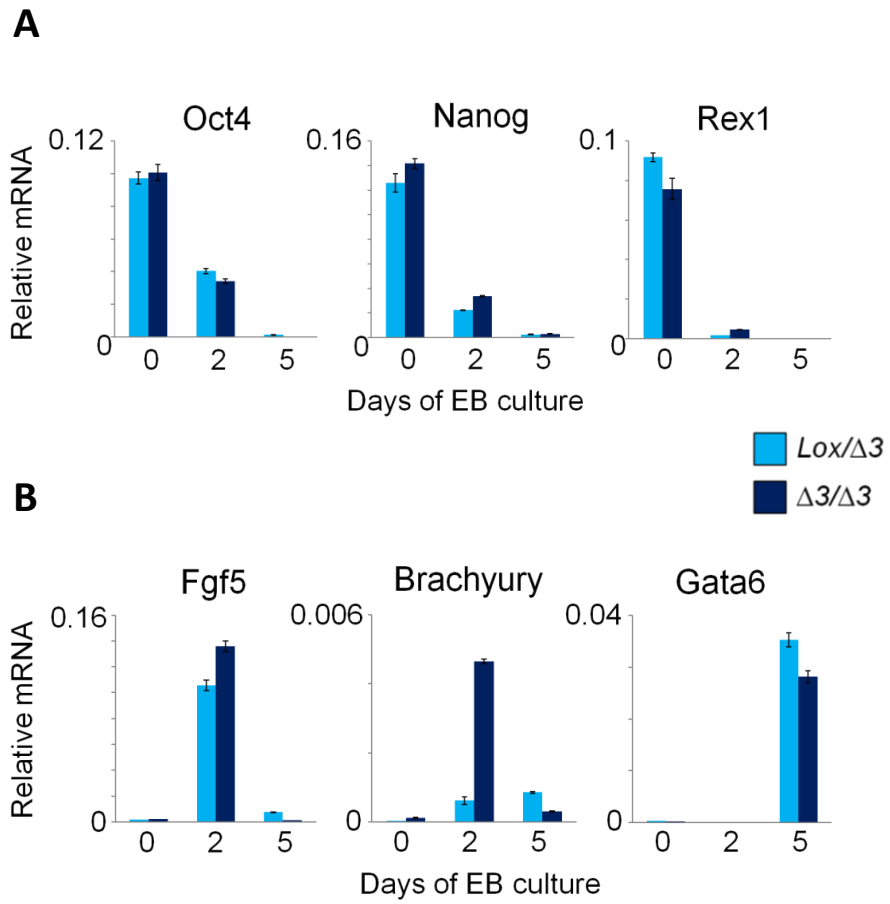

Figure 3.13 Differentiation of ES cells lacking LSD1 is associated with repression of pluripotency factors but perturbed transcriptional regulation in mesoderm development. (A) Quantitative RT-PCR data for genes characteristic of undifferentiated ES cells (Oct4, Nanog, Rex1) was performed on mRNA extracted at 0, 2 and 5 days during EB differentiation.. (B) The same data is displayed for genes indicative of primitive ectoderm (*Fgf5*), mesoderm (*Brachyury*) and primitive endoderm (*Gata6*). Expression of the *Gata6* and *Fgf5* is unaffected, but precocious expression of *Brachyury* is observed. One cDNA sample was amplified in three parallel PCR reactions and mean values +/- S.E.M are plotted. Values indicate expression of the specific gene relative to the GAPDH control gene, measured using Roche UPL hydrolysis probes

Extended culture of surviving EBs beyond 12 days revealed that that EBs consisting of LSD1 knockout cells were less than half the size of controls (Figure 3.14A and B). This comparative size to controls is less than at day 5, suggesting that differentiation and growth is restricted over a further 7 days of EB culture. Also, clumps of dead cells were apparent (Figure 3.14A, arrow), which was further evidence of significant cell death throughout this differentiation assay. At day 15, qRT-PCR revealed a lack of mesodermal cell types in LSD1-deleted EBs and significantly increased levels of genes characteristic of extra-embryonic endoderm, which is derived from primitive endoderm (Figure 3.14C). These results corroborated gene expression observations in 5 day-developed EBs (Figure 3.13B; loss of *Brachyury* expression and maintenance of *Gata6* expression). Notably, *Tal1* and *CD34* expression was non-existent compared to controls at day 12 (data not shown) and day 15 (Figure 3.14C), suggesting that haematopoietic cell types did not develop at all in $Lsd1^{\Delta 3/\Delta 3}$ EBs. Much higher expression of genes indicative of parietal and visceral endoderm lineage (*TTR, AFP* and *HNF-1*β) suggested that embryonic cell types died, supporting a developmental block of epiblast-derived lineages in the post-implantation embryo. The absence of mesodermally-derived cells may be due to death due to earlier over-expression of *Brachyury*, which could also emphasise the enrichment of endodermal markers, especially considering the abnormal size and morphology of LSD1-deleted EBs at this later stage (Figure 3.14A and B). This expression data in day 15 EBs was corroborated recently by a report showing that teratomas derived from LSD1 knockout ES cells have enrichment for extra-embryonic endodermal cell types and a similar lack of mesoderm cells types (Macfarlan *et al.* 2011). These observations were explained by an expanded fate potential of LSD1 knockout ES cells, where ES cells derived from the

ICM acquire the ability to develop into embryonic and extra-embryonic derivatives (Macfarlan *et al.* 2011).

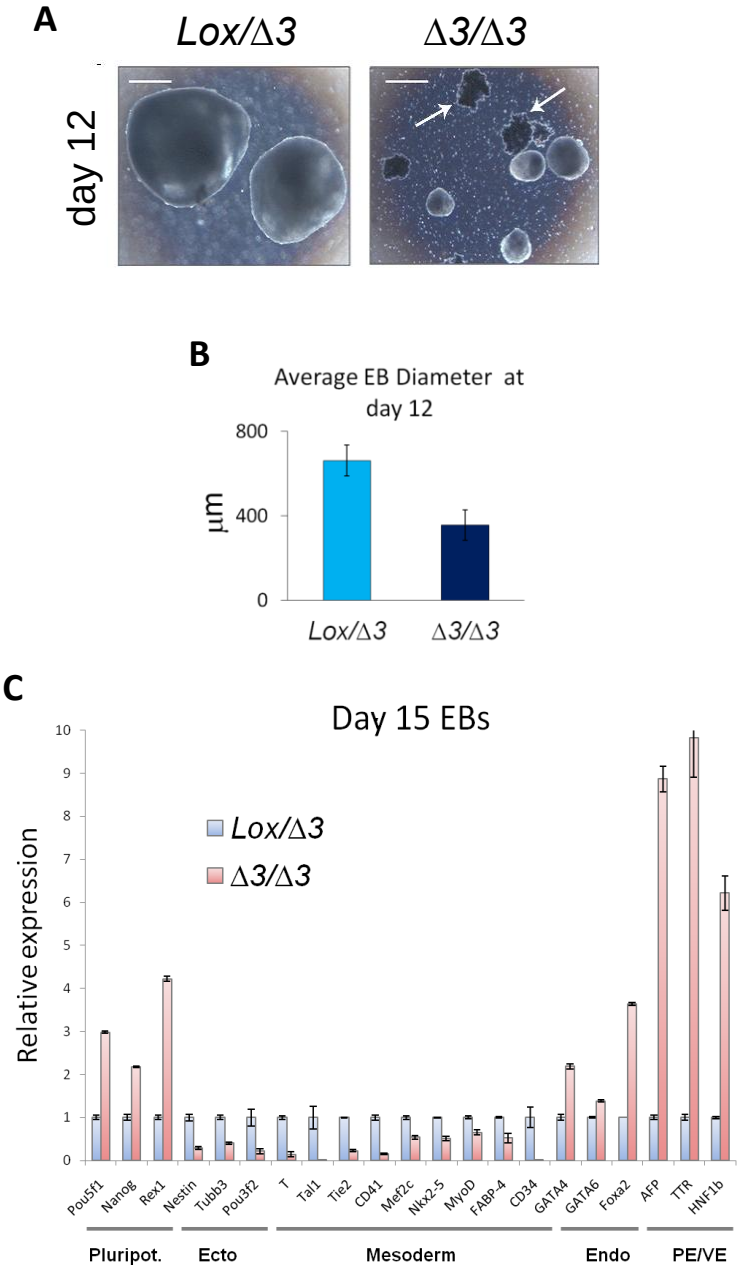

Figure 3.14 Extended culture of EBs reveals an absence of mesodermal cell types and enrichment for endodermal cell types. (A) Representative bright field image of EBs after 12 days of culture. Arrows indicate clumps of dead cells that accumulate in *Lsd1*$^{\Delta 3/\Delta 3}$ cultures. Scale bar = 300µM. (B) Diameter of EBs of the indicated genotype observed after 12 days of culture. (C) Quantitiative RT-PCR was performed for a range of markers of pluripotent cells and primary lineages. Pluripot. = pluripotency factors; Ecto = definitive ectoderm; mesoderm; Endo = endoderm; PE/VE = parietal/ visceral endoderm. One cDNA sample was amplified in three parallel PCR reactions and mean values +/- S.E.M are plotted. Values indicate expression of the specific gene relative to GAPDH.

3.3 Conclusions

ES cells lacking LSD1 proliferate normally under standard ES cell culture conditions and retain stem cell characteristics (*AP, Oct4, Nanog* and *Rex1* expression), but display increased levels of cell death upon differentiation, accompanying an aberrant mesoderm transcriptional programme and defects in full embryonic lineage development in EBs. Differentiation-associated cell death and restriction of embryonic lineage propagation correlate with a similar temporal impairment of embryonic development, suggesting that LSD1 is required to control the onset of lineage development from the primitive ectoderm cells of the epiblast. This developmental block may however be due to de-regulation of further genes in the epiblast, yet to be revealed, due to limited gene expression analysis. As well as this, the association with HDAC1 and 2 in a multi-protein co-repressor complex is likely to be critical for the role played by LSD1.

4 Understanding the role of LSD1 in embryonic gene regulation

4.1 Introduction

The previous chapter reported a number of observations seen upon conditional deletion of LSD1 in ES cells; results suggested that an underlying cause of the differentiation-associated cell death phenotype in *Lsd1*$^{\Delta 3/\Delta 3}$ ES cells was transcriptional de-regulation. This was explored further by biochemical analysis of the CoREST complex in the absence of LSD1, as well as assessment of the effect of LSD1 depletion on histone methylation and acetylation. These experiments were instigated by prior knowledge of LSD1-associated proteins and the known enzymatic redundancy towards H3K4me2/me1. As LSD1 is involved in the removal of a modification that marks actively transcribed genes, to understand how LSD1 regulates epiblast development through control of transcriptional networks, global comparative gene expression analysis was performed in ES cells.

LSD1 can form a complex with different CoREST family corepressors (CoREST1-3) in different cell types. It remained unknown if different CoREST proteins functioned specifically in ES cells until a report in May 2011 showed that CoREST2 is predominantly expressed in ES cells and forms a complex with LSD1, facilitating its nucleosomal demethylation activity (Yang *et al*. 2011). These data were published after work documented in this thesis had been completed. The interaction and functionality of LSD1 with CoREST1 (Rcor1/mKIAA0071/CoREST) was originally

identified and had therefore been much scrutinised in previous publications, though these studies were performed using HEK293 and HeLa cells (Lee *et al.* 2005, Shi *et al.* 2005). The knockdown of CoREST2 in ES cells inhibited proliferation and severely impaired pluripotency, which contrasts with LSD1 knockout ES cell data in Chapter 3, suggesting CoREST2 may have additional functions outside the LSD1/CoREST/HDAC complex (Yang *et al.* 2011). Experiments in this Chapter were performed using an antibody specific to CoREST1 (anti-CoREST Millipore 07-455), thereby restricting the analysis to the effects of LSD1 deletion on CoREST1.

The interaction of LSD1 with CoREST1 (hereby refered to as CoREST) is known to be critical for the recognition and demethylation of nucleosomal substrates (Lee *et al*. 2005, Shi *et al*. 2005). This suggests that the association with CoREST would endow some substrate specificity to LSD1, and underpins the essential requirement for LSD1 over other H3K4me2 demethylases such as JARID1A and LSD2 (Klose *et al.* 2007, Ciccone *et al*. 2009). The stability of LSD1 is dependent on CoREST and the binding affinity of LSD1 and CoREST is high, implying that the function of LSD1 relies on ability to form a multi-protein complex (Shi *et al.* 2005, Hwang *et al*. 2011). In addition, the ability to associate with HDACs is important for LSD1 activity, as hypoacetylated histone tails serve as a more effective substrate for demethylation (Shi *et al.* 2005, Lee *et al.* 2006). A previous study has demonstrated the interplay between LSD1 and deacetylase activities; where the only detectable global change upon LSD1 deletion was in H3K9 acetylation, with H3K4 methylation being unaffected (Wang *et al.* 2009). This implies that the requirement for LSD1 might be manifested though deacetylases.

As direct and indirect gene de-regulation is likely to be identified in microarray analyses, and ultimately ascertaining direct LSD1 targets in ES cells is an aim in this investigation, information from previously published data from large-scale ChIP studies in other cell types may be informative. LSD1 gene targets in MEL cells (Saleque *et al.* 2007) and MCF-7 cells (Garcia-Bassets *et al.* 2007, Wang *et al*. 2009a) have been previously reported. Notably, in one of these reports, the *Brachyury* promoter was identified as a target of LSD1, through association with the NuRD complex (Wang *et al.* 2009a). This observation was in a somatic cell system, in which the chromatin state of genes is different compared to ES cells. However, the preliminary identification of *Brachyury* de-regulation suggests that this gene may be under direct control by LSD1 in ES cells (Chapter 3, Figure 3.13B).

4.2 Results

4.2.1 Loss of LSD1 causes a reduction in the level of CoREST

The co-repressor, CoREST is a central binding partner of LSD1 in cells and together with HDAC1 and 2, forms a core repressor complex (You *et al*. 2001, Hakimi *et al*. 2002, Lee *et al*. 2005, Shi *et al*. 2005, Yang *et al*. 2006, Lee *et al*. 2006b). The first experiment performed was to assess the effect of LSD1 deletion on members of this complex by a comparative western blot. The results here gave an initial indication that the levels of CoREST were reduced in *Lsd1*$^{\Delta 3/\Delta 3}$ ES cells though the levels of HDAC1 and 2 were unchanged (Figure 4.1). The direct binding of CoREST with LSD1 and the fact that CoREST is only found in this protein complex (as opposed to HDAC1 and 2 that are present in diverse repressor complexes) supported the notion that removal of LSD1 would affect CoREST. Since LSD1 stability is reduced in the absence of CoREST, a reciprocal dependence for stability appears to occur (Shi *et al*. 2005).

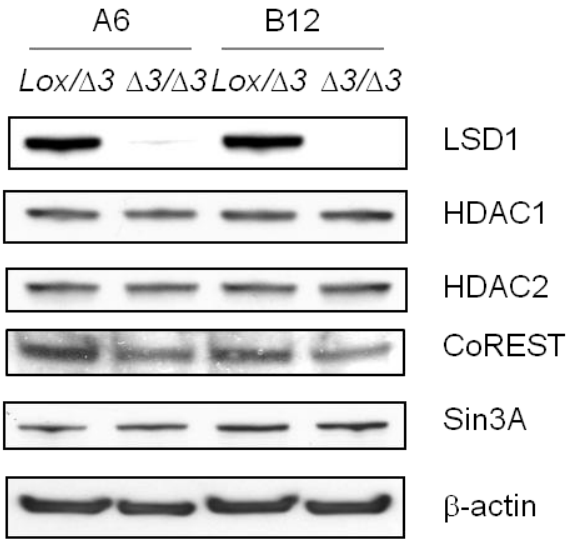

Figure 4.1 Loss of LSD1 does not affect HDAC1 and 2 levels but results in reduced CoREST levels. Western blotting revealed that the level of HDAC 1 and 2 are unchanged in the absence of LSD1, but CoREST levels appear reduced. Sin3A and β-actin were used as protein loading controls. Clones A6 and B12 were assessed at 7 days after 4-OHT treatment .

The reduced levels of CoREST were verified further by western blotting titration using four varying amounts of cell extract (Figure 4.2A). The lane with 10μg of whole cell extract revealed significantly less CoREST in *Lsd1*$^{\Delta 3/\Delta 3}$ ES cells compared to controls. A reduction in protein stability was implicated since CoREST mRNA was unaffected (Figure 4.2B). Revovery of the levels of CoREST protein through inhibition of the proteasome was attempted, though 4 hour treatment of ES cells with MG132 did not seem to result in a quantifiable increase in CoREST protein (Figure 4.2C). This was unsurprising as the half-life of CoREST following synthesis is estimated to be considerably more that 4 hours. MG132 inhibition of the proteasome proved to be a difficult assay to perform, as a vast amount of cell death occurred within a couple of hours of treatment. A longer inhibition time may well be required for more evident rescue of CoREST protein levels, where 24 hours treatment with proteasome inhibitor rescues LSD1 protein expression in cells expressing CoREST shRNA (Shi *et al.* 2005).

To test the integrity of the remaining complex in the absence of LSD1, CoREST was purified from *Lsd1*$^{\Delta 3/\Delta 3}$ cells and tested for ability to interact with HDAC1 and 2. In control cells, CoREST co-precipitated with LSD1, HDAC1 and HDAC2 (Figure 4.3A lane 5). In the absence of LSD1, a decrease in the level of CoREST protein was again observed (Figure 4.3A compare lane 1 with 6). The reduction in CoREST correlated with a decrease in the association of HDAC1 and 2 (Figure 4.3A compare lane 5 with 10 in rows 3 and 4) and associated deacetylase activity (Figure 4.3B; $p<0.05$). However, although the association was reduced, as CoREST levels were lower, a physical and biochemical association of CoREST with HDACs could still be monitored, suggesting

that this portion of the complex was still intact. Whether this portion of the complex was still functioning in gene regulation remained to be seen. As a control, the association of HDAC1 with a distinct co-repressor protein, Sin3A, was tested and found to be unaffected by loss of LSD1 (Figure 4.3A compare lane 4 with 9 in row 5). Full complex assembly, including LSD1, is likely to be essential for CoREST complex function, and depletion of LSD1 was expected to hinder HDAC function in gene regulation based on this result. The natural progression was therefore to analyse effects on global histone acetylation in addition to methylation. Importantly, there was no change in overall deacetylase activity of HDAC1 in *Lsd1*$^{\Delta 3/\Delta 3}$ cells (Figure 4.3B), implying that any possible changes in histone acetylation levels in the cell would be attributed to LSD1/CoREST/HDAC-target loci. These results (Figure 4.3) were generated from analysis of clone A6; identical results were observed in clone B12 analysis (Figure 4.4A and B), which ruled out any false positive results occurring through grossly unequal loading of purified proteins onto the gel or into the deacetylase assays.

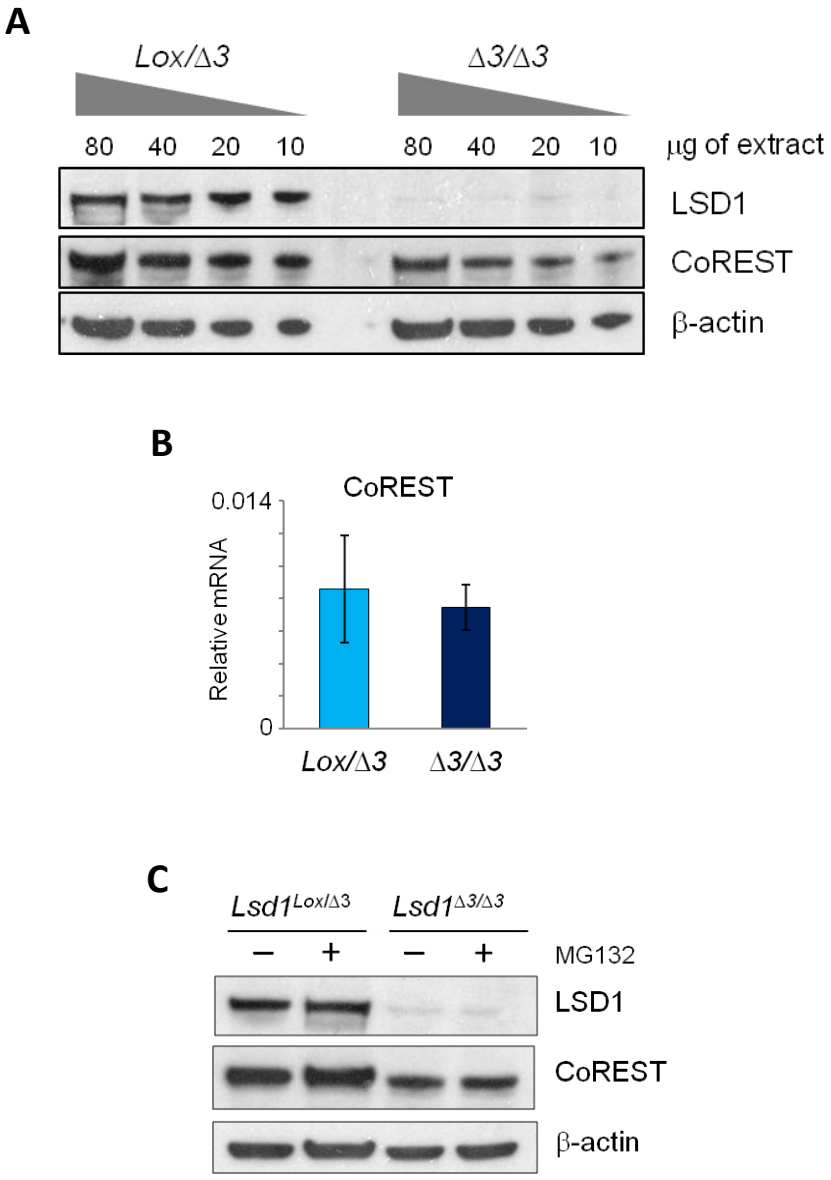

Figure 4.2 Loss of LSD1 results in reduced CoREST protein stability. (A) Western blot using a titration of nuclear extract quantities from *Lsd1*$^{Lox/\Delta3}$ and *Lsd1*$^{\Delta3/\Delta3}$ ES cells revealed a reduction in CoREST protein in the absence of LSD1. This is most noticeable at 10μg. β-actin was used as a loading control. (B) Quantitative RT-PCR revealed that CoREST is not regulated by LSD1 through transcriptional control. CoREST mRNA levels, normalised to GAPDH, are similar in *Lsd1*$^{Lox/\Delta3}$ and *Lsd1*$^{\Delta3/\Delta3}$ ES cells. (C) Treatment of ES cells for 4 hours with a proteasome inhibitor, MG132, showed a modest increase in CoREST levels in *Lsd1*$^{\Delta3/\Delta3}$ ES cells, confirming that in the absence of LSD1, CoREST protein is unstable and degraded.

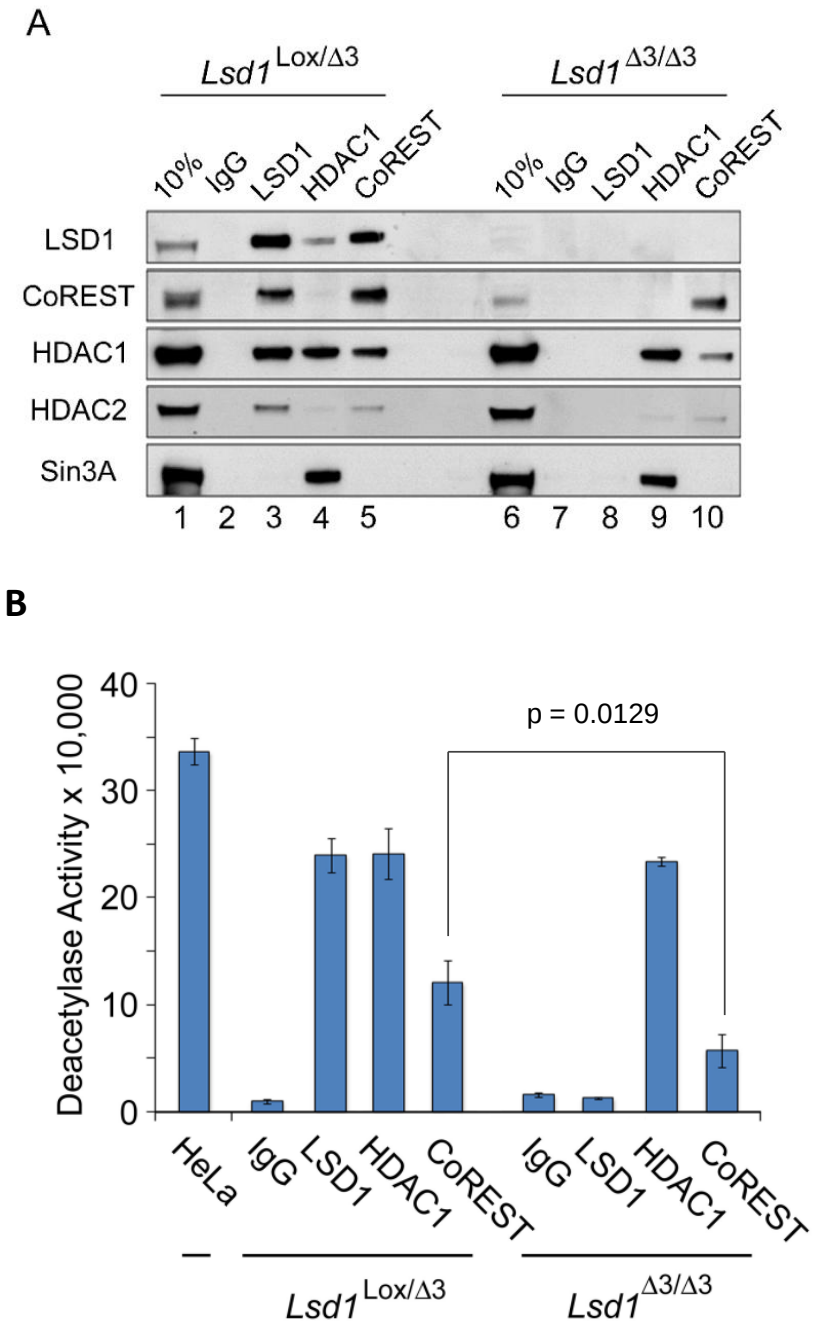

Figure 4.3 Loss of LSD1 results in decreased CoREST protein levels and a reduction in HDAC association within the CoREST complex. (A) Specific antibodies to the indicated proteins were used to immunoprecipitate LSD1, HDAC1 and CoREST from *Lsd1*$^{Lox/\Delta3}$ and *Lsd1*$^{\Delta3/\Delta3}$ ES cells (clone A6). Normal rabbit IgG was used as a non-specific antibody control. Co-immunoprecipitating proteins were assessed by immunoblot (indicated on the left of the figure). (B) The amount of deacetylase activity associated with each immunoprecipitation was measured using a commercially available kit. The amount of deacetylase activity co-immunoprecipitated with CoREST in *Lsd1*$^{\Delta3/\Delta3}$ cells was less than half that of *Lsd1*$^{Lox/\Delta3}$ cells ($p<0.05$).

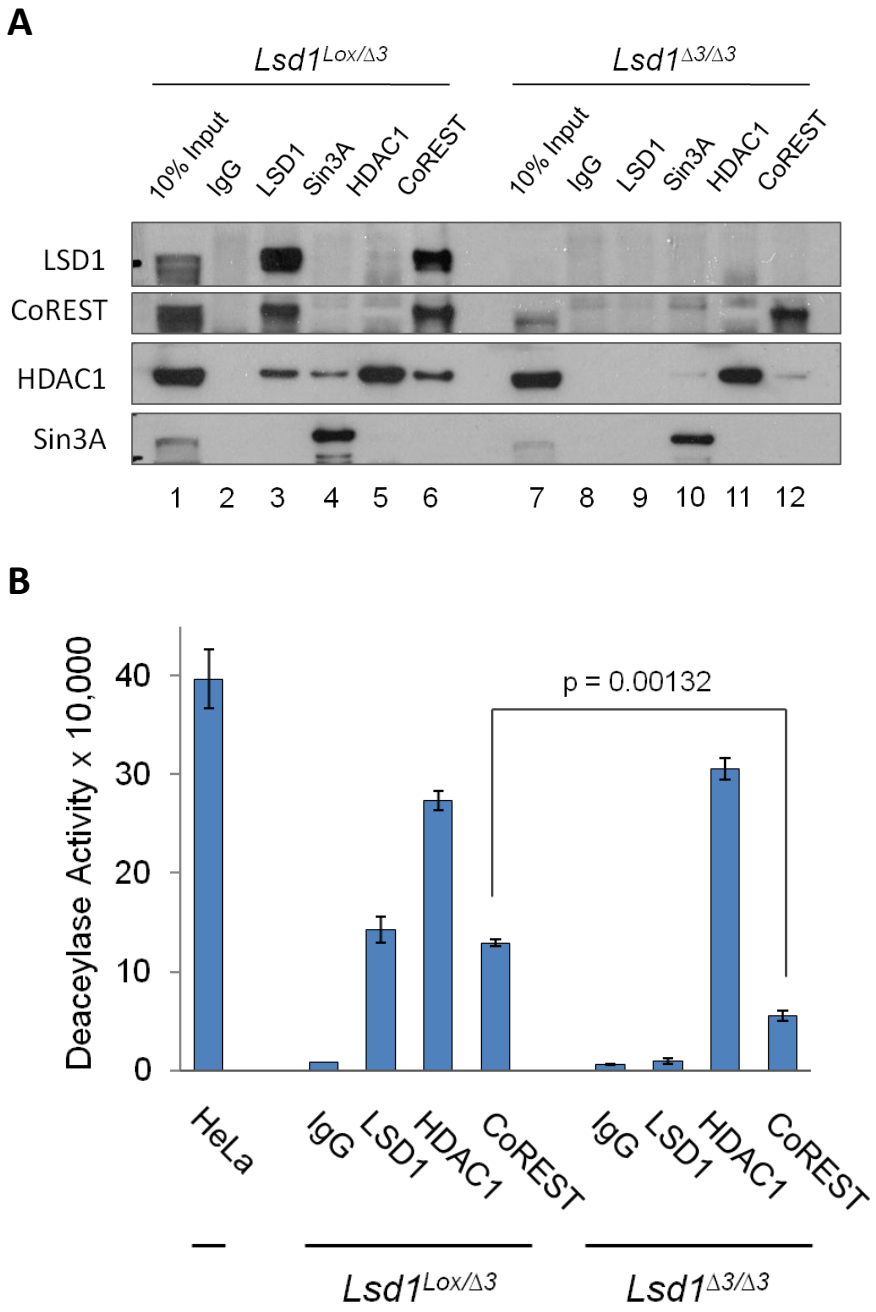

Figure 4.4 Loss of LSD1 results in decrease CoREST protein levels and a reduction in HDAC association within the CoREST complex. (A) Specific antibodies to the indicated proteins were used to immunoprecipitate LSD1, HDAC1 and CoREST from *Lsd1*$^{Lox/\Delta3}$ and *Lsd1*$^{\Delta3/\Delta3}$ ES cells (clone B12). Normal rabbit IgG was used as a non-specific antibody control. Co-immunoprecipitating proteins were assessed by immunoblot (indicated on the left of the figure). (B) The amount of deacetylase activity associated with each immunoprecipitation was measured using a commercially available kit. The amount of deacetylase activity co-immunoprecipitated with CoREST in *Lsd1*$^{\Delta3/\Delta3}$ cells was less than half that of *Lsd1*$^{Lox/\Delta3}$ cells ($p<0.01$).

4.2.2 Loss of LSD1 results in increased global histone acetylation

Knowledge of the catalytic activity of LSD1 towards mono- and di-methylated histone H3K4 (Shi *et al*. 2005, Forneris *et al*. 2005a, Forneris *et al*. 2006) as well as the observed reduction in the deacetylase activity of the LSD1-deficient CoREST complex, prompted the comparative examination of post-translational modification of histone H3. Loss of LSD1 produced only a small increase in the global levels of the substrates of the enzyme, H3K4me1 and H3K4me2, suggesting that locus-specific changes in methylation may occur (Figure 4.5A). These differences were statistically significant, with very similar results recapitulated in all three biological replicates ($p<0.01$). A modest H3K4me3 increase was also seen, implying that removal of LSD1 allows the accumulation of this mark. More extensive changes were observed in lysine acetylation. A 1.3-fold increase in H3K9 acetylation and a 2-fold increase in H3K56 acetylation were observed in *Lsd1*$^{\Delta 3/\Delta 3}$ cells (Figure 4.5A and B), consistent with a decrease in the HDAC activity associated with CoREST (Figure 4.3B). The larger increase in acetylation than methylation suggests that there is more redundancy among demethylases towards H3K4me2/me1 than among HDACs to H3K9ac and H3K56ac. It may also reflect the observation that LSD1 enzymatic activity can regulate deacetylation by HDAC1, where purified complexes containing catalytically inactive LSD1 display decrease deacetylase activity (Lee *et al*. 2006a). However the similarities in levels of HDAC1 protein to the deacetylase activity purified with CoREST suggest this is not the case *in vivo* (Figure 4.3 and 4.4). However, these two sites may be considered as substrates for the CoREST complex and it appears that LSD1 can regulate global histone modifications through stabilisation of the CoREST complex in ES cells.

Histone H3K56 acetylation is a modification associated with DNA damage (Das *et al*. 2009, Tjeertes *et al.* 2009), nucleosome assembly (Das *et al*. 2009) and the activity of stem cell factors (Xie *et al*. 2009). This large change in H3K56ac is in agreement with Dovey *et al.* 2010, where changes in acetylation could be dependent on the relative abundances of different acetyl-lysines in ES cells. Histone tails appear to be hyperacetyated on H3K9/K14 in ES cells, as the deletion of HDAC1 or treatment with TSA results in smaller increases in H3K9/K14ac in ES cells compared to MEFs (Dovey *et al.* 2010b). In contrast, acetylated H3K56 is a relatively rare modification in mammalian cells and deletion of HDAC1 or TSA treatment results in larger H3K56ac increases in ES cells (Das *et al*. 2009, Xie *et al.* 2009, Dovey *et al.* 2010b). The 2-fold increase in H3K56ac in the absence of LSD1 may occur due to this situation with the relative hyperacetylation of H3K9/K14 in ES cells perhaps masking the detection of increased H3K9/K14 acetylation due to loss of LSD1 and reduced complex-associated HDAC activity.

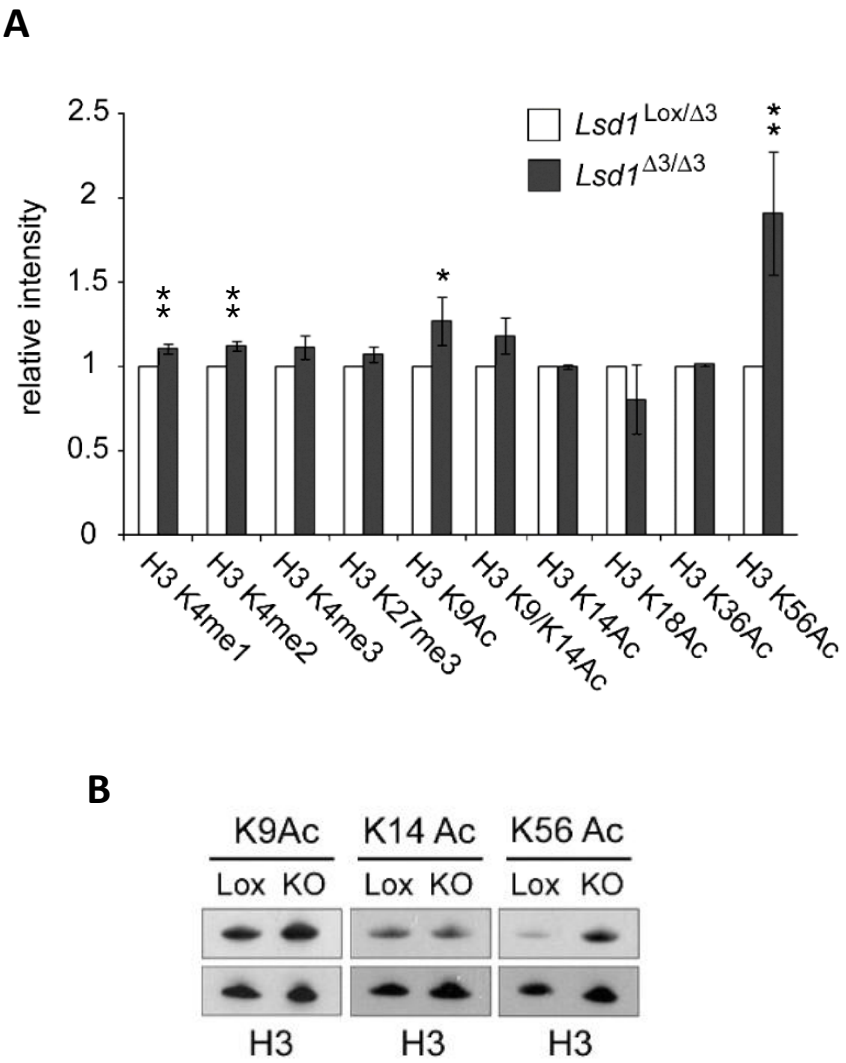

Figure 4.5 Loss of LSD1 results in an increase in global histone H3 acetylation (A) The methylation and acetylation status of histone H3 was detected using quantitative western blotting. Histones were acid extracted from three different clone (A6, B12 and C10). LiCOR fluorescent secondary antibodies were used (480 and 560nm) and the signal of the specific modification was normalised to the total amount of histone H3 using the LiCOR Odyssey Scanner (**p<0.01, *p<0.05 students t-test). (B) Three representative blots against specific acetyl modifications are shown.

4.2.3 LSD1 regulates the embryonic transcriptome

Global changes in histone acetylation in *Lsd1*$^{\Delta 3/\Delta 3}$ ES cells prompted examination of the ES cell transcriptome. RNA was isolated from *Lsd1*$^{Lox/\Delta 3}$ and *Lsd1*$^{\Delta 3/\Delta 3}$ cells to perform a comparative microarray analysis using an Illumina Whole-Genome Expression BeadChip platform that covers 45,200 different mouse transcripts. RNA was harvested from *Lsd1*$^{Lox/\Delta 3}$ cells and *Lsd1*$^{\Delta 3/\Delta 3}$ cells 10 days after addition of 4-OHT and impurities were removed by a further round of phenol-chloroform extraction. Various assessments of RNA quality were performed before proceeding to the microarray protocols. The RNA was analysed with the Nanodrop™ spectrophotometer, by agorose gel electrophoresis and on the Agilent Bioanlyser. The RNA was of good quality judging by integrity of the 26S and 18s ribosomal RNA bands and the smaller RNA species on the gel (Figure 4.6). This was confirmed by the Bioanalyser in the Genomics Core Facility, with robust rRNA peaks.

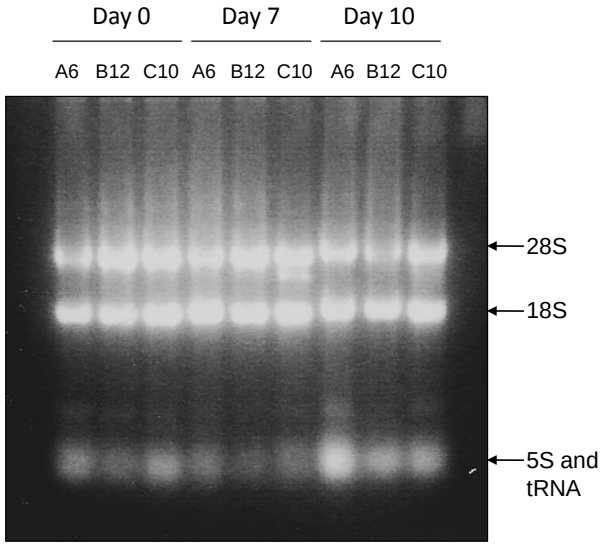

Figure 4.6 RNA sample quality used in microarray hybridisation. The agarose gel image confirms that RNA used in the array had not degraded. High abundance rRNA (28S, 18S and 5S) and tRNA are easily seen; mRNA species are of varying sizes and in low abundance produce no clear band on the gel.

Transcripts that were up- or down-regulated by greater than 1.4-fold (*p-value*<0.05), across three independent experiments involving different biological clones, were identified using ArrayTrack analysis software. In total, 588 transcripts were differentially regulated, with considerably more up-regulated than down-regulated (362 up compared to 226 down; Figure 4.7 and Appendix Table A3). This data gave no indication of the direct role LSD1 could play in both transcriptional repression and activation at specific genes, though the large number of down-regulated genes suggested LSD1 could play a role as a transcriptional activator at targets. However, the larger number of up-regulated genes observed was still consistent with a role for LSD1 transcriptional repression. The raw data files of the analysis have been deposited at the Gene Expression Omnibus database at NCBI (GEO Accession number GSE21131). *Lsd1* (*AOF2*) itself was the transcript down-regulated most (3-fold down), as show previously through qRT-PCR (Figure 3.5B). This result served as a useful internal control for the experimental system. The LSD1 Illumina probe was specific to a region within exon 19 (the final exon), confirming the occurrence of nonsense mediated decay (NMD) of the LSD1 mRNA and ruling out exon 4 skipping and splicing into exon 5 for production of a functional transcript. This 3-fold lower transcript abundance on the microarray was comparable to a 10-fold decrease revealed through qRT-PCR (Figure 3.5B), which was an initial indication that expression changes revealed through the array were lower than those in qRT-PCR analysis. This was a perhaps an artefact of higher background or weaker label detection in the microarray platform. Another immediate observation was that *Brachyury*, which was identified previously as being up-regulated in undifferentiated LSD1-deleted cells (Figure 3.13B), was increased 1.47-fold in the array (p =0.0007).

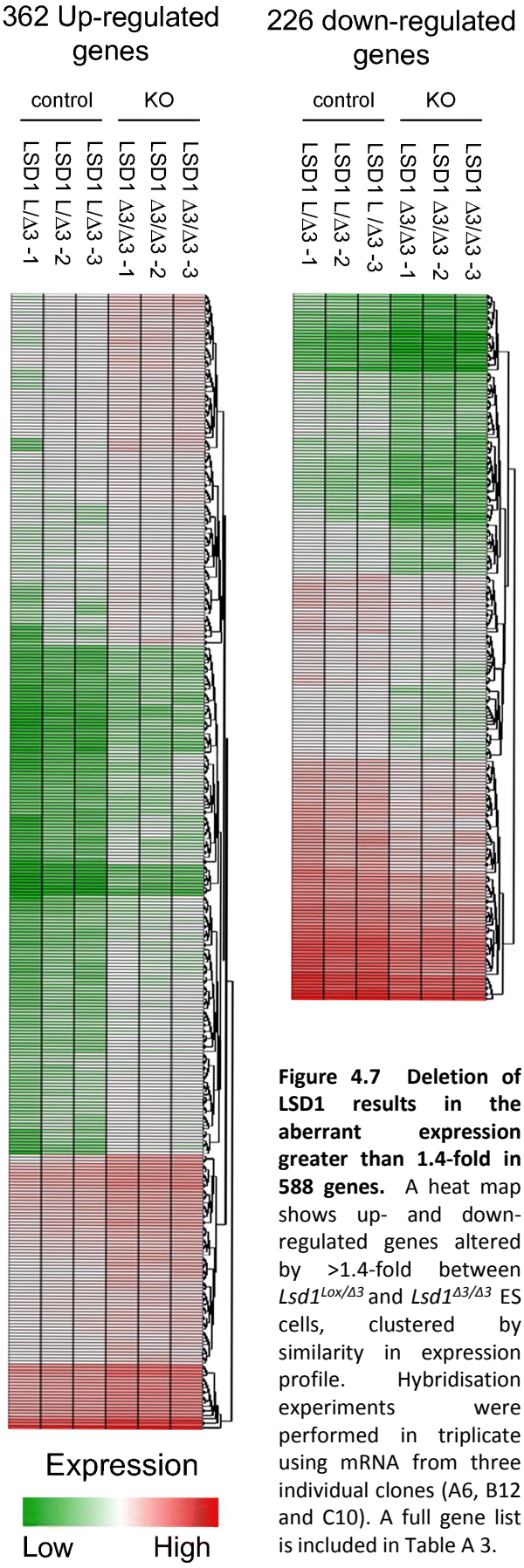

Figure 4.7 Deletion of LSD1 results in the aberrant expression greater than 1.4-fold in 588 genes. A heat map shows up- and down-regulated genes altered by >1.4-fold between *Lsd1*$^{Lox/\Delta 3}$ and *Lsd1*$^{\Delta 3/\Delta 3}$ ES cells, clustered by similarity in expression profile. Hybridisation experiments were performed in triplicate using mRNA from three individual clones (A6, B12 and C10). A full gene list is included in Table A 3.

To verify the microarray results, the levels of 8 up-regulated, 5 down-regulated and 4 unchanged transcripts were quantified by qRT-PCR using the same three RNA samples (Figure 4.8A). All 17 transcripts corroborated the microarray result, though for many genes a more robust change in transcript levels, as expected judging from the LSD1 transcript data, was observed (for example BRDT was 1.9-fold up-regulated by microarray compared to 5.5-fold using qRT-PCR). The over-expression of *Brachyury* (2.5-fold) was also reported through qRT-PCR analysis on these samples. The comparison of expression levels was performed using $Lsd1^{\Delta 3/\Delta 3}$ cells 10 days after 4-OHT treatment against $Lsd1^{Lox/\Delta 3}$ ES cells in order for expression data to be comparable to the *in vitro* differentiation assay data, as well as to rule out effects of genomic hypomethylation on transcriptional changes. Gene expression analysis at four time points over the 10 days was performed to assess the temporal nature of gene de-regulation following 4-OHT addition. *Brachyury, Hoxb7* and *Rasgrp3* all showed significant up-regulation beyond the 7 day point (Figure 4.8B), suggesting that a complete deletion of LSD1 protein was only achieved at 7 days (beyond detection by Western blotting in Figure 3.5A). This justified the choice of the 10 day stage of comparative analysis; with the trend of up-regulation also suggesting these genes are under the direct control of LSD1.

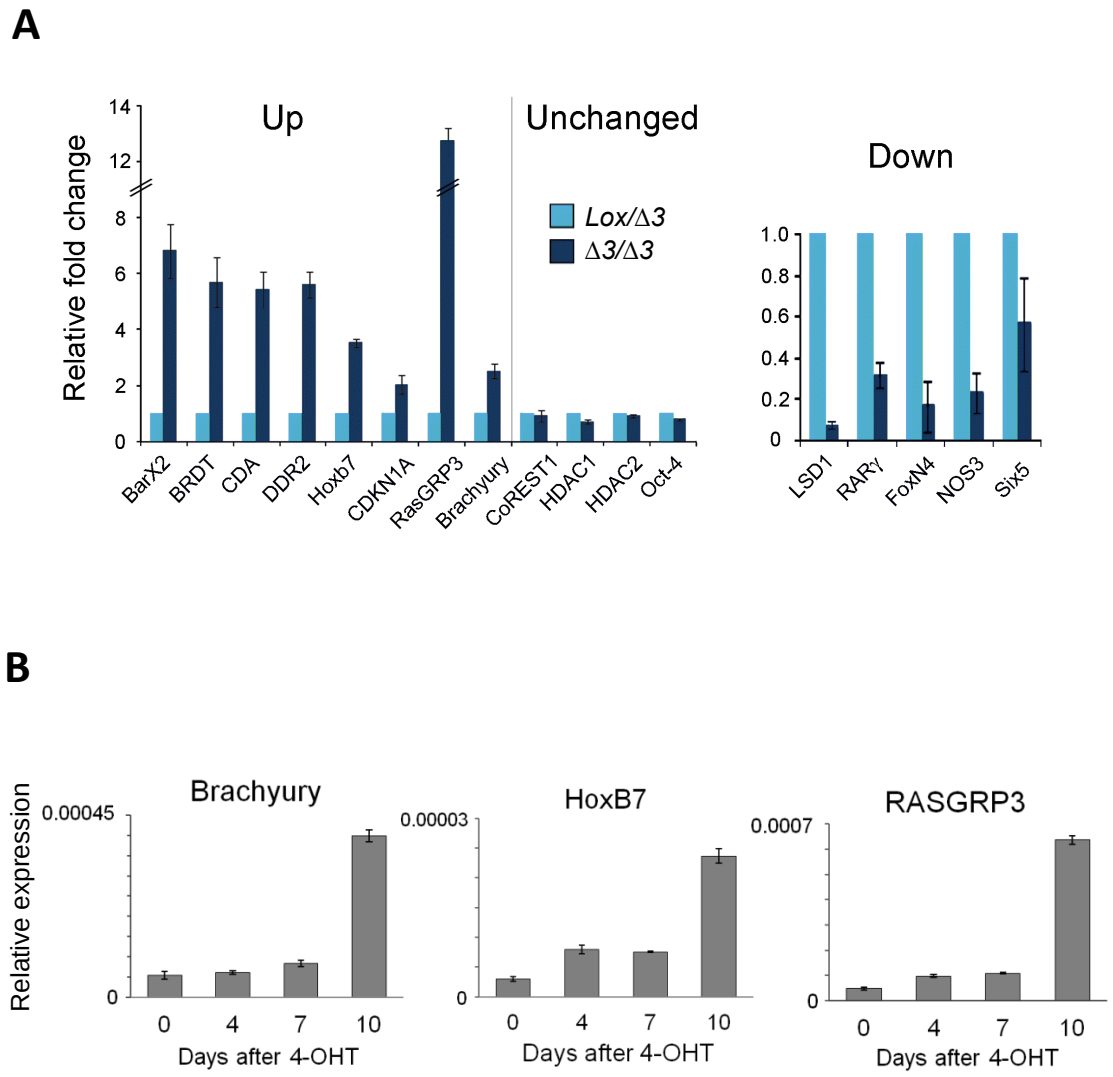

Figure 4.8 Gene expression changes are corroborated by candidate gene analysis. (A) Quantitative RT-PCR validation of genes up-regulated, unchanged and down-regulated genes in *Lsd1*$^{\Delta 3/\Delta 3}$ ES cells at day 10 post 4-OHT addition. Experiments were performed in triplicate (n=3) using the mRNA hybridised to the array. Expression was normalised to GAPDH and values are expressed relative to the level of transcript in *Lsd1*$^{Lox/\Delta 3}$ cells, which is calibrated to 1. (B) Quantitative RT-PCR to analyse the temporal trends of gene expression change, normalised to GAPDH, following addition of 4-OHT. These results justify the day 10 time-point for global analysis. Experiments were performed in biological triplicate, where 3 different cell line RNA samples were used in PCR. Mean values +/- S.E.M plotted.

A survey of the functional annotations of genes de-regulated in the absence of LSD1 by gene ontology revealed a wide spectrum of biological activities (Figure 4.9). A number of genes with a role in embryonic development were identified. These were of particular interest as their aberrant expression might relate to the embryonic lethal phenotype of the *Lsd1*$^{\beta\text{-}geo/\beta\text{-}geo}$ embryos. Thirteen transcription factors were de-regulated (Figure 4.9; GO: 0045893, positive regulation of transcription), of which some, including *Brachyury, Gli2* and *RAR*γ, have functions in tissue specification and notochord/neural tube development (GO: 0030903). In addition, a number of homeobox containing proteins were up-regulated, including *Hoxb7, Hoxd8* and *Barx2,* which are involved in early embryo patterning. This implied that multiple developmental programs might be regulated by LSD1 in ES cells.

An analysis of functionally related gene groups among the up-regulated gene list using DAVID (Huang *et al.* 2009) revealed enrichment for genes involved in processes related to cardiac and striated muscle (Figure 4.10). A number of these genes in fact encode muscle protein; with four genes involved in most of the processes within the muscular and circulatory systems (*Gm4392, Ankyrin, Troponin I and Troponin TI*). These systems are derivatives of the mesoderm, of which Brachyury is a master regulator in the developing embryo. Up-regulation of *Brachyury* in undifferentiated ES cells might cause increased expression of muscle-specific genes. Thus, an altered transcriptional program, including aberrant expression of a mesoderm-specification factor and derivatives may contribute to the impaired developmental phenotype of LSD1 knockout ES cells and embryos.

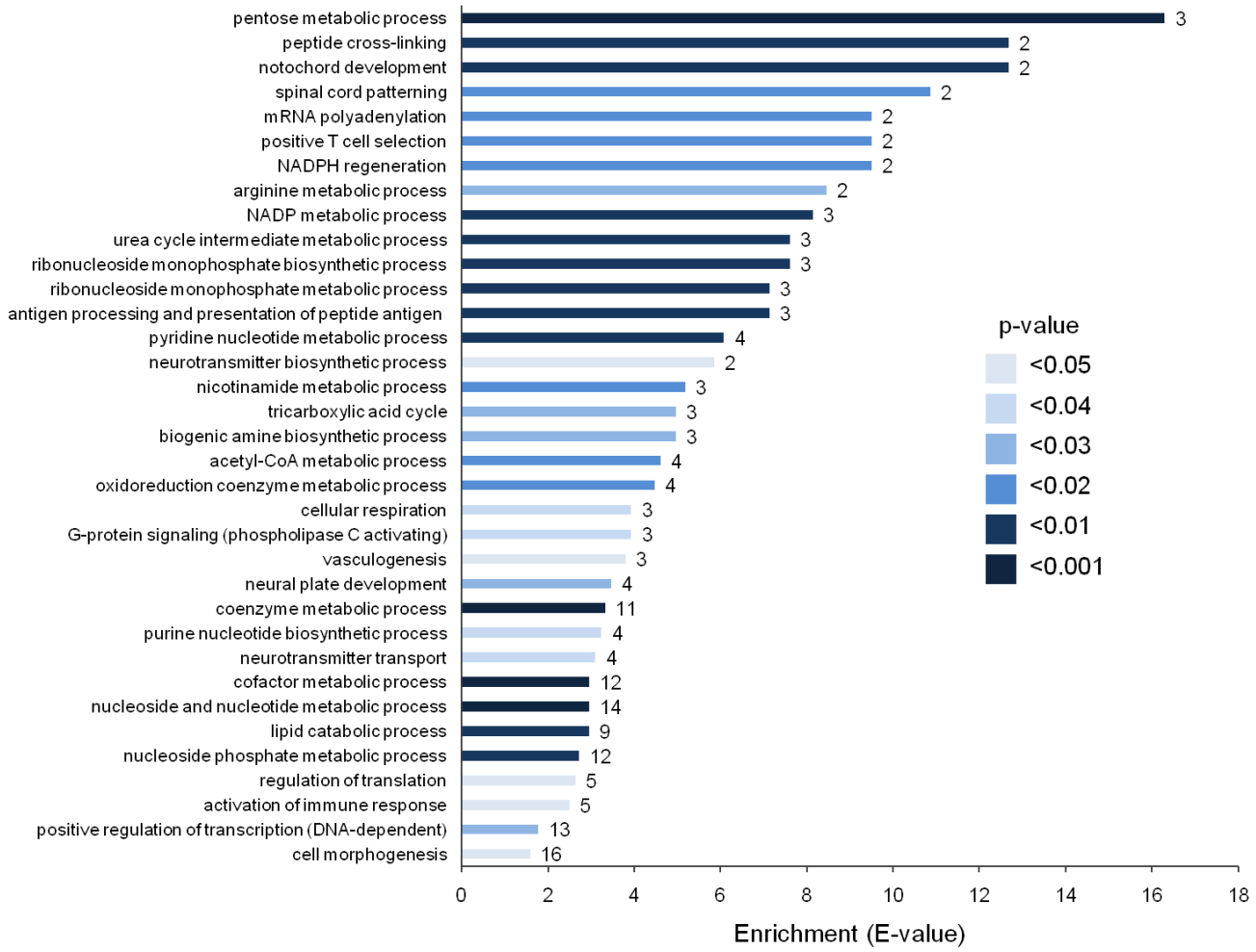

Figure 4.9 A multitude of biological processes are affected by the deletion of LSD1. Enrichment of gene ontology biological process terms in *Lsd1*$^{\Delta 3/\Delta 3}$ ES cells is plotted.. Enrichment was calculated from the number of de-regulated genes within the process compared to the total number of genes on the array within the process. The number of de-regulated genes in each category is shown next to the bars and colours represent *p values* according to the key

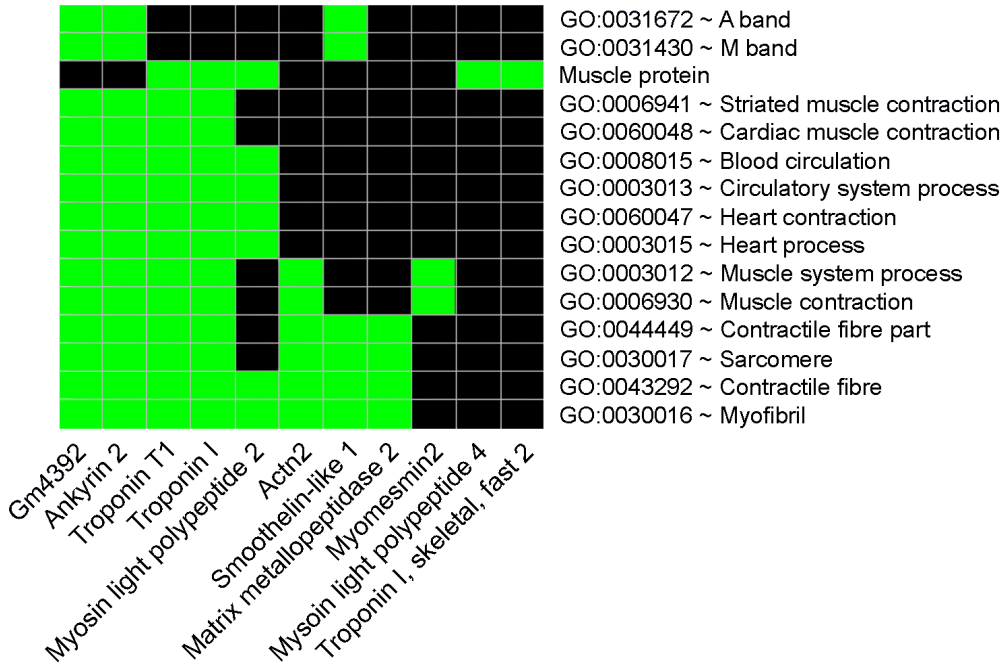

Figure 4.10 Loss of LSD1 results in up-regulation of a cluster of genes with a muscle-specific function. Functional annotation clustering of up-regulated genes using DAVID identifies an enrichment for genes with a muscle-specific function. Gene names and associated gene ontology (GO) terms for PANTHER biological processes are listed. A green block indicates a corresponding gene-term association positively reported.

Since LSD1 controls gene expression via regulation of H3K4 methylation, and with the knowledge that many genes with lineage-specific function are bivalent in ES cells (Azuara *et al*. 2006, Bernstein *et al*. 2006a, Mikkelsen *et al.* 2007) (Chapter 1.9), it was decided to determine the initial chromatin state of genes altered by loss of LSD1. Using available histone modification datasets for mouse ES cells (Mikkelsen *et al*. 2007, Ku *et al*. 2008), genes up-regulated in the absence of LSD1 were sub-divided into four classes based on their methylation status at H3K4 and H3K27 (Figure 4.11). Among the up-regulated transcripts, a significant enrichment for genes that possess the bivalent modification was observed ($p = 0.0145$), with an even higher association of gene up-regulation with the possession of neither modification ($p = 2.34 \times 10^{7}$). Notably, *Brachyury* and other developmental genes, such as *Barx2, Hoxb7* and *Reln* are bivalent*;* therefore LSD1 could play a role in the maintenance of the transcriptionally primed state of bivalently modified genes through removal of the H3K4me2 modification. At unmodified genes, LSD1 may function to maintain unmethylated H3K4 in order to contribute to gene repression. Only two bivalent genes are down-regulated upon removal of LSD1; this result is a useful control, as by definition, down-regulated genes must be initially active. Unsurprisingly, of the down-regulated genes, there was a very high enrichment for genes possessing only the H3K4me3 modification, which marks a transcriptionally active state.

Chromatin State	Number of LSD1 Up-regulated genes	Genes with modifcation on WG-6 v2 array	P value
K27me3	3	131	0.351
K4me3	95	9210	0.999
K4me3/K27me3	54	2520	0.0145
None	112	4589	2.34×10^{-7}
	264	16450	

Figure 4.11 LSD1 preferentially regulates bivalent or K4/K27 unmodified genes. Up-regulated genes were subdivided by their original chromatin state in mouse ES cells (Bernstein *et al.* 2005). Genes were classified by the presence of either H3K4me3, H3K27me3, both modifications, or no modification. The number of up-regulated genes with these chromatin states, the number of genes present on the WG-2-v2 array with the particular modification and the enrichment of genes with one of the four potential states is indicated (p-value calculated using a hyper-geometric test).

4.2.4 Chromatin state changes in up-regulated genes

To further understand how the initial chromatin state of genes relates to up-regulation in gene expression upon removal of an H3K4me1/me2 demethylase, ChIP was performed using antibodies against H3K4me1, H3K4me2, H3K4me3 and H3K27me3 modifications to analyse three gene promoters with different initial chromatin states. The H3K4me2 and H3K4me3 antibodies were tested for specificity using primers at genomic regions classified as either H3K4me3-positive or negative (Table 2.1 and Figure 4.12A and B). This would determine the efficacy of the antibodies in precipitating genomic regions possessing this histone modification and therefore was a crude test of their specificity. This method is often used to test the quality of an antibody for use in ChIP. The H3K4me3 antibody appeared highly specific and effective at recognising high leveles of H3K4me3. Regions classified as positive for this modification were highly enriched over histone input DNA, whereas regions classified as lacking this modification are less enriched (Figure 4.12A). The H3K4me2 antibody was also validated using these regions, as H3K4me2 is known to be concordant with H3K4me3 in ES cells (Orford *et al*. 2008). The PCR results showed that H3K4me2 was specific, though variations in enrichment compared to the H3K4me3 data indicated that either the antibody was not as specific as the H3K4me3 antibody, or that H3K4me3-positive regions have differential levels of the H4K4me2 mark (Figure 4.12). Notably, at the *Oct4* promoter (which is highly active in ES cells), very high enrichment of H3K4me2 is seen (50-fold over input), which meant that H3K4me2 persists at higher levels in this region in ES cells, or that this antibody is more effective at precipitating chromatin. Overall, these tests justified the use of these antibodies in ChIP assays.

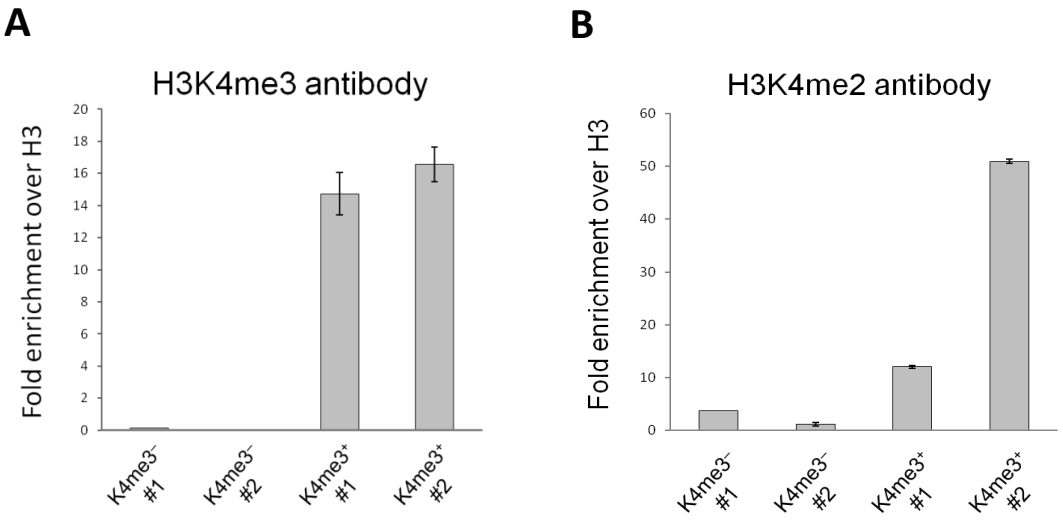

Figure 4.12 Testing the specificity of commercially available histone modification antibodies. Two genomic regions classified to be lacking the H3K4me3 modification ($K4me3^-$) or possessing the modification ($K4me3^+$) based on ChIP-seq data (Mikkelsen *et al.* 2007*,* Stock *et al.* 2008) were used to validate the affinity of (A) an H3K4me3 antibody (Sigma D5692) and (B) an H3K4me2 antibody (Millipore 07-473) for their specified epitopes.

The promoters of three genes, with either bivalent, H3K27me3 alone or H3K4/K27 unmodified initial chromatin state, were examined. The bivalent gene, *Brachyury,* showed increases in all three methylation states of H3K4 upon removal of LSD1, fitting with increase in gene transcription (Figure 4.13A). An increase in mono- and dimethyation was not unsurprising as these are the substrates for LSD1. However, the increase in tri-methylation, a modification that is already present, suggested a role for LSD1 in the acute regulation of methylation levels. *Hoxd8,* a gene with H3K27me3 but without H3K4me2/me3, showed an increase in the H3K4me mark and a decrease in the repressive H3K27me3 mark upon LSD1 deletion (Figure 4.13B), with the later change most likely linked to an increase in gene expression, suggesting an indirect of LSD1 removal on the change in expression of *Hoxd8.* An increase in H3K4me2/me3 levels at the H3K4/K27 unmodified promoter was observed, correlating with increased expression as well as the removal of an enzyme that demethylates H3K4me2 (Figure 4.13C). Regardless of confirmation of LSD1 binding, it was interesting to understand how these chromatin states might change upon up-regulation.

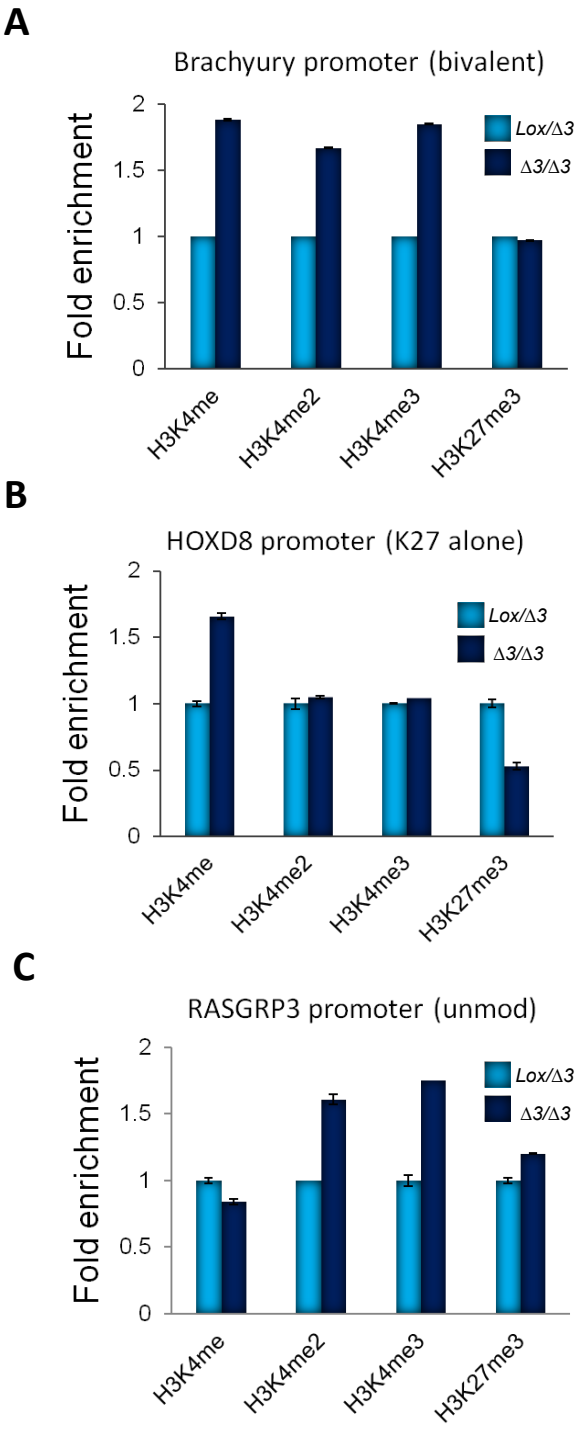

Figure 4.13 Up-regulation of genes in the absence of LSD1 is associated with initial chromatin state-dependent changes in histone methylation at the promoter,. ChIP was performed to identify changes in enrichment of methylation states of histone H3 at promoter regions of three up-regulated genes in LSD1-deleted ES cells, including (A) *Brachyury,* a gene that initially possesses both H3K4me3 and H3K27me3 in *Lsd1*$^{Lox/\Delta 3}$ ES cells; (B) *HOXD8*, a gene that possesses only H3K27me3 in *Lsd1*$^{Lox/\Delta 3}$ ES cells; (C) *RASGRP3*, a gene that is unmodified at both H3K4 and H3K27 in *Lsd1*$^{Lox/\Delta 3}$ ES cells.

4.2.5 *Brachyury* is a direct target of LSD1

A correlation between LSD1 loss, increased *Brachyury* expression and the activation of mesodermal, notably muscle-specific genes, prompted the investigation of the relationship between LSD1 and *Brachyury* further. Examination of Brachyury transcript and protein levels was performed in $Lsd1^{Lox/\Delta 3}$ and $Lsd1^{\Delta 3/\Delta 3}$ cells that were either cultured in the presence of LIF, or absence of LIF to stimulate ES cell differentiation as a monolayer. LIF withdrawal led to an increase in mRNA levels in both control and LSD1-deleted cells, although expression was still considerably higher in the absence of LSD1 (Figure 4.14A). This result recapitulated the previously observed over-expression in undifferentiated ES cells (Figure 3.13B and 4.8A) and supported the expression data recorded at day 2 of EB differentiation (Figure 3.13B). Over-expression of *Brachyury* in undifferentiated ES cells was consistently recorded at 2 to 5-fold. Brachyury protein levels were similarly increased in the absence of LSD1 in undifferentiated (3.3-fold) and differentiated (2.24-fold) ES cells (Figure 4.14B). All results have confirmed that LSD1 negatively regulates *Brachyury* expression.

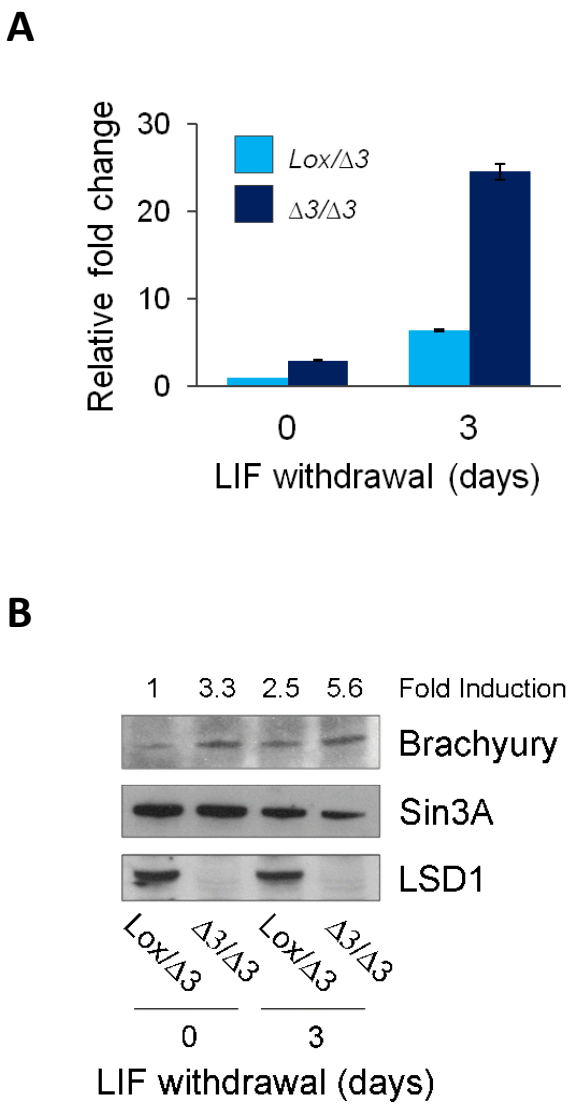

Figure 4.14 Brachyury is over-expressed in undifferentiated and 3 day differentiated *Lsd1*$^{\Delta 3/\Delta 3}$ ES cells. (A) Quantitative RT-PCR shows up-regulation of *Brachyury* mRNA in *Lsd1*$^{\Delta 3/\Delta 3}$ ES cells with (day 0) and without LIF (day 3). mRNA levels are normalised to GAPDH and values are represented relative to the level of transcript in *Lsd1*$^{Lox/\Delta 3}$ cells with LIF, calibrated to 1. Triplicates represent one cDNA sample amplified in 3 parallel reactions. (B) Western blot shows an increase in Brachyury protein levels in *Lsd1*$^{\Delta 3/\Delta 3}$ ES cells with (day 0) and without LIF (day 3). The fold induction of Brachyury protein was calculated relative to the Sin3A control.

The next experimental direction was therefore to test if this regulation was a consequence of direct recruitment of LSD1 to the *Brachyury* gene. Chromatin immunoprecipitation (ChIP) was performed to look for enrichment of DNA fragments representing the promoter region of the *Brachyury* gene. The region 600bp upstream of the transcriptional start site (TSS) was technically easier to amplify in PCR as regions closer to the TSS are very GC-rich, making specific amplification difficult. The resolution of ChIP analysis was approximately 200-400bp, based on the average size of sonicated chromatin fragments (Figure 4.15), which meant that -600bp was a reasonable reflection of LSD1 association with the proximal promoter region. PCR primers were designed to detect DNA representing regions downstream of the TSS (+400bp), the proximal promoter (-600bp) and a site remote from the TSS as a negative control (-4500bp) (Figure 4.16A). It was shown that LSD1 was associated with the promoter region; with a maximal enrichment (2.5-fold) approximately 600bp upstream of the transcriptional start site (Figure 4.16B). Reduced LSD1 binding was detected downstream of the first exon, with no association detected with a more distal 5' region of the *Brachyury* locus. The enrichment reflected the ability of the LSD1 antibody to specifically IP from the crosslinked material and the *Lsd1*$^{\Delta 3/\Delta 3}$ cells were effectively a negative control as no LSD1 protein was present in these cells. ChIP was also performed using antibodies to histone modifications. In the absence of LSD1, an increase in the level of H3K4me2 (2.5-fold) was detected at the -600pb region (Figure 4.16C), indicative of increased transcription and the loss of LSD1 enzymatic activity. Indeed, the trend of LSD1 binding and H3K4me2 levels overlapped well at all regions. The level of H3K4me3 was also increased at -600bp (2-fold) in *Lsd1*$^{\Delta 3/\Delta 3}$ cells (Figure 4.16D), correlating with increased transcription from this promoter but also

suggesting that LSD1 may hinder the accumulation of this mark, even though H3K4me3 is not an LSD1 substrate. As global H3K9 acetylation was increased in *Lsd1*$^{\Delta 3/\Delta 3}$ cells (Figure 4.5A and B), this mark was also assessed by ChIP. An increase in H3K9ac (4-fold) was observed at -600pb (Figure 4.16E), again indicative of increased transcription, but also suggesting that gene-specific function of HDACs could be perturbed in the absence of LSD1. This reflects the earlier identification of reduced HDAC association within the CoREST complex in the absence of LSD1 (Figure 4.3 and 4.4). It therefore seemed likely that LSD1 regulated *Brachyury* expression as part of an HDAC-containing repressor.

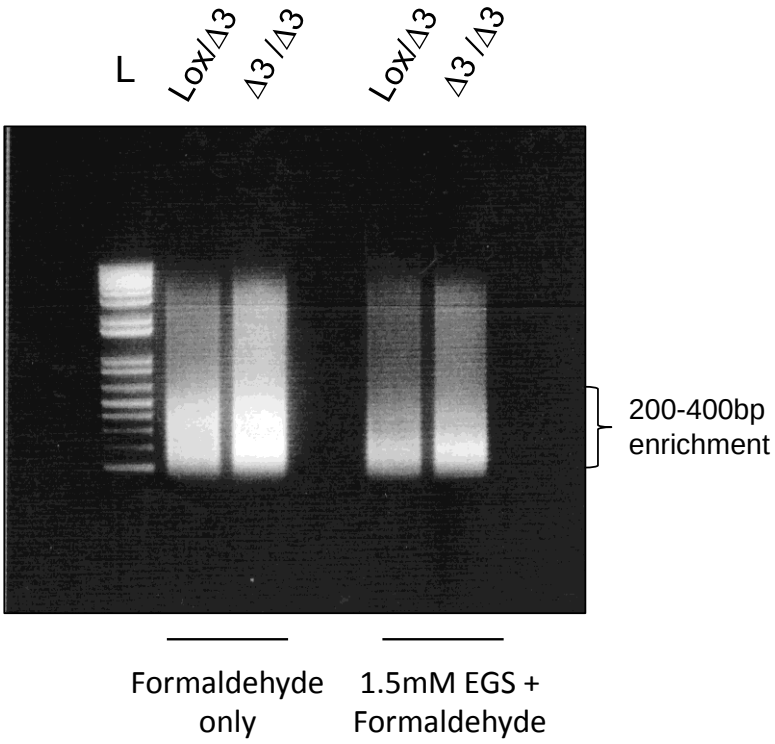

Figure 4.15 Sonication of crosslinked chromatin generates enrichment for 200-400pb DNA fragments In single crosslinked samples 15 minutes sonication was required on the HIGH setting with 30 second on/off cycles. For double crosslinked samples, 20 minutes sonication was required using the same Bioruptor settings

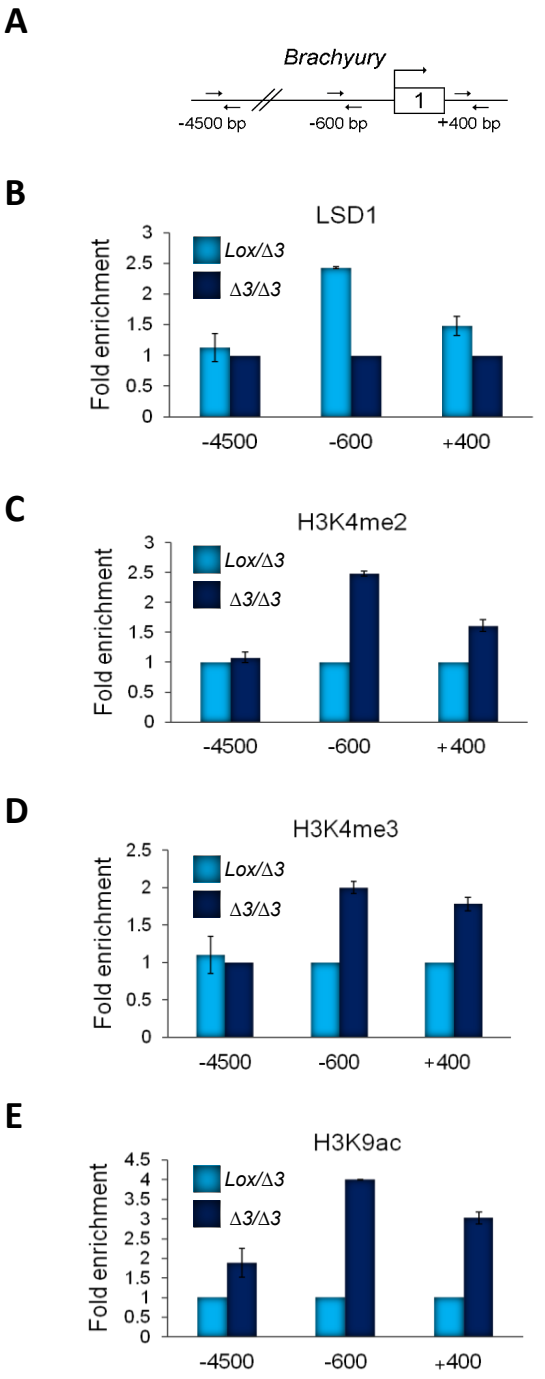

Figure 4.16 Brachyury is a direct target gene of LSD1 (A)Schematic of the *Brachyury* gene shows the relative position of the primers used for the quantitative PCR following chromatin immunoprecipitation. (B) The region -600bp from the transcriptional start site (TSS) is enriched in LSD1 ChIP from *Lsd1*$^{Lox/\Delta3}$ cells but not *Lsd1*$^{\Delta3/\Delta3}$ cells. Less enrichment is seen at +400bp with no enrichment at -4500bp, indicating that LSD1 associates with the gene just upstream of the TSS. Loss of LSD1 results in (C) increased H3K4me2, (D) increased H3K4me3 and (E) increased in H3K9ac at -600bp and +400bp sites. Increased enrichment of these modifications at the Brachyury promoter supports activation of transcription.

To further investigate whether LSD1 is recruited to the *Brachyury* promoter as part of the CoREST complex, ChIP using an antibody to CoREST was performed. LSD1 ChIP was performed simultaneously in this assay, with a recapitulation of LSD1 binding at -600bp (Figure 4.17B). Interestingly, relative DNA enrichment of the -600bp region was also seen in CoREST ChIP from *Lsd1*$^{Lox/\Delta 3}$ cells to a similar extent as LSD1 ChIP (Figure 4.17C). This suggested that loss of LSD1 resulted in loss of association of CoREST protein with the *Brachyury* promoter; and therefore presumably also HDAC1 and 2, which is reflected by increased H3K9 acetylation at this gene (Figure 4.16E). The similar levels of enrichment across the three amplified regions could reflect the very similar abilities of LSD1 and CoREST antibodies to immunoprecipitate the specific protein (see Figure 4.3A lanes 3 and 5). Overall, these data support biochemical observations of the integrity of the CoREST complex in LSD1-depleted ES cells and confirm that the CoREST repressor complex regulates *Brachyury* in ES cells by way of possession of H3K4me1/me2 demethylase and deacetylase activities.

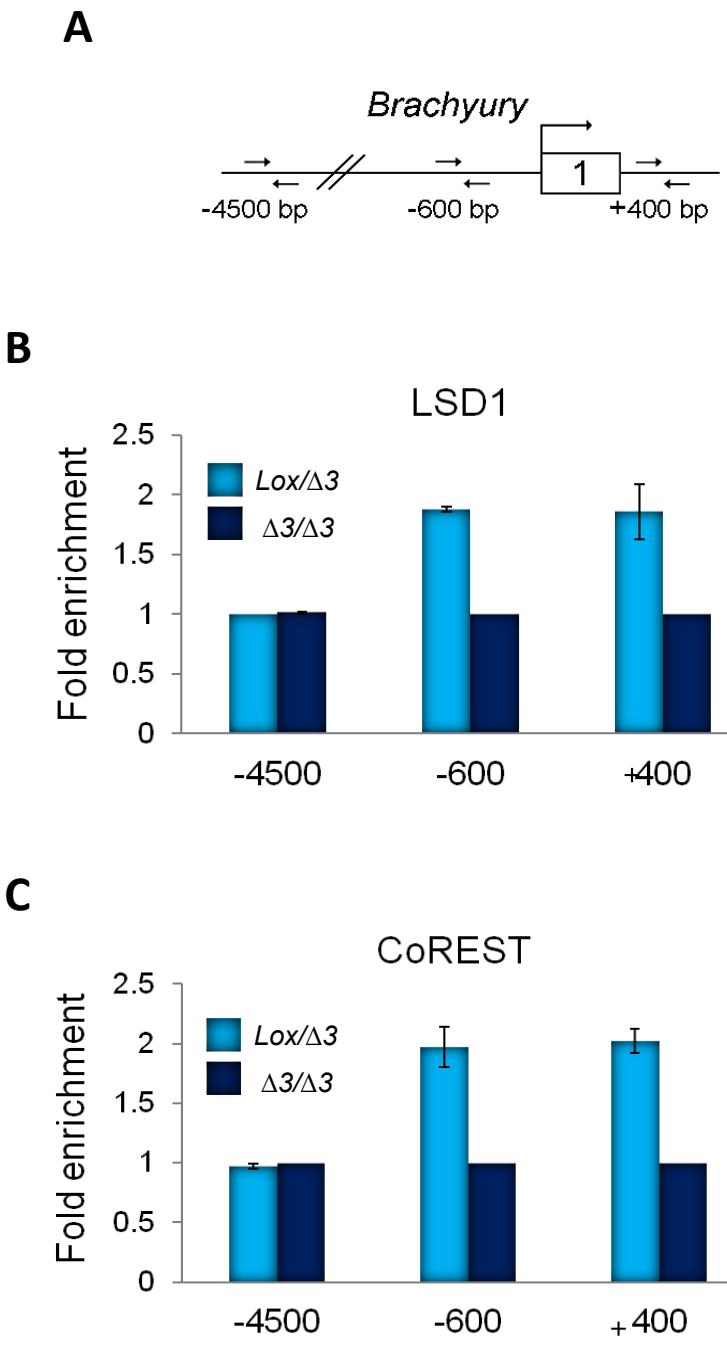

Figure 4.17 Loss of LSD1 results in a similar loss of CoREST from the *Brachyury* promoter (A) A repeat LSD1 ChIP assay was performed, which result in a recapitulation of the previous data (with slightly less -600bp enrichment in $Lsd1^{Lox/\Delta 3}$ cells LSD1 ChIP. (B) CoREST ChIP was performed simultaneously and revealed a similar pattern of enrichment in $Lsd1^{Lox/\Delta 3}$ cells over $Lsd1^{\Delta 3/\Delta 3}$ cells at -600bp and +400bp from the TSS.

4.2.6 *Brachyury* is up-regulated in E6.5 *Lsd1*$^{\beta\text{-}geo/\beta\text{-}geo}$ embryos

Due to observations of differentiation-associated cell death in *Lsd1*$^{\Delta 3/\Delta 3}$ ES cells and the early embryonic lethality of LSD1 knockout embryos (Chapter 3), it was a now an aim to relate the increase in *Brachyury* expression observed in *Lsd1*$^{\Delta 3/\Delta 3}$ ES cells back to the *in vivo Lsd1*$^{\beta\text{-}geo/\beta\text{-}geo}$ embryo model. Timed mates were set up with *Lsd1*$^{+/\beta\text{-}geo}$ heterozygous mice, and vaginal plugs were monitored and reported in order to isolate embryos at the appropriate time. *WT, Lsd1*$^{+/\beta\text{-}geo}$ and *Lsd1*$^{\beta\text{-}geo/\beta\text{-}geo}$ E6.5 embryos were harvested from euthanized pregnant females by Dr Shaun Cowley. The whole embryo was used for RNA extraction, followed by cDNA synthesis and qRT-PCR. *Brachyury* expression was increased significantly (almost 20-fold) in *Lsd1*$^{\beta\text{-}geo/\beta\text{-}geo}$ embryos compared to *Lsd1*$^{+/\beta\text{-}geo}$ heterozygous controls (Figure 4.18). *RASGRP3* and *CDA*, two genes up-regulated in *Lsd1*$^{\Delta 3/\Delta 3}$ ES cells, were also up-regulated in *Lsd1*$^{\beta\text{-}geo/\beta\text{-}geo}$ embryos, though to a lesser extent. As a control, the expression of *HDAC1* and *HDAC2,* whose protein and mRNA levels were unchanged by loss of LSD1 in ES cells (Figure 4.1 and 4.8A) was found to be unaltered between all embryonic genotypes (Figure 4.18), demonstrating a consistent relationship between the *in vitro* and *in vivo* systems. Overall these data infer that LSD1 is recruited directly to the *Brachyury* locus in order to restrict expression prior to differentiation in ES cells and gastrulation in the developing embryo.

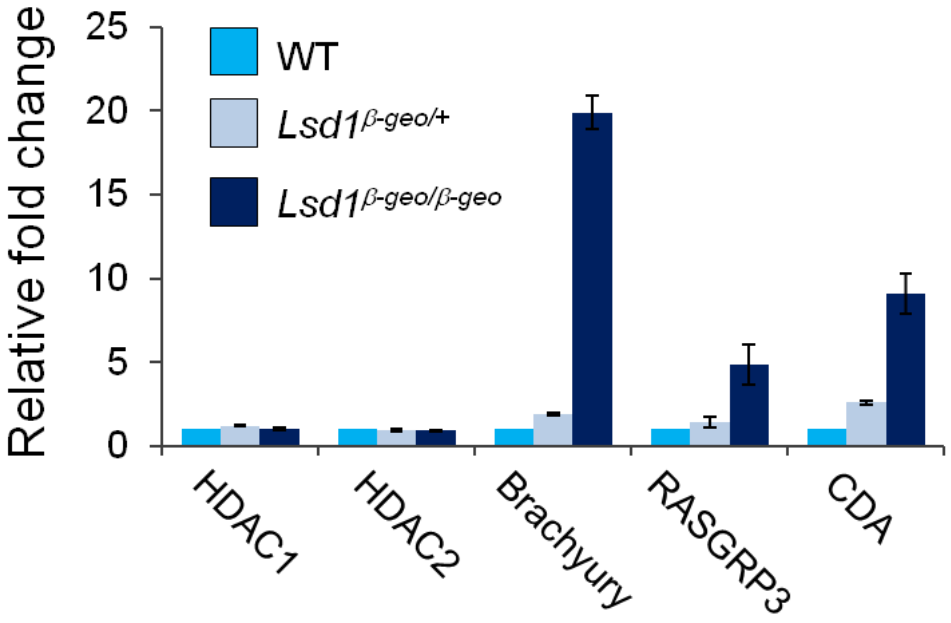

Figure 4.18 *Brachyury* is de-repressed in *Lsd1*$^{\beta\text{-geo}/\beta\text{–geo}}$ genetrap embryos. Quantitative RT-PCR analysis of E6.5 embryos revealed that homozygous (*Lsd1*$^{\beta\text{-geo}/\beta\text{–geo}}$) embryos have a 20-fold increase in *Brachyury* mRNA compared to wild-type and heterozygous (*Lsd1*$^{\beta\text{-geo}/+}$) embryos. Additionally, *RASGRP3* and *CDA* mRNAs were increased 5-fold and 10-fodld, respectively in *Lsd1*$^{\beta\text{-geo}/\beta\text{–geo}}$ embryos, where HDAC1 and 2 levels remained unchanged. Assays were performed in biological triplicate, using RNA samples from three different embryos of each genotype in PCR. Expression was normalised to GAPDH and values are represented relative to the level of transcript in *WT* embryos, which is calibrated to 1. Mean values (n=3) +/- S.E.M are plotted.

4.3 Conclusions

In conclusion, biochemical and transcriptional analyses in LSD1-deleted ES cells indicate a role for LSD1 in transcriptional contol through regulation of histone modification. Comparative microarray analysis of *Lsd1*$^{Lox/\Delta 3}$ and *Lsd1*$^{\Delta 3/\Delta 3}$ ES cells revealed that 62% more genes were up-regulated (362) than down-regulated (226). Transcriptional up-regulation of 362 genes was consistent with a reduction in levels of the co-repressor, CoREST, reduced deacetylase activity associated with the CoREST complex, and global increase in H3K9 and H3K56 acetylation. The down-regulation of genes in the absence of LSD1 either represents off-target effects or suggests LSD1 acts as an activator of transcription at around 40% of its targets. These possibilities have yet to be questioned in any detail. The de-regulation of number of genes with a role in embryonic development appeared to be of significance, considering that LSD1 loss results in early embryonic lethality. Moreover, upon functional analysis of up-regulated genes, the identification of enrichment for genes involved in processes related to cardiac and striated muscle function indicated that up-regulation of the mesoderm lineage master-regulator, *Brachyury,* was informative. Subsequently, the confirmation that *Brachyury* was a direct target of LSD1 and CoREST and that deletion of LSD1 resulted in the increase in marks of gene activation (H3K4me2/me3 and H3K9ac), provided insight into *in vivo* functionality of LSD1/CoREST/HDAC gene control. The acknowledgement that *Brachyury* contains the bivalent chromatin domain, poising it for activation in ES cells, in addition to an identification of bivalent gene up-regulation in *Lsd1*$^{\Delta 3/\Delta 3}$ ES cells, broadened the scope of understanding of LSD1 function.

5 Investigating the requirement for the catalytic activity of LSD1

5.1 Introduction

Rescue of LSD1 knockout ES cells by re-expressing LSD1 was planned in order to confirm the specificity of the phenotype resulting from LSD1 deletion. Three phenotypes of LSD1-deleted ES cells could be analysed in rescued cells, including the reduction in CoREST protein levels, increased expression of *Brachyury* and differentiation-associated cell death. The up-regulation of a directly targeted bivalent gene in the absence of LSD1 and detected increases in H3K4me2 and H3K4me3 indicated that association of an H3K4me2 demethylase is required to prevent modification overbalance towards H3K4me2/me3 at the bivalent domain, which would cause inappropriate expression of the gene. Increase in the H3K9ac mark was also reported upon up-regulation of *Brachyury,* suggesting that less CoREST-associated deacetylase activity in the absence of LSD1 causes hyper-acetylation of histones around the promoter, which could underpin gene over-expression. The aims were to determine whether active demethylase activity is required for gene regulation, or whether CoREST interaction and HDAC association is of more importance. The precedence of this investigation is the report that the H3K9 methyltransferase, G9a, can still repress *Oct4* expression through recruitment of *de novo* DNA methyltransferases independent of its histone KMT activity (Epsztejn-Litman *et al.* 2008). Here, SET-domain mutated G9a can recruit Dnmt3a through an ankyrin domain, with the catalysis of H3K9me3 and subsequent HP1 recruitment dispensible for DNA methylation of the promoter. As the biochemical environment of LSD1 is

analogous with that of G9a, in that they both have protein interaction domains with which to harness further catalytic functions, similar questions about the primary molecular function of LSD1 were asked. To determine whether the demethylase activity is essential for gene repression and hence co-ordination of embryonic development, re-expression of a catalytically inactive form of LSD1 (lysine 661→alanine; Lee *et al*. 2005) in *Lsd1*$^{\Delta 3/\Delta 3}$ cells was performed. The importance of the interaction with CoREST was also investigated by re-expressing a mutated form of LSD1 that would not be able to associate with CoREST through its TOWER domain.

5.2 Results

5.2.1 Generation of LSD1 expression constructs

Five forms of LSD1 were generated by PCR with primers containing tails of 'family D vector homology' for cloning into pLEIC21 expression vectors provided by the PROTEX service at the University of Leicester. Insertion into this vector would endow an EGFP (enhanced green fluorescent protein) tag to the N-terminus of the LSD1 protein. The creation of EGFP fusion proteins was designed to enable assessment of recombinant protein transfection efficiency by FACS and selection of EGFP-positive ES cells through cell sorting if transfection efficiencies were low. GFP is a protein produced by the jellyfish *Aequorea victoria* which fluoresces in the lower green portion of the visible spectrum (Prasher *et al.* 1992, Chalfie *et al*. 1994, Inouye & Tsuji 1994). The gene for GFP is often used in molecular biology as a tool to fluorescently label expressed recombinant protein in order to monitor its expression levels or track its localisation within a cell. Wild-type GFP has two excitation peaks at 395nm and 475nm and an emission peak at 509nm (green). Problems with rapid quenching of *WT* GFP fluorescense instigated the generation of several mutants of GFP, which have increased fluorescence and red-shifted the major excitation peak to 490nm. This excitation peak shift is better for FITC filtersets in fluorescence microscopy and FACS as the main laserline for FITC excitation is from the argon laser at 488nm. EGFP has a double mutation of phenylalanine 64 to leucine and serine 65 to threonine, which has been optimised for brighter fluroscence (Cormack *et al.* 1996).

Full-length LSD1 (Figure 5.1A) and LSD1 with an N-terminal deletion (Figure 5.1B) were designed to behave like wild-type protein. The N-terminal region has been shown to be dispensable for LSD1 activity and is an unstructured region (Forneris *et al*. 2005a), with the removal of this region also possibly aiding the toleration of the 27kDa EGFP tag N-terminally of the functional domains of the protein. A further truncated protein without residue 1-277 was also created to further investigate the requirement of the SWIRM domain of LSD1 (Figure 5.1C). A catalytically inactive form of LSD1 with a lysine to alanine mutation introduced at residue 661 (K661A, referred to from here on as KA), was created by site-directed mutagenesis (Figure 5.1D). This conserved lysine is known to be essential for flavin cofactor interactions in monoamine oxidases and its mutation to alanine abrogates demethylation activity of LSD1 (Binda *et al*. 1999, Binda *et al*. 2003, Lee *et al*. 2005). Two mutations were introduced to full-length LSD1 in order to create a protein that would fail to bind CoREST (Figure 5.1E). The hydrophobic residues mutated (valine and leucine) are within the TOWER domain and assessment of the Protein Data Bank deposits of LSD1-CoREST using the 3D-Mol viewer suggested they would be essential in creating an interface for CoREST association. Expression of this mutant aimed to analyse the requirement for CoREST binding by LSD1 and the role of HDACs in gene expression regulation as part of the CoREST complex.

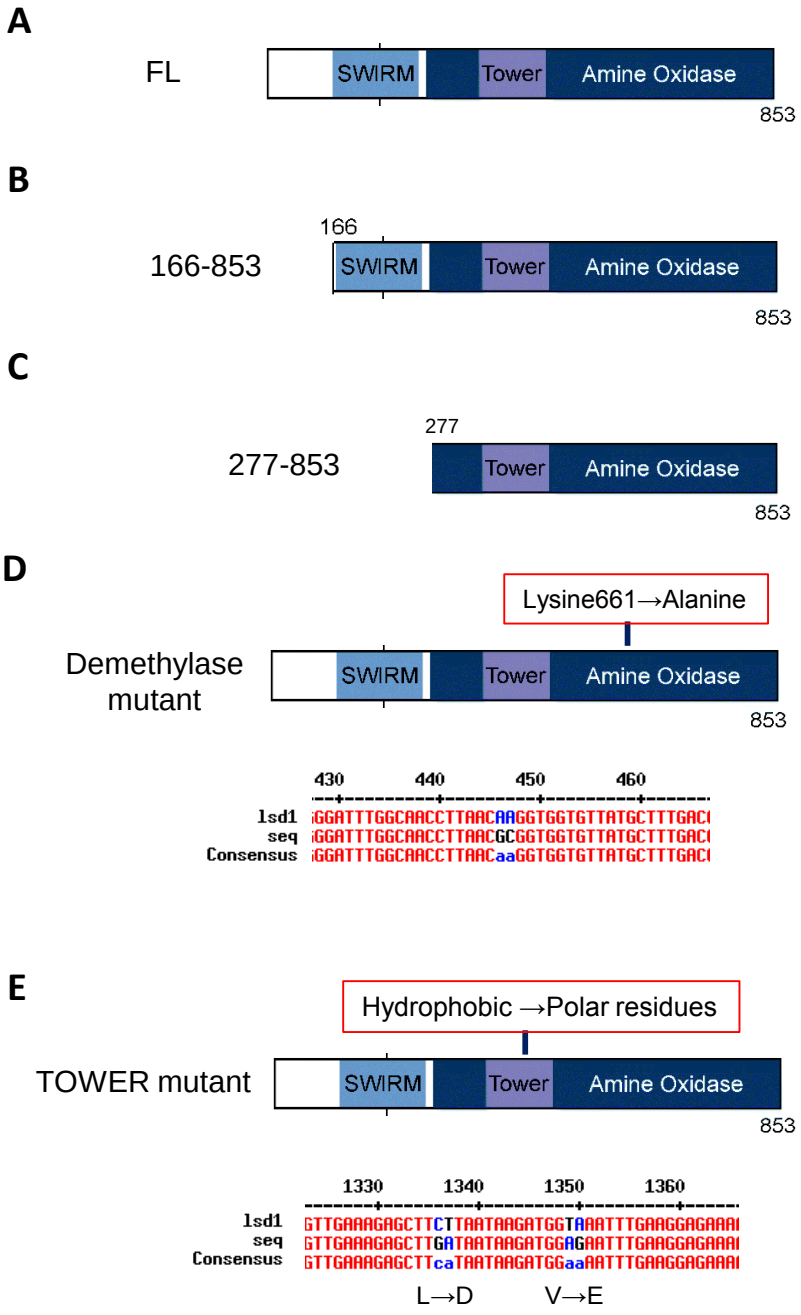

Figure 5.1 LSD1 rescue and mutant schematics for cloning into pLEIC21 vectors. (A) Full length and (B) N-terminal truncated LSD1 used as WT forms of LSD1 to rescue the knockout ES cells. (C) SWIRM domain truncated LSD1. (D) Catalytically inactive LSD1 with lysine 661 mutated to alanine (Lee *et al.* 2005) with sequencing alignment confirming mutagenesis of two nucleotides to alter the amino acid. (E) Mutated TOWER domain to disrupt the interaction with CoREST, with sequencing alignment confirming mutagenesis of leucine 446 to apartic acid and valine 450 to glutamic acid.

An initial expression trial of EGFP-LSD1$^{166\text{-}853}$ (here on referred to as EGFP-LSD1^{166}) in the pLEIC21 vector was performed. FACS analysis showed that GFP expression in ES cells was less than 2% after 48 hours of transfection with pLEIC EGFP-LSD1$^{166\text{-}853}$, and western blots proved that LSD1 protein was barely detectable compared to control *Lsd1*$^{Lox/\Delta 3}$ cells (Figure 5.2). The pLEIC vectors are derived from the pcDNA family of vectors and contain a cytomegalovirus (CMV) promoter. Recombinant protein expression from this vector was foreseen to be difficult as low constitutive activity and even inactivation of the CMV promoter has been previously observed in mouse ES cells (Chung *et al.* 2002, Barrow *et al.* 2006). ES cells can also be difficult to transfect; therefore these two features were ultimately manifested in poor recombinant protein expression. The EGFP-LSD1 fusions were subsequently shuttled into a pCAGGS vector containing a chicken α-globin promoter (Figure 5.3A). pCAGGS-Flpe had previously been utilised for expressing Flpe in ES cells, with reasonable expression observed. A linearised vector backbone was generated from the pCAGGS-Flpe construct using PCR with a high-fidelity KOD polymerase (Figure 5.3B). This removed the Flpe ORF and also omitted the puromycin resistance gene, as the ES cells already contained this gene at the *ROSA26* locus, rendering puromycin expression from this construct redundant. All E-LSD1 ORFs were amplified by PCR from the appropriate pLEIC21 constructs using primers with 15bp tails of homology to the ends of the linear pCAGGS vector (Chapter 2; Table 2.3**)**. The PCR reactions were assessed for presence of a single specific DNA species (Figure 5.3C) and inserts were then cloned into the pCAGGS vector by annealing the tails of homology to the 5' and 3' ends of the linear backbone using an In-Fusion® enzyme. New pCAGGS constructs were identified by colony PCR and newly

inserted ORFs were sequenced before endotoxin-free preparations of plasmids was performed for transfection into ES cells.

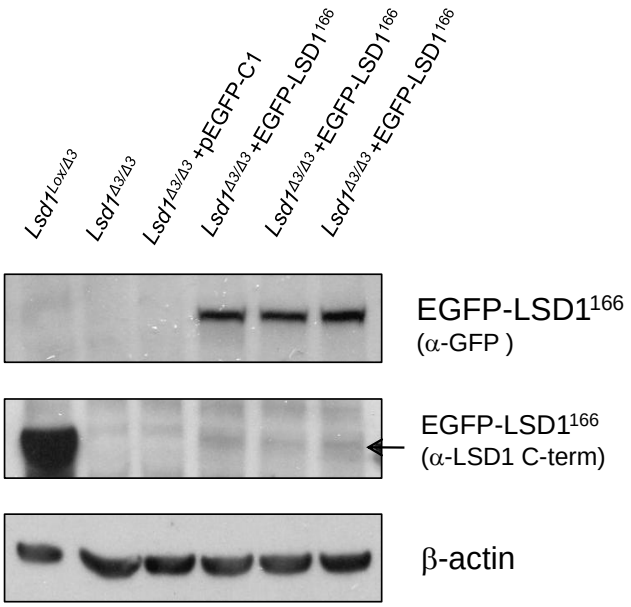

Figure 5.2. Expressed of EGFP-LSD1$^{166\text{-}853}$ from the pLEIC21 vector is very low in ES cells A GFP antibody reveals that 48hr transient transfection of pLEIC12 EGFP–LSD1^{166} results in recombinant protein expression in *Lsd1$^{\Delta3/\Delta3}$* ES cells (top panel) . However, use of the LSD1 antibody shows that this protein is expressed at very low levels compared to endogenous LSD1 in *Lsd1$^{Lox/\Delta3}$* cells (middle panel). β-actin was used as a protein loading control. Plasmids from three different transformed bacterial clones were tested.

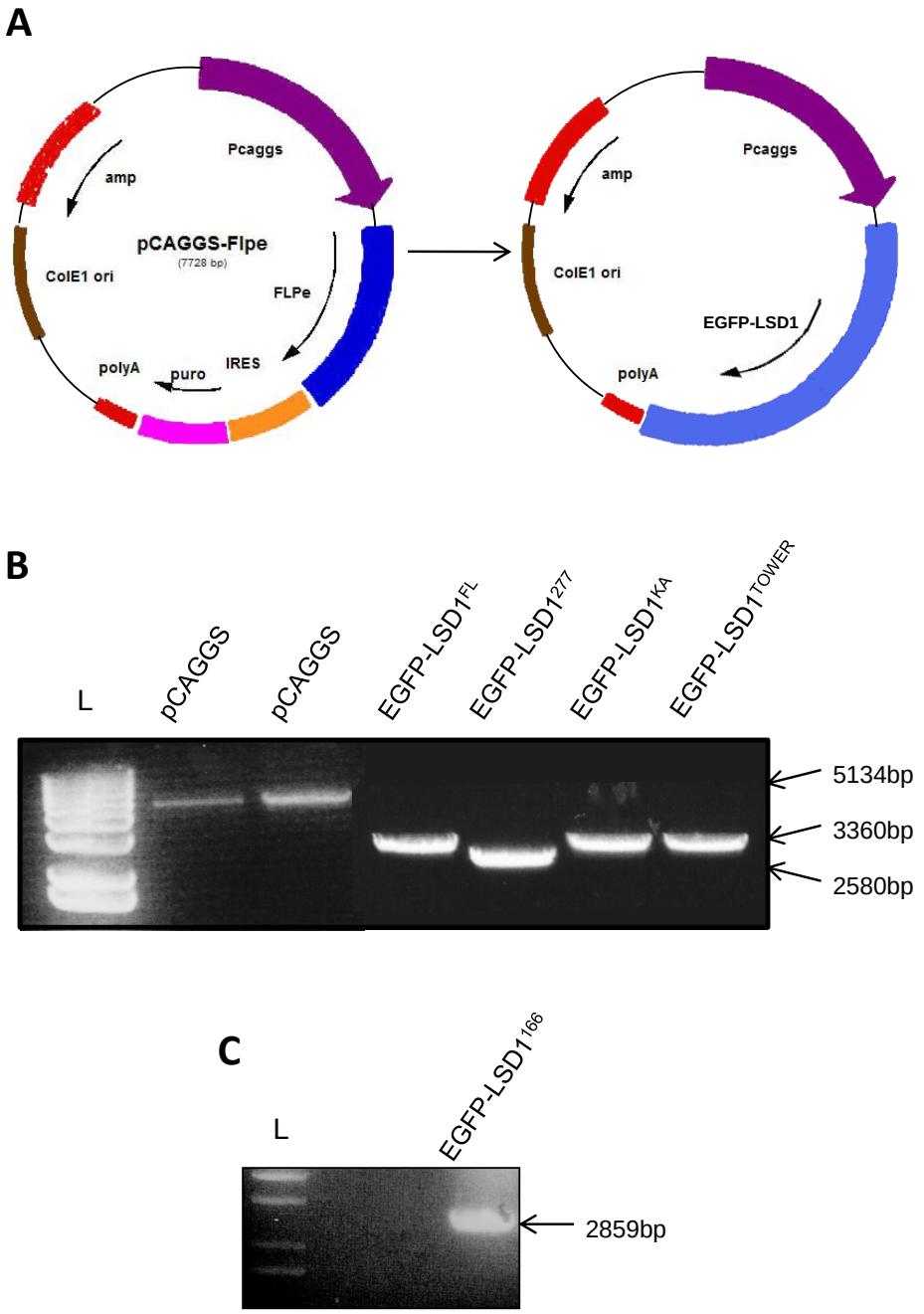

Figure 5.3 Generation of the pCAGGS-EGFP-LSD1 constructs by PCR and InFusion cloning. (A) Schematic of the convesion of pCAGGS-Flpe to pCAGGS-EGFP-LSD1. (B-C) The cloning strategy involved KOD PCR amplification of EGFP-LSD1 inserts from pLEIC21 construct with 15bp arms of homology to the pCAGGS backbone, which itself was generated by KOD PCR. PCR products were verified by agarose gel electrophoresis and then treated appropriately before use in the InFusion cloning procedure (2.14). Sizes of PCR products are indicated. All primers used in cloning procedures are listed in Table 2.3.

5.2.2 Expression of pCAGGS EGFP-LSD1 constructs in ES cells

The EGFP N-terminal tag could be used to assess the success of recombinant protein expression following transfection by FACS analysis. Excitation of EGFP is achieved using the FITC excitation wavelength (488nm) in FACS. The analysis of EGFP-LSD1 expression from the pLEIC21 vector by western blot had revealed very low expression levels that were not adequate for a rescue of the LSD1-null ES cell phenotype (Figure 5.2). FACS analysis indicated that the percentage of cells expressing EGFP 24 hours after transfection with pCAGGS constructs was only between 12 and 21% (Figure 5.4A). However, upon analysis of fusion protein expression by Western blot using the LSD1 C-terminal antibody, high protein expression was observed at this time of cell harvesting (Figure 5.4B). This expression was in fact higher than endogenous LSD1 levels. The combined results indicated that under a quarter of the cell population was expressing recombinant protein at extremely high levels, which was not a recapitulation of the cellular state of *Lsd1*$^{Lox/\Delta 3}$ ES cells. This was an early indication that selection or sorting of recombinant protein-expressing cells was necessary. Notably, at 24 hours after transfection, no obvious increase in CoREST levels was observed in LSD1 rescued cells (Figure 5.4B middle panel). This suggested that the next essential experiment was to assess the ability for recombinant LSD1 to associate with the CoREST complex and that longer transient re-expression of LSD1 might be required to rescue CoREST levels. This strong expression of LSD1 could be harnessed nonetheless for LSD1 immunoprecipitation and co-purification of CoREST and HDAC1.

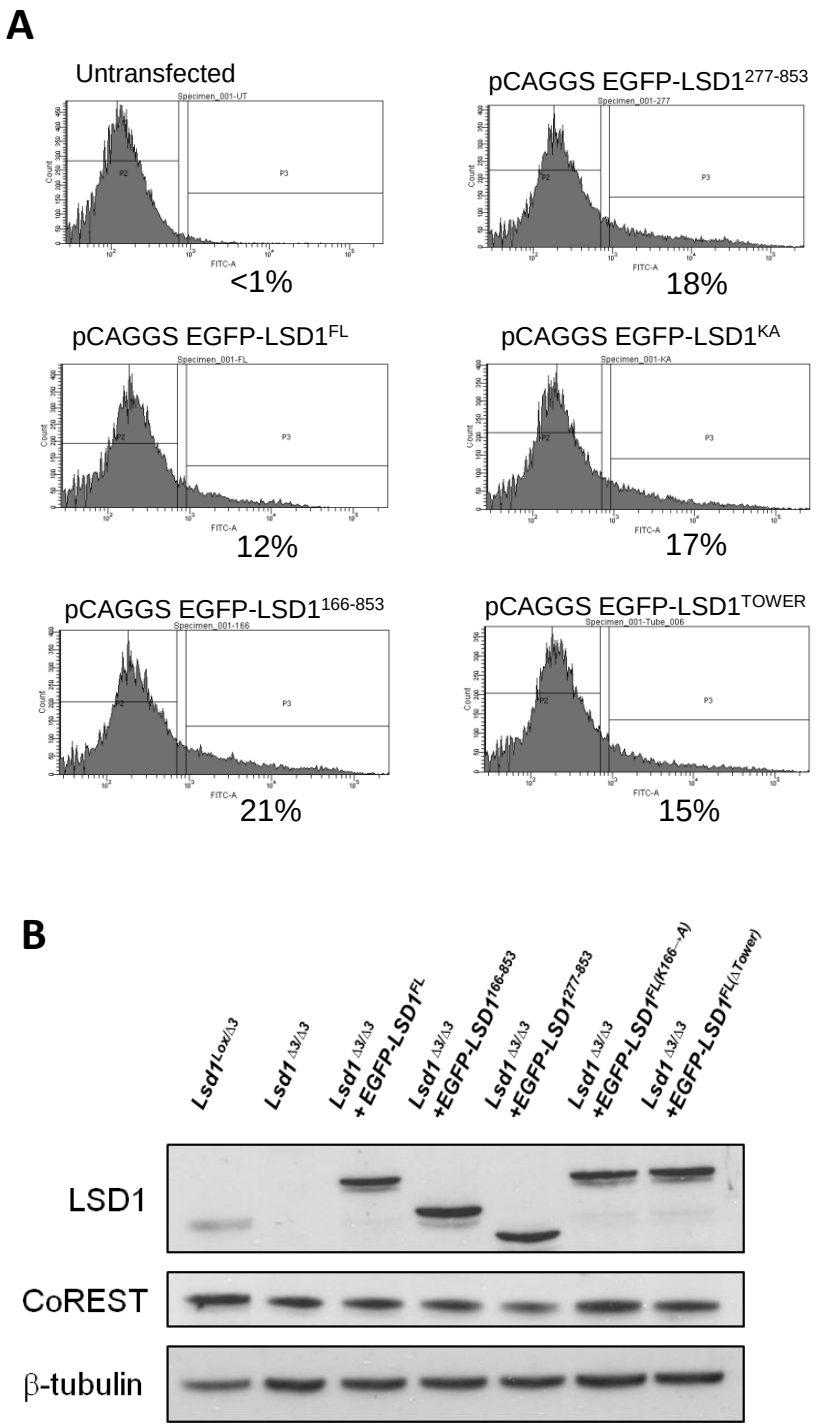

Figure 5.4 Transfection efficiency and expression of all rescue constructs 24 hours after transfection (A) FACS analysis to identify GFP-positive cell populations identified a transfection efficiency between 12-21% with pCAGGS rescue constructs. (B) Western blotting revealed high expression of rescue constructs at 24 hours post transfection. The size of EGFP is 27KDa, therefore this tag increases the sizes of detectable LSD1. β-tubulin was used as a protein loading control. Note the unequal loading of protein in the first lane.

5.2.3 Analysis of recombinant LSD1 protein interactions

Preliminary analysis of recombinant protein expression levels showed that expression was highest at 24 hours after transfection and then decreased, either due to exclusion of the expression vector from ES cells or diminishing promoter function. Therefore, protein was harvested at 24 hours to test the ability of all forms of recombinant LSD1 to contribute to reformation of the CoREST complex. LSD1 was purified from ES cell extracts using the C-terminal LSD1 antibody and the co-purification of CoREST and HDAC1 was assessed. LSD1 was successfully immunoprecipitated from *Lsd1*$^{Lox/\Delta 3}$ ES cells but no LSD1 was immunoprecipitated from *Lsd1*$^{\Delta 3/\Delta 3}$ ES cells transfected with pEGFP-C1 which expressed EGFP alone (Figure 5.5A, top panel lanes 3 and 5). This data was in accordance with immunoprecipitation experiments documented in Chapter 4. All recombinant proteins could be immunoprecipitated with the LSD1 antibody (Figure 5.4A, top panel). Importantly, whereas CoREST could not be co-purified with LSD1 in *Lsd1*$^{\Delta 3/\Delta 3}$ ES cells (lane 5), CoREST protein was co-purified with recombinant WT LSD1 (FL and 166), as well as 277, KA and surprisingly TOWER mutants (lanes 7, 9, 11, 13, 15). Deacetylase assays of LSD1 immunoprecipitates showed that all recombinant LSD1 proteins could also co-purify deacetylase activity (Figure 5.4B), even though HDAC1 co-purification could not be easily identified through western blotting (Figure 5.4A). This biochemical data suggested that the TOWER mutant did not function as intended as it could co-purify CoREST (Figure 5.4A lane 15) and deacetylase activity (Figure 5.4B). Overall, all forms of re-expressed LSD1 could bind within the CoREST complex and therefore presumably rescue reduced CoREST levels if expressed for longer than 24 hours. The TOWER mutant was discarded from analysis at this point due to wild-type biochemical behaviour.

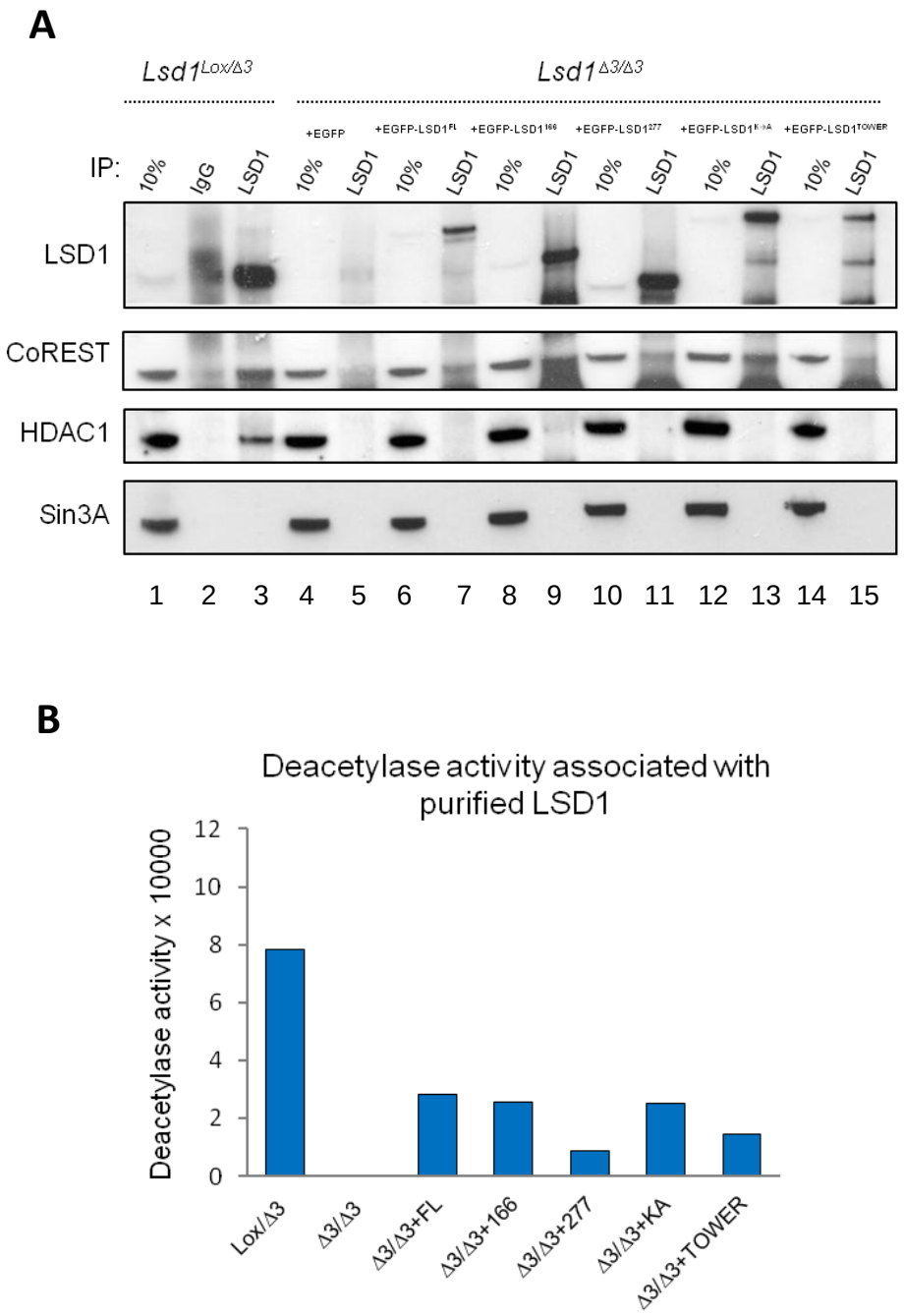

Figure 5.5 Recombinant LSD1 is incorporated into an HDAC-containing complex. (A) Immunoprecipitation of LSD1 in *Lsd1*$^{Lox/\Delta3}$, *Lsd1*$^{\Delta3/\Delta3}$ and *Lsd1* $^{\Delta3/\Delta3}$ ES cells re-expressing recombinant LSD1 shows that LSD1 can be purified and CoREST co-purified in all cells, including the TOWER domain mutant. Sin3A was used as a negative control, which does not bind LSD1. HDAC1 co-immunoprecipitation was inconclusive through Western blotting however (B) shows that deacetylase activity is co-purified with all forms of recombinant LSD1, including the TOWER domain mutant.

5.2.4 Analysis of the ability for re-expressed wild-type LSD1 to rescue CoREST levels and gene expression

EGFP-LSD1^{166} could bind CoREST/HDAC1, with FACS and western blot data indicating that it was the most highly expressed recombinant protein. It was therefore used to see if phenotypes of *Lsd1*$^{\Delta 3/\Delta 3}$ ES cells could be rescued following a longer period of transient re-expression, as there was no obvious effect on CoREST protein levels at 24 hours. A titration of Lipofectamine 2000 (6μl, 8μl and 10μl) was used in transfections to increase the expression level of EGFP-LSD1^{166} and assess corresponding levels of CoREST. Two different quantities of plasmid were also used in transfection (1μg and 2μg). ES cells were harvested 48 hours after transfection in order to allow more time for recovery of CoREST protein levels, as CoREST protein stability had previously be shown to be dependent on the ability to bind LSD1. An increase in the quantity of Lipofectamine 2000 resulted in an increase in EGFP-LSD1^{166} protein level (Figure 5.6A and B), which correlated with an increase in CoREST protein level (Figure 5.6A and C). This data confirmed that EGFP-LSD1^{166} rescued CoREST protein levels by allowing re-formation of the CoREST complex. This effect consequently resulted in the rescue of expression of three genes that were de-regulated in *Lsd1*$^{\Delta 3/\Delta 3}$ ES cells (Figure 5.7A-C). The unchanged levels of *HDAC2* (Figure 5.7D) confirmed that the trend in rescue of *Brachyury, DDR2* and *RASGRP3* was specific to expression of EGFP-LSD1^{166}. The rescue of *Brachyury* expression is also further confirmation that LSD1 represses *Brachyury* as part of the CoREST complex (Chapter 4).

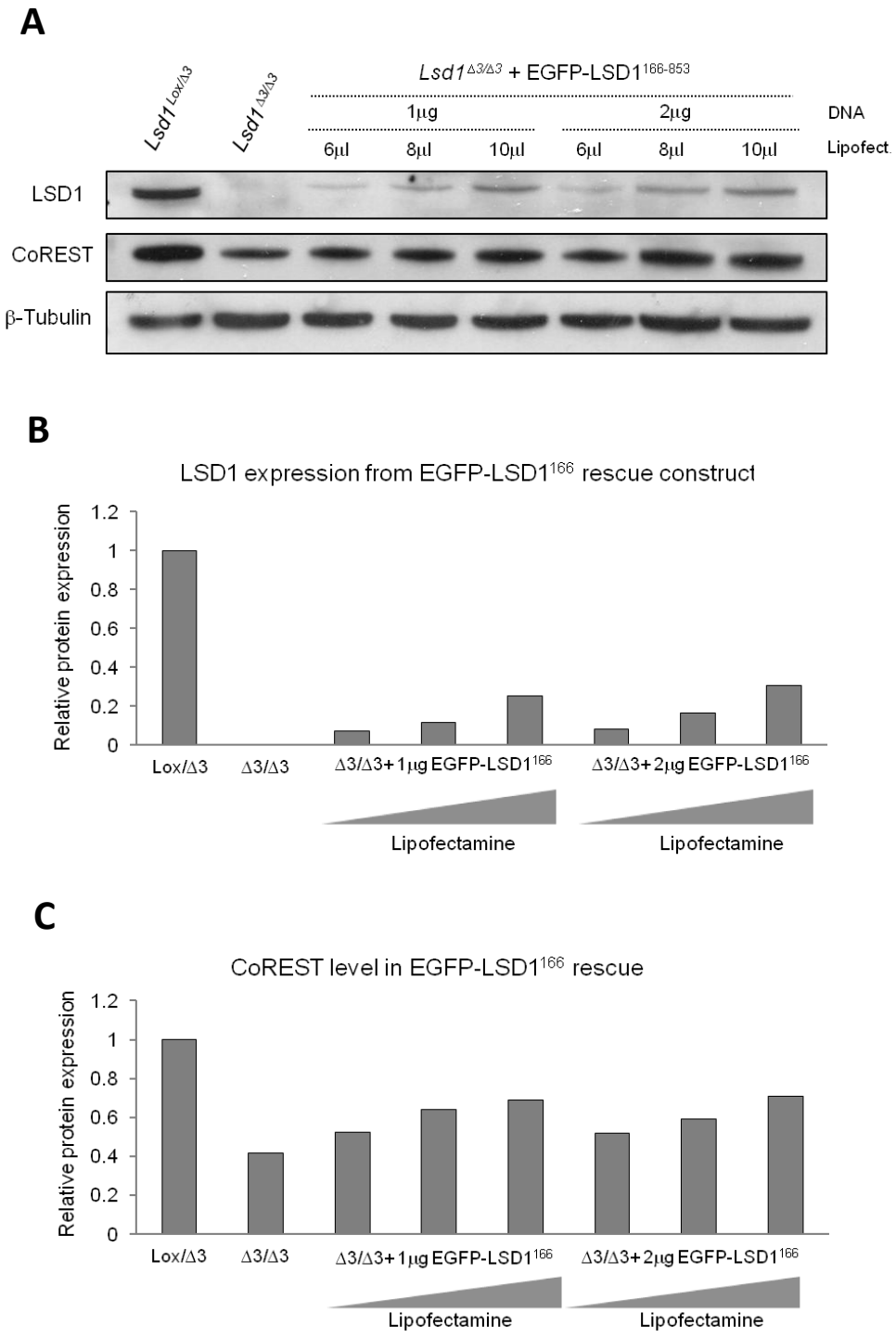

Figure 5.6 Titration of WT rescue construct expression identifies a recovery of CoREST levels in *Lsd1$^{Lox/Δ3}$* ES cells. (A) Increasing Lipofectamine 2000 reagent quantities with 1μg and 2μg of pCAGGS-EGFP-LSD1^{166} plasmid correlates with an increase in transient expression of recombinant protein. Protein extracts were harvested at 48 hours after transfection. (B) Quantification of EGFP-LSD1^{166} protein expression from (A). (C) Quantification of CoREST protein levels from (A). Protein levels were calculated relative to the protein loading control, β-tubulin.

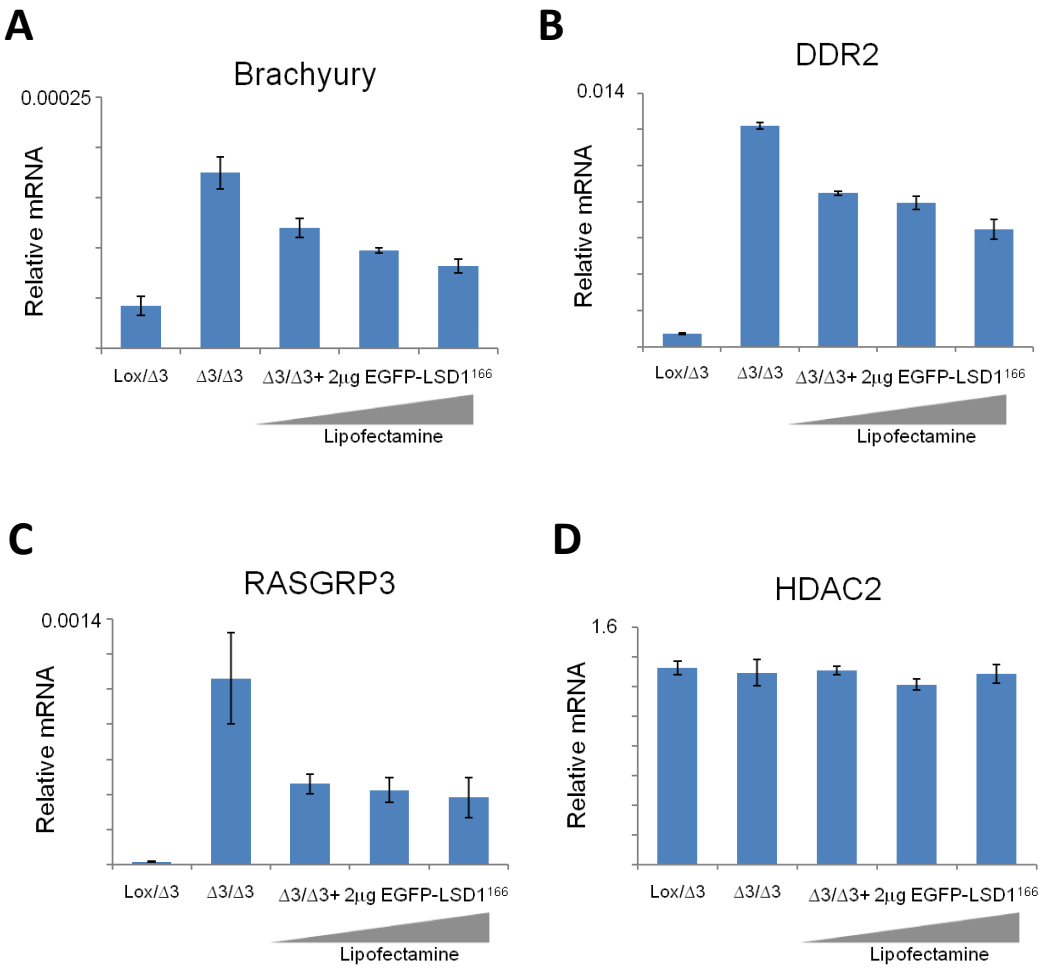

Figure 5.7 Expression of EGFP-LSD1^{166} rescues the expression of genes up-regulated in *Lsd1$^{Lox/Δ3}$* ES cells. Increasing expression of EGFP-LSD1^{166} as represented in Figure 5.6A and B (2μg plasmid quantity) causes a correlative re-repression of (A) *Brachyury*, (B) *DDR2* and (C) *RASGRP3*, but no change in (D) *HDAC2*, a gene unaffected by loss of LSD1.

5.2.5 LSD1 demethylase activity is not required for gene repression

The observation that less than 20% of ES cells were over-expressing exogenous LSD1 at above physiological levels (Figure 5.4) prompted the move to sort or select plasmid-expressing cells. This could also be combined with longer culture of cells following transfection in attempt to rescue gene expression to original levels. FACS sorting of GFP-positive cells was unsuccessful as most of the cells died during the sorting processes and therefore there were insufficient cells to harvest or even establish further cell cultures with. It appeared that the expression plasmids were being rejected from cells beyond 24 hours after transfection, therefore selection of cells that retained the plasmid was performed. This involved co-transfecting ES cells with the pCAGGS construct and a plasmid containing a Hygromycin resistance gene (Hyg^R). The culture of ES cells in the presence of 50μM hygromycin would kill untransfected and plasmid-excluding cells over a 5 day period, to allow the propagation of $Lsd1^{\Delta 3/\Delta 3}$ ES cells expressing recombinant LSD1. Previous analysis of ES cell kill curves using 50μM hygromycin had been assessed by the Geneta laboratory, concluding that this drug concentration killed all non-resistant ES cells within 5 days of drug exposure.

To investigate the effects of the catalytically inactive LSD1 mutant, EGFP-$LSD1^{KA}$ was compared to the EGFP-$LSD1^{FL}$. The mutation was introduced into full-length LSD1 and therefore the most reliable comparison was with wild-type FL protein. Firstly, the EGFP-$LSD1^{KA}$ mutant was confirmed to be catalytically impaired as the demethylase activity in EGFP-$LSD1^{KA}$-transfected cells was comparable to LSD1 knockout cells (Figure 5.8). In addition to this, the significant difference in detectable demethylase

activity towards a recombinant H3K4me2 substrate in the *Lsd1*$^{Lox/\Delta 3}$ to *Lsd1*$^{\Delta 3/\Delta 3}$ cells confirmed the assay was sensitive to demethylase activity associated with LSD1 ($p<0.05$).

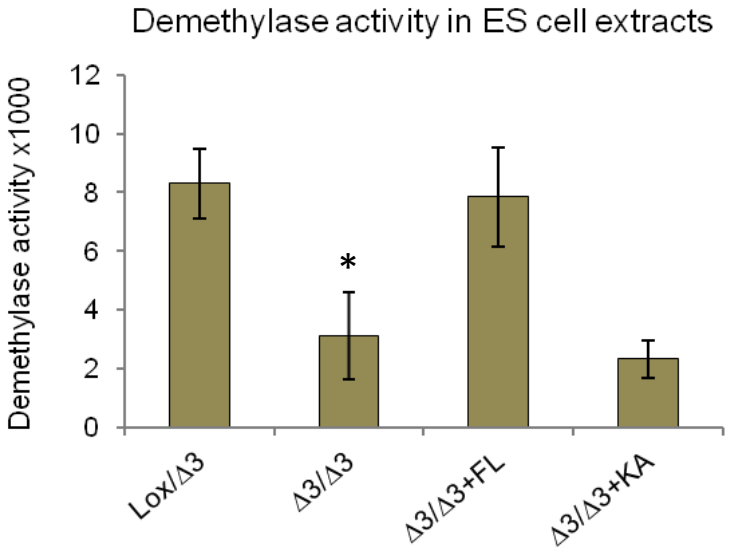

Figure 5.8 The EGFP-LSD1^{KA} construct expressed catalytically inactive protein. ES cells extracts were harvested and protein concentrations were equalised before catalytic activity was measured by formaldehyde production from a demethylation reaction with a recombinant H3K4me2 substrate (Active Motif). n=3 +/- S.E.M. * $p<0.05$

Assessment of co-transfected cells after 5 days showed enrichment for recombinant LSD1 in cells grown under hygromycin selection (Figure 5.9A). This selected population also showed a significant increase in CoREST levels (Figure 5.9A and B). This result suggested that even though recombinant LSD1 expression was not identical to *Lsd1*$^{Lox/\Delta 3}$ expression, the 5 day period of expression within a more homogenously behaving population of cells could more effectively rescue phenotypes. Moreover, gene expression analysis showed that selection resulted in complete rescue of *DDR* mRNA levels in both EGFP-LSD1^{FL} and EGFP-LSD1^{KA}-transfected ES cells (Figure 5.9C). This suggested demethylase activity was not required for repression of *DDR2*. This observation in EGFP-LSD1^{KA}-transfected ES cells prompted more extensive analyses of gene expression between ES cells transfected with EGFP-LSD1^{FL} and EGFP-LSD1^{KA}. Quantitative RT-PCR analysis demonstrated that 5 day expression of EGFP-LSD1^{FL} rescued expression in seven out of seven over-expressed genes, with the *HDAC1* control gene unchanged (Figure 5.10). Notably though, expression of the catalytic mutant form of LSD1 also rescued expression of all these genes (Figure 5.10). Therefore the demethylase activity of LSD1 was dispensible in the rescue of de-regulated genes, implying demethylase activity is not essential for gene repression. However, slightly higher expression of all genes in EGFP-LSD1^{KA} transfected cells (most recognisable in *BARX2*) suggests that demethylase activity may be required to maintain repression. Further culture of ES cells expressing the mutated LSD1 might have revealed release of repression of these genes in the absence of an active demethylase. The presence of the bivalent modification at the *Brachyury* promoter suggests that active demethylation by LSD1 would not govern gene regulation. Increases in H3K4me2 and H3K4me3 at the *Brachyury* promoter following LSD1

deletion may simply be a by-product of increased transcription, and changes in acetylation state possibly dictate an increase in expression. An alternative thought is that the LSD1/HDAC/CoREST repressor complex serves as an obstruction to TrxG complexes that can apply the H3K4me3 modification and facilitate gene activation. Other bivalent genes (*Barx2, Spink2* and *Thy1)*, not yet confirmed as direct targets of LSD1, may be responding through similar mechanisms. The analysis of the TOWER mutant in these experiments would have been very useful in determining whether the ability of LSD1 to re-associate with HDACs (via CoREST) was sufficient to re-repress genes at this 5 day time point. Ultimately, stable transfection of rescue constructs and analysis of gene expression over an extended period of time would provide more explicit data on the biological interplay of LSD1 catalytic activity and HDACs in target gene repression.

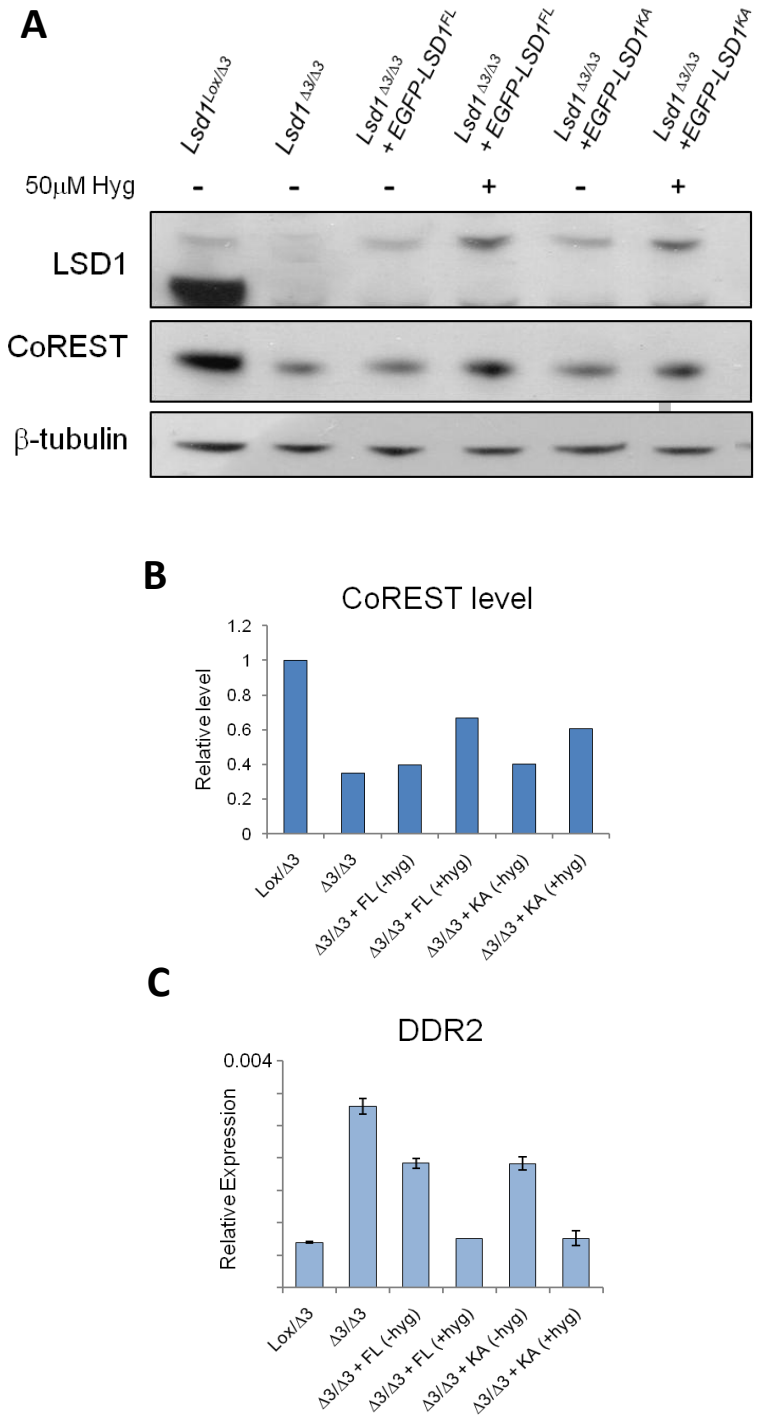

Figure 5.9 Five-day selection of transfected FL and KA constructs shows more effective rescue of CoREST levels and gene expression. (A) Western blotting shows selection for plasmid expression ES cells, following co-transfection of FL and KA rescue constructs with a *Hyg*^{R} plasmid. This results in enrichment for recombinant protein expression in *Lsd1*$^{\Delta 3/\Delta 3}$ ES cells. The enrichment for FL and KA protein correlates with enhanced rescue of (B) CoREST protein levels and (C) *DDR2* gene expression levels. *DDR* expression was normalised to GAPDH. n=3 +/- S.E.M.

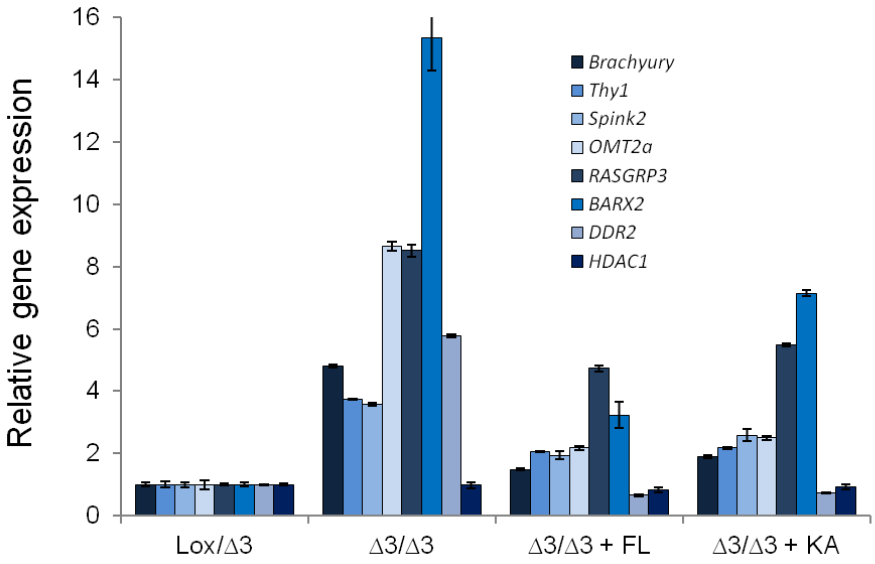

Figure 5.10 Catalytically inactive LSD1 can rescue gene expression in *Lsd1*$^{\Delta 3/\Delta 3}$ ES cells. Gene expression analysis of 7 up-regulated genes in *Lsd1*$^{\Delta 3/\Delta 3}$ ES cells, cultured for 5 days under hygromycin selection, shows that catalytically inactive LSD1 (KA) re-represses gene expression to a similar extent as the fully-functional demethylase (FL). *HDAC1,* a gene unaffected by loss of LSD1 was used as a control, which remains unchanged following FL and KA transfection. Gene expression levels were normalised to GAPDH and represented as a fold change relative to *Lsd1*$^{Lox/\Delta 3}$ expression. n=3 +/- S.E.M.

5.3 Conclusions

The results reported in this chapter constitute attempts to rescue *Lsd1*$^{\Delta 3/\Delta 3}$ ES cells. Importantly, the re-expression of WT LSD1 increased CoREST levels and re-repressed genes that are up-regulated in LSD1 knockout ES cells. These results proved that observations in *Lsd1*$^{\Delta 3/\Delta 3}$ ES cells were specific to the deletion of the protein of interest. However, there are further assays that were planned to test the specificity of phenotypes in *Lsd1*$^{\Delta 3/\Delta 3}$ ES cells. These included assessment of the ability to rescue differentiated-associated cell death, global H3K56 acetylation levels and histone modifications at the *Brachyury* locus. Ultimately a stable transfection of WT and KA LSD1 is most likely required for these experiments. However, the ability to remove one of the catalytic components of the CoREST complex by re-expressing a 'demethylase-dead' form of LSD1, allowed insights into the mechanisms of LSD1 functions. Incorporation of a catalytically inactive form of LSD1 into the CoREST complex had the ability to not only recover CoREST levels, as expected, but also cause re-repression of genes over-expressed in LSD1 knockout ES cells. The deacetylase activity of this reconstituted complex can explain re-repression of genes; though there was an indication that demethylation of H3K4me2 might be required to maintain repression. However, the presence of a repressor complex at target genes is postulated to be sufficient to prevent association of activating complexes which contain methyltransferases to catalyse addition of the H3K4me3.

6 Discussion

6.1 An essential role for LSD1 in early embryonic development

LSD1 was initially identified as an FAD-binding protein found in a complex containing the co-repressor of REST, CoREST, the carboxy-terminal binding protein, CtBP, and specific histone deacetylases, HDAC1 and 2 (Humphrey *et al*. 2001, You *et al*. 2001, Hakimi *et al*. 2002, Shi *et al.* 2003). It can function as a histone H3K4me1/me2 and H3K9me1/me2 demethylase (Shi *et al.* 2004, Metzger *et al*. 2005). LSD1 is known to mediate the regulation of genes involved in cell-specific proliferation and differentiation through LSD1/CoREST/HDAC association with a number of transcription factors, including REST, Gfi, TAL1, TLX, Mef2c and MyoD (Shi *et al*. 2004, Shi *et al*. 2005, Saleque *et al*. 2007, Hu *et al*. 2009, Ouyang *et al*. 2009, Sun *et al*. 2010, Choi *et al*. 2010).

Before the publication of data contained in this thesis, reporting an explanation for the essential role of LSD1 in embryonic development, two other germline LSD1 knockout mouse studies had been published. The timing of death in the LSD1 knockout embryos is consistent with these previous reports (Wang *et al*. 2007, Wang *et al*. 2009). However, neither of these reports provided embryonic analyses that could convincingly explain pre-gastrulation embryonic lethality. The study in 2007 demonstrated that LSD1 is required for late cell-type differentiation in the pituitary through activation of *Pit1*-dependent target genes (*Gh, Prl* and *Tshb)* at E16.5-17.5.

These analyses of a conditional LSD1 deletion failed to provide reasoning for a much earlier developmental block within the embryo (Wang *et al.* 2007). The phenotype of the LSD1 knockout published in 2009 was attributed to increased cell death and impaired cell cycle progression of LSD1 deleted ES cells, which resulted from decreased levels of the maintenance DNA methyltranferase DNMT1 and subsequent hypomethylation of DNA (Wang *et al.* 2009). However, embryonic lethality is unlikely to be solely caused by reduced DNMT1, since *Dnmt1* mutant embryos survive to mid-gestation, whereas *Lsd1* mutants die at the onset of gastrulation (Wang *et al*. 2007, Li *et al.* 1992).

The previously reported non-viability of embryos with a germline deletion for LSD1 as well as our $Lsd1^{\beta\text{-}geo/\beta\text{-}geo}$ genetrap embryo data prompted the generation of ES cells where LSD1 may be conditionally deleted. The indication from one publication that LSD1-deleted ES cells might not be viable also instigated a conditional deletion strategy (Wang *et al*. 2009). Control of protein deletion would enable assessment of the impacts of LSD1 removal in cells that are equivalent to those of the embryonic epiblast. If the viability of undifferentiated ES cells was unaffected then the impact of LSD1 loss on early differentiation events in the post-implantation embryo could be analysed through *in vitro* differentiation assays, which recapitulate this period of development. Data from our $Lsd1^{\beta\text{-}geo/\beta\text{-}geo}$ genetrap embryos and $Lsd1^{\Delta 3/\Delta 3}$ ES cells has provided a better understanding of the essential role of LSD1 in the survival of the post-implantation embryo. Prior to implantation, $Lsd1^{\beta\text{-}geo/\beta\text{-}geo}$ blastocysts occur at expected Mendelian ratios and appear morphologically normal. *In vitro* cultured of

Lsd1$^{\beta\text{-}geo/\beta\text{-}geo}$ blastocysts show robust outgrowth of the ICM (Figure 3.1K-M) and *Lsd1*$^{\Delta 3/\Delta 3}$ ES cells show no reduction in proliferative potential (Figure 3.7A and B), suggesting that embryonic lethality does not occur due to impaired cell cycle progression within the epiblast, as stated by Wang *et al.* 2009, but a developmental block shortly after implantation. The conditional deletion of LSD1 in ES cells allowed assessment of the DNA hypomethylation phenotype previously reported (Wang *et al.* 2009). The observation that DNA methylation was unaffected at 6 days after the complete loss of LSD1 protein (Figure 3.5A and Figure 3.9A lane 3) suggested there would be no defects in maintenance methylation in E6.5 embryos. Ultimately, if defects in maintenance DNA methylation were solely causal of embryonic death in *Lsd1*$^{\beta\text{-}geo/\beta\text{-}geo}$ embryos, reduced Dnmt1 at 11 days (4 to 15 days) after loss of LSD1 protein (Figure 3.8B compare day 4 to 15) should correlate with a mid-gestation time of embryonic death, which is the case in *Dnmt1*$^{-/-}$ embryos (Li *et al.* 1992). At this stage of the research, it was proposed that death of the *Lsd1*$^{\beta\text{-}geo/\beta\text{-}geo}$ genetrap embryo was likely due to a developmental block, underpinned by mechanisms independent of Dnmt1 and DNA methylation. A recent publication in fact corroborated this dissociation of LSD1 from Dnmt1 in the early embryo and ES cells (Macfarlan *et al*. 2011).

Unlike the ubiquitous expression pattern involved in the head-fold stage and beyond (Figure 3.1D and E), LSD1 expression in the post-implantation embryo is restricted to the embryonic portion of the embryo (Figure 3.1F and G). Based on the expression pattern, it appears that *Lsd1*$^{\beta\text{-}geo/\beta\text{-}geo}$ embryos lack extra-embryonic tissue, indicating

developmental stall before the elongation of the epiblast and an inability to form extra-embryonic tissue. However, the ability for *Lsd1*$^{\Delta 3/\Delta 3}$ ES cells to repress *Oct4* suggests that trophectoderm development might not be perturbed (Figure 3.13A). Outgrowth of the ICM in blastocyst outgrowth assays indicated that pluripotent ES cells could be derived from the ICM in the absence of LSD1 (Figure3.1K-M). This further suggests that LSD1-deficient cells of the ICM maintain normal levels of Oct4 and Nanog, as lack of these factors results in failure to maintain the epiblast and pluripotency in ES cells (Nichols *et al*. 1998, Mitsui *et al*. 2003). This was confirmed through the ES cells generated from gene targeting, which maintained self-renewal capacity and normal expression of *Oct4* and *Nanog* (Figure 3.7, 3.10A and B, Figure 3.13A).

The *Oct4* promoter shows progressive decrease in H3K4 methylation during differentiation of ES cells in the absence of LIF and retinoic acid-mediated differentiation of embryonic carcinoma cells, implicating a potential role for LSD1 (Lee *et al.* 2004b, Feldman *et al*. 2006). However, *Oct4* is successfully repressed in absence of LSD1, which would suggest that LSD1 is not required for repression of *Oct4* upon ES cell differentiation, and hence the involvement of an alternative H3K4-specific lysine demethylase (KDM). This was interesting because LSD1 and CoREST localise to the CR4 region of *Oct4* in P19 embryonic carcinoma cells to repress *Oct4,* with inhibition of LSD1 causing *Oct4* de-repression (Lee *et al*. 2006b). P19 cells represent those of the primitive ectoderm where as ES cells are derived from the pluripotent ICM. The contrasting observations between the two cell types may reflect enzymatic

redundancy for the removal of H3K4 methylation in ES cells, which is not a feature of P19 cells. Additionally, the report that Oct4 protein associates with LSD1 in ES cells suggests that LSD1 would not have an essential role in the repression of *Oct4* gene itself (Pardo *et al*. 2010). The related amine oxidase, LSD2 can demethylate mono- and di-methylated H3K4 (Karytinos *et al*. 2009) and several JmjC domain containing enzymes also contain specificity to H3K4me2, including JARID1A, JARID1B, JARID1C, JARID1D, with all but JARID1D expressed in ES cells (Su *et al*. 2004, Christensen *et al*. 2007, Iwase *et al.* 2007, Klose *et al*. 2007, Lee *et al*. 2007a). Knockout mice have been generated for LSD2 (Ciccone *et al*. 2009) and JARID1A (Klose *et al*. 2007), but neither is essential for embryonic development. Therefore possibly JARID1B, JARID1C may have a role in demethylation of H3K4 at the *Oct4* promoter upon ES cell differentiation. A developmental block was also not attributed to the inability to differentiate through repression of other pluripotent factors. LSD1-deleted ES cells were still able to down-regulate alkaline phosphatase (AP) upon LIF withdrawal and repress transcription of *Nanog* and *Rex1* upon EB differentiation (Figure 3.10A and Figure 3.13A). The inability to repress *Nanog* in particular is known to cause resistance to retinoic acid-induced differentiation, which was not the case here. ES cell aggregation as EBs, which requires *Nanog* repression, could also be achieved in the absence of LSD1, albeit with increased levels of cell death (Figure 3.11).

LSD1 has been identified as one of a number of co-repressor proteins that bind Oct4 in ES cells (Pardo *et al*. 2010, van den Berg *et al.* 2010). LSD1 may therefore play a direct role in mediating transcriptional regulation by Oct4. A key role of Oct4 is to control

repression of developmental genes in order to maintain stem cell pluripotency and self-renewal (Boyer *et al.* 2006, Loh *et al*. 2006). This indicates that repression of some developmental genes is controlled by co-occupancy of Oct4, LSD1 and associated repressors. Many repressed targets of Oct4 are co-occupied by PcG repressor proteins (Lee *et al.* 2006), where deletion of PRC2 components also results in post-implantation embryonic lethality (O'Carroll *et al.* 2001, Pasini *et al*. 2004). The loss of LSD1 does not diminish the ability for Oct4 to maintain pluripotency and self-renewal, since *Lsd1*$^{\Delta 3/\Delta 3}$ ES cells do not spontaneously differentiate in culture (Figure 3.10A and B). This is comparable to reports that PRC2 activity is not necessary for the maintenance of the pluripotent state in ES cells, where even though developmental regulators are over-expressed in EED-null ES cells, the positive regulation of pluripotency factors is sufficient for functional pluripotency (Chamberlain *et al.* 2008). This all suggests that LSD1 could be repressing developmental genes, though it would be unsurprising if these LSD1 and PRC2-proteins were found to have different gene specificities.

6.2 LSD1 regulates the transcriptome during embryonic development

Comparative microarray analysis of *Lsd1*$^{Lox/\Delta 3}$ versus *Lsd1*$^{\Delta 3/\Delta 3}$ ES cells revealed that 60% more genes were up-regulated (362) than down-regulated (226), supporting the loss of a direct repressive factor (Figure 4.7). This is consistent with the global increase in H3K9 and H3K56 acetylation (Figure 4.5). However, the down-regulation of a considerable number of genes in the absence of LSD1 makes it is clear that either there are off-target effects or that Lsd1 also acts as an activator on 40% of the targets. These transcriptional changes occur independently of the reduced genomic methylation, since levels of DNA methylation was unchanged 10 days after induction of LSD1 deletion, when ES cells were analysed. Furthermore, recent genome-wide methylation analysis in human ES cells has shown that nearly one-quarter of all methylation identified is in a non-CpG context, suggesting there is lower correlation between CpG methylation and gene expression in ES cells (Lister *et al*. 2009). Results in this thesis therefore identify a correlation between LSD1-dependent gene regulation and histone modifications, rather than DNA methylation.

The figure of 588 transcripts is relatively small in comparison to the number of potential LSD1 gene targets identified in three global ChIP studies in MEL and MCF7 cells (5191 and 4212/1913, respectively; Garcia-Bassets *et al*. 2007, Saleque *et al*. 2007, Wang *et al*. 2009a). These global ChIP studies were performed in somatic cells, though the data infers that LSD1 activity may not be essential for the repression (or potentially activation) of all targets in ES cells. It is noteworthy that Gfi-1/1b and the oestrogen receptor, factors which determine LSD1 recruitment to target promoters in

these studies, are not expressed in ES cells. A very recent report that LSD1 binds 2144 genes in human ES cells also supports the idea that not all LSD1 targets are affected by LSD1 deletion (Adamo *et al.* 2011). A complete list of genomic binding sites of LSD1 in mouse ES cells has not yet been compiled and ultimately global ChIP analysis would reveal which of these 588 genes are direct targets as well as identify additional targets that are not de-regulated upon LSD1 deletion.

Altered transcripts encompassed a wide range of biological processes and molecular functions (Figure 4.9). This was expected due to the nature of LSD1 as a chromatin modifier in a repressor complex, as opposed to being a direct DNA binding protein downstream of a specific intracellular signalling pathway. Gene ontology analyses of de-regulated genes reveals enrichment for genes involved in various metabolic processes and developmental processes (Figure 4.9). Notably, notochord development and spinal cord patterning are developmental processes and include genes encoding the transcription factors Brachyury, Gli2 and Reelin (Figure 4.9 and Appendix Table A3). Considering the perturbation of ES cell differentiation and embryogenesis, the de-regulation of other transcription factors with roles in anterior/posterior patterning and tissue specific development (Hoxb7, Hoxd8, Barx2, RARγ) appears noteworthy. Interestingly, the recent findings in human ES cells demonstrated that LSD1 directly controls developmental regulators (including *Brachyury, FOXA2, EOMES* and *BMP2*) and knockdown of LSD1 causes up-regulation of these genes and spontaneous ES cells differentiation (Adamo *et al*. 2011). However, the up-regulation of many developmental factors and the significant enrichment for

genes with a muscle-specific function (Figure 4.9 and 4.10) does not cause loss of pluripotency in ES cells (Figure 3.10), indicating differing tolerance to aberrant expression of developmental genes in human and mouse ES cells. It is important to note that our identification of LSD1 as a direct regulator of *Brachyury* in ES cells pre-dates this publication.

LSD1 appears to function crucially by controlling the expression of lineage-specific genes, for example *Brachyury*. Altered expression of this key developmental regulator as well as *Hoxb7, Hoxd8, Barx2* and *RARγ* in undifferentiated *Lsd1*$^{\Delta 3/\Delta 3}$ ES cells supports the hypothesis that embryonic lethality is caused by multiple aberrant and conflicting developmental signals. *Brachyury* expression should be barely detectable in undifferentiated ES cells, with induction of this gene expected at day 3 of ES cell differentiation (Keller *et al*. 1993). In the embryo, *Brachyury* expression is equivalently up-regulated at the onset of gastrulation in the primitive streak and axial mesoderm (Kispert & Herrmann 1994). EB differentiation assays demonstrate that this dramatic over-expression of *Brachyury* at day 2 is followed by loss of expression at day 5 (Figure 3.13B); this precocious expression pattern correlates with a period of significant differentiation-associated cell death induced by RA and LIF withdrawal in serum-free media (Figure 3.12A and B). Subsequent experiments showed a striking over-expression of *Brachyury* in *Lsd1*$^{\beta\text{-}geo/\beta\text{-}geo}$ embryos at E6.5, just before embryonic death (Figure 4.18). This was an important *in vivo* corroboration of ES cell based results, which justified use of the ES cell system to interpret an early embryonic phenotype.

The loss of LSD1 causes a 3- to 5-fold increase in Brachyury mRNA, whereas induction of differentiation results in a 20-30 fold increase in transcript abundance (Figure 3.13B and 4.14A). The removal of repressive factors (LSD1 and HDAC1/2) causes a modest increase in gene expression (approximately 3-fold; Figure 3.13B, 4.8A, 4.14A), which is amplified upon differentiation (approximately 25-fold; Figure 3.13B, 4.14A). Even though *Brachyury* is up-regulated in undifferentiated ES cells, the onset of differentiation appears to cause cell death. This effect supports the recent report from the Ramanathan lab that only at 48 hours after removal of pluripotency-promoting conditions (LIF and serum) do ES cells become competent to respond to differentiation-inducing signals, such as over-expression of developmental genes (Thomson *et al*. 2011). The molecular basis of this ES cell differentiation-responsive state was found to be down-regulation of Nanog levels at 48 hours after LIF and serum removal. This was backed-up by the observation that addition of a Wnt agonist, to stimulate mesoendodermal differentiation, could only activate *Brachyury* expression, in pluripotent-promoting conditions, when Nanog was depleted by siRNA (Thomson *et al*. 2011). The observation of down-regulation of *Nanog* at 2 days of EB differentiation and correlation with an amplified increase in *Brachyury* expression are corroborated by these recent findings (Figure 3.13A and B). Data in Thomson *et al.* and in this thesis also verifies the prior indication that over-expression of *Brachyury* and other developmental regulators in undifferentiated LSD1 knockout cells does not override the ability for stem cell factors such as Nanog to maintain the pluripotent state (Chamberlain *et al.* 2008). It has also been shown that ES cells overespressing Nanog are resistant to differentiation induced by retinoic acid (Chambers *et al.* 2003, Loh *et al.* 2006). It is therefore presumable that repression of *Nanog* allows cells to respond

to developmental gene expression patterns, which is defective in LSD1 deleted cells, consequently resulting in cellular crisis and cell death. To test this hypothesis, an interesting further experiment would have been to attempt to maintain the expression of Nanog during the induction of differentiation, to see if this prevents the onset of a differentiation-responsive state and subsequent cell death in *Brachyury* over-expressing, *Lsd1*$^{\Delta 3/\Delta 3}$ cells.

As *Brachyury* should not be expressed in ES cells or cells of the embryonic epiblast, an RNAi-mediated knock-down of this gene in LSD1-depleted ES cells could have been implemented to assess the significance of the over-expression of this key developmental regulator at the onset of differentiation. If aberrant over-expression of *Brachyury* was the main contributer to differentiation-associated cell death, reduction of its expression might alleviate this phenotype. It was also assumed that over-expression of *Brachyury* at day 2 of EB differentiation and in embryos is restricted to appropriately fated cell-types (axial mesoderm and primitive streak). However analysis of day 15 EBs revealed that ectoderm cell-types die as well (Figure 3.14), suggesting that inappropriate ectopic expression of *Brachyury* might occur in regions fated to give rise to ectoderm. These events have been previously observed with *Brachyury* transcripts in the early embryo (Faust *et al*. 1995). *In situ* hybridisation of *Brachyury* mRNA in *Lsd1*$^{\beta\text{-}geo/\beta\text{-}geo}$ embryos at E6.5 would have been a key experiment to address this hypothesis. However, difficulties in harvesting knockout embryos at this stage made this assay unfeasible. Alternatively, defects in ectoderm development may arise through other mechanisms.

ES cell differentiation assays can illustrate which lineages have the potential to develop in the absence of certain factors. ES cell differentiation in EBs occurs in a disorganised fashion (Murry & Keller 2008), therefore to understand more precisely which lineages are development impeded in the absence of LSD1, refined EB formation techniques or more specific types of differentiation assay using defined growth factors could be implemented. *In vitro* differentiation assays that actively inhibit development of primitive ectoderm could be performed. The formation of the primitive ectoderm (*FGF5* up-regulation; *Rex1* repression) and differentiation into ectoderm, mesoderm and definitive endoderm requires the withdrawal of LIF (Shen & Leder 1992, Murray & Edgar 2001). Aggregation of EBs in the presence of LIF would only permit the formation of primitive endoderm (Hamazaki *et al.* 2004), a lineage that survives in *Lsd1*$^{\Delta 3/\Delta 3}$ EBs. Therefore, this technique could be implemented to prevent the onset of primitive ectoderm development; potentially rescuing the cell death phenotype of *Lsd1*$^{\Delta 3/\Delta 3}$ EBs. On the other hand, mesoderm-inducing conditions could be used to corroborate the link between cell death and mesoderm development. The induction of a primitive streak-like region and differentiation in mesendodermal progenitors can be achieved in EBs through activation of the Wnt pathway by exogenous Wnt3a (ten Berge *et al*. 2008). This assay in fact mediates the local execution of a gastrulation-like process, therefore would be an effective way to verify the requirement for LSD1 at the onset of gastrulation in the developing embryo. Alternatively, differentiation of ES cells into haemangioblasts would substantiate the correlation of precocious *Brachyury* activation and differentiation-associated cell death. This assay induces the formation of *Brachyury*- and *Flk1*-positive cell types, which act as haematogenic precursors (Fraser *et al*. 2003). The inability for *Tal1* and

CD34 expressing cells to develop in *Lsd1*$^{\Delta 3/\Delta 3}$ EBs suggests that these precursors cannot be generated in the absence of LSD1 (Figure 3.14C). The depletion of LSD1 and CoREST has also been shown to impair haematopoietic differentiation in studies performed in MEL, megakaryoblastic and myeloid cell lines, as well as primary haematopoietic cells (Saleque *et al*. 2007). This is due to up-regulation of Gfi-1/1b target gene expression upon LSD1 deletion. The Gfi-1/LSD1/CoREST/HDAC complex represses target genes in order to control differentiation of several haematopoietic lineages via regulation of the H3K4 methylation state. These reports are supporting of a situation whereby LSD1 and CoREST regulate mesoderm development in ES cells and the embryo.

6.3 LSD1 knockout ES cells have reduced CoREST levels and increased histone acetylation

Conditional deletion of LSD1 in ES cells results in a reduction of CoREST protein, consistent with previous demonstration that knockdown of CoREST reduces LSD1 levels (Shi *et al*. 2005). This suggests a co-dependence on protein stability. The levels of HDAC1 and HDAC2 were unaffected, most likely due to their occurrence in multiple complexes (Yang & Seto 2008). In the absence of LSD1, CoREST, although reduced, still has the ability to interact with HDAC1/2 via an N-terminal ELM2 domain in an LSD1-independent manner (Lee *et al*. 2005, Lee *et al*. 2006a).

Perturbation of the LSD1/CoREST/HDAC complex encouraged examination of the effects on global histone methylation and acetylation levels. Deletion of LSD1 causes a number of small, but reproducible changes in global histone methylation (Figure 4.5A). The levels of the LSD1 substrates, H3K4me1/me2, are increased only slightly, in accordance with the results of Wang and colleagues, who state that 4% of promoters gain H3K4me2 in LSD1-deleted cells (Wang *et al*. 2009, Baltus and Kadam unpublished). The androgen and estrogen receptors, factors reported to switch the LSD1 substrate specificity from H3K4me1/me2 to H3K9me1/me2 (Metzger *et al*. 2005, Garcia-Bassets *et al*. 2007, Wissmann *et al*. 2007), are absent in ES cells. Therefore, this modification was not scrutinised in detail, with the methylation status of H3K4 the focus. ChIP-on-chip data in MCF7 and MEL cells suggests that LSD1 is associated with a large number of gene promoters (Garcia-Bassets *et al*. 2007, Saleque *et al*. 2007, Wang *et al*. 2009a), and that many of these genes are active (74% expressed in MCF7)

and therefore positive for H3K4me3. It is therefore not surprising that H3K4me2 (and H3K4me3) are relatively unchanged upon loss of LSD1. Alternatively, this change represents a much smaller set of genes in ES cells which are directly regulated by LSD1 and show increase H3K4 methylation upon LSD1 removal.

In contrast, the LSD1 dependent reduction in CoREST protein and HDAC1/2 associated with the complex (Figure 4.3 and 4.4) results in a 1.3-fold increase in H3K9 acetylation and a 2-fold increase in H3K56 acetylation (Figure 4.5A and B). This supports the notion that a fully active protein complex no longer operates at gene promoters in the absence of LSD1. *In vitro* analysis of LSD1/COREST/HDAC complex activity towards nucleosomes has shown that CoREST and LSD1 are required for mediating nucleosomal deacetylation (Lee *et al*. 2006a). This indicates that, even though there is detectable deacetylase activity co-purified with CoREST in the absence of LSD1 (Figure 4.3B), this is not active towards histone substrates as part of this remaining complex. Thus, large increases in global histone acetylation are observed. A recent publication has corroborated this data by showing that knockdown of LSD1 with siRNA results in increased acetylation of H3K9 (Huang *et al*. 2011). H3K56ac is a modification associated with the DNA damage response, histone deposition and the activity of pluripotency factors in higher eukaryotes (Schneider *et al.* 2006, Driscoll *et al.* 2007, Han et al. 2007, Tjeertes *et al.* 2009, Xie et al. 2009). The observation that H3K56ac levels are affected more than other acetylated lysines within histone H3 is likely a reflection of relative abundances of acetyl-lysines in ES cells. The increase in H3K9/K14ac and H4ac levels in ES cells treated with TSA is relatively modest compared

to somatic cells (Dovey *et al.* 2010b), suggesting that histone tails are already in a hyperacetylated state. In contrast, only 1% of histone H3 is acetylated at H3K56 in ES cells, which would put an emphasis on any small changes in H3K56ac levels (Xie *et al*. 2009). Increased H3K56ac correlates with reduced CoREST levels and reduced deacetylase activity associated with CoREST (where cellular HDAC1 and 2 levels remain constant). Our lab has previously provided evidence that H3K56ac is a substrate of HDAC1 (Dovey *et al.* 2010b), with data presented in this thesis indicating that H3K56 acetylation is regulated by HDAC1 within the LSD1/CoREST/HDAC complex.

A wave of deacetylation occurs on histones associated with the *Oct4* promoters upon differentiation (Fuhrmann *et al*. 2001, Feldman *et al*. 2006). Successful repression of pluripotent genes in *Lsd1*$^{\Delta 3/\Delta 3}$ ES cell differentiation confirms LSD1/COREST/HDAC does not regulate their repression and that H3K9 is deacetylated at the *Oct4* promoter by a different HDAC-containing complex. However, developmental genes may rely on histone deacetylation in ES cells and the early embryo, with inability to selectively deacetylate lineage-specific genes, due to HDAC1/2 disruption, contributing to differentiation defects. Notably, deletion of HDAC1 in ES cells, which is results in reduced deacetylase activity associated with the Sin3A, NuRD and CoREST complexes, causes precocious differentiation into mesodermal and ectodermal lineages in EBs (Dovey *et al.* 2010b). This demonstrates that HDAC1 is required to restrict developmental gene expression. Moreover, given the degree of enzymatic redundancy towards H3K4me1/me2, the essential requirement for LSD1 may be attributed to the ability for LSD1 to interact with CoREST and HDAC1/2. Thus, it

appears that LSD1, a lysine demethylase, functions in part by regulating the lysine acetylation status of chromatin by enabling HDACs to function at genomic loci as part of a core complex. The ternary complex, which is enzymatically more active than individual components (Lee *et al*. 2005, Lee *et al*. 2006a) is then capable of function independently (You *et al*. 2001, Saleque *et al*. 2007) or as a module of broader super-complexes containing multiple chromatin-associated factors (Hakimi *et al*. 2002, Shi *et al*. 2003, , Lee *et al*. 2005, Shi *et al*. 2005).

6.4 Catalytic activity of LSD1 is dispensable for gene regulation

LSD1/CoREST/HDAC has so been shown here to directly repress a key developmental gene in pluripotent ES cells. It is possible that this may be through association with Oct4, based on the report that Oct4-LSD1 proteins interact and Oct4 binds the *Brachyury* promoter in ES cells (Loh *et al*. 2006, Kim *et al*. 2008, Pardo *et al*. 2010). The ablation of a Nanog- and Oct4-associated HDAC complex has previously been shown to cause the inappropriate activation of numerous developmental genes in ES cells (Liang *et al*. 2008). Here we show that a distinct HDAC complex, which may be directed to targets by Oct4, is involved in developmental gene repression, though its disruption does not cause loss of pluripotency of ES cells due to activation of developmental genes; rather differentiation-associated cell death.

Within the set of genes up-regulated by loss of LSD1 there is enrichment of bivalent genes, which possess the H3K4me2/me3 modification. This includes *Brachyury* (Bernstein *et al*. 2006a), confirmed as a direct LSD1/CoREST/HDAC target (Figure 4.16). As LSD1 is an H3K4me2 demethylase, this observation invites much discussion of possible molecular mechanisms of LSD1 function at bivalent target genes. Individual gene analysis prior to these reports, indicated that the *Brachyury* gene promoter possesses H3K4me2 modification in undifferentiated ES cells, with a specific increase in H3K4me3 at day 5 of EB differentiation, coinciding with the time of highest *Brachyury* induction (Lee *et al.* 2004a). Removal of LSD1 from this locus in undifferentiated ES cells causes the accumulation of the H3K4me3 state that is

proposed to coincide with *Brachyury* activation during differentiation (Figure 4.16). As results in this thesis have demonstrated that LSD1 catalytic activity is dispensable for gene repression (Figure 5.10), the LSD1/CoREST/HDAC complex is suggested to have a role in preventing the accumulation of H3K4me3 at H3K4me2-positive promoters, possibly through preventing the association TrxG complexes that contain H3K4me3-specific KMTs, such as MLL2. The fact that LSD1 is not serving as an active demethylase at bivalent genes that already possess H3K4me2 (the LSD1 substrate) is further evidence that LSD1-containing complexes play an obstructive role at bivalent genes. Interestingly, MLL2 knockout ES cells display a delay in the development of germ layers upon *in vitro* differentiation, including a slight delay in *Brachyury* expression (Lubitz *et al*. 2007). This suggests that LSD1- and MLL2-complexes act antagonistically at common genes. Data in this thesis shows analogy with the H3K4me2/me3 demethylase JARID1 (RBP2), which resides on a number of bivalent *Hox* genes (*Hoxa1*, *Hoxa5*, and *Hoxa7*) in undifferentiated ES cells to prevent the accumulation of H3K4me3 and hence their expression (Bernstein *et al.* 2006a, Christensen *et al.* 2007). RBP2 is displaced from *Hox* genes upon ES cell differentiation, correlating with their activation (Christensen *et al*. 2007).

A recent analysis of LSD1 in human ES cells, found that LSD1 regulates bivalent genes in human ES cells through direct association. However, the knockdown of LSD1 results in spontaneous differentiation of human ES cells, suggesting a different tolerance to developmental gene de-regulation in the absence of LSD1 between mouse and human ES cells (Adamo *et al.* 2011). Importantly, this study has shown that 17% of genes de-

regulated upon LSD1 deletion can be rescued by catalytically inactive LSD1 (K661A), corroborating data in this thesis (Figure 5.10).

As the CoREST complex contains two enzymatic activities, with synergistic effects, it may be expected that chromatin modification regulation beyond control of H3K4 and H3K27 methylation level is required for activation of genes bound by LSD1/CoREST/HDAC. A persuasive argument for this is that the deletion of the PRC2 components, EZH2, SUZ12 and EED, and a consequent decrease in H3K27me3 level, do not reveal up-regulation of *Brachyury* (Boyer *et al*. 2006, Lee *et al.* 2006, Chamberlain *et al.* 2008, Shen *et al.* 2008a). Data has revealed that reconstitution of the LSD1/CoREST association and re-association of deacetylase activity with LSD1 (Figure 5.5), is sufficient to rescue gene expression in LSD1 knockout ES cells (Figure 5.10). The identification of deacetylase activity co-purifying with recombinant LSD1 confirms that the substantial increase in global histone acetylation observed in LSD1-depleted cells is specific to disruption of the LSD1/CoREST/HDAC complex (Figure 4.3 and 4.4). Since biochemical experiments have shown that histone tail deacetylation by the CoREST complex occurs before H3K4 demethylation (Forneris *et al*. 2006, Lee *et al.* 2006a), it seems likely that deacetylation could prime gene repression and the localisation of the reformed CoREST complex can mediate gene expression regardless of demethylase activity. In addition, the reformed complex could displace H3K4me3-specific KMTs (such as MLL2), which maintain the H3K4me3 modification in activated genes; hence directly rescuing acetylation levels and indirectly rescuing H3K4 methylation state. Alternatively, the regulation of histone acetylation may simply be

more influential in the control of expression of genes bound by LSD1/CoREST/HDAC. This is supported by the ability to rescue the expression of genes initially unmodified at H3K4, which would presumably require active LSD1 demethylation to enforce this chromatin state (Figure 5.10; *DDR2, RASGRP3* and *Omt2a*). Failure for the TOWER mutant to function as intended prevented complete confirmation that deacetylase activity is solely sufficient. The identification of up-regulation of bivalent genes and rescue with catalytically inactive LSD1 gives significance to a previous report showing that the Rpd3 histone deacetylase interacts with the PRC2 complex and enhances PcG complex-mediated gene repression through histone deacetylation (van der Vlag & Otte 1999, Tie *et al.* 2003). Furthermore, in *Drosophila,* the mediation of transcriptional activation by TrxG complexes, which antagonise PcG complex function, is endowed by the ability to inhibit histone deacetylation (Lee *et al.* 2009). This supports a crucial accompanying role of HDACs with LSD1 in gene repression.

It has been suggested that around 4% of promoters gain H3K4me2 in LSD1 deleted cells, which was proposed to underpin the gene-specific regulation of H3K4me2 methylation (Wang *et al.* 2009). The figure of 4% figure might represent a small proportion of genes bound by LSD1/CoREST/HDAC that require the demethylase or it may be representative of H3K4me2 increase as a by-product of transcriptional activation, which is mainly instigated by an increase in local histone acetylation. However, further ChIP experiments are required to investigate the effect of re-expressing WT and catalytically inactive LSD1 on the levels of H3K4me2, H4K4me3 and H3K9ac at gene loci. ChIP followed by next generation sequencing (ChIP-seq)

experiments have recently been performed in collaboration with Ana Pombo, in order to compare locus-specific H3K4me2 levels in *Lsd1*$^{Lox/\Delta 3}$ and *Lsd1*$^{\Delta 3/\Delta 3}$ ES cells. This data is still being analysed and has not been presented in this thesis. In addition to these experiments, devising a new strategy to create an LSD1 mutant that cannot associate with CoREST should be pursued to examine the requirement for CoREST complex deacetylase activity at target genes. The expectation is that perturbation of this interaction will produce analogous results to the full LSD1 protein deletion, as the decrease in CoREST levels in the absence of LSD1 seems to be a poignant phenotype of the knockout. This is the most feasible way of assessing HDAC involvement, as the use of class I HDAC inhibitors will affect deacetylase activity in multiple repressor complexes. Finally, to further investigate the proposed obstructive mechanism of an LSD1-contained complex in controlling H3K4me3 levels, supported by the seemingly opposite effects of LSD1 and MLL2 deletion on differentiation events (Lubitz *et al*. 2007), a combined conditional deletion of LSD1 and MLL2, or a knockdown of MLL2 in LSD1 knockout ES cells should be pursued. The combinational ablation of the catalysis of H3K4me3 may reveal reversion of gene up-regulation that relies on an increase in this chromatin modification.

6.5 Concluding Remarks

Data in this thesis strongly argues for an essential role for LSD1 in development due to an ability to regulate embryonic gene expression through histone modification control. The ability for LSD1 to form a fully functional class I HDAC-containing CoREST complex is suggested to be important in LSD1-mediated gene regulation within the pre-gastrulation embryo. Perturbation of repressor complex function through removal of LSD1 directly results in de-repression of a key developmental regulator, *Brachyury.* Numerous other developmentally-linked genes are de-repressed in the absence of LSD1, though these genes are as yet not known to be under direct control. A direct role of LSD1 in gene activation has however not been ruled out, where ChIP-seq experiments must be performed in order to discover which genes that are de-regulated in the absence of LSD1 are direct targets. Most notably, disruption of the ES cell transcriptome and significant differentiation-associated cell death in LSD1-deleted cells correlates with gene de-regulation and a developmental block in LSD1 genetrap embryos.

The function of the CoREST complex appears to be independent of its demethylase activity, where catalytically inactive LSD1 can rescue the expression of de-regulated genes. It is proposed that reconstitution of the complex containing just deacetylase activity is sufficient to re-repress genes, where deacetylase activity can solely regulate gene expression and/or the CoREST complex potentially serves as an impediment to activator complexes that can catalyse tri-methylation of H3K4. These results reveal insights into mechanisms of multi-protein repressor complex function that contain

multiple enzymatic activities towards histone substrates. Data also raises questions about the relative importance of two synergistic enzymatic activities with a common complex. It elucidates how an acetylation state might be sufficient to establish transcriptional states, though the methylation state is secondary to this and fulfils a purpose in epigenetic memory of transcriptional states.

Appendices

Table A1 List of antibodies used in the study

Antibody	Clonality	Source	Dilution	Company	Catalogue #	Application
hdac1	polyclonal	rabbit	1:2000	Santa Cruz	sc-7872	WB
hdac1	monoclonal	mouse	1:2000	Abcam	ab46985	IP
hdac2	polyclonal	rabbit	1:2000	Santa Cruz	sc-7899	IP
hdac2	monoclonal	mouse	1:2000	Millipore	05-814	WB
CoREST	polyclonal	rabbit	1:500	Millipore	07-455	WB/IP
LSD1	polyclonal	rabbit	1:1000	Sigma	L4418	WB
LSD1	polyclonal	rabbit	1:2000	Abcam	ab37165	WB/IP/ChIP
mSin3a	polyclonal	rabbit	1:1000	Santa Cruz	sc-767	IP
mSin3a	monoclonal	mouse	1:2000	In house	-	WB
Brachyury	polyclonal	rabbit	1:500	Sigma	B8436	WB
Dnmt1	monoclonal	mouse	1:500	Abcam	ab92453	WB
Oct4	polyclonal	rabbit	1:1000	Sigma	P0056	WB
β-actin	monoclonal	mouse	1:5000	Sigma	ac-74	WB
β–tubulin	monoclonal	mouse	1:5000	Sigma	T6199	WB
H3	monoclonal	mouse	1:2000	Millipore	05-499	WB/ChIP
H3K4me1	polyclonal	rabbit	1:1000	Sigma	M4819	WB
H3K4me2	polyclonal	rabbit	1:1000	Sigma	D5692	WB/ChIP
H3K4me3	polyclonal	rabbit	1:1000	Millipore	07-473	WB/ChIP
H3K27me3	polyclonal	rabbit	1:1000	Millipore	07-499	WB/ChIP
H3K9/14ac	polyclonal	rabbit	1:1000	Millipore	06-599	WB
H3K9ac	polyclonal	Rabbit	1:1000	Millipore	06-942	WB/ChIP
H3K18ac	polyclonal	rabbit	1:1000	Millipore	07-354	WB
H3K27ac	polyclonal	rabbit	1:1000	Active Motif	39132	WB
H3K36ac	polyclonal	rabbit	1:1000	Millipore	07-540	WB
H3K56ac	polyclonal	rabbit	1:1000	Active Motif	39281	WB

Table A2 List of primers used quantitative RT-PCR

Gene	UPL Probe #	Primers	Amplicon (nt)
Pou5fl	82	cacgagtggaaagcaactca	125
		cttctgcagggctttcatgt	
Nanog	25	agcctccagcagatgcaa	76
		ggttttgaaaccaggtcttaacc	
Sox2	70	ggacttctttttgggggact	86
		cagatctatacatggtccgattcc	
Rex1	33	tcgctgtgggcattagaga	94
		gctgcactgcacactcactc	
FGF5	89	gagccctgaaggaaactcg	76
		gcgaaacaaaatgacctgact	
Wnt3	48	gccaagagtgtattcgcatcta	86
		gatccagccgcacaatctac	
Brachyury	88	cgagatgattgtgaccaagaac	65
		ggcctgacacatttaccttca	
Nkx2.5	53	gacgtagcctggtgtctcg	70
		gtgtggaatccgtcgaaagt	
MEF2c	77	tctgccctcagtcagttgg	63
		cgtggtgtgttgtgggtatc	
MyoD	52	ccaggacacgactgctttct	76
		cacaccggctgtcctctac	
Gata4	13	ggaagacaccccaatctcg	75
		catggccccacaattgac	
Gata6	40	ggtctctacagcaagatgaatgg	94
		tggcacaggacagtccaag	
Sox17	52	ggtctgaagtgcggttgg	109
		tgtcttccctgtcttggttga	
Foxa2	77	gagcagcaacatcaccacag	64
		cgtaggccttgaggtccat	
Flk1 (VEGFR2)	18	ccccaaattccattatgacaa	69
		cggctctttcgcttactgtt	
CD34	2	ttgggcaccactggttattt	96
		ttttcttcccaacagccatc	
Tal1	60	cgcctcactaggcagtgg	75
		ctcttcacccggttgttgtt	
Tie2	110	gaggacgcttccacattcc	75
		gacccaaggatggctatgag	
FABP-4	31	gaaaacgagatggtgacaagc	76
		gccctttcataaactcttgtgg	
Tubb3 (beta III Tubulin)	78	ggcaactatgtaggggactcag	87
		cctgggcacatacttgtgag	
Nestin	2	tgcaggccactgaaaagtt	89
		ttccaggatctgagcgatct	

Brn2 (Pou3f2)	1	gacacgccgacctcagac	60
		gatccgcctctgcttgaat	
HNF1b	109	atccccagcaatctcagaac	82
		gcttgggaggtgttgagg	
AFP	63	catgctgcaaagctgacaa	62
		ctttgcaatggatgctctctt	
TTR	76	catgaattcgcggatgtg	60
		gatggtgtagtggcgatgg	
LSD1	67	atccagctgacgtttgaagc	74
		cggtggacaagcacagtatc	
CoREST	69	aagtccccagaaagctccat	75
		tgcgtatcttacgtcgagga	
Hdac1	89	gagtacctggagaagatcaagca	121
		cttcatccccactctcttcg	
Hdac2	45	ctccacgggtggttcagt	71
		cccaattgacagccatatca	
DDR2	63	cgaaagcttccagagtttgc	61
		gcttcacaacaccactgcac	
HoxB7	1	ctggatgcgaagctcagg	109
		ccgagtcaggtagcgattgta	
OMT2a	106	cttgcaatctccggacca	87
		tgaagtacctccggttccac	
RARG	17	ggcttactacgcagagccact	104
		ctggtgctctgtgtctccac	
RASGRP3	91	cacatcagcctcatggacata	92
		gcctttccccttttggatac	
Cdkn1a	21	tccacagcgatatccagaca	90
		ggcacactttgctcctgtg	
TRIM46	33	aagagaccatcaggcacactg	89
		ttccagcacagcccctagt	
BARX2	17	aagatgaacagccaggctca	70
		ggggttcagaggaagcttgt	
BRDT	68	ggatgaacgagtgcagcat	69
		acttgcagctgctgatgaac	
CDA	17	ctgccgacaagtcatgagag	122
		ggtcttcaggtccaaacgag	
FOXN4	103	agcatcatggacttcgctct	64
		ggctgaagctgtcctcctt	
NOS3	5	gaccctcaccgctacaacat	62
		gtcctggtgtccagatccat	
SIX5	69	aacttccctcgtccactgc	71
		agtgacaatggggctaccag	
RELN	100	gcatggcaatgctgtcac	72
		gttgtgttcaggcatgtggt	
Dusp26	45	ggagggaaaggatgggtct	60
		ctccgtcaccaggtaggtgt	

SNCA	102	ggaaggagtggttcatggag tgctcctccaacatttgtca	73
Spink2	4	tgttcgctgcacaggaga tgagaatcggaagagtcgaga	130
Thy1	63	gaaaactgcgggcttcag ccaagagttccgacttggat	102
Tspan8	40	gctgtggagctgtgaaagaaa ggtttgaaagcggctccta	112
Krt23	25	tcatgaagaaacgccatgag ccttgaagtcactcggcaag	60
Them5	95	accgtctatgccaagtcctc gtggccactgagtcatcaag	96

Table A3 List of genes that are de-regulated >1.4-fold in LSD1 knockout ES cells

Up-regulated Genes	Fold Change	Down-regulated Genes	Fold Change
Echdc2	1.4003	Aof2	0.3241
Tmem62	1.4007	Atp2a3	0.384
1700003M02Rik	1.4009	C330036H15Rik	0.4425
Slc16a9	1.4012	Atp2a3	0.465
9130230L23Rik	1.4023	Gli2	0.4686
Myom3	1.4024	Naprt1	0.4717
Tnfrsf17	1.4034	Metrn	0.4899
A330049M08Rik	1.4036	Tgm2	0.4947
Sftpd	1.404	Tgm1	0.5004
Hoxb7	1.4042	Wdr90	0.5029
Zc4h2	1.4057	Adap1	0.5044
Impdh1	1.4063	Lrfn3	0.5057
Taf1d	1.4104	Bdh2	0.5084
Gm766	1.4124	Cplx1	0.5138
Dync1i1	1.4125	Naprt1	0.5162
2410078J06Rik	1.4128	Cotl1	0.5198
Cyp2j9	1.4132	Ccdc28b	0.5213
Zfp521	1.4135	Arg2	0.5246
Map1lc3a	1.4137	Gm129	0.5351
Oc90	1.4138	Cox6a2	0.5448
Klk10	1.4152	1700029P11Rik	0.5449
Cpne2	1.416	Gng13	0.5453
Atg10	1.4161	Ift172	0.554
Nrg4	1.4168	Itgb4	0.5568
Gpha2	1.4179	3230401M21Rik	0.5599
AU022751	1.4204	2310022B05Rik	0.5642
2810025M15Rik	1.421	Akap9	0.5688
Mogat2	1.421	Dis3l	0.569
Rnf182	1.4241	Btbd1	0.5701
2810439F02Rik	1.425	Rarg	0.5706
Hsh2d	1.4254	Itgb4	0.574
AI317395	1.4263	Cotl1	0.5766
Fhl1	1.4272	Akap9	0.5777
Rnf170	1.4274	Eno3	0.5799
Mtap2	1.43	Gfpt2	0.5812
Crabp1	1.4301	BC003993	0.5828
Gstm6	1.4307	Nos3	0.5829
Ppp2r2c	1.4318	Plcd1	0.5836
LOC634731	1.432	Ddit3	0.5876
Elovl4	1.4335	Gna11	0.5886
Plxdc1	1.4358	Ddx25	0.5891

Prx	1.4366	Arpp19	0.5892
Fmr1nb	1.4369	Gm129	0.5898
LOC382001	1.4375	Cul7	0.5903
B230358A15Rik	1.4377	Bcam	0.5954
Ank2	1.4386	Nme3	0.5983
Trpv2	1.4455	Ndst2	0.6008
Mdfic	1.4479	Aplp1	0.6041
Ccl25	1.4482	Nisch	0.6081
Mup2	1.4483	Pgls	0.6083
Klf17	1.4508	LOC626152	0.6094
Cda	1.4512	Celsr3	0.6104
Tph2	1.4521	Tia1	0.6116
Tmem159	1.4531	Jmjd2b	0.6134
Ccbl1	1.4534	Snai3	0.6145
LOC100045780	1.4544	C030046I01Rik	0.6154
Klk13	1.4546	B3gnt1	0.6162
BC018465	1.4558	Grasp	0.6162
Bahd1	1.4573	LOC673578	0.6167
Ly6e	1.4613	LOC100044468	0.6187
Actn2	1.4627	Grasp	0.6197
Bbs7	1.4641	Cxxc6	0.6215
H6pd	1.4642	Otub2	0.6218
Clic6	1.4658	Tk1	0.6228
Gpr143	1.468	Cpe	0.6267
Gca	1.4704	Pex11a	0.6287
T	1.4713	Tbc1d2	0.629
Abcc5	1.4714	Bcam	0.6291
Gstm5	1.4748	Naprt1	0.6301
Cdkn1a	1.475	Sec14l1	0.6301
Tm7sf4	1.4752	Foxn4	0.6309
Edg2	1.4768	Gna11	0.6313
Lmo7	1.4768	5133400G04Rik	0.6342
Nlrp4c	1.4771	5133400G04Rik	0.6351
Epb4.1l4b	1.4776	Rarres2	0.636
LOC382264	1.4782	Ldoc1l	0.6363
Gmpr	1.4797	D430042O09Rik	0.6365
LOC381471	1.48	Mslnl	0.6366
ORF9	1.4822	Zfp579	0.6384
EG368203	1.4823	Sec14l1	0.6392
Defcr3	1.4848	Npepl1	0.6393
Gjb4	1.4854	E030007N04Rik	0.6394
Cdc42ep5	1.4872	2310045N01Rik	0.6404
Lgals3bp	1.4876	Fkbp6	0.6416
Padi6	1.4876	1190005N23Rik	0.6423
Ebi3	1.4892	Evc	0.6425
Cyp2c44	1.49	Lrrc40	0.6427

Nin	1.5004	Krt7	0.6429
Tekt1	1.5019	Diras1	0.6441
Best1	1.5026	Wipi2	0.6446
LOC245892	1.5031	2410018G20Rik	0.646
Gtsf1l	1.5032	Elac1	0.6467
Itgae	1.5035	Myd88	0.6472
Selplg	1.5052	Adap1	0.6492
Cxcl14	1.5053	F2r	0.6493
Abca14	1.511	Vrk1	0.65
Alg14	1.5145	Zfp810	0.6502
4933412E12Rik	1.5148	Dnajc7	0.6505
AW551984	1.516	Suclg2	0.6525
Taf9b	1.518	1190003J15Rik	0.6535
Col2a1	1.5192	Mrpl10	0.656
App	1.521	1810014F10Rik	0.6579
5930412G12Rik	1.5223	Ltbp3	0.6606
Mt1	1.5234	Dhodh	0.6612
Clcnkb	1.5248	Bckdha	0.6621
Aox3	1.527	Sox15	0.6637
Prickle1	1.5291	Irf2bp1	0.6647
EG638695	1.53	Rassf1	0.6649
Slc26a4	1.5319	Ykt6	0.6666
Smtnl1	1.5319	Dgkq	0.6669
Fgl1	1.532	Il11ra1	0.6672
LOC100046049	1.5342	Coro1a	0.6682
Pdlim4	1.5363	Riok3	0.6684
Xk	1.5364	Slc25a44	0.67
D12Ertd647e	1.5386	Ciz1	0.6701
Agrp	1.5403	BC003993	0.6714
Cyp2c55	1.5423	Haghl	0.6714
BC026585	1.5431	Pias3	0.672
Lyzl4	1.544	Zcwpw1	0.6721
LOC224532	1.5488	Rbks	0.6722
Mx2	1.5525	Drg2	0.6725
Sh3rf2	1.5543	Fam110a	0.6733
Pof1b	1.5562	Tia1	0.6743
Aim2	1.5564	Mthfd2	0.6756
Ptpn22	1.5567	Itga3	0.6763
Clca3	1.5569	Rac3	0.6763
Npw	1.5587	Slc6a9	0.6771
Pla1a	1.559	Ube2e1	0.6772
Tuba3a	1.5594	Ap1b1	0.6775
Acot1	1.5632	Dnd1	0.6781
Gpr137b	1.5684	9930033H14Rik	0.6785
LOC100039227	1.5704	Tmem141	0.6785
Cox7a1	1.574	Mrpl35	0.6786

Fam154a	1.5761	Ankra2	0.6788
Magea4	1.5765	4833442J19Rik	0.6791
Rbm47	1.5767	Pard6a	0.6794
L3mbtl3	1.577	Echs1	0.6806
Reln	1.5792	Ap2b1	0.6808
C430014G13Rik	1.5833	Gm129	0.6808
Defcr6	1.5836	C330024D21Rik	0.6809
4921531P07Rik	1.5879	Ppp1r14d	0.6814
Mansc1	1.5885	Ankrd13a	0.6828
Mycl1	1.5918	Lrch4	0.6834
2410164B09Rik	1.5922	Ubr7	0.6838
Htatip2	1.5933	Rccd1	0.6844
4932431H17Rik	1.5935	Nt5c3l	0.6845
Ctsa	1.594	scl0001379.1_70	0.6847
620807	1.5957	6330569M22Rik	0.6859
Gpr113	1.5965	5133400G04Rik	0.6861
Slc6a13	1.5991	Agxt2l2	0.6863
Popdc3	1.601	1190005F20Rik	0.6866
Hoxd8	1.6022	Pola2	0.6867
1520401A03Rik	1.6034	Cdc20	0.687
Cdh3	1.6038	Rars2	0.6872
Idh1	1.6044	Coro1a	0.6873
2310039L15Rik	1.6059	2310022K01Rik	0.6876
3110049J23Rik	1.6081	Idh3a	0.6877
Srd5a2	1.6087	Cpsf3l	0.6881
Myom2	1.6088	Snx17	0.6883
Snca	1.6091	Chkb	0.6884
Mllt3	1.6094	Lztr1	0.6887
LOC385274	1.6104	H3f3a	0.6889
OTTMUSG00000019001	1.6109	Tmem131	0.6893
4930550L24Rik	1.6115	Ankmy2	0.6899
Bfsp2	1.6131	Wipi2	0.6899
Chi3l1	1.6138	Rps6ka4	0.6901
Hspb8	1.6153	Dusp11	0.6904
Pld1	1.6169	Otub2	0.6905
LOC385368	1.6201	9830002L24Rik	0.6908
EG546250	1.6217	Bub1b	0.6908
Ela1	1.6229	LOC100040799	0.6913
Lama3	1.6246	Tubgcp2	0.6919
Hebp2	1.6316	Eif3s8	0.692
1600013E24Rik	1.6325	Pou2f1	0.6924
Pnlip	1.6378	Suclg2	0.6924
Timm8a2	1.6395	Nat6	0.6925
Omt2b	1.6419	Ctbp2	0.6926
Uroc1	1.6451	Npepl1	0.6928
Kiss1	1.6499	Pik3r2	0.6929

Fxyd5	1.651	Gprk6	0.6942
C8b	1.6512	Blcap	0.6945
Ube2l6	1.6519	Ift172	0.6946
Nat2	1.6544	Crip2	0.6957
Sult2b1	1.6545	0610010E21Rik	0.6963
LOC272693	1.6551	Triobp	0.6964
Stk32a	1.6578	LOC100045019	0.6966
Gm44	1.6579	Nos3	0.6971
LOC382163	1.659	Slc28a1	0.6971
Usp29	1.6633	Tcea3	0.6988
Copz2	1.664	Rdm1	0.6992
Magea10	1.6672	Shc1	0.6993
H2-Ab1	1.6675	Ddx27	0.6997
Oas1g	1.6699	Dcxr	0.7003
BC049762	1.6709	scl0002368.1_75	0.7004
Syt5	1.6726	Spryd4	0.7004
Sytl3	1.6743	Wars	0.7006
Si	1.6811	Cml1	0.7009
1700020N15Rik	1.682	Ankzf1	0.7015
Kcnu1	1.6858	LOC675567	0.7017
Bcas1	1.6862	Acot8	0.7019
OTTMUSG00000010552	1.6875	Sap30	0.7022
Pga5	1.6921	1110014J17Rik	0.7032
Aass	1.6987	EG434402	0.7037
C130073F10Rik	1.6992	6530415H11Rik	0.7038
Diras2	1.6998	Gtpbp2	0.7038
Lst1	1.7061	Vps45	0.7041
4930583H14Rik	1.7065	Ppp2r4	0.7054
LOC100046087	1.7087	3830406C13Rik	0.7055
Pde6a	1.7112	Scly	0.7064
LOC674912	1.7195	2810432D09Rik	0.7068
Tnnt1	1.7227	Trabd	0.707
Sepp1	1.7229	Atp11b	0.7078
Xpnpep2	1.7235	Tmem186	0.708
Gm1679	1.7239	2310014L17Rik	0.7089
Dpysl3	1.7254	Gcat	0.709
Ddr2	1.7266	Cc2d2a	0.7098
Mboat1	1.7273	Mthfd2	0.7102
Gsta3	1.728	Rapgef3	0.7103
Spnb3	1.7313	Tfdp1	0.7105
Defb30	1.7326	Ube2d3	0.7106
Mlana	1.7402	LOC435145	0.711
Adh4	1.7405	Rnmt	0.712
Igh-VJ558	1.7411	Taf5	0.7126
Barx2	1.7447	Tk1	0.7126
Ntrk2	1.7448	Echs1	0.7127

1700022P22Rik	1.7452	Plod1	0.7129
4930486L24Rik	1.751	A930009M04Rik	0.713
C330016K18Rik	1.7553	E130014J05Rik	0.7132
Slc5a4a	1.7568	A230070D14Rik	0.7138
OTTMUSG00000010438	1.7614		
Slc36a3	1.7617		
Cpn1	1.7801		
LOC385256	1.7811		
LOC380655	1.785		
Rbms2	1.7862		
Gm566	1.7883		
Mmp2	1.7982		
Fetub	1.8034		
Mgst2	1.8087		
Aqp9	1.8122		
Akr1c18	1.8178		
Pcolce2	1.8231		
Rasgrp3	1.8246		
Crygs	1.8317		
Zfp393	1.8369		
Brdt	1.8381		
Tspan2	1.8421		
Cd74	1.8434		
Hecw2	1.8454		
Igl-5	1.8465		
Tst	1.8475		
Lpl	1.8508		
Ott	1.855		
Clps	1.8694		
Dusp26	1.8715		
C030033M19Rik	1.8728		
Krt23	1.8734		
Mbl2	1.8795		
4930502E18Rik	1.8874		
Omt2a	1.8899		
1700011F14Rik	1.8903		
Gm773	1.891		
Stx11	1.8916		
Tulp4	1.8956		
Xlr5a	1.8983		
Xlr4a	1.8998		
4930591A17Rik	1.9034		
Slc15a2	1.9064		
LOC630179	1.9079		
Scml2	1.9082		
4931407G18Rik	1.9085		

Dmrtc1c	1.9089		
Myl4	1.9128		
Tpbg	1.9131		
Tnni2	1.9176		
Myl2	1.9194		
LOC383642	1.9204		
Agmat	1.9286		
LOC383368	1.9305		
Spic	1.9309		
Tex19.2	1.9316		
Rragd	1.9326		
Igbp1b	1.9329		
Dnajc5g	1.9387		
A730037C10Rik	1.9393		
2010204K13Rik	1.9405		
Rhox4d	1.9496		
Crxos1	1.9543		
Tex13	1.9551		
Tsx	1.9574		
Ela2a	1.9684		
Liph	1.969		
Magea8	1.9713		
LOC270344	1.9837		
Gm41	1.9844		
2200001I15Rik	1.9908		
Ifitm1	1.9948		
9530077C05Rik	2.0012		
Cd3d	2.0129		
Klk1b4	2.0283		
1700011M02Rik	2.0308		
Slc5a4b	2.0309		
Acss1	2.0317		
4930524B15Rik	2.0337		
Aim1	2.0353		
Cpne9	2.0581		
Ndp52	2.0597		
Cntnap2	2.066		
Klk1b27	2.0724		
Plac8	2.0847		
Them5	2.0921		
Alox5ap	2.0929		
OTTMUSG00000017677	2.1193		
Qpct	2.1195		
Tspan8	2.1341		
Acpp	2.1354		
Boll	2.1474		

Slamf9	2.1506		
Klk1b5	2.1585		
Ly6g6e	2.1603		
1700006H03Rik	2.1607		
Ng23	2.1837		
Itsn1	2.19		
Nckap1l	2.1917		
2410088K16Rik	2.2373		
Klk1b26	2.2414		
C230070D10Rik	2.2499		
LOC100045342	2.2517		
Cd200	2.254		
Tmem40	2.2835		
Ly6a	2.2977		
4933408N05Rik	2.2996		
LOC641366	2.319		
Otog	2.3531		
Cct6b	2.3756		
Klk1	2.3871		
LOC385308	2.3976		
Crygd	2.4702		
Slc30a3	2.4942		
Ovol2	2.5243		
Magea2	2.5497		
LOC100040016	2.591		
Defb42	2.6075		
Thy1	2.6288		
LOC98434	2.6335		
Magea5	2.6651		
LOC100040479	2.6676		
Pramel7	2.6879		
Obox6	2.6962		
Rcsd1	2.701		
A730017C20Rik	2.7211		
Zscan5b	2.7235		
Mt3	2.7717		
1700080O16Rik	2.9609		
4921521F21Rik	3.0268		
H2-Eb1	3.1767		
Spink2	3.193		
Reg1	3.2291		
Ybx3	3.3365		
Pkd2l1	3.3582	3.3582	

Bibliography

Aasland, R., Stewart, A.F. & Gibson, T. 1996, "The SANT domain: A putative DNA-binding domain in the SWI-SNF and ADA complexes, the transcriptional corepressor N-CoR and TFIIIB", *Trends in biochemical sciences,* vol. 21, no. 3, pp. 87-88.

Adamo, A., Sesé, B., Boue, S., Castaño, J., Paramonov, I., Barrero, M.J. & Izpisua Belmonte, J.C. 2011, "LSD1 regulates the balance between self-renewal and differentiation in human embryonic stem cells.", *Nature Cell Biology,* vol. 13, no. 6, pp. 652-660.

Agalioti, T., Chen, G.Y. & Thanos, D. 2002, "Deciphering the transcriptional histone acetylation code for a human gene", *Cell,* vol. 111, no. 3, pp. 381-392.

Agger, K., Cloos, P.A.C., Christensen, J., Pasini, D., Rose, S., Rappsilber, J., Issaeva, I., Canaani, E., Salcini, A.E. & Helin, K. 2007, "UTX and JMJD3 are histone H3K27 demethylases involved in HOX gene regulation and development", *Nature,* vol. 449, no. 7163, pp. 731-U10.

Alland, L., David, G., Hong, S.L., Potes, J., Muhle, R., Lee, H.C., Hou, H., Chen, K. & DePinho, R.A. 2002, "Identification of mammalian Sds3 as an integral component of the Sin3/histone deacetylase corepressor complex", *Molecular and cellular biology,* vol. 22, no. 8, pp. 2743-2750.

Allfrey, V.G., Faulkner, R. & Mirsky, A.E. 1964, "Acetylation and Methylation of Histones and their Possible Role in the Regulation of Rna Synthesis.", *Proc Natl Acad Sci U S A,* vol. 51, pp. 786-794.

Ambrosetti, D.C., Basilico, C. & Dailey, L. 1997, "Synergistic activation of the fibroblast growth factor 4 enhancer by Sox2 and Oct-3 depends on protein-protein interactions facilitated by a specific spatial arrangement of factor binding sites", *Molecular and cellular biology,* vol. 17, no. 11, pp. 6321-6329.

Andres, M.E., Burger, C., Peral-Rubio, M.J., Battaglioli, E., Anderson, M.E., Grimes, J., Dallman, J., Ballas, N. & Mandel, G. 1999, "
CoREST: a functional corepressor required for regulation of neural-specific gene expression", *Proceedings of the National Academy of Sciences USA,* vol. 96, no. 17, pp. 9873-9678.

Anton, R., Kestler, H.A. & Kuehl, M. 2007, "beta-Catenin signaling contributes to stemness and regulates early differentiation in murine embryonic stem cells", *FEBS letters,* vol. 581, no. 27, pp. 5247-5254.

Avilion, A.A., Nicolis, S.K., Pevny, L.H., Perez, L., Vivian, N. & Lovell-Badge, R. 2003, "Multipotent cell lineages in early mouse development depend on SOX2 function", *Genes & development,* vol. 17, no. 1, pp. 126-140.

Azuara, V., Perry, P., Sauer, S., Spivakov, M., Jorgensen, H.F., John, R.M., Gouti, M., Casanova, M., Warnes, G., Merkenschlager, M. & Fisher, A.G. 2006, "Chromatin signatures of pluripotent cell lines", *Nature cell biology,* vol. 8, no. 5, pp. 532-U189.

Bain, G., Kitchens, D., Yao, M., Huettner, J.E. & Gottlieb, D.I. 1995, "Embryonic Stem-Cells Express Neuronal Properties In-Vitro", *Developmental biology,* vol. 168, no. 2, pp. 342-357.

Ballas, N., Battaglioli, E., Atouf, F., Andres, M.E., Chenoweth, J., Anderson, M.E., Burger, C., Moniwa, M., Davie, J.R., Bowers, W.J., Federoff, H.J., Rose, D.W., Rosenfeld, M.G., Brehm, P. & Mandel, G. 2001, "Regulation of neuronal traits by a novel transcriptional complex", *Neuron,* vol. 31, no. 3, pp. 353-365.

Baltus, G.A., Kowalski, M.P., Tutter, A.V. & Kadam, S. 2009, "A positive regulatory role for the mSin3A-HDAC complex in pluripotency through Nanog and Sox2", *Journal of Biological Chemistry,* vol. 284, no. 11, pp. 6998-7006.

Bannister, A.J., Schneider, R. & Kouzarides, T. 2002, "Histone modification: dynamic or static?", *Cell,* vol. 109, pp. 801-806.

Bannister, A.J., Schneider, R., Myers, F.A., Thorne, A.W., Crane-Robinson, C. & Kouzarides, T. 2005, "Spatial distribution of di- and tri-methyl lysine 36 of histone H3 at active genes", *Journal of Biological Chemistry,* vol. 280, no. 18, pp. 17732-17736.

Bannister, A.J., Zegerman, P., Partridge, J.F., Miska, E.A., Thomas, J.O., Allshire, R.C. & Kouzarides, T. 2001, "Selective recognition of methylated lysine 9 on histone H3 by the HP1 chromo domain", *Nature,* vol. 410, no. 6824, pp. 120-124.

Barrow, K.M., Perez-Campo, F.M. & Ward, C.M. 2006, "Use of the cytomegalovirus promoter for transient and stable transgene expression in mouse embryonic stem cells.", *Methods in Molecular Biology,* vol. 329, pp. 283-294.

Barski, A., Cuddapah, S., Cui, K., Roh, T., Schones, D.E., Wang, Z., Wei, G., Chepelev, I. & Zhao, K. 2007, "High-resolution profiling of histone methylations in the human genome", *Cell,* vol. 129, no. 4, pp. 823-837.

Beddington, R.S.P. 1983, "Histogenetic and Neoplastic Potential of Different Regions of the Mouse Embryonic Egg Cylinder", *Journal of embryology and experimental morphology,* vol. 75, no. JUN, pp. 189-204.

Bernstein, B.E., Mikkelsen, T.S., Xie, X.H., Kamal, M., Huebert, D.J., Cuff, J., Fry, B., Meissner, A., Wernig, M., Plath, K., Jaenisch, R., Wagschal, A., Feil, R., Schreiber, S.L. & Lander, E.S. 2006a, "A bivalent chromatin structure marks key developmental genes in embryonic stem cells", *Cell,* vol. 125, no. 2, pp. 315-326.

Bernstein, E., Duncan, E.M., Masui, O., Gil, J., Heard, E. & Allis, C.D. 2006b, "Mouse polycomb proteins bind differentially to methylated histone H3 and RNA and are enriched in facultative heterochromatin", *Molecular and cellular biology,* vol. 26, no. 7, pp. 2560-2569.

Bhaumik, S.R., Smith, E. & Shilatifard, A. 2007, "Covalent modifications of histones during development and disease pathogenesis", *Nature Structural & Molecular Biology,* vol. 14, no. 11, pp. 1008-1016.

Binda, C., Coda, A., Angelini, R., Federico, R., Ascenzi, P. & Mattevi, A. 1999, "A 30 angstrom long U-shaped catalytic tunnel in the crystal structure of polyamine oxidase", *Structure with Folding & design,* vol. 7, no. 3, pp. 265-276.

Binda, C., Li, M., Hubalek, F., Restelli, N., Edmondson, D.E. & Mattevi, A. 2003, "Insights into the mode of inhibition of human mitochondrial monoamine oxidase B from high-resolution crystal structures", *Proceedings of the National Academy of Sciences of the United States of America,* vol. 100, no. 17, pp. 9750-9755.

Bird, A. 2002, "DNA methylation patterns and epigentic memory", *Genes and Development,* vol 16, pp. 6-21.

Birnboim, H. & Doly, J. 1979, "Rapid Alkaline Extraction Procedure for Screening Recombinant Plasmid DNA", *Nucleic acids research,* vol. 7, no. 6, pp. 1513-1523.

Borde, V., Robine, N., Lin, W., Bonfils, S., Geli, V. & Nicolas, A. 2009, "Histone H3 lysine 4 trimethylation marks meiotic recombination initiation sites", *Embo Journal,* vol. 28, no. 2, pp. 99-111.

Borun, T.W., Pearson, D., & Paik, W.K. 1972, "Studies of histone methylation during the HeLa S-3 cell cycle. *J. Biol. Chem.* vol. 247, pp. 4288-4298.

Boyd, J.M., Subramanian, T., Schaeper, U., Laregina, M., Bayley, S. & Chinnadurai, G. 1993, "A Region in the C-Terminus of Adenovirus-2/5 E1a Protein is Required for Association with a Cellular Phosphoprotein and Important for the Negative Modulation of T24-Ras Mediated Transformation, Tumorigenesis and Metastasis", *Embo Journal,* vol. 12, no. 2, pp. 469-478.

Boyer, L.A., Lee, T.I., Cole, M.F., Johnstone, S.E., Levine, S.S., Zucker, J.R., Guenther, M.G., Kumar, R.M., Murray, H.L., Jenner, R.G., Gifford, D.K., Melton, D.A., Jaenisch, R. & Young, R.A. 2005a, "Core transcriptional regulatory circuitry in human embryonic stem cells", *Cell,* vol. 122, no. 6, pp. 947-956.

Boyer, L.A., Plath, K., Zeitlinger, J., Brambrink, T., Medeiros, L.A., Lee, T.I., Levine, S.S., Wernig, M., Tajonar, A., Ray, M.K., Bell, G.W., Otte, A.P., Vidal, M., Gifford, D.K., Young, R.A. & Jaenisch, R. 2006, "Polycomb complexes repress developmental regulators in murine embryonic stem cells", *Nature,* vol. 441, no. 7091, pp. 349-353.

Boyer, L.A., Mathur, D. & Jaenisch, R. 2006, "Molecular control of pluripotency", *Current opinion in genetics & development,* vol. 16, no. 5, pp. 455-462.

Bracken, A.P., Dietrich, N., Pasini, D., Hansen, K.H. & Helin, K. 2006, "Genome-wide mapping of Polycomb target genes unravels their roles in cell fate transitions", *Genes & development,* vol. 20, no. 9, pp. 1123-1136.

Bradley, A., Evans, M., Kaufman, M.H. & Robertson, E. 1984, "Formation of Germ-Line Chimeras from Embryo-Derived Teratocarcinoma Cell-Lines", *Nature,* vol. 309, no. 5965, pp. 255-256.

Brehm, A., Miska, E.A., McCance, D.J., Reid, J.L., Bannister, A.J. & Kouzarides, T. 1998, "Retinoblastoma protein recruits histone deacetylase to repress transcription", *Nature,* vol. 391, no. 6667, pp. 597-601.

Brook, F.A. & Gardner, R.L. 1997, "The origin and efficient derivation of embryonic stem cells in the mouse.", *Proceedings of the National Academy of Sciences of the United States of America,* vol. 94, no. 11, pp. 5709-5712.

Brown, M.A., Sims,Robert J.,,III, Gottlieb, P.D. & Tucker, P.W. 2006, "Identification and characterization of Smyd2: a split SET/MYND domain-containing histone H3 lysine 36-specific methyltransferase that interacts with the Sin3 histone deacetylase complex", *Molecular Cancer,* vol. 5, pp. 26.

Brownell, J.E. & Allis, C.D. 1996, "Special HATs for special occasions: Linking histone acetylation to chromatin assembly and gene activation", *Current opinion in genetics & development,* vol. 6, no. 2, pp. 176-184.

Buard, J., Barthes, P., Grey, C. & de Massy, B. 2009, "Distinct histone modifications define initiation and repair of meiotic recombination in the mouse", *Embo Journal,* vol. 28, no. 17, pp. 2616-2624.

Buchholz, F., Angrand, P.O. & Stewart, A.F. 1998, "Improved properties of FLP recombinase evolved by cycling mutagenesis", *Nature biotechnology,* vol. 16, no. 7, pp. 657-662.

Byvoet, P., Shepherd, G.R., Hardin, J.M. & Noland, B.J. 1972, " The distribution and turnover of labelled methyl groups in histone fractions of cultured mammalian cells", *Arch. Biochem. Biophys.* vol. 148, pp. 558-567.

Cao, R. & Zhang, Y. 2004, "SUZ12 is required for both the histone methyltransferase activity and the silencing function of the EED-EZH2 complex", *Molecular cell,* vol. 15, no. 1, pp. 57-67.

Capo-chichi, C.D., Rula, M.E., Smedberg, J.L., Vanderveer, L., Parmacek, M.S., Morrisey, E.E., Godwin, A.K. & Xu, X.X. 2005, "Perception of differentiation cues by GATA factors in primitive endoderm lineage determination of mouse embryonic stem cells", *Developmental biology,* vol. 286, no. 2, pp. 574-586.

Carmen, A.A., Milne, L. & Grunstein, M. 2002, "Acetylation of the yeast histone H4N terminus regulates its binding to heterochromatin protein SIR3", *Journal of Biological Chemistry,* vol. 277, no. 7, pp. 4778-4781.

Carrozza, M.J., Li, B., Florens, L., Suganuma, T., Swanson, S.K., Lee, K.K., Shia, W.J., Anderson, S., Yates, J., Washburn, M.P. & Workman, J.L. 2005, "Histone H3 methylation by Set2 directs deacetylation of coding regions by Rpd3S to suppress spurious intragenic transcription", *Cell,* vol. 123, no. 4, pp. 581-592.

Chalfie, M., Tu, Y., Euskirchen, G., Ward, W.W. & Prasher, D.C. 1994, "Green Fluorescent Protein as a Marker for Gene-Expression", *Science,* vol. 263, no. 5148, pp. 802-805.

Chamberlain, S.J., Yee, D. & Magnuson, T. 2008, "Polycomb repressive complex 2 is dispensable for maintenance of embryonic stem cell pluripotency", *Stem cells,* vol. 26, no. 6, pp. 1496-1505.

Chambers, I., Colby, D., Robertson, M., Nichols, J., Lee, S., Tweedie, S. & Smith, A. 2003, "Functional expression cloning of Nanog, a pluripotency sustaining factor in embryonic stem cells", *Cell,* vol. 113, no. 5, pp. 643-655.

Chambers, I. & Smith, A. 2004, "Self-renewal of teratocarcinoma and embryonic stem cells", *Oncogene,* vol. 23, no. 43, pp. 7150-7160.

Chambeyron, S., Da Silva, N.R., Lawson, K.A. & Bickmore, W.A. 2005, "Nuclear re-organisation of the Hoxb complex during mouse embryonic development", *Development,* vol. 132, no. 9, pp. 2215-2223.

Chen, Y., Yang, Y., Wang, F., Wan, K., Yarnane, K., Zhang, Y. & Lei, M. 2006, "Crystal structure of human histone lysine-specific demethylase 1 (LSD1)", *Proceedings of the National Academy of Sciences of the United States of America,* vol. 103, no. 38, pp. 13956-13961.

Cheung, P., Allis, C.D. & Sassone-Corsi, P. 2000, "Signaling to chromatin through histone modifications", *Cell,* vol. 103, no. 2, pp. 263-271.

Chew, J.L., Loh, Y.H., Zhang, W.S., Chen, X., Tam, W.L., Yeap, L.S., Li, P., Ang, Y.S., Lim, B., Robson, P. & Ng, H.H. 2005, "Reciprocal transcriptional regulation of Pou5f1 and Sox2 via the Oct4/Sox2 complex in embryonic stem cells", *Molecular and cellular biology,* vol. 25, no. 14, pp. 6031-6046.

Chinnadurai, G. 2002, "CtBP, an unconventional transcriptional corepressor in development and oncogenesis", *Molecular cell,* vol. 9, no. 2, pp. 213-224.

Choi, J., Jang, H., Kim, H., Kim, S., Cho, E. & Youn, H. 2010, "Histone demethylase LSD1 is required to induce skeletal muscle differentiation by regulating myogenic factors", *Biochemical and biophysical research communications,* vol. 401, no. 3, pp. 327-332.

Chong, J.A., Tapia-Ramírez, J., Kim, S., Toledo-Aral, J.J., Zheng, Y., Boutros, M.C., Altshuller, Y.M., Frohman, M.A., Kraner, S.D. & Mandel, G. 1995, "REST: a mammalian silencer protein that restricts sodium channel gene expression to neurons.", *Cell,* vol. 80, no. 6, pp. 949-957.

Christensen, J., Agger, K., Cloos, P.A.C., Pasini, D., Rose, S., Sennels, L., Rappsilber, J., Hansen, K.H., Salcini, A.E. & Helin, K. 2007, "RBP2 belongs to a family of demethylases, specific for tri- and dimethylated lysine 4 on histone 3", *Cell,* vol. 128, no. 6, pp. 1063-1076.

Chuikov, S., Kurash, J.K., Wilson, J.R., Xiao, B., Justin, N., Ivanov, G.S., McKinney, K., Tempst, P., Prives, C., Gamblin, S.J., Barlev, N.A. & Reinberg, D. 2004, "Regulation of p53 activity through lysine methylation", *Nature,* vol. 432, no. 7015, pp. 353-360.

Chung, S., Andersson, T., Sonntag, K.C., Björklund, L., Isacson, O. & Kim, K.S. 2002, "Analysis of Different Promoter Systems for Efficient Transgene Expression in Mouse Embryonic Stem Cell Lines", *Stem Cells,* vol. 20, no. 2, pp. 139-145.

Ciccone, D.N., Su, H., Hevi, S., Gay, F., Lei, H., Bajko, J., Xu, G., Li, E. & Chen, T. 2009, "KDM1B is a histone H3K4 demethylase required to establish maternal genomic imprints", *Nature,* vol. 461, no. 7262, pp. 415-U115.

Clark, D.J. & Kimura, T. 1990, "Electrostatic Mechanism of Chromatin Folding", *Journal of Molecular Biology,* vol. 211, no. 4, pp. 883-896.

Cloos, P.A.C., Christensen, J., Agger, K. & Helin, K. 2008, "Erasing the methyl mark: histone demethylases at the center of cellular differentiation and disease", *Genes & development,* vol. 22, no. 9, pp. 1115-1140.

Cloos, P.A.C., Christensen, J., Agger, K., Maiolica, A., Rappsilber, J., Antal, T., Hansen, K.H. & Helin, K. 2006, "The putative oncogene GASC1 demethylates tri- and dimethylated lysine 9 on histone H3", *Nature,* vol. 442, no. 7100, pp. 307-311.

Cormack, B.P., Valdivia, R.H. & Falkow, S. 1996, "FACS-optimized mutants of the green fluorescent protein (GFP)", *Gene,* vol. 173, no. 1, pp. 33-38.

Coucouvanis, E. & Martin, G.R. 1995, "Signals for Death and Survival - a 2-Step Mechanism for Cavitation in the Vertebrate Embryo", *Cell,* vol. 83, no. 2, pp. 279-287.

Couture, J., Collazo, E., Ortiz-Tello, P.A., Brunzelle, J.S. & Trievel, R.C. 2007, "Specificity and mechanism of JMJD2A, a trimethyllysine-specific histone demethylase", *Nature Structural & Molecular Biology,* vol. 14, no. 8, pp. 689-695.

Cowley, S.M., Iritani, B.M., Mendrysa, S.M., Xu, T., Cheng, P.F., Yada, J., Liggitt, H.D. & Eisenman, R.N. 2005, "The mSin3A chromatin-modifying complex is essential for embryogenesis and T-cell development", *Molecular and cellular biology,* vol. 25, no. 16, pp. 6990-7004.

Da, G.P., Lenkart, J., Zhao, K.H., Shiekhattar, R., Cairns, B.R. & Marmorstein, R. 2006, "Structure and function of the SWIRM domain, a conserved protein module found in chromatin regulatory complexes", *Proceedings of the National Academy of Sciences of the United States of America,* vol. 103, no. 7, pp. 2057-2062.

Dannenberg, J.H., David, G., Zhong, S., van der Torre, J., Wong, W.H. & DePinho, R.A. 2005, "mSin3A corepressor regulates diverse transcriptional networks governing normal and neoplastic growth and survival", *Genes & development,* vol. 19, no. 13, pp. 1581-1595.

Das, C., Lucia, M.S., Hansen, K.C. & Tyler, J.K. 2009, "CBP/p300-mediated acetylation of histone H3 on lysine 56", *Nature,* vol. 459, no. 7243, pp. 113-U123.

David, G., Grandinetti, K.B., Finnerty, P.M., Simpson, N., Chu, G.C. & DePinho, R.A. 2008, "Specific requirement of the chromatin modifier mSin3B in cell cycle exit and cellular differentiation", *Proceedings of the National Academy of Sciences of the United States of America,* vol. 105, no. 11, pp. 4168-4172.

De Ruijter, A.J.M., Van Gennip, A.H., Caron, H.N., Kemp, S. & Van Kuilenburg, A.B.P. 2003, "Histone deacetylases (HDACs): characterization of the classical HDAC family", *Biochemical Journal,* vol. 370, pp. 737-749.

De Santa, F., Totaro, M.G., Prosperini, E., Notarbartolo, S., Testa, G. & Natoli, G. 2007, "The histone H3 lysine-27 demethylase Jmjd3 links inflammation to inhibition of polycomb-mediated gene silencing", *Cell,* vol. 130, no. 6, pp. 1083-1094.

Denslow, S.S. & Wade, P.A. 2007, "
"The human Mi-2/NuRD complex and gene regulation.", *Oncogene,* vol. 26, no. 37, pp. 5433-5438.

Dhalluin, C., Carlson, J.E., Zeng, L., He, C., Aggarwal, A.K. & Zhou, M.M. 1999, "Structure and ligand of a histone acetyltransferase bromodomain", *Nature,* vol. 399, no. 6735, pp. 491-496.

Ding, Z., Gillespie, L. & Paterno, G. 2003, "Human MI-ER1 alpha and beta function as transcriptional repressors by recruitment of histone deacetylase 1 to their conserved ELM2 domain", *Molecular and cellular biology,* vol. 23, no. 1, pp. 250-258.

Dodge, J.E., Kang, Y.K., Beppu, H., Lei, H. & Li, E. 2004, "Histone H3-K9 methyltransferase ESET is essential for early development", *Molecular and cellular biology,* vol. 24, no. 6, pp. 2478-2486.

Doetschman, T.C., Eistetter, H., Katz, M., Schmidt, W. & Kemler, R. 1985, "The Invitro Development of Blastocyst-Derived Embryonic Stem-Cell Lines - Formation of Visceral Yolk-Sac, Blood Islands and Myocardium", *Journal of embryology and experimental morphology,* vol. 87, no. JUN, pp. 27-&.

Dong, K.B., Maksakova, I.A., Mohn, F., Leung, D., Appanah, R., Lee, S., Yang, H.W., Lam, L.L., Mager, D.L., Schuebeler, D., Tachibana, M., Shinkai, Y. & Lorincz, M.C. 2008, "DNA methylation in ES cells requires the lysine methyltransferase G9a but not its catalytic activity", *Embo Journal,* vol. 27, no. 20, pp. 2691-2701.

Dovey, O.M., Foster, C.T. & Cowley, S.M. 2010a, "Emphasizing the positive: A role for histone deacetylases in transcriptional activation", *Cell Cycle,* vol. 9, no. 14, pp. 2700-2701.

Dovey, O.M., Foster, C.T. & Cowley, S.M. 2010b, "Histone deacetylase 1 (HDAC1), but not HDAC2, controls embryonic stem cell differentiation", *Proceedings of the National Academy of Sciences of the United States of America,* vol. 107, no. 18, pp. 8242-8247.

Driscoll, R., Hudson, A. & Jackson, S.P. 2007, "Yeast Rtt109 promotes genome stability by acetylating histone H3 on lysine 56", *Science,* vol. 315, no. 5812, pp. 649-652.

Duerre, J.A. & Lee, C.T. 1974, "In vivo methylation and turnover of rat brain histones", *Journal of* Neurochemistry, vol. 23, pp. 541–547

Duvic, M., Talpur, R., Ni, X., Zhang, C., Hazarika, P., Kelly, C., Chiao, J.H., Reilly, J.F., Ricker, J.L., Richon, V.M. & Frankel, S.R. 2007, "Phase 2 trial of oral vorinostat (suberoylanilide hydroxamic acid, SAHA) for refractory cutaneous T-cell lymphoma, (CTCL)", *Blood,* vol. 109, no. 1, pp. 31-39.

Epsztejn-Litman, S., Feldman, N., Abu-Remaileh, M., Shufaro, Y., Gerson, A., Ueda, J., Deplus, R., Fuks, F., Shinkai, Y., Cedar, H. & Bergman, Y. 2008, "De novo DNA methylation promoted by G9a prevents reprogramming of embryonically silenced genes", *Nature Structural & Molecular Biology,* vol. 15, no. 11, pp. 1176-1183.

Ernst, M., Oates, A. & Dunn, A.R. 1996, "gp130-mediated signal transduction in embryonic stem cells involves activation of Jak and Ras/mitogen-activated protein kinase pathways", *Journal of Biological Chemistry,* vol. 271, no. 47, pp. 30136-30143.

Evans, M.J. & Kaufman, M.H. 1981, "Establishment in Culture of Pluripotential Cells from Mouse Embryos", *Nature,* vol. 292, no. 5819, pp. 154-156.

Faust, C., Schmacher, A., Holdener, B. & Magnuson, T. 1995, "The Eed Mutation Disrupts Anterior Mesoderm Production in Mice", *Development,* vol. 121, no. 2, pp. 273-285.

Fehling, H.J., Lacaud, G., Kubo, A., Kennedy, M., Robertson, S., Keller, G. & Kouskoff, V. 2003, "Tracking mesoderm induction and its specification to the hemangioblast during embryonic stem cell differentiation", *Development,* vol. 130, no. 17, pp. 4217-4227.

Feil, R., Brocard, J., Mascrez, B., LeMeur, M., Metzger, D. & Chambon, P. 1996, "Ligand-activated site-specific recombination in mice", *Proceedings of the National Academy of Sciences of the United States of America,* vol. 93, no. 20, pp. 10887-10890.

Feldman, N., Gerson, A., Fang, J., Li, E., Zhang, Y., Shinkai, Y., Cedar, H. & Bergman, Y. 2006, "G9a-mediated irreversible epigenetic inactivation of Oct-3/4 during early embryogenesis.", *Nature cell biology,* vol. 8, no. 2, pp. 188-194.

Finch, J.T., Noll, M. & Kornberg, R.D. 1975, "Electron microscopy of defined lengths of chromatin.", *Proceedings of the National Academy of Sciences of the United States of America,* vol. 72, no. 9, pp. 3320-3322.

Fischle, W., Wang, Y., Jacobs, S., Kim, Y., Allis, C. & Khorasanizadeh, S. 2003, "Molecular basis for the discrimination of repressive methyl-lysine marks in histone H3 bv Polvcomb and HP1 chromodomains", *Genes & development,* vol. 17, no. 15, pp. 1870-1881.

Folger, K.R., Wong, E.A., Wahl, G. & Capecchi, M.R. 1982, "Patterns of Integration of Dna Micro-Injected into Cultured Mammalian-Cells - Evidence for Homologous Recombination between Injected Plasmid Dna-Molecules", *Molecular and cellular biology,* vol. 2, no. 11, pp. 1372-1387.

Forneris, F., Binda, C., Vanoni, M.A., Battaglioli, E. & Mattevi, A. 2005a, "Human histone demethylase LSD1 reads the histone code", *Journal of Biological Chemistry,* vol. 280, no. 50, pp. 41360-41365.

Forneris, F., Binda, C., Vanoni, M.A., Mattevi, A. & Battaglioli, E. 2005b, "Histone demethylation catalysed by LSD1 is a flavin-dependent oxidative process", *FEBS letters,* vol. 579, no. 10, pp. 2203-2207.

Forneris, F., Binda, C., Adamo, A., Battaglioli, E. & Mattevi, A. 2007, "Structural basis of LSD1-CoREST selectivity in histone H3 recognition", *Journal of Biological Chemistry,* vol. 282, no. 28, pp. 20070-20074.

Forneris, F., Binda, C., Battaglioli, E. & Mattevi, A. 2008, "LSD1: oxidative chemistry for multifaceted functions in chromatin regulation", *Trends in biochemical sciences,* vol. 33, no. 4, pp. 181-189.

Forneris, F., Binda, C., Dall'Aglio, A., Fraaije, M.W., Battaglioli, E. & Mattevi, A. 2006, "A highly specific mechanism of histone H3-K4 recognition by histone demethylase LSD1", *Journal of Biological Chemistry,* vol. 281, no. 46, pp. 35289-35295.

Foster, C.T., Dovey, O.M., Lezina, L., Luo, J.L., Gant, T.W., Barlev, N., Bradley, A. & Cowley, S.M. 2010, "Lysine-Specific Demethylase 1 Regulates the Embryonic Transcriptome and CoREST Stability", *Molecular and cellular biology,* vol. 30, no. 20, pp. 4851-4863.

Fouse, S.D., Shen, Y., Pellegrini, M., Cole, S., Meissner, A., Van Neste, L., Jaenisch, R. & Fan, G. 2008, "Promoter CpG methylation contributes to ES cell gene regulation in parallel with

Oct4/Nanog, PcG complex, and histone H3K4/K27 trimethylation", *Cell Stem Cell,* vol. 2, no. 2, pp. 160-169.

Fraga, M.F., Ballestar, E., Villar-Garea, A., Boix-Chornet, M., Espada, J., Schotta, G., Bonaldi, T., Haydon, C., Ropero, S., Petrie, K., Iyer, N.G., Perez-Rosado, A., Calvo, E., Lopez, J.A., Cano, A., Calasanz, M.J., Colomer, D., Piris, M.A., Ahn, N., Imhof, A., Caldas, C., Jenuwein, T. & Esteller, M. 2005, "Loss of acetylation at Lys16 and trimethylation at Lys20 of histone H4 is a common hallmark of human cancer", *Nature genetics,* vol. 37, no. 4, pp. 391-400.

Fraser, S.T., Yamashita, J., Jakt, L.M., Okada, M., Ogawa, M., Nishikawa, S. & Nishikawa, S.I. 2003, "In vitro differentiation of mouse embryonic stem cells: Hematopoietic and vascular cell types", *Differentiation of Embryonic Stem Cells,* vol. 365, pp. 59-72.

Fuhrmann, G., Chung, A.C., Jackson, K.J., Hummelke, G., Baniahmad, A., Sutter, J., Sylvester, I., Scholer, H.R. & Cooney, A.J. 2001, "Mouse germline restriction of Oct4 expression by germ cell nuclear factor.", *Developmental Cell,* vol. 1, no. 3, pp. 377-387.

Fujikura, J., Yamato, E., Yonemura, S., Hosoda, K., Masui, S., Nakao, K., Miyazaki, J. & Niwa, H. 2002, "Differentiation of embryonic stem cells is induced by GATA factors", *Genes & development,* vol. 16, no. 7, pp. 784-789.

Garcia-Bassets, I., Kwon, Y., Telese, F., Prefontaine, G.G., Hutt, K.R., Cheng, C.S., Ju, B., Ohgi, K.A., Wang, J., Escoubet-Lozach, L., Rose, D.W., Glass, C.K., Fu, X. & Rosenfeld, M.G. 2007, "Histone methylation-dependent mechanisms impose ligand dependency for gene activation by nuclear receptors", *Cell,* vol. 128, no. 3, pp. 505-518.

Gardner, R.L. & Rossant, J. 1979, "Investigation of the Fate of 4.5 Day Post-Coitum Mouse Inner Cell Mass Cells by Blastocyst Injection", *Journal of embryology and experimental morphology,* vol. 52, no. AUG, pp. 141-152.

Giambra, V., Volpi, S., Emelyanov, A.V., Pflugh, D., Bothwell, A.L.M., Norio, P., Fan, Y., Ju, Z., Skoultchi, A.I., Hardy, R.R., Frezza, D. & Birshtein, B.K. 2008, "Pax5 and linker histone H1 coordinate DNA methylation and histone modifications in the 3 ' regulatory region of the immunoglobulin heavy chain locus", *Molecular and cellular biology,* vol. 28, no. 19, pp. 6123-6133.

Ginsburg, M., Snow, M.H.L. & Mclaren, A. 1990, "Primordial Germ-Cells in the Mouse Embryo during Gastrulation", *Development,* vol. 110, no. 2, pp. 521-&.

Goll, M.G. % Bestor, T.H. 2005, "Eukaryotic Cytosine Methyltransferases". *Annual Review in Biochemistry*, vol. 74, pp. 481-514.

Goren, A., Tabib, A., Hecht, M. & Cedar, H. 2008, "DNA replication timing of the human beta-globin domain is controlled by histone modification at the origin", *Genes & development,* vol. 22, no. 10, pp. 1319-1324.

Grunstein, M. 1997, "Histone acetylation in chromatin structure and transcription", *Nature,* vol. 389, no. 6649, pp. 349-352.

Gu, P., LeMenuet, D., Chung, A.C., Mancini, M., Wheeler, D.A. & Cooney, A.J. 2005, "Orphan nuclear receptor GCNF is required for the repression of pluripotency genes during retinoic

acid-induced embryonic stem cell differentiation.", *Molecular & Cellular Biology,* vol. 25, no. 19, pp. 8507-8519.

Haberland, M., Montgomery, R.L. & Olson, E.N. 2009, " The many roles of histone deacetylases in development and physiology: implications for disease and therapy.", *Nature Reviews Genetics,* vol. 10, no.1, pp.32-42.

Hakimi, M.A., Bochar, D.A., Chenoweth, J., Lane, W.S., Mandel, G. & Shiekhattar, R. 2002, "A core-BRAF35 complex containing histone deacetylase mediates repression of neuronal-specific genes", *Proceedings of the National Academy of Sciences of the United States of America,* vol. 99, no. 11, pp. 7420-7425.

Hamazaki, T., Oka, M., Yamanaka, S. & Terada, N. 2004, "Aggregation of embryonic stem cells induces Nanog repression and primitive endoderm differentiation", *Journal of cell science,* vol. 117, no. 23, pp. 5681-5686.

Han, J., Zhou, H., Horazdovsky, B., Zhang, K., Xu, R. & Zhang, Z. 2007, "Rtt109 acetylates histone H3 lysine 56 and functions in DNA replication", *Science,* vol. 315, no. 5812, pp. 653-655.

Hassig, C.A., Tong, J.K., Fleischer, T.C., Owa, T., Grable, P.G., Ayer, D.E., & Schreiber, S.L. 1998, "A role for histone deacetylase activity in HDAC1-mediated transcriptional repression", *Proc. Natl. Acad. Sci.* vol. 95, pp. 3519–3524.

Hattori, N., Nishino, K., Ko, Y.G., Hattori, N., Ohgane, J., Tanaka, S. & Shiota, K. 2004, "Epigenetic control of mouse Oct-4 gene expression in embryonic stem cells and trophoblast stem cells", *Journal of Biological Chemistry,* vol. 279, no. 17, pp. 17063-17069.

Haub, O. & Goldfarb, M. 1991, "Expression of the Fibroblast Growth Factor-5 Gene in the Mouse Embryo", *Development,* vol. 112, no. 2, pp. 397.

Hayes, J.J. & Hansen, J.C. 2001. "Nucleosomes and the chromatin fibre" *Curr. Opin. Genet. Dev.* vol. 11, pp. 124–129

Hebbes, T.R., Thorne, A.W. & Crane-Robinson. C. 1988, "A Direct Link between Core Histone Acetylation and Transcriptionally Active Chromatin", *EMBO Journal,* vol 7, no. 5, pp. 1395-1402

Hebert, J.M., Boyle, M. & Martin, G.R. 1991, "Messenger-RNA Localization Studies Suggest that Murine Fgf-5 Plays a Role in Gastrulation", *Development,* vol. 112, no. 2, pp. 407-415.

Heintzman, N.D., Hon, G.C., Hawkins, R.D., Kheradpour, P., Stark, A., Harp, L.F., Ye, Z., Lee, L.K., Stuart, R.K., Ching, C.W., Ching, K.A., Antosiewicz-Bourget, J.E., Liu, H., Zhang, X., Green, R.D., Lobanenkov, V.V., Stewart, R., Thomson, J.A., Crawford, G.E., Kellis, M. & Ren, B. 2009, "Histone modifications at human enhancers reflect global cell-type-specific gene expression", *Nature,* vol. 459, no. 7243, pp. 108-112.

Heintzman, N.D., Stuart, R.K., Hon, G., Fu, Y., Ching, C.W., Hawkins, R.D., Barrera, L.O., Van Calcar, S., Qu, C., Ching, K.A., Wang, W., Weng, Z., Green, R.D., Crawford, G.E. & Ren, B. 2007, "Distinct and predictive chromatin signatures of transcriptional promoters and enhancers in the human genome", *Nature genetics,* vol. 39, no. 3, pp. 311-318.

Hendrich, B. & Bird, A. 1998, "Identification and characterization of a family of mammalian methyl-CpG binding proteins", *Molecular and cellular biology,* vol. 18, no. 11, pp. 6538-6547.

Hendrich, B., Guy, J., Ramsahoye, B., Wilson, V.A. & Bird, A. 2001, "Closely related proteins MBD2 and MBD3 play distinctive but interacting roles in mouse development", *Genes & development,* vol. 15, no. 6, pp. 710-723.

Hernandez-Munoz, I., Taghavi, P., Kuijl, C., Neefjes, J. & van Lohuizen, M. 2005, "Association of BMI1 with polycomb bodies is dynamic and requires PRC2/EZH2 and the maintenance DNA methyltransferase DNMT1", *Molecular and cellular biology,* vol. 25, no. 24, pp. 11047-11058.

Herrmann, B.G., Labeit, S., Poustka, A., King, T.R. & Lehrach, H. 1990, "Cloning of the T-Gene Required in Mesoderm Formation in the Mouse", *Nature,* vol. 343, no. 6259, pp. 617-622.

Hewish, D.R. & Burgoyne, L.A. 1973, "Chromatin sub-structure. The digestion of chromatin DNA at regularly spaced sites by a nuclear deoxyribonuclease.", *Biochemical & Biophysical Research Communications,* vol. 52, no. 2, pp. 504-510.

Holland, P.W.H. & Hogan, B.L.M. 1988, "Expression of Homeo Box Genes during Mouse Development - a Review", *Genes & development,* vol. 2, no. 7, pp. 773-782.

Hu, X., Li, X., Valverde, K., Fu, X., Noguchi, C., Qiu, Y. & Huang, S. 2009, "LSD1-mediated epigenetic modification is required for TAL1 function and hematopoiesis", *Proceedings of the National Academy of Sciences of the United States of America,* vol. 106, no. 25, pp. 10141-10146.

Huang, Y., Vasilatos, S.N., Boric, L., Shaw, P.G. & Davidson, N.E. 2011, "Inhibitors of histone demethylation and histone deacetylation cooperate in regulating gene expression and inhibiting growth in human breast cancer cells.", *Breast Cancer Research and Treatment,* .

Huang, D.W., Sherman, B.T. & Lempicki, R.A. 2009, "Systematic and integrative analysis of large gene lists using DAVID bioinformatics resources", *Nature Protocols,* vol. 4, no. 1, pp. 44-57.

Huang, J., Sengupta, R., Espejo, A.B., Lee, M.G., Dorsey, J.A., Richter, M., Opravil, S., Shiekhattar, R., Bedford, M.T., Jenuwein, T. & Berger, S.L. 2007, "p53 is regulated by the lysine demethylase LSD1", *Nature,* vol. 449, no. 7158, pp. 105-U80.

Huang, Y., Fang, J., Bedford, M.T., Zhang, Y. & Xu, R.M. 2006, "Recognition of histone H3 lysine-4 methylation by the double tudor domain of JMJD2A", *Science,* vol. 312, no. 5774, pp. 748-751.

Hughes, C.M., Rozenblatt-Rosen, O., Milne, T.A., Copeland, T.D., Levine, S.S., Lee, J.C., Hayes, D.N., Shanmugam, K.S., Bhattacharjee, A., Biondi, C.A., Kay, G.F., Hayward, N.K., Hess, J.L. & Meyerson, M. 2004, "Menin associates with a trithorax family histone methyltransferase complex and with the Hoxc8 locus", *Molecular cell,* vol. 13, no. 4, pp. 587-597.

Humphrey, G.W., Wang, Y.H., Russanova, V.R., Hirai, T., Qin, J., Nakatani, Y. & Howard, B.H. 2001, "Stable histone deacetylase complexes distinguished by the presence of SANT

domain proteins CoREST/kiaa0071 and Mta-L1", *Journal of Biological Chemistry,* vol. 276, no. 9, pp. 6817-6824.

Hwang, S., Schmitt, A.A., Luteran, A.E., Toone, E.J. & McCafferty, D.G. 2011, "Thermodynamic Characterization of the Binding Interaction between the Histone Demethylase LSD1/KDM1 and CoREST", *Biochemistry,* vol. 50, no. 4, pp. 546-557.

Ikura, T., Ogryzko, V.V., Grigoriev, M., Groisman, R., Wang, J., Horikoshi, M., Scully, R., Qin, J. & Nakatani, Y. 2000, "Involvement of the TIP60 histone acetylase complex in DNA repair and apoptosis", *Cell,* vol. 102, no. 4, pp. 463-473.

Inouye, S. & Tsuji, F.I. 1994, "Aequorea Green Fluorescent Protein - Expression of the Gene and Fluorescence Characteristics of the Recombinant Protein", *FEBS letters,* vol. 341, no. 2-3, pp. 277-280.

Issaeva, I., Zonis, Y., Rozovskaia, T., Orlovsky, K., Croce, C.M., Nakamura, T., Mazo, A., Eisenbach, L. & Canaani, E. 2007, "Knockdown of ALR (MLL2) reveals ALR target genes and leads to alterations in cell adhesion and growth", *Molecular and cellular biology,* vol. 27, no. 5, pp. 1889-1903.

Iwase, S., Lan, F., Bayliss, P., de la Torre-Ubieta, L., Huarte, M., Qi, H.H., Whetstine, J.R., Bonni, A., Roberts, T.M. & Shi, Y. 2007, "The X-linked mental retardation gene SMCX/JARID1C defines a family of histone H3 lysine 4 demethylases", *Cell,* vol. 128, no. 6, pp. 1077-1088.

Jenuwein, T. & Allis, C.D. 2001, "Translating the histone code", *Science,* vol. 293, no. 5532, pp. 1074-1080.

Joshi, A.A. & Struhl, K. 2005, "Eaf3 chromodomain interaction with methylated H3-K36 links histone deacetylation to Pol II elongation", *Molecular cell,* vol. 20, no. 6, pp. 971-978.

Kadosh, D. & Struhl, K. 1997, "Repression by Ume6 involves recruitment of a complex containing Sin3 corepressor and Rpd3 histone deacetylase to target promoters", *Cell,* vol. 89, no. 3, pp. 365-371.

Kaji, K., Caballero, I.M., MacLeod, R., Nichols, J., Wilson, V.A. & Hendrich, B. 2006, "The NuRD component Mbd3 is required for pluripotency of embryonic stem cells", *Nature cell biology,* vol. 8, no. 3, pp. 285-292.

Karytinos, A., Forneris, F., Profumo, A., Ciossani, G., Battaglioli, E., Binda, C. & Mattevi, A. 2009, "A Novel Mammalian Flavin-dependent Histone Demethylase", *Journal of Biological Chemistry,* vol. 284, no. 26, pp. 17775-17782.

Kasten, M.M., Dorland, S. & Stillman, D.J. 1997, "Large protein complex containing the yeast Sin3p and Rpd3p transcriptional regulators", *Molecular and cellular biology,* vol. 17, no. 8, pp. 4852-4858.

Keller, G. 2005, "Embryonic stem cell differentiation: emergence of a new era in biology and medicine", *Genes & development,* vol. 19, no. 10, pp. 1129-1155.

Keller, G., Kennedy, M., Papayannopoulou, T. & Wiles, M.V. 1993, "Hematopoietic Commitment during Embryonic Stem-Cell Differentiation in Culture", *Molecular and cellular biology,* vol. 13, no. 1, pp. 473-486.

Keller, G.M. 1995, "In-Vitro Differentiation of Embryonic Stem-Cells", *Current opinion in cell biology,* vol. 7, no. 6, pp. 862-869.

Keogh, M.C., Kurdistani, S.K., Morris, S.A., Ahn, S.H., Podolny, V., Collins, S.R., Schuldiner, M., Chin, K.Y., Punna, T., Thompson, N.J., Boone, C., Emili, A., Weissman, J.S., Hughes, T.R., Strahl, B.D., Grunstein, M., Greenblatt, J.F., Buratowski, S. & Krogan, N.J. 2005, "Cotranscriptional Set2 methylation of histone H3 lysine 36 recruits a repressive Rpd3 complex", *Cell,* vol. 123, no. 4, pp. 593-605.

Kim, S., Benoiton, L., & Paik, W.K. 1964,"Alkyllsinase. Purification and properties of the enzyme", *Journal of Biological Chemistry,* vol. 239, pp. 3790–3796.

Kim, J., Sif, S., Jones, B., Jackson, A., Koipally, J., Heller, E., Winandy, S., Viel, A., Sawyer, A., Ikeda, T., Kingston, R. & Georgopoulos, K. 1999, "
Ikaros DNA-binding proteins direct formation of chromatin remodeling complexes in lymphocytes", *Immunity,* vol. 10, no. 3, pp. 345-355.

Kim, J., Daniel, J., Espejo, A., Lake, A., Krishna, M., Xia, L., Zhang, Y. & Bedford, M.T. 2006, "Tudor, MBT and chromo domains gauge the degree of lysine methylation", *EMBO reports,* vol. 7, no. 4, pp. 397-403.

Kim, J., Chu, J., Shen, X., Wang, J. & Orkin, S.H. 2008, "An extended transcriptional network for pluripotency of embryonic stem cells", *Cell,* vol. 132, no. 6, pp. 1049-1061.

Kinder, S.J., Tsang, T.E., Quinlan, G.A., Hadjantonakis, A.K., Nagy, A. & Tam, P.P.L. 1999, "The orderly allocation of mesodermal cells to the extraembryonic structures and the anteroposterior axis during gastrulation of the mouse embryo", *Development,* vol. 126, no. 21, pp. 4691-4701.

Kingston, R.E. and Narlikar, G.J. 1999, "ATP-dependent remodeling and acetylation as regulators of chromatin fluidity", *Genes & Dev.* vol. 13, pp. 2339–2352.

Kispert, A. & Herrmann, B.G. 1994, "Immunohistochemical Analysis of the Brachyury Protein in Wild-Type and Mutant Mouse Embryos", *Developmental biology,* vol. 161, no. 1, pp. 179-193.

Klose, R.J., Yamane, K., Bae, Y., Zhang, D., Erdjument-Bromage, H., Tempst, P., Wong, J. & Zhang, Y. 2006, "The transcriptional repressor JHDM3A demethylates trimethyl histone H3 lysine 9 and lysine 36", *Nature,* vol. 442, no. 7100, pp. 312-316.

Klose, R.J., Yan, Q., Tothova, Z., Yamane, K., Erdjument-Bromage, H., Tempst, P., Gilliland, D.G., Zhang, Y. & Kaelin, W.G., Jr. 2007, "The retinoblastoma binding protein RBP2 is an H3K4 demethylase", *Cell,* vol. 128, no. 5, pp. 889-900.

Kohlmaier, A., Savarese, F., Lachner, M., Martens, J., Jenuwein, T. & Wutz, A. 2004, "A chromosomal memory triggered by Xist regulates histone methylation in X inactivation", *Plos Biology,* vol. 2, no. 7, pp. 991-1003.

Kolasinska-Zwierz, P., Down, T., Latorre, I., Liu, T., Liu, X.S. & Ahringer J. 2009, "Differential chromatin marking of introns and expressed exons by H3K36me3", *Nature Genetics*, vol. 41, no. 3, pp. 376-381.

Kontaki, H. & Talianidis, I. 2010, "Lysine Methylation Regulates E2F1-Induced Cell Death", *Molecular cell,* vol. 39, no. 1, pp. 152-160.

Kornberg, R.D. 1974, "Chromatin Structure - Repeating Unit of Histones and DNA", *Science,* vol. 184, no. 4139, pp. 868-871.

Kornberg, R.D. and Lorch, Y. 1999. "Twenty-five years of the nucleosome, fundamental particle of the eukaryote chromosome" *Cell,* vol. 98, pp. 285–294

Kossel. A. 1884, *Physiol. Chem.,* vol. 8, pp. 511–515.

Kouzarides, T. 2007, "Chromatin modifications and their function", *Cell,* vol. 128, no. 4, pp. 693-705.

Ku, M., Koche, R.P., Rheinbay, E., Mendenhall, E.M., Endoh, M., Mikkelsen, T.S., Presser, A., Nusbaum, C., Xie, X., Chi, A.S., Adli, M., Kasif, S., Ptaszek, L.M., Cowan, C.A., Lander, E.S., Koseki, H. & Bernstein, B.E. 2008, "Genomewide Analysis of PRC1 and PRC2 Occupancy Identifies Two Classes of Bivalent Domains", *Plos Genetics,* vol. 4, no. 10, pp. e1000242.

Kunath, T., Saba-El-Leil, M.K., Almousailleakh, M., Wray, J., Meloche, S. & Smith, A. 2007, "FGF stimulation of the Erk1/2 signalling cascade triggers transition of pluripotent embryonic stem cells from self-renewal to lineage commitment", *Development,* vol. 134, no. 16, pp. 2895-2902.

Kuo, M.H., Zhou, J., Jambeck, P., Churchill, M.E., & Allis, C.D. 1998, "Histone acetyltransferase activity of yeast Gcn5p is required for the activation of target genes in vivo", *Genes & Dev.* vol. 12, pp. 627–63.

Kurdistani, S.K., Robyr, D., Tavazoie, S. & Grunstein, M. 2002, "Genome-wide binding map of the histone deacetylase Rpd3 in yeast", *Nature genetics,* vol. 31, no. 3, pp. 248-254.

Kuzmichev, A. & Reinberg, D. 2001, "Role of histone deacetylase complexes in the regulation of chromatin metabolism", *Curr. Top. Microbiol. Immunol.* vol. 254, pp.35–58.

Lachner, M. & Jenuwein, T. 2002, "The many faces of histone lysine methylation", *Current opinion in cell biology,* vol. 14, no. 3, pp. 286-298.

Lachner, M., O'Carroll, N., Rea, S., Mechtler, K. & Jenuwein, T. 2001, "Methylation of histone H3 lysine 9 creates a binding site for HP1 proteins", *Nature,* vol. 410, no. 6824, pp. 116-120.

Lachner, M., O'Sullivan, R.J. & Jenuwein, T. 2003, "An epigenetic road map for histone lysine methylation", *Journal of cell science,* vol. 116, no. 11, pp. 2117-2124.

Lagger, G., O'Carroll, D., Rembold, M., Khier, H., Tischler, J., Weitzer, G., Schuettengruber, B., Hauser, C., Brunmeir, R., Jenuwein, T. & Seiser, C. 2002, "Essential function of histone

deacetylase 1 in proliferation control and CDK inhibitor repression.", *EMBO Journal,* vol. 21, no. 11, pp. 2672-2681.

Laherty, C.D., Yang, W.M., Sun, J.M., Davie, J.R., Seto, E. & Eisenman, R.N. 1997, "Histone deacetylases associated with the mSin3 corepressor mediate Mad transcriptional repression", *Cell,* vol. 89, no. 3, pp. 349-356.

Lai, A., Kennedy, B.K., Barbie, D.A., Bertos, N.R., Yang, X.J., Theberge, M.C., Tsai, S.C., Seto, E., Zhang, Y., Kuzmichev, A., Lane, W.S., Reinberg, D., Harlow, E. & Branton, P.E. 2001, "RBP1 recruits the mSIN3-histone deacetylase complex to the pocket of retinoblastoma tumor suppressor family proteins found in limited discrete regions of the nucleus at growth arrest", *Molecular and cellular biology,* vol. 21, no. 8, pp. 2918-2932.

Lake, J.A., Rathjen, J., Remiszewski, J. & Rathjen, P.D. 2000, "Reversible programming of pluripotent cell differentiation", *Journal of cell science,* vol. 113, no. 3, pp. 555-566.

Lan, F., Collins, R.E., De Cegli, R., Alpatov, R., Horton, J.R., Shi, X., Gozani, O., Cheng, X. & Shi, Y. 2007, "Recognition of unmethylated histone H3 lysine 4 links BHC80 to LSD1-mediated gene repression", *Nature,* vol. 448, no. 7154, pp. 718-U14.

Lan, F., Nottke, A.C. & Shi, Y. 2008, "Mechanisms involved in the regulation of histone lysine demethylases", *Current opinion in cell biology,* vol. 20, no. 3, pp. 316-325.

Lande-Diner, L., Zhang, J. & Cedar, H. 2009, "Shifts in Replication Timing Actively Affect Histone Acetylation during Nucleosome Reassembly", *Molecular cell,* vol. 34, no. 6, pp. 767-774.

Lee, M.G., Wynder, C., Bochar, D.A., Hakimi, M.A., Cooch, N. & Shiekhattar, R. 2006a, "Functional interplay between histone demethylase and deacetylase enzymes.", *Molecular and Cellular Biology,* vol. 26, no. 17, pp. 6395-6402.

Lee, M.G., Wynder, C., Schmidt, D.M., McCafferty, D.G. & Shiekhatter, R. 2006b, " Histone H3 lysine 4 demethylation is a target of nonselective antidepressive medications", *Chemical Biology,* vol. 13, pp. 563-567.

Lee, J.H., Hart, S.R.L. & Skalnik, D.G. 2004a, "Histone deacetylase activity is required for embryonic stem cell differentiation", *Genesis,* vol. 38, no. 1, pp. 32-38.

Lee, J.H., Hart, S.R.L. & Skalnik, D.G. 2004b, "Histone deacetylase activity is required for embryonic stem cell differentiation", *Genesis,* vol. 38, no. 1, pp. 32-38.

Lee, J., Smith, E. & Shilatifard, A. 2010, "The Language of Histone Crosstalk", *Cell,* vol. 142, no. 5, pp. 682-685.

Lee, M.G., Wynder, C., Cooch, N. & Shiekhattar, R. 2005, "An essential role for CoREST in nucleosomal histone 3 lysine 4 demethylation", *Nature,* vol. 437, no. 7057, pp. 432-435.

Lee, M.G., Wynder, C., Schmidt, D.M., McCafferty, D.G. & Shiekhattar, R. 2006, "Histone H3 lysine 4 demethylation is a target of nonselective antidepressive medications", *Chemistry & biology,* vol. 13, no. 6, pp. 563-567.

Lee, M.G., Norman, J., Shilatifard, A. & Shiekhattar, R. 2007a, "Physical and functional association of a trimethyl H3K4 demethylase and Ring6a/MBLR, a polycomb-like protein", *Cell,* vol. 128, no. 5, pp. 877-887.

Lee, M.G., Villa, R., Trojer, P., Norman, J., Yan, K., Reinberg, D., Di Croce, L. & Shiekhattar, R. 2007b, "Demethylation of H3K27 regulates polycomb recruitment and H2A ubiquitination", *Science,* vol. 318, no. 5849, pp. 447-450.

Lee, N., Erdjument-Bromage, H., Tempst, P., Jones, R.S. & Zhang, Y. 2009, "The H3K4 Demethylase Lid Associates with and Inhibits Histone Deacetylase Rpd3", *Molecular and cellular biology,* vol. 29, no. 6, pp. 1401-1410.

Lee, T.I., Jenner, R.G., Boyer, L.A., Guenther, M.G., Levine, S.S., Kumar, R.M., Chevalier, B., Johnstone, S.E., Cole, M.F., Isono, K., Koseki, H., Fuchikami, T., Abe, K., Murray, H.L., Zucker, J.P., Yuan, B., Bell, G.W., Herbolsheimer, E., Hannett, N.M., Sun, K., Odom, D.T., Otte, A.P., Volkert, T.L., Bartel, D.P., Melton, D.A., Gifford, D.K., Jaenisch, R. & Young, R.A. 2006, "Control of developmental regulators by Polycomb in human embryonic stem cells", *Cell,* vol. 125, no. 2, pp. 301-313.

Li, E., Bestor, T.H. & Jaenisch, R. 1992, "Targeted Mutation of the Dna Methyltransferase Gene Results in Embryonic Lethality", *Cell,* vol. 69, no. 6, pp. 915-926.

Li, H.T., Ilin, S., Wang, W.K., Duncan, E.M., Wysocka, J., Allis, C.D. & Patel, D.J. 2006, "Molecular basis for site-specific read-out of histone H3K4me3 by the BPTF PHD finger of NURF", *Nature,* vol. 442, no. 7098, pp. 91-95.

Li B, Jackson J, Simon MD, Fleharty B, Gogol M, Seidel C, Workman JL, Shilatifard A. 2009, "Histone H3 lysine 36 dimethylation (H3K36me2) is sufficient to recruit the Rpd3s histone deacetylase complex and to repress spurious transcription", *Journal of Biological Chemistry,* vol. 284, no. 12, pp. 7970-7976

Liang, J., Wan, M., Zhang, Y., Gu, P., Xin, H., Jung, S.Y., Qin, J., Wong, J., Cooney, A.J., Liu, D. & Zhou Songyang 2008, "Nanog and Oct4 associate with unique transcriptional repression complexes in embryonic stem cells", *Nature cell biology,* vol. 10, no. 6, pp. 731-739.

Lin, W.C. & Dent, S.Y.R. 2006, "Functions of histone-modifying enzymes in development", *Current opinion in genetics & development,* vol. 16, no. 2, pp. 137-142.

Lister, R., Pelizzola, M., Dowen, R.H., Hawkins, R.D., Hon, G., Tonti-Filippini, J., Nery, J.R., Lee, L., Ye, Z., Ngo, Q., Edsall, L., Antosiewicz-Bourget, J., Stewart, R., Ruotti, V., Millar, A.H., Thomson, J.A., Ren, B. & Ecker, J.R. 2009, "Human DNA methylomes at base resolution show widespread epigenomic differences RID B-9144-2008", *Nature,* vol. 462, no. 7271, pp. 315-322.

Litt, M.D., Simpson, M., Gaszner, M., Allis, C.D. & Felsenfeld, G. 2001, "Correlation between histone lysine methylation and developmental changes at the chicken beta-globin locus", *Science,* vol. 293, pp. 2453-2455.

Liu, P.T., Wakamiya, M., Shea, M.J., Albrecht, U., Behringer, R.R. & Bradley, A. 1999, "Requirement for Wnt3 in vertebrate axis formation", *Nature genetics,* vol. 22, no. 4, pp. 361-365.

Liu, Z., Li, T., Liu, Y., Jia, Z., Li, Y., Zhang, C., Chen, P., Ma, K., Affara, N. & Zhou, C. 2009, "WNT signaling promotes Nkx2.5 expression and early cardiomyogenesis via downregulation of Hdac1", *Biochimica Et Biophysica Acta-Molecular Cell Research,* vol. 1793, no. 2, pp. 300-311.

Loh, Y.H., Wu, Q., Chew, J.L., Vega, V.B., Zhang, W.W., Chen, X., Bourque, G., George, J., Leong, B., Liu, J., Wong, K.Y., Sung, K.W., Lee, C.W.H., Zhao, X.D., Chiu, K.P., Lipovich, L., Kuznetsov, V.A., Robson, P., Stanton, L.W., Wei, C.L., Ruan, Y.J., Lim, B. & Ng, H.H. 2006, "The Oct4 and Nanog transcription network regulates pluripotency in mouse embryonic stem cells", *Nature genetics,* vol. 38, no. 4, pp. 431-440.

Loh, Y., Zhang, W., Chen, X., George, J. & Ng, H. 2007, "Jmjd1a and Jmjd2c histone H3 Lys 9 demethylases regulate self-renewal in embryonic stem cells", *Genes & development,* vol. 21, no. 20, pp. 2545-2557.

Lowry, W.E., Richter, L., Yachechko, R., Pyle, A.D., Tchieu, J., Sridharan, R., Clark, A.T. & Plath, K. 2008, "Generation of human induced pluripotent stem cells from dermal fibroblasts", *Proceedings of the National Academy of Sciences of the United States of America,* vol. 105, no. 8, pp. 2883-2888.

Lubitz, S., Glaser, S., Schaft, J., Stewart, A.F. & Anastassiadis, K. 2007, "Increased apoptosis and skewed differentiation in mouse embryonic stem cells lacking the histone methyltransferase Mll2 RID A-8944-2010", *Molecular biology of the cell,* vol. 18, no. 6, pp. 2356-2366.

Luco, R.F., Pan, Q., Tominaga, K., Blencowe, B.J., Pereira-Smith, O.M. & Misteli, T. 2010, "Regulation of Alternative Splicing by Histone Modifications", *Science,* vol. 327, no. 5968, pp. 996-1000.

Lunyak, V.V., Burgess, R., Prefontaine, G.G., Nelson, C., Sze, S.H., Chenoweth, J., Schwartz, P., Pevzner, P.A., Glass, C., Mandel, G. & Rosenfeld, M.G. 2002, "Corepressor-dependent silencing of chromosomal regions encoding neuronal genes", *Science,* vol. 298, no. 5599, pp. 1747-1752.

Luo, R.X., Postigo, A.A. & Dean, D.C. 1998, "Rb interacts with histone deacetylase to repress transcription", *Cell,* vol. 92, no. 4, pp. 463-473.

Ma, Y.G., Rosfjord, E., Huebert, C., Wilder, P., Tiesman, J., Kelly, D. & Rizzino, A. 1992, "Transcriptional Regulation of the Murine K-Fgf Gene in Embryonic-Cell Lines", *Developmental biology,* vol. 154, no. 1, pp. 45-54.

Macfarlan, T.S., Gifford, W.D., Agarwal, S., Driscoll, S., Lettieri, K., Wang, J., Andrews, S.E., Franco, L., Rosenfeld, M.G., Ren, B. & Pfaff, S.L. 2011, "Endogenous retroviruses and neighboring genes are coordinately repressed by LSD1/KDM1A", *Genes & development,* vol. 25, no. 6, pp. 594-607.

Magnaghi-Jaulin, L., Groisman, R., Naguibneva, I., Robin, P., Lorain, S., Le Villain, J.P., Troalen, F., Trouche, D. & Harel-Bellan, A. 1998, "Retinoblastoma protein represses transcription by recruiting a histone deacetylase", *Nature,* vol. 391, no. 6667, pp. 601-605.

Maherali, N., Sridharan, R., Xie, W., Utikal, J., Eminli, S., Arnold, K., Stadtfeld, M., Yachechko, R., Tchieu, J., Jaenisch, R., Plath, K. & Hochedlinger, K. 2007, "Directly reprogrammed fibroblasts show global epigenetic remodeling and widespread tissue contribution", *Cell Stem Cell,* vol. 1, no. 1, pp. 55-70.

Margueron, R., Trojer, P. & Reinberg, D. 2005, "The key to development: interpreting the histone code?", *Current opinion in genetics & development,* vol. 15, no. 2, pp. 163-176.

Marks, P.A. & Xu, W.-. 2009, "Histone Deacetylase Inhibitors: Potential in Cancer Therapy", *Journal of cellular biochemistry,* vol. 107, no. 4, pp. 600-608.

Martin, C. & Zhang, Y. 2005, "The diverse functions of histone lysine methylation.", *Nature Reviews Molecular Cell Biology,* vol. 6, pp. 838-849.

Martin, G.R. 1981, "Isolation of a Pluripotent Cell-Line from Early Mouse Embryos Cultured in Medium Conditioned by Teratocarcinoma Stem-Cells", *Proceedings of the National Academy of Sciences of the United States of America-Biological Sciences,* vol. 78, no. 12, pp. 7634-7638.

Mayshoopes, L., Brown, A. & Huang, R. 1983, "Methylation and Rearrangement of Mouse Intracisternal a Particle Genes in Development, Aging, and Myeloma", *Molecular and cellular biology,* vol. 3, no. 8, pp. 1371-1380.

Mcclelland, M. 1981, "The Effect of Sequence Specific Dna Methylation on Restriction Endonuclease Cleavage", *Nucleic acids research,* vol. 9, no. 22, pp. 5859-5866.

Meissner, A., Wernig, M. & Jaenisch, R. 2007, "Direct reprogramming of genetically unmodified fibroblasts into pluripotent stem cells", *Nature biotechnology,* vol. 25, no. 10, pp. 1177-1181.

Mellor, J., Dudek, P. & Clynes, D. 2008, "A glimpse into the epigenetic landscape of gene regulation", *Current opinion in genetics & development,* vol. 18, no. 2, pp. 116-122.

Meshorer, E., Yellajoshula, D., George, E., Scambler, P.J., Brown, D.T. & Mistell, T. 2006, "Hyperdynamic plasticity in pluripotent embryonic of chromatin proteins stem cells", *Developmental Cell,* vol. 10, no. 1, pp. 105-116.

Metzger, E., Wissmann, M., Yin, N., Muller, J.M., Schneider, R., Peters, A.H.F.M., Gunther, T., Buettner, R. & Schule, R. 2005, "LSD1 demethylates repressive histone marks to promote androgen-receptor-dependent transcription", *Nature,* vol. 437, pp. 436-439.

Metzger, D., Clifford, J., Chiba, H. & Chambon, P. 1995, "Conditional Site-Specific Recombination in Mammalian-Cells using a Ligand-Dependent Chimeric Cre Recombinase", *Proceedings of the National Academy of Sciences of the United States of America,* vol. 92, no. 15, pp. 6991-6995.

Mikkelsen, T.S., Ku, M., Jaffe, D.B., Issac, B., Lieberman, E., Giannoukos, G., Alvarez, P., Brockman, W., Kim, T., Koche, R.P., Lee, W., Mendenhall, E., O'Donovan, A., Presser, A., Russ, C., Xie, X., Meissner, A., Wernig, M., Jaenisch, R., Nusbaum, C., Lander, E.S. & Bernstein, B.E. 2007, "Genome-wide maps of chromatin state in pluripotent and lineage-committed cells", *Nature,* vol. 448, no. 7153, pp. 553-U2.

Miller, T., Krogan, N.J., Dover, J., Erdjument-Bromage, H., Tempst, P., Johnston, M., Greenblatt, J.F. & Shilatifard, A. 2001, "COMPASS: A complex of proteins associated with a trithorax-related SET domain protein", *Proceedings of the National Academy of Sciences of the United States of America,* vol. 98, no. 23, pp. 12902-12907.

Millerhance, W.C., Lacorbiere, M., Fuller, S.J., Evans, S.M., Lyons, G., Schmidt, C., Robbins, J. & Chien, K.R. 1993, "In-Vitro Chamber Specification during Embryonic Stem-Cell Cardiogenesis - Expression of the Ventricular Myosin Light Chain-2 Gene is Independent of Heart Tube Formation", *Journal of Biological Chemistry,* vol. 268, no. 33, pp. 25244-25252.

Milne, T.A., Briggs, S.D., Brock, H.W., Martin, M.E., Gibbs, D., Allis, C.D. & Hess, J.L. 2002, "MLL targets SET domain methyltransferase activity to Hox gene promoters", *Molecular cell,* vol. 10, no. 5, pp. 1107-1117.

Mitsui, K., Tokuzawa, Y., Itoh, H., Segawa, K., Murakami, M., Takahashi, K., Maruyama, M., Maeda, M. & Yamanaka, S. 2003, "The homeoprotein Nanog is required for maintenance of pluripotency in mouse epiblast and ES cells.", *Cell,* vol. 113, no. 5, pp. 631-642.

Montgomery, N.D., Yee, D., Chen, A., Kalantry, S., Chamberlain, S.J., Otte, A.P. & Magnuson, T. 2005, "The murine polycomb group protein Eed is required for global histone H3 lysine-27 methylation", *Current Biology,* vol. 15, no. 10, pp. 942-947.

Montgomery, R.L., Hsieh, J., Barbosa, A.C., Richardson, J.A. & Olson, E.N. 2009, "Histone deacetylases 1 and 2 control the progression of neural precursors to neurons during brain development", *Proceedings of the National Academy of Sciences of the United States of America,* vol. 106, no. 19, pp. 7876-7881.

Murray, P. & Edgar, D. 2001, "The regulation of embryonic stem cell differentiation by leukaemia inhibitory factor (LIF)", *Differentiation,* vol. 68, no. 4-5, pp. 227-234.

Murry, C.E. & Keller, G. 2008, "Differentiation of embryonic stem cells to clinically relevant populations: lesson from embryonic development", *Cell,* vol. 132, no. 4, pp. 661-680.

Nagy, L., Kao, H.Y., Chakravarti, D., Lin, R.J., Hassig, C.A., Ayer, D.E., Schreiber, S.L. & Evans, R.M. 1997, "Nuclear receptor repression mediated by a complex containing SMRT, mSin3A, and histone deacetylase.", *Cell,* vol. 89, no. 3, pp. 373-380.

Nakano, T., Kodama, H. & Honjo, T. 1994, "Generation of Lymphohematopoietic Cells from Embryonic Stem-Cells in Culture", *Science,* vol. 265, no. 5175, pp. 1098-1101.

Nakayam, J., Rice, J.C., Strahl, B.D., Allis, C.D. & Grewal, S.I.S. 2001, "Role of histone H3 lysine 9 methylation in epigenetic control of heterochromatin assembly", *Science,* vol. 292, no. 5514, pp. 110-113.

Ng, H.H., Robert, F., Young, R.A. & Struhl, K. 2003, "Targeted recruitment of set1 histone methylase by elongating pol II provides a localized mark and memory of recent transcriptional activity", *Molecular cell,* vol. 11, no. 3, pp. 709-719.

Ng, S.S., Kavanagh, K.L., McDonough, M.A., Butler, D., Pilka, E.S., Lienard, B.M.R., Bray, J.E., Savitsky, P., Gileadi, O., von Delft, F., Rose, N.R., Offer, J., Scheinost, J.C., Borowski, T., Sundstrom, M., Schofield, C.J. & Oppermann, U. 2007, "Crystal structures of histone

demethylase JMJD2A reveal basis for substrate specificity", *Nature,* vol. 448, no. 7149, pp. 87-91.

Nichols, J., Zevnik, B., Anastassiadis, K., Niwa, H., Klewe-Nebenius, D., Chambers, I., Scholer, H. & Smith, A. 1998, "Formation of pluripotent stem cells in the mammalian embryo depends on the POU transcription factor Oct4.", *Cell,* vol. 95, no. 3, pp. 379-391.

Nicolas, E., Lee, M.G., Hakimi, M., Cam, H.P., Grewal, S.I.S. & Shiekhattar, R. 2006, "Fission yeast homologs of human histone H3 lysine 4 demethylase regulate a common set of genes with diverse functions", *Journal of Biological Chemistry,* vol. 281, no. 47, pp. 35983-35988.

Nielsen, S.J., Schneider, R., Bauer, U.M., Bannister, A.J., Morrison, A., O'Carroll, D., Firestein, R., Cleary, M., Jenuwein, T., Herrera, R.E. & Kouzarides, T. 2001, "Rb targets histone H3 methylation and HP1 to promoters", *Nature,* vol. 412, no. 6846, pp. 561-565.

Nishikawa, S., Nishikawa, S., Hirashima, M., Matsuyoshi, N. & Kodama, H. 1998, "Progressive lineage analysis by cell sorting and culture identifies FLK1(+)VE-cadherin(+) cells at a diverging point of endothelial and hemopoietic lineages", *Development,* vol. 125, no. 9, pp. 1747-1757.

Nishioka, K., Chuikov, S., Sarma, K., Erdjument-Bromage, H., Allis, C.D., Tempst, P. & Reinberg, D. 2002, "Set9, a novel histone H3 methyltransferase that facilitates transcription by precluding histone tail modifications required for heterochromatin formation", *Genes & development,* vol. 16, no. 4, pp. 479-489.

Niwa, H., Burdon, T., Chambers, I. & Smith, A. 1998, "Self-renewal of pluripotent embryonic stem cells is mediated via activation of STAT3", *Genes & development,* vol. 12, no. 13, pp. 2048-2060.

Niwa, H., Miyazaki, J. & Smith, A.G. 2000, "Quantitative expression of Oct-3/4 defines differentiation, dedifferentiation or self-renewal of ES cells", *Nature genetics,* vol. 24, no. 4, pp. 372-376.

Niwa, H., Toyooka, T., Shimosato, D., Strumpf, D., Takahashi, K., Yagi, R. & Rossant, J. 2005, "Interaction between Oct3/4 and Cdx2 determines trophectoderm differentiation", *Cell,* vol. 123, no. 5, pp. 917-929.

Noll, M. 1974, "Subunit structure of chromatin.", *Nature,* vol. 251, no. 5472, pp. 249-251.

Noma, K., Allis, C.D. & Grewal, S.I.S. 2001, "Transitions in distinct histone H3 methylation patterns at the heterochromatin domain boundaries", *Science,* vol. 293, pp. 1150-1155.

O'Carroll, D., Erhardt, S., Pagani, M., Barton, S.C., Surani, M.A. & Jenuwein, T. 2001, "The Polycomb-group gene Ezh2 is required for early mouse development", *Molecular and cellular biology,* vol. 21, no. 13, pp. 4330-4336.

Okita, K., Ichisaka, T. & Yamanaka, S. 2007, "Generation of germline-competent induced pluripotent stem cells", *Nature,* vol. 448, no. 7151, pp. 313-U1.

Okita, K., Nakagawa, M., Hong, H., Ichisaka, T. & Yamanaka, S. 2008, "Generation of Mouse Induced Pluripotent Stem Cells Without Viral Vectors", *Science,* vol. 322, no. 5903, pp. 949-953.

Ooi, S.K.T., Qiu, C., Bernstein, E., Li, K., Jia, D., Yang, Z., Erdjument-Bromage, H., Tempst, P., Lin, S., Allis, C.D., Cheng, X. & Bestor, T.H. 2007, "DNMT3L connects unmethylated lysine 4 of histone H3 to de novo methylation of DNA", *Nature,* vol. 448, no. 7154, pp. 714-U13.

Orford, K., Kharchenko, P., Lai, W., Dao, M.C., Worhunsky, D.J., Ferro, A., Janzen, V., Park, P.J. & Scadden, D.T. 2008, "Differential H3K4 methylation identifies developmentally poised hematopoietic genes", *Developmental Cell,* vol. 14, no. 5, pp. 798-809.

Oudet, P., Gross-Bellard, M. & Chambon, P. 1975, "Electron microscopic and biochemical evidence that chromatin structure is a repeating unit", *Cell,* vol. 4, no. 4, pp. 281-300.

Ouyang, J., Shi, Y., Valin, A., Xuan, Y. & Gill, G. 2009, "Direct binding of CoREST1 to SUMO-2/3 contributes to gene-specific repression by the LSD1/CoREST/HDAC1 complex", *Molecular Cell,* vol. 34, pp. 145-154.

Paik, W.K. & Kim, S. 1973, "Enzymatic demethylation of calf thymus histones", *Biochem*. *Biophys. Res. Commun*. vol, 51, pp. 781–788.

Paik, W.K. & Kim, S. 1974, "Epsilon-alkyllysinase. New assay method, purificational and biological significance", *Arch. Biochem. Biophys.* vol. 165, pp. 369–378.

Pan, G., Tian, S., Nie, J., Yang, C., Ruotti, V., Wei, H., Jonsdottir, G.A., Stewart, R. & Thomson, J.A. 2007, "Whole-genome analysis of histone H3 lysine 4 and lysine 27 methylation in human embryonic stem cells", *Cell Stem Cell,* vol. 1, no. 3, pp. 299-312.

Pardo, M., Lang, B., Yu, L., Prosser, H., Bradley, A., Babu, M.M. & Choudhary, J. 2010, "An Expanded Oct4 Interaction Network: Implications for Stem Cell Biology, Development, and Disease", *Cell Stem Cell,* vol. 6, no. 4, pp. 382-395.

Park, I., Zhao, R., West, J.A., Yabuuchi, A., Huo, H., Ince, T.A., Lerou, P.H., Lensch, M.W. & Daley, G.Q. 2008, "Reprogramming of human somatic cells to pluripotency with defined factors", *Nature,* vol. 451, no. 7175, pp. 141-U1.

Pasini, D., Bracken, A.P., Jensen, M.R., Denchi, E.L. & Helin, K. 2004, "Suz12 is essential for mouse development and for EZH2 histone methyltransferase activity", *Embo Journal,* vol. 23, no. 20, pp. 4061-4071.

Pazin, M.J. and Kadonaga, J.T. 1997, "What's up and down with histone deacetylation and transcription?", *Cell,* vol. 89, pp. 325–328.

Pegoraro, G., Kubben, N., Wickert, U., Goehler, H., Hoffmann, K. & Misteli, T. 2009, "Ageing-related chromatin defects through loss of the NURD complex", *Nature cell biology,* vol. 11, no. 10, pp. 1261-U251.

Pena, P.V., Davrazou, F., Shi, X.B., Walter, K.L., Verkhusha, V.V., Gozani, O., Zhao, R. & Kutateladze, T.G. 2006, "Molecular mechanism of histone H3K4me3 recognition by plant homeodomain of ING2", *Nature,* vol. 442, no. 7098, pp. 100-103.

Peters, A.H.F.M., Mermoud, J.E., O'Carroll, D., Pagani, M., Schweizer, D., Brockdorff, N. & Jenuwein, T. 2002, "Histone H3 lysine 9 methylation is an epigenetic imprint of facultative heterochromatin", *Nature genetics,* vol. 30, no. 1, pp. 77-80.

Peterson, C.L. & Laniel, M.A. 2004, "Histones and histone modifications", *Current Biology,* vol. 14, no. 14, pp. R546-R551.

Prasher, D.C., Eckenrode, V.K., Ward, W.W., Prendergast, F.G. & Cormier, M.J. 1992, "Primary Structure of the Aequorea-Victoria Green-Fluorescent Protein", *Gene,* vol. 111, no. 2, pp. 229-233.

Qian, C.M., Zhang, Q., Li, S.D., Zeng, L., Walsh, M.J. & Zhou, M.M. 2005, "Structure and chromosomal DNA binding of the SWIRM domain", *Nature Structural & Molecular Biology,* vol. 12, no. 12, pp. 1078-1085.

Rathjen, J., Lake, J.A., Bettess, M.D., Washington, J.M., Chapman, G. & Rathjen, P.D. 1999, "Formation of a primitive ectoderm like cell population, EPL cells, from ES cells in response to biologically derived factors", *Journal of cell science,* vol. 112, no. 5, pp. 601-612.

Rea, S., Eisenhaber, F., O'Carroll, N., Strahl, B.D., Sun, Z.W., Schmid, M., Opravil, S., Mechtler, K., Ponting, C.P., Allis, C.D. & Jenuwein, T. 2000, "Regulation of chromatin structure by site-specific histone H3 methyltransferases", *Nature,* vol. 406, no. 6796, pp. 593-599.

Ridsdale, J.A., Hendzel, M.J., Delcuve, G.P. & Davie, J.R. 1990, "Histone acetylation alters the capacity of the H1 histones to condense transcriptionally active/competent chromatin.", *Journal of Biological Chemistry,* vol. 265, no. 9, pp. 5150-5156.

Ringrose, L. & Paro, R. 2004, "Epigenetic regulation of cellular memory by the polycomb and trithorax group proteins", *Annual Review of Genetics,* vol. 38, pp. 413-443.

Risau, W., Sariola, H., Zerwes, H.G., Sasse, J., Ekblom, P., Kemler, R. & Doetschman, T. 1988, "Vasculogenesis and Angiogenesis in Embryonic-Stem-Cell-Derived Embryoid Bodies", *Development,* vol. 102, no. 3, pp. 471-478.

Robert, F., Pokholok, D.K., Hannett, N.M., Rinaldi, N.J., Chandy, M., Rolfe, A., Workman, J.L., Gifford, D.K. & Young, R.A. 2004, "Global position and recruitment of HATs and HDACs in the yeast genome", *Molecular cell,* vol. 16, no. 2, pp. 199-209.

Robertson, E., Bradley, A., Kuehn, M. & Evans, M. 1986, "Germ-Line Transmission of Genes Introduced into Cultured Pluripotential Cells by Retroviral Vector", *Nature,* vol. 323, no. 6087, pp. 445-448.

Robinson, P.J.J., An, W., Routh, A., Martino, F., Chapman, L., Roeder, R.G. & Rhodes, D. 2008, "30 nm Chromatin Fibre Decompaction Requires both H4-K16 Acetylation and Linker Histone Eviction", *Journal of Molecular Biology,* vol. 381, no. 4, pp. 816-825.

Rogers, M.B., Hosler, B.A. & Gudas, L.J. 1991, "Specific Expression of a Retinoic Acid-Regulated, Zinc-Finger Gene, Rex-1, in Preimplantation Embryos, Trophoblast and Spermatocytes", *Development,* vol. 113, no. 3, pp. 815-824.

Roh, T., Cuddapah, S., Cui, K. & Zhao, K. 2006, "The genomic landscape of histone modifications in human T cells", *Proceedings of the National Academy of Sciences of the United States of America,* vol. 103, no. 43, pp. 15782-15787.

Rohwedel, J., Maltsev, V., Bober, E., Arnold, H.H., Hescheler, J. & Wobus, A.M. 1994, "Muscle-Cell Differentiation of Embryonic Stem-Cells Reflects Myogenesis In-Vivo - Developmentally-Regulated Expression of Myogenic Determination Genes and Functional Expression of Ionic Currents", *Developmental biology,* vol. 164, no. 1, pp. 87-101.

Ropero, S., Fraga, M.F., Ballestar, E., Hamelin, R., Yamamoto, H., Boix-Chornet, M., Caballero, R., Alaminos, M., Setien, F., Paz, M.F., Herranz, M., Palacios, J., Arango, D., Orntoft, T.F., Aaltonen, L.A., Schwartz, S. & Esteller, M. 2006, "A truncating mutation of HDAC2 in human cancers confers resistance to histone deacetylase inhibition", *Nature genetics,* vol. 38, no. 5, pp. 566-569.

Rosner, M.H., Vigano, M.A., Ozato, K., Timmons, P.M., Poirier, F., Rigby, P.W.J. & Staudt, L.M. 1990, "A Pou-Domain Transcription Factor in Early Stem-Cells and Germ-Cells of the Mammalian Embryo", *Nature,* vol. 345, no. 6277, pp. 686-692.

Rossant, J. & Ofer, L. 1977, "Properties of Extra-Embryonic Ectoderm Isolated from Postimplantation Mouse Embryos", *Journal of embryology and experimental morphology,* vol. 39, no. JUN, pp. 183-194.

Roth, S.Y., Denu, J.M. & Allis, C.D. 2001, "Histone acetyltransferases", *Annual Review of Biochemistry,* vol. 70, pp. 81-120.

Rudolph, T., Yonezawa, M., Lein, S., Heidrich, K., Kubicek, S., Schaefer, C., Phalke, S., Walther, M., Schmidt, A., Jenuwein, T. & Reuter, G. 2007, "Heterochromatin formation in Drosophila is initiated through active removal of H3K4 methylation by the LSD1 homolog SU(VAR)3-3", *Molecular cell,* vol. 26, no. 1, pp. 103-115.

Rundlett, S.E., Carmen, A.A., Kobayashi, R., Bavykin, S., Turner, B.M. & Grunstein, M. 1996, "HDA1 and RPD3 are members of distinct yeast histone deacetylase complexes that regulate silencing and transcription", *Proceedings of the National Academy of Sciences of the United States of America,* vol. 93, no. 25, pp. 14503-14508.

Ruthenburg, A.J., Li, H., Patel, D.J. & Allis, C.D. 2007, "Multivalent engagement of chromatin modifications by linked binding modules", *Nature Reviews Molecular Cell Biology,* vol. 8, no. 12, pp. 983-994.

Saito, M. & Ishikawa, F. 2002, "The mCpG-binding domain of human MBD3 does not bind to mCpG but interacts with NuRD/Mi2 components HDAC1 and MTA2", *Journal of Biological Chemistry,* vol. 277, no. 38, pp. 35434-35439.

Saleque, S., Kim, J., Rooke, H.M. & Orkin, S.H. 2007, "Epigenetic regulation of hematopoietic differentiation by Gfi-1 and Gfi-1b is mediated by the cofactors CoREST and LSD1", *Molecular cell,* vol. 27, no. 4, pp. 562-572.

Santos-Rosa, H., Schneider, R., Bannister, A.J., Sherriff, J., Bernstein, B.E., Emre, N.C.T., Schreiber, S.L., Mellor, J. & Kouzarides, T. 2002, "Active genes are tri-methylated at K4 of histone H3", *Nature,* vol. 419, pp. 407-411.

Sato, N., Meijer, L., Skaltsounis, L., Greengard, P. & Brivanlou, A.H. 2004, "Maintenance of pluripotency in human and mouse embryonic stem cells through activation of Wnt signaling by a pharmacological GSK-3-specific inhibitor", *Nature medicine,* vol. 10, no. 1, pp. 55-63.

Sauer, B. 1987, "Functional Expression of the Cre-Lox Site-Specific Recombination System in the Yeast Saccharomyces-Cerevisiae", *Molecular and cellular biology,* vol. 7, no. 6, pp. 2087-2096.

Sauer, B. & Henderson, N. 1988, "Site-Specific Dna Recombination in Mammalian-Cells by the Cre Recombinase of Bacteriophage-P1", *Proceedings of the National Academy of Sciences of the United States of America,* vol. 85, no. 14, pp. 5166-5170.

Schaeper, U., Boyd, J.M., Verma, S., Uhlmann, E., Subramanian, T. & Chinadurai, G. 1995, "Molecular-Cloning and Characterization of a Cellular Phosphoprotein that Interacts with a Conserved C-Terminal Domain of Adenovirus E1a Involved in Negative Modulation of Oncogenic Transformation", *Proceedings of the National Academy of Sciences of the United States of America,* vol. 92, no. 23, pp. 10467-10471.

Schneider, R., Bannister, A.J., Myers, F.A., Thorne, A.W., Crane-Robinson, C. & Kouzarides, T. 2004, "Histone H3 lysine 4 methylation patterns in higher eukaryotic genes", *Nature Cell Biology,* vol. 6, pp. 73-77.

Schneider, J., Bajwa, P., Johnson, F.C., Bhaumik, S.R. & Shilatifard, A. 2006, "Rtt109 is required for proper H3K56 acetylation - A Chromatin mark associated with the elongating RNA polymerase II", *Journal of Biological Chemistry,* vol. 281, no. 49, pp. 37270-37274.

Schoenherr, C.J. & Anderson, D.J. 1995, "The neuron-restrictive silencer factor (NRSF): a coordinate repressor of multiple neuron-specific genes.", *Science,* vol. 267, no. 5202, pp. 1360-1363.

Schotta, G., Lachner, M., Sarma, K., Ebert, A., Sengupta, R., Reuter, G., Reinberg, D. & Jenuwein, T. 2004, "A silencing pathway to induce H3-K9 and H4-K20 trimethylation at constitutive heterochromatin", *Genes & development,* vol. 18, no. 11, pp. 1251-1262.

Schreiber, S.L. & Bernstein, B.E. 2002, "Signaling network model of chromatin", *Cell,* vol. 111, no. 6, pp. 771-778.

Schuettengruber, B., Chourrout, D., Vervoort, M., LeBlanc, B. & Cavalli, G. 2007, "Genome Regulation by Polycomb and Trithorax Proteins", *Cell,* vol. 128, no. 4, pp. 735-745.

Shahbazian, M.D. & Grunstein, M. 2007, "Functions of site-specific histone acerylation and deacetylation", *Annual Review of Biochemistry,* vol. 76, pp. 75-100.

Shechter, D., Dormann, H.L., Allis, C.D. & Hake, S.B. 2007, "Extraction, purification and analysis of histones", *Nature Protocols,* vol. 2, no. 6, pp. 1445-1457.

Shen, M.M. & Leder, P. 1992, "Leukemia Inhibitory Factor is Expressed by the Preimplantation Uterus and Selectively Blocks Primitive Ectoderm Formation Invitro", *Proceedings of the National Academy of Sciences of the United States of America,* vol. 89, no. 17, pp. 8240-8244.

Shen, X., Liu, Y., Hsu, Y., Fujiwara, Y., Kim, J., Mao, X., Yuan, G. & Orkin, S.H. 2008a, "EZH1 Mediates Methylation on Histone H3 Lysine 27 and Complements EZH2 in Maintaining Stem Cell Identity and Executing Pluripotency", *Molecular cell,* vol. 32, no. 4, pp. 491-502.

Shen, X., Liu, Y., Hsu, Y., Fujiwara, Y., Kim, J., Mao, X., Yuan, G. & Orkin, S.H. 2008b, "EZH1 Mediates Methylation on Histone H3 Lysine 27 and Complements EZH2 in Maintaining Stem Cell Identity and Executing Pluripotency", *Molecular cell,* vol. 32, no. 4, pp. 491-502.

Shi, Y., Lan, F., Matson, C., Mulligan, P., Whetstine, J.R., Cole, P.A., Casero, R.A. & Shi, Y. 2004, "Histone demethylation mediated by the nuclear amine oxidase homolog LSD1", *Cell,* vol. 119, pp. 941-953.

Shi, X.B., Hong, T., Walter, K.L., Ewalt, M., Michishita, E., Hung, T., Carney, D., Pena, P., Lan, F., Kaadige, M.R., Lacoste, N., Cayrou, C., Davrazou, F., Saha, A., Cairns, B.R., Ayer, D.E., Kutateladze, T.G., Shi, Y., Cote, J., Chua, K.F. & Gozani, O. 2006, "ING2 PHD domain links histone H3 lysine 4 methylation to active gene repression", *Nature,* vol. 442, no. 7098, pp. 96-99.

Shi, Y.J., Matson, C., Lan, F., Iwase, S., Baba, T. & Shi, Y. 2005, "Regulation of LSD1 histone demethylase activity by its associated factors", *Molecular cell,* vol. 19, no. 6, pp. 857-864.

Shi, Y.J., Sawada, J., Sui, G.C., Affar, E.B., Whetstine, J.R., Lan, F., Ogawa, H., Luke, M.P.S., Nakatani, Y. & Shi, Y. 2003, "Coordinated histone modifications mediated by a CtBP co-repressor complex", *Nature,* vol. 422, no. 6933, pp. 735-738.

Shi, Y. & Whetstine, J.R. 2007, "Dynamic regulation of histone lysine methylation by demethylases", *Molecular cell,* vol. 25, no. 1, pp. 1-14.

Shilatifard, A. 2006, "Chromatin modifications by methylation and ubiquitination: Implications in the regulation of gene expression", *Annual Review of Biochemistry,* vol. 75, pp. 243-269.

Shogren-Knaak, M., Ishii, H., Sun, J.M., Pazin, M.J., Davie, J.R. & Peterson, C.L. 2006, "Histone H4-K16 acetylation controls chromatin structure and protein interactions", *Science,* vol. 311, no. 5762, pp. 844-847.

Silverstein, R.A. & Ekwall, K. 2005, "Sin3: a flexible regulator of global gene expression and genome stability", *Current genetics,* vol. 47, no. 1, pp. 1-17.

Sims, R.J III & Reinberg, D. 2006, "Histone H3 Lys 4 methylation: caught in a bind?", *Genes & development,* vol. 20, no. 20, pp. 2779-2786.

Smith, A.G. 2001, "Embryo-derived stem cells: Of mice and men", *Annual Review of Cell and Developmental Biology,* vol. 17, pp. 435-462.

Smith, A.G., Heath, J.K., Donaldson, D.D., Wong, G.G., Moreau, J., Stahl, M. & Rogers, D. 1988, "Inhibition of Pluripotential Embryonic Stem-Cell Differentiation by Purified Polypeptides", *Nature,* vol. 336, no. 6200, pp. 688-690.

Smithies, O., Gregg, R.G., Boggs, S.S., Koralewski, M.A. & Kucherlapati, R.S. 1985, "Insertion of Dna-Sequences into the Human Chromosomal Beta-Globin Locus by Homologous Recombination", *Nature,* vol. 317, no. 6034, pp. 230-234.

Snow, M.H.L. 1977, "Gastrulation in Mouse - Growth and Regionalization of Epiblast", *Journal of embryology and experimental morphology,* vol. 42, no. DEC, pp. 293-303.

Solari, F., Bateman, A. & Ahringer, J. 1999, "The Caenorhabditis elegans genes egl-27 and egr-1 are similar to MTA1, a member of a chromatin regulatory complex, and are redundantly required for embryonic patterning", *Development,* vol. 126, no. 11, pp. 2483-2494.

Southern, E.M. 1975, "Detection of Specific Sequences among Dna Fragments Separated by Gel-Electrophoresis", *Journal of Molecular Biology,* vol. 98, no. 3, pp. 503-&.

Spies, N., Nielsen, C.B., Padgett, R.A. & Burge, C.B. 2009, "Biased Chromatin Signatures around Polyadenylation Sites and Exons", *Molecular cell,* vol. 36, no. 2, pp. 245-254.

Spivakov, M. & Fisher, A.G. 2007, "Epigenetic signatures of stem-cell identity", *Nature Reviews Genetics,* vol. 8, no. 4, pp. 263-271.

Stadtfeld, M., Nagaya, M., Utikal, J., Weir, G. & Hochedlinger, K. 2008, "Induced Pluripotent Stem Cells Generated Without Viral Integration", *Science,* vol. 322, no. 5903, pp. 945-949.

Sterner, D.E. & Berger, S.L. 2000, "Acetylation of histones and transcription-related factors", *Microbiology and Molecular Biology Reviews,* vol. 64, no. 2, pp. 435-+.

Stock, J.K., Giadrossi, S., Casanova, M., Brookes, E., Vidal, M., Koseki, H., Brockdorff, N., Fisher, A.G. & Pombo, A. 2007, "Ring1-mediated ubiquitination of H2A restrains poised RNA polymerase II at bivalent genes in mouse ES cells", *Nature cell biology,* vol. 9, no. 12, pp. 1428-U174.

Strahl, B. & Allis, C.D. 2000, "The language of covalent histone modifications", *Nature,* vol. 403, pp. 41-45.

Strumpf, D., Mao, C.A., Yamanaka, Y., Ralston, A., Chawengsaksophak, K., Beck, F. & Rossant, J. 2005, "Cdx2 is required for correct cell fate specification and differentiation of trophectoderm in the mouse blastocyst", *Development,* vol. 132, no. 9, pp. 2093-2102.

Stucki, M. & Jackson, S.P. 2004, "Tudor domains track down DNA breaks", *Nature cell biology,* vol. 6, no. 12, pp. 1150-1152.

Su, A.I., Wiltshire, T., Batalov, S., Lapp, H., Ching, K.A., Block, D., Zhang, J., Soden, R., Hayakawa, M., Kreiman, G., Cooke, M.P., Walker, J.R. & Hogenesch, J.B. 2004, "A gene atlas of the mouse and human protein-encoding transcriptomes", *Proceedings of the National Academy of Sciences of the United States of America,* vol. 101, no. 16, pp. 6062-6067.

Sun, G., Alzayady, K., Stewart, R., Ye, P., Yang, S., Li, W. & Shi, Y. 2010, "Histone Demethylase LSD1 Regulates Neural Stem Cell Proliferation", *Molecular and cellular biology,* vol. 30, no. 8, pp. 1997-2005.

Sun, J., Zhang, Q. & Schlick, T. 2005, "Electrostatic mechanism of nucleosomal array folding revealed by computer simulation", *Proceedings of the National Academy of Sciences of the United States of America,* vol. 102, no. 23, pp. 8180-8185.

Surani, M.A., Hayashi, K. & Hajkova, P. 2007, "Genetic and epigenetic regulators of pluripotency", *Cell,* vol. 128, no. 4, pp. 747-762.

Szutorisz, H., Canzonetta, C., Georgiou, A., Chow, C.M., Tora, L. & Dillon, N. 2005, "Formation of an active tissue-specific chromatin domain initiated by epigenetic marking at the embryonic stem cell stage", *Molecular and cellular biology,* vol. 25, no. 5, pp. 1804-1820.

Tachibana, M., Matsumura, Y., Fukuda, M., Kimura, H. & Shinkai, Y. 2008, "G9a/GLP complexes independently mediate H3K9 and DNA methylation to silence transcription", *Embo Journal,* vol. 27, no. 20, pp. 2681-2690.

Takahashi, K., Tanabe, K., Ohnuki, M., Narita, M., Ichisaka, T., Tomoda, K. & Yamanaka, S. 2007, "Induction of pluripotent stem cells from adult human fibroblasts by defined factors", *Cell,* vol. 131, no. 5, pp. 861-872.

Takahashi, K. & Yamanaka, S. 2006, "Induction of pluripotent stem cells from mouse embryonic and adult fibroblast cultures by defined factors", *Cell,* vol. 126, no. 4, pp. 663-676.

Talasz, H., Lindner, H.H., Sarg, B. & Helliger, W. 2005, "Histone H4-lysine 20 monomethylation is increased in promoter and coding regions of active genes and correlates with hyperacetylation", *Journal of Biological Chemistry,* vol. 280, no. 46, pp. 38814-38822.

Tam, P.P.L. & Behringer, R.R. 1997, "Mouse gastrulation: the formation of a mammalian body plan", *Mechanisms of development,* vol. 68, no. 1-2, pp. 3-25.

Tanay, A., O'Donnell, A.H., Damelin, M. & Bestor, T.H. 2007, "Hyperconserved CpG domains underlie Polycomb-binding sites", *Proceedings of the National Academy of Sciences of the United States of America,* vol. 104, no. 13, pp. 5521-5526.

Taplick, J., Kurtev, V., Kroboth, K., Posch, M., Lechner, T. & Seiser, C. 2001, "Homo-oligomerisation and nuclear localisation of mouse histone deacetylase 1", *Journal of Molecular Biology,* vol. 308, no. 1, pp. 27-38.

Taunton, J., Hassig, C.A. & Schreiber, S.L. 1996, "A mammalian histone deacetylase related to the yeast transcriptional regulator Rpd3p", *Science,* vol. 272, no. 5260, pp. 408-411.

Taverna, S.D., Li, H., Ruthenburg, A.J., Allis, C.D. & Patel, D.J. 2007, "How chromatin-binding modules interpret histone modifications: lessons from professional pocket pickers", *Nature Structural & Molecular Biology,* vol. 14, no. 11, pp. 1025-1040.

ten Berge, D., Koole, W., Fuerer, C., Fish, M., Eroglu, E. & Nusse, R. 2008, "Wnt signalling mediates self-organisation and axis formation in embryoid bodies.", *Cell Stem Cell,* vol. 3, no. 5, pp. 508-518.

Thomas, K.R. & Capecchi, M.R. 1987, "Site-Directed Mutagenesis by Gene Targeting in Mouse Embryo-Derived Stem-Cells", *Cell,* vol. 51, no. 3, pp. 503-512.

Thomson, M., Liu, S.J., Zou, L., Smith, Z., Meissner, A. & Ramanathan, S. 2011, "Pluripotency Factors in Embryonic Stem Cells Regulate Differentiation into Germ Layers", *Cell,* vol. 145, no. 6, pp. 875-889.

Tie, F., Prasad-Sinha, J., Birve, A., Rasmuson-Lestander, A. & Harte, P.J. 2003, "A 1-megadalton ESC/E(Z) complex from Drosophila that contains polycomblike and RPD3", *Molecular and cellular biology,* vol. 23, no. 9, pp. 3352-3362.

Tjeertes, J.V., Miller, K.M. & Jackson, S.P. 2009, "Screen for DNA-damage-responsive histone modifications identifies H3K9Ac and H3K56Ac in human cells", *Embo Journal,* vol. 28, no. 13, pp. 1878-1889.

Tong, J.K., Hassig, C.A., Schnitzler, G.R., Kingston, R.E. & Schreiber, S.L. 1998, "Chromatin deacetylation by an ATP-dependent nucleosome remodelling complex", *Nature,* vol. 395, no. 6705, pp. 917-921.

Torres-Padilla, M., Parfitt, D., Kouzarides, T. & Zernicka-Goetz, M. 2007, "Histone arginine methylation regulates pluripotency in the early mouse embryo", *Nature,* vol. 445, no. 7124, pp. 214-218.

Trewick, S.C., McLaughlin, P.J. & Allshire, R.C. 2005, "Methylation: lost in hydroxylation?", vol. 6, no. 4, pp. 320.

Tse, C., Sera, T., Wolffe, A.P. & Hansen, J.C. 1998, "Disruption of higher-order folding by core histone acetylation dramatically enhances transcription of nucleosomal arrays by RNA polymerase III", *Molecular and cellular biology,* vol. 18, no. 8, pp. 4629-4638.

Tsukada, Y., Fang, J., Erdjument-Bromage, H., Warren, M.E., Borchers, C.H., Tempst, P. & Zhang, Y. 2006, "Histone demethylation by a family of JmjC domain-containing proteins", *Nature,* vol. 439, no. 7078, pp. 811-816.

Turner, B.M. 2005, "Reading signals on the nucleosome with a new nomenclature for modified histones", *Nature Structural & Molecular Biology,* vol. 12, no. 2, pp. 110-112.

Turner, B.M. 2002, "Cellular memory and the histone code", *Cell,* vol. 111, no. 3, pp. 285-291.

Vakoc, C.R., Sachdeva, M.M., Wang, H. & Blobel, G.A. 2006, "Profile of histone lysine methylation across transcribed mammalian chromatin", *Molecular and cellular biology,* vol. 26, no. 24, pp. 9185-9195.

van den Berg, D.L., Snoek, T., Mullin, N.P., Yates, A., Bezstarosti.,K., Demmers, J., Chambers, I. & Poot, R.A. 2010 "An Oct4-centred protein interaction network in embryonic stem cells", *Cell Stem Cell,* vol. 6, no. 4, pp. 369-381.

van der Vlag, J. & Otte, A.P. 1999, "Transcriptional repression mediated by the human polycomb-group protein EED involves histone deacetylation", *Nature genetics,* vol. 23, no. 4, pp. 474-478.

van Leeuwen, F., Gafken, P.R. & Gottschling, D.E. 2002, "Dot1p modulates silencing in yeast by methylation of the nucleosome core", *Cell,* vol. 109, no. 6, pp. 745-756.

Vangelder, R., Vonzastrow, M., Yool, A., Dement, W., Barchas, J. & Eberwine, J. 1990, "Amplified Rna Synthesized from Limited Quantities of Heterogeneous Cdna Rid B-2247-2010", *Proceedings of the National Academy of Sciences of the United States of America,* vol. 87, no. 5, pp. 1663-1667.

Vidal, M. & Gaber, R.F. 1991, "Rpd3 Encodes a 2nd Factor Required to Achieve Maximum Positive and Negative Transcriptional States in Saccharomyces-Cerevisiae", *Molecular and cellular biology,* vol. 11, no. 12, pp. 6317-6327.

Vignali, M., Hassan, A.H., Neely, K.E., & Workman, J.L. 2000, "ATP-dependent chromatin-remodeling complexes", *Molecular and Cellular Bioliogy,* vol. 20, pp. 1899–1910.

Wang, J., Hevi, S., Kurash, J.K., Lei, H., Gay, F., Bajko, J., Su, H., Sun, W., Chang, H., Xu, G.L., Gaudet, F., Li, E. & Chen, T. 2009, "The lysine demethylase LSD1 (KDM1) is required for maintenance of global DNA methylation", *Nature Genetics,* vol. 41, pp. 125-129.

Wang, J.X., Scully, K., Zhu, X., Cai, L., Zhang, J., Prefontaine, G.G., Krones, A., Ohgi, K.A., Zhu, P., Garcia-Bassets, I., Liu, F., Taylor, H., Lozach, J., Jayes, F.L., Korach, K.S., Glass, C.K., Fu, X.D. & Rosenfeld, M.G. 2007, "Opposing LSD1 complexes function in developmental gene activation and repression programmes", *Nature,* vol. 446, pp. 882-887.

Wang, A., Kurdistani, S.K. & Grunstein, M. 2002, "Requirement of Hos2 histone deacetylase for gene activity in yeast", *Science,* vol. 298, no. 5597, pp. 1412-1414.

Wang, H.B., Cao, R., Xia, L., Erdjument-Bromage, H., Borchers, C., Tempst, P. & Zhang, Y. 2001, "Purification and functional characterization of a histone H3-lysine 4-specific methyltransferase", *Molecular cell,* vol. 8, no. 6, pp. 1207-1217.

Wang, J., Rao, S., Chu, J., Shen, X., Levasseur, D.N., Theunissen, T.W. & Orkin, S.H. 2006, "A protein interaction network for pluripotency of embryonic stem cells", *Nature,* vol. 444, no. 7117, pp. 364-368.

Wang, J., Scully, K., Zhu, X., Cai, L., Zhang, J., Prefontaine, G.G., Krones, A., Ohgi, K.A., Zhu, P., Garcia-Bassets, I., Liu, F., Taylor, H., Lozach, J., Jayes, F.L., Korach, K.S., Glass, C.K., Fu, X. & Rosenfeld, M.G. 2007, "Opposing LSD1 complexes function in developmental gene activation and repression programmes", *Nature,* vol. 446, no. 7138, pp. 882-887.

Wang, Y., Zhang, H., Chen, Y., Sun, Y., Yang, F., Yu, W., Liang, J., Sun, L., Yang, X., Shi, L., Li, R., Li, Y., Zhang, Y., Li, Q., Yi, X. & Shang, Y. 2009a, "LSD1 Is a Subunit of the NuRD Complex and Targets the Metastasis Programs in Breast Cancer", *Cell,* vol. 138, no. 4, pp. 660-672.

Wang, Z., Zang, C., Cui, K., Schones, D.E., Barski, A., Peng, W. & Zhao, K. 2009b, "Genome-wide Mapping of HATs and HDACs Reveals Distinct Functions in Active and Inactive Genes", *Cell,* vol. 138, no. 5, pp. 1019-1031.

Wernig, M., Meissner, A., Foreman, R., Brambrink, T., Ku, M., Hochedlinger, K., Bernstein, B.E. & Jaenisch, R. 2007, "In vitro reprogramming of fibroblasts into a pluripotent ES-cell-like state", *Nature,* vol. 448, no. 7151, pp. 318-324.

Whetstine, J.R., Nottke, A., Lan, F., Huarte, M., Smolikov, S., Chen, Z.Z., Spooner, E., Li, E., Zhang, G.Y., Colaiacovo, M. & Shi, Y. 2006, "Reversal of histone lysine trimethylation by the JMJD2 family of histone demethylases", *Cell,* vol. 125, no. 3, pp. 467-481.

Wiles, M.V. & Keller, G. 1991, "Multiple Hematopoietic Lineages Develop from Embryonic Stem (Es) Cells in Culture", *Development,* vol. 111, no. 2, pp. 259-&.

Wilkinson, D.G., Bhatt, S. & Herrmann, B.G. 1990, "Expression Pattern of the Mouse T-Gene and its Role in Mesoderm Formation", *Nature,* vol. 343, no. 6259, pp. 657-659.

Wissmann, M., Yin, N., Mueller, J.M., Greschik, H., Fodor, B.D., Jenuwein, T., Vogler, C., Schneider, R., Guenther, T., Buettner, R., Metzger, E. & Schuele, R. 2007, "Cooperative demethylation by JMJD2C and LSD1 promotes androgen receptor-dependent gene expression", *Nature cell biology,* vol. 9, no. 3, pp. 347-U176.

Wu, J. & Grunstein, M. 2000, "25 years after the nucleosomemodel: Chromatin modifications", *Trends Biochem. Sci.* vol. 25, pp. 619–623.

Wysocka, J., Swigut, T., Xiao, H., Milne, T.A., Kwon, S.Y., Landry, J., Kauer, M., Tackett, A.J., Chait, B.T., Badenhorst, P., Wu, C. & Allis, C.D. 2006, "A PHD finger of NURF couples histone H3 lysine 4 trimethylation with chromatin remodelling", *Nature,* vol. 442, no. 7098, pp. 86-90.

Xiao, B., Jing, C., Kelly, G., Walker, P.A., Muskett, F.W., Frenkiel, T.A., Martin, S.R., Sarma, K., Reinberg, D., Gamblin, S.J. & Wilson, J.R. 2005, "Specificity and mechanism of the histone methyltransferase Pr-Set7", *Genes & development,* vol. 19, no. 12, pp. 1444-1454.

Xie, J.X., Pierce, M., Gailus-Durner, V., Wagner, M., Winter, E. & Vershon, A.K. 1999, "Sum1 and Hst1 repress middle sporulation-specific gene expression during mitosis in Saccharomyces cerevisiae", *Embo Journal,* vol. 18, no. 22, pp. 6448-6454.

Xie, W., Song, C., Young, N.L., Sperling, A.S., Xu, F., Sridharan, R., Conway, A.E., Garcia, B.A., Plath, K., Clark, A.T. & Grunstein, M. 2009, "Histone H3 Lysine 56 Acetylation Is Linked to the Core Transcriptional Network in Human Embryonic Stem Cells", *Molecular cell,* vol. 33, no. 4, pp. 417-427.

Yamane, K., Toumazou, C., Tsukada, Y., Erdjument-Bromage, H., Tempst, P., Wong, J.M. & Zhang, Y. 2006, "JHDM2A, a JmjC-containing H3K9 dernethylase, facilitates transcription activation by androgen receptor", *Cell,* vol. 125, no. 3, pp. 483-495.

Yang, M., Culhane, J.C., Szewczuk, L.M., Gocke, C.B., Brautigam, C.A., Tomchick, D.R., Machius, M., Cole, P.A. & Yu, H. 2007, "Structural basis of histone demethylation by LSD1 revealed by suicide inactivation", *Nature Structural & Molecular Biology,* vol. 14, no. 6, pp. 535-539.

Yang, M., Gocke, C.B., Luo, X., Borek, D., Tomchick, D.R., Machius, M., Otwinowski, Z. & Yu, H. 2006, "Structural basis for CoREST-dependent demethylation of nucleosomes by the human LSD1 histone demethylase", *Molecular cell,* vol. 23, no. 3, pp. 377-387.

Yang, X. & Seto, E. 2008, "The Rpd3/Hda1 family of lysine deacetylases: from bacteria and yeast to mice and men", *Nature Reviews Molecular Cell Biology,* vol. 9, no. 3, pp. 206-218.

Ying, Q.L., Nichols, J., Chambers, I. & Smith, A. 2003, "BMP induction of Id proteins suppresses differentiation and sustains embryonic stem cell self-renewal in collaboration with STAT3", *Cell,* vol. 115, no. 3, pp. 281-292.

Ying, Q.L. & Smith, A.G. 2003, "Defined conditions for neural commitment and differentiation", *Differentiation of Embryonic Stem Cells,* vol. 365, pp. 327-+.

Ying, Q., Wray, J., Nichols, J., Batlle-Morera, L., Doble, B., Woodgett, J., Cohen, P. & Smith, A. 2008, "The ground state of embryonic stem cell self-renewal", *Nature,* vol. 453, no. 7194, pp. 519-U5.

You, A., Tong, J.K., Grozinger, C.M. & Schreiber, S.L. 2001, "CoREST is an integral component of the CoREST-human histone deacetylase complex", *Proceedings of the National Academy of Sciences of the United States of America,* vol. 98, no. 4, pp. 1454-1458.

Yu, J., Vodyanik, M.A., Smuga-Otto, K., Antosiewicz-Bourget, J., Frane, J.L., Tian, S., Nie, J., Jonsdottir, G.A., Ruotti, V., Stewart, R., Slukvin, I.I. & Thomson, J.A. 2007, "Induced pluripotent stem cell lines derived from human somatic cells", *Science,* vol. 318, no. 5858, pp. 1917-1920.

Zeng, L. & Zhou, M.M. 2002, "Bromodomain: an acetyl-lysine binding domain", *FEBS letters,* vol. 513, no. 1, pp. 124-128.

Zeng, P., Vakoc, C.R., Chen, Z., Blobel, G.A. & Berger, S.L. 2006, "In vivo dual cross-linking for identification of indirect DNA-associated proteins by chromatin immunoprecipitation", *BioTechniques,* vol. 41, no. 6, pp. 694-+.

Zhang, Y., LeRoy, G., Seelig, H.P., Lane, W.S. & Reinberg, D. 1998, "
The dermatomyositis-specific autoantigen Mi2 is a component of a complex containing histone deacetylase and nucleosome remodeling activities", *Cell,* vol. 95, no. 2, pp. 279-289.

Zhang, Y. & Reinberg, D. 2001, "Transcription regulation by histone methylation: interplay between different covalent modifications of the core histone tails", *Genes and Development,* vol. 15, pp. 2343-2360.

Zhou, W., Zhu, P., Wang, J., Pascual, G., Ohgi, K.A., Lozach, J., Glass, C.K. & Rosenfeld, M.G. 2008, "Histone H2A monoubiquitination represses transcription by inhibiting RNA polymerase II transcriptional elongation", *Molecular cell,* vol. 29, no. 1, pp. 69-80.